Chemotherapy induces a genotoxic bystander effect in cell lines from the human bone marrow; evaluation of the role of the redox microenvironment

Okeke Kelechi Celine

This thesis is submitted in partial fulfilment of the requirements of the University of the West of England for the degree of Doctor of Philosophy in Biomedical Science

Faculty of Health and Applied Sciences, University of the West of England, Bristol

August, 2019

Abstract

Modern chemotherapeutic regimens for adult and childhood leukaemia rely on the use of a combination of various cytotoxic agents. Unfortunately, haematopoietic stem cell transplant, a last resort treatment for haematologic malignancies requires high dose of chemotherapy prior to transplant. Despite advances in cancer chemotherapy, occurrence of secondary malignancies such as donor cell leukaemia (DCL) persist due to the random targets of actively dividing cells by chemotherapy. DCL is a rare condition whereby infused donor cells become toxic in the patient, despite the donor apparently remaining healthy. To date, the cause of DCL is unknown, therefore this thesis sought to explore the role of chemotherapy-induced bystander effect (CIBE) in DCL.

To investigate CIBE, a co-culture bystander model was developed, promoting cell-to-cell communication *in vitro* and permitting isolation of the bystander cells for cytotoxicity and genotoxicity assessment post exposure to chemotherapeutic agents. For the first time, a panel of 22 chemotherapeutic agents were screened for CIBE and were found to promote genotoxicity in bystander cells. Four drugs (chlorambucil, carmustine, etoposide and mitoxantrone) later studied in detail suggested mitoxantrone induced mainly aneugenic events, but a mixed mode of function for the other three drugs swaying towards aneugenicity in the pancentromeric labelling of micronucleus assay. Interestingly, these analyses demonstrated a novel finding that the donor or bystander cells or both, may play an important role in the occurrence of CIBE, as responses within the TK6, AHH-1 and Kasumi-1 bystander cells differed throughout the research.

The role of the tumour microenvironment in potentiating CIBE also appears important as genotoxicity peaked at day 3 and continued up to 5 days post chemotherapy exposure. Use of the comet assay did not demonstrate significant DNA fragmentation but addition of hOGG1 and Fpg endonucleases suggested a role for redox disruption and generation of reactive oxygen species (ROS). Investigation of the redox status showed an increase in ROS in the bone marrow microenvironment (HS-5 cells), but show little evidence of ROS in bystander cells, despite the increased oxidative damage in the comet assay. The Agilent Seahorse extracellular flux (XF) mitochondrial stress test supported redox disruption in the HS-5 cells, but analyses of antioxidant expression in both compartments showed limited evidence of any response (either increased or decreased).

Collectively this research has demonstrated the capacity for chemotherapeutic agents to induce a bystander effect with the capacity to promote development of a mutated clone within a supportive tumour microenvironment. Currently the mechanism of this bystander effect is unknown, with redox disruption unlikely to play a major direct role. However, given the understanding of ROS in cellular signalling, and the observation of increased oxidative damage, this may promote cell survival within a genotoxic environment, which warrants further investigation. The data notionally could support a role for CIBE in the development of DCL, but also raises important questions in the wider applications of genotoxicity testing and models used as hitherto, the focus has been on outcomes from direct exposure, with monocultures used as the mainstay. This raises important implications for the assessment of human risk and support the idea of more complex multicellular and 3-dimensional study models.

Acknowledgements

I sincerely owe my immense gratitude to God in whom my existence was made possible. He alone granted me the free breath of life, strength, sound health of mind and body. All that I have achieved so far in life are by your grace and mercy alone. For the provisions of necessary life needs, which contributed to the excellent delivery of this PhD work, I say a big thank you Lord. And to our dearest mother Mary, you certainly have no replica and your stronghold and abundant love in my life is deeply appreciated.

To my very own star, Dr Ruth Morse, you are indeed a woman of substance. You were not only a director of studies but you stood in that gap as my tutor, mentor, parents and a friend. You nurtured me into the professional researcher I have become today. I am humbled by your patience with my research developmental processes. You encouraged me when times were hard and you never ceased to share in my happiness, as you would tap me on the back to say well done girl! These words of encouragements served as my red bull to facilitate the output of this research. I forever remain grateful and loyal to your mentorship. Thank you specially for coming through for me in the course of this write up, I sincerely appreciate.

Complimentary to the efforts of my DOS is an icon (Professor Myra Conway). Very subtle with words and highly professional. You taught me to pay attention to details and to focus on and specific with things. Your contributions to the achievement of this quality research is highly remarkable and I sincerely appreciate all your support.

A special recognition goes to Ebonyi State University (EBSU), Abakaliki, whom through the funds of the Tertiary Education trust Fund (TETFUND) sponsored this research work. I highly applaud Dr Amos Nworie who believed so much in me to have put me forward for this staff development scholarship award, may God continue to bless you abundantly. I sincerely hope

to transfer all skills and knowledge acquired to future graduates of EBSU Medical Laboratory Science in every manner possible.

Let me also acknowledge the efforts of my professional colleagues, other academics support and that of the technical team of Centre for Biosciences (CRIB) laboratory, particularly David Corry (flow cytometry, confocal and fluorescent microscopy expert), Jeff Davey (cell culture and chemiluminescence work) and Paul Bowdler (LCMS). I sincerely appreciate all your support, transferred skills, knowledge and expertise. I also acknowledge Adam Thomas for his guide on the HPRT assay and thanks to Sultan Almaki for the help with my bystander model drawing.

To my adorable and most loving parents (Sir and Lady B.C Okeke), I appreciate your choice of me and I shall continue to make you both proud. May God kindly reward you for all your care and supports. To my partners in crime and happiness (my darling siblings) in the person of Chika, Uchenna, Chinwe, Chiderah and Ifeanyichukwu; thanks for your understanding of my frustrated moments and for tolerating all my excesses during the course of this work. Your love, moral, emotional, financial and social support is well recognised.

For all my dear friends and team members (Alex, Arinze, Sultan and Harshini), admirers, lovers and ex-lovers who in one way or the other contributed to the success of this research, I say thank you. Apologies to all those I had lost their contacts, people I refused to hang out with because of tight schedules; it's all over now, so let's celebrate.

Table of Contents

List of Figures

List of Tables

Abbreviations

µg	Microgram
µl	Microlitre
µM	Micromolar
^{0}C	Degree Celsius
4-HHE	4-Hydroxy-Trans-Hexenale
5-OHMeU	5-Hydroxymethyl Uracil
8-OHdG	8-Dihydroxy-2'-deoxyguanosine
AGEP	Advanced Glycation End Products
AHH	Aryl hydrocarbon hydroxylase
ALL	Acute lymphoid leukaemia
AML	Acute myeloid leukaemia
AOPP	Advanced Oxidation Protein Products
APS	Ammonium per sulfate
ATCC	American type culture collection
ATP	Adenosine Triphosphate
BCA	Bicinchoninic acid
BM	Bone Marrow
BSA	Bovine serum albumin
BVDV	Bovine viral diarrhea virus
CAT	Catalase
CIBE	Chemotherapy-induced Bystander Effect
CLL	Chronic lymphoid leukaemia
CML	Chronic myeloid leukaemia
CO_2	Carbondioxide
COSHH	Control of substances hazardous to health
COX-2	Cyclooxygenase-2
DAPI	4',6-Diamindine-2-phenylindole
DCFDA	2',7'-dichlorodihydrofluorescein diacaetate
DCL	Donor cell leukaemia
DEM	Diethylemaleate
DMEM/F12	Dulbecco's Modified Eagle Medium with Ham's factor 12 nutrient

DMEM/HG	Dulbecco's Modified Eagle Medium with high glucose
DMEM/LG	Dulbecco's Modified Eagle Medium with low glucose
DMF	Dimethyl formamide
DMSO	Dimethylsulphoxide
DNA	Deoxyribonucleic Acid
EBV	Epstein Barr virus
ECAR	Extracellular acidification rate
ECAR	Extracellular Acidification Rate
EDTA	Ethylenediaminetetraacetic acid
ELISA	Enzyme Linked Immunosorbent Assay
ESI	Electrospray ionization
ETO	Eight twenty one
FaPyAde	4,6-diamino-5-formamidopyrimide
FaPyGua	2,6-diamino-4-hydroxy-5-formamidopyrimidine
FBS	Foetal bovine serum
FCCP	Fluoro Carbonyl Cyanide-P-trifluoromethoxy Phenyl-Hydrazon
FCS	Foetal Calf Serum
FISH	Fluorescent *in situ* hybridisation
FITC	Fluorescein isothiocyanate
Fpg	Formamido pyrimidine DNA-glycosylase
g/l	Gram per litre
H_2O_2	Hydrogen peroxide
HAT	Hypoxathine-aminopterin-thymidine
HCL	Hydrochloric acid
HEPES	4-(2-hydroxyethyl)-1-piperazineethanesulfonic acid
HI-FBS	Heat inactivated foetal bovine serum
hOGGI	Human 8-oxoguanine DNA-N-glycosylase 1
HPLC	High performance liquid chromatography
HRP	Horseradish peroxidase
HSC	Haematopoietic stem cells
HSCT	Haematopoietic stem cell transplant
HTLV	Human T-cell lymphocytic virus
IL	Interleukin

$KBrO_3$	Potassium bromate
KCL	Potassium chloride
LCMS	Liquid Chromatography and Mass Spectrometer
MAPK	Mitogen-Activated Protein Kinase
MDA	Malondialdehyde
MDS	Myelodysplastic syndrome
MFI	Median Fluorescent Intensity
ml	Millilitre
mM	Millimolar
mmol/L	Millimole per litre
MRM	Multiple reaction monitoring
NAC	N-acetylcysteine
NaCl	Sodium chloride
nM	Nanomolar
OCR	Oxygen Consumption Rate
OECD	Organisation for Economic Co-operation and Development
OxoGua	Oxo-7,8- dihydroguanine
PBS	Phosphate buffered saline
PCR	Polymerase Chain Reaction
PET	Polyethylene terephthalate
PFA	Paraformaldehyde
PFA	Paraformaldehyde
pg/ml	Picogram per millilitre
PVDF	Polyvinylidene difluoride
RIPA	Radio immune precipitation assay
RNA	Ribonucleic acid
ROS	Reactive oxygen species
RPMI	Roswell park memorial institute
SDS- PAGE	Sodium dodecyl sulphate polyacrylamide gel electrophoresis
SOD	Superoxide Dismutase
STR	Short tandem repeat
TEMED	Tetramethylethylenediamine
TMB	Tetramethylbenzene
Tnf-α	Tumour necrosis factor alpha

TRL	Therapy related leukaemia
TRX	Thioredoxin

CHAPTER 1

INTRODUCTION

1.1 Haematopoiesis and the bone marrow microenvironment

Haematopoiesis describes the process by which the repertoire of blood cell lineages are produced from haematopoietic stem cells (HSCs). This hierarchical development of cell lineages eventually results in the production of red cells (erythropoiesis), white cells (leukopoiesis) and platelets (thrombopoiesis) (Mikkola and Orkin, 2006). HSCs are produced at various anatomical sites (yolk sac, placenta, foetal liver, aorta-gonad-mesonephros region) and are responsible for maintaining the blood pool throughout life. HSCs further colonize the bone marrow (BM) in adulthood maintaining a quiescent steady state (homeostasis) through 'their' self-renewal, differentiation and proliferation capacity, thus producing nearly a trillion mature blood cells daily (Boulais and Frenette, 2015).

HSCs are maintained in a BM specialized microenvironment called the niche (Figure 1.1); the niche cells are responsible for regulation of HSCs during normal haematopoiesis (Gleitz *et al.*, 2018). Traditionally, the two main identified niches are the endosteal and vascular niches, but according to the classification by Sean Morrison and Simon Mendez-Ferrer, BM niches are continuously evolving, with new discoveries for mesenchymal and haematopoietic lineages (Beerman *et al*., 2017). The identified niches comprise majorly of endothelial (arterioles, transition zone vessels and sinusoids) and mesenchymal stromal cells (mesenchymal stem cells, osteo-lineages, adipocytes, chondrocytes, myocytes and haematopoietic progenitor cells). These cells are the key players in the maintenance of BM steady state and the continued generation of HSCs. The stromal cells include the CXCL12-abundant reticular (CAR) cells, leptin receptor positive cells (LepR+), and $CD144^{-}CD146^{-}Sca\text{-}1^{+}$ cells; these together highly express niche factors such as CXCL12 (also known as stromal derived factor; SDF-1) and stem cell factor (SCF) that support HSC (Ding and Morrison, 2013 and Greenbaum *et al*., 2013), alongside the Treg cells that provides immunoprivilege sites for HSCs. The endothelial cells produce some angiocrine factors like bone morphogenic protein (BMP) 2 and 4, notch ligands, SCF, CXCL12, wingless-type mouse

mammary tumour virus (MMTV) integration site (WNT5a), cytokines and insulin growth factor binding protein 2; all contributing to HSC maintenance within the niche (Butler *et al*., 2010). The role of osteocytes in HSC maintenance remains controversial but it appears to play a role in HSC mobilization through the granulocyte-colony stimulating factor (G-CSF; Asada, 2018).

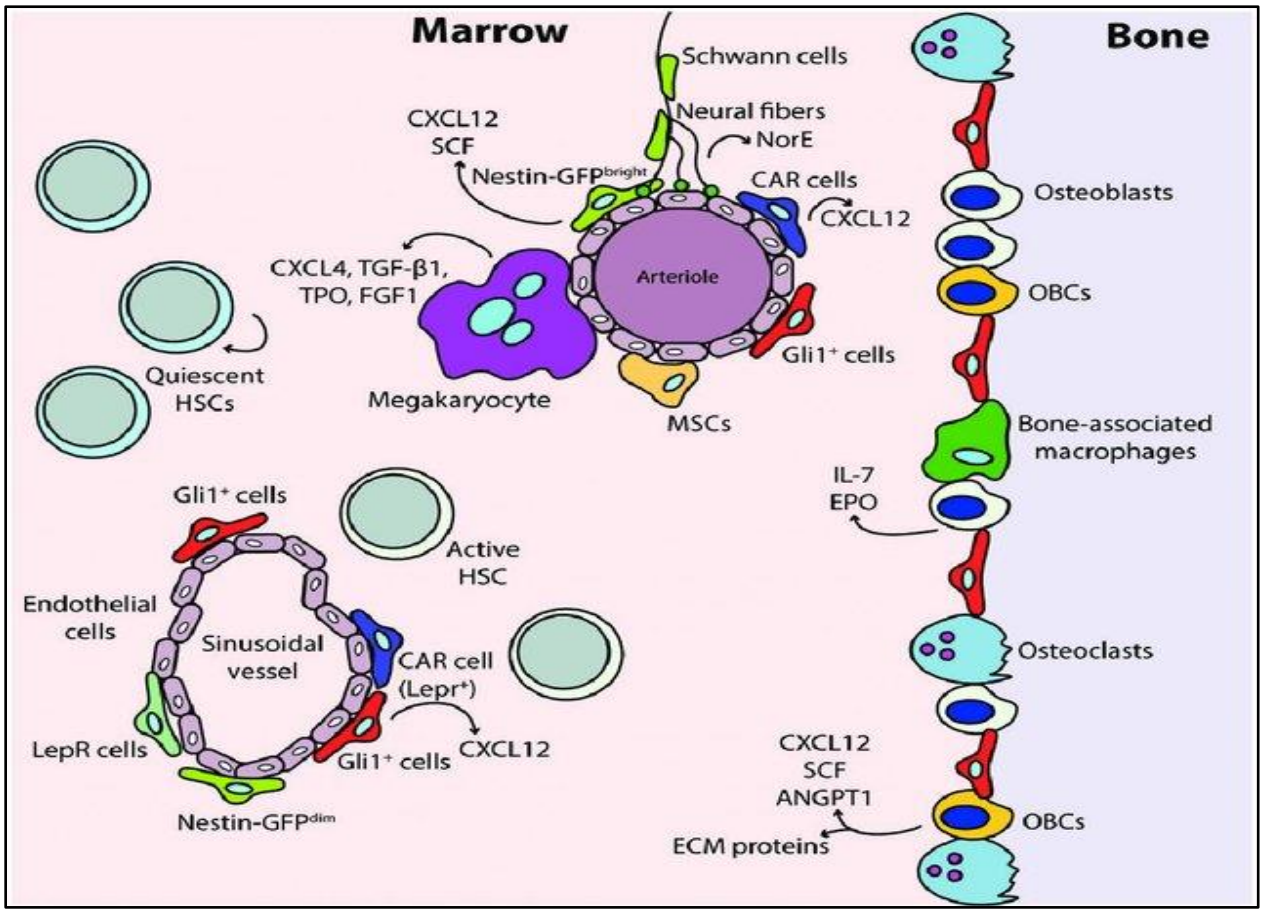

Figure 1.1 The bone marrow (BM) in normal homeostasis. The BM cells reside in niches including the endosteal, reticular and the vascular niches. Haemopoietic stem cells (HSCs) are in contact with the endosteal niche and endothelial cells within the BM. The mesenchymal stem (MSCs) and progenitor cells produce the bone forming cells (osteoblasts) and osteoblastic cells (OBCs) which produces erythropoietin (EPO), interleukin-7 (IL-7) and expresses other HSC formation vital factors like the C-X-C motif chemokine ligand 12 (CXCL12), stem cell factor (SCF), angiopoietin-1 (ANGPT1) and extracellular matrix proteins. The osteoclasts (bone-resorbing cells) are associated with macrophages and the primitive MSCs like CXCL12-abundant reticular cells (CAR) and the nestin-expressing cells. The bright nestin–green fluorescent protein (Nestin-GFPbright), neural-glial antigen (Gli 1+ cells) MSCs are associated with bone transition zone vessels and arterioles while the Nestin-GFPdim, leptin receptor (LEPR) and CXCL12-CAR cells MSCs are associated with the sinusoids in the center of BM. All these various cells interplay alongside the cytokines aid the maintenance of BM homeostasis. Image copied from Gleitz *et al.,* 2018 under the free creative common license.

1.2 Alterations to bone marrow microenvironment during leukaemogenesis

Normal haematopoiesis (Figure 1.2) involves a complex interaction between the BM niche and haematopoietic cells. HSCs operates a restricted and controlled cell autonomous process through the regulation of the hierarchical haemopoietic system where the pluripotent HSCs continuously regenerates to replace the blood pool. Although they are self-renewing (Morrison *et al*., 2002), they sometimes receive signals from the microenvironment through the cell-cell interactions, integrating them to produce progenies that support the haematopoiesis (Hoffman and Calvi, 2014).

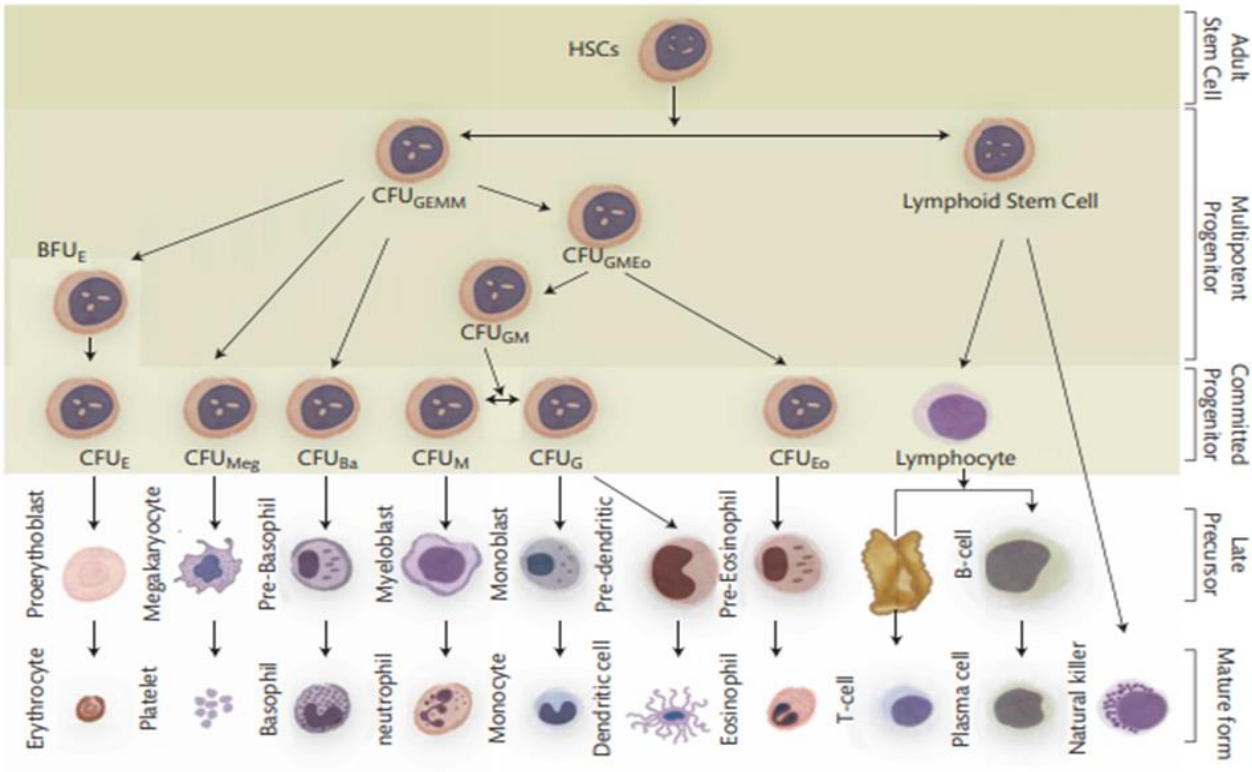

Figure 1.2: The developmental sequence of haematopoietic cells in human. The haemopoietic stem cells (HSCs) are responsible for production of blood cells. Under the influence of cytokines expressed by bone marrow (BM) stroma cells, HSCs proliferates and differentiates to generate progenitor cells of myeloid (originating from colony forming unit for granulocyte, erythrocyte, monocyte and megakaryocyte - CFU_{GEMM}) and lymphoid lineages. The committed myeloid lineages produces erythrocyte, developed from the burst and colony forming unit erythrocyte (BFU_E and CFU_E); platelets, developed from the colony forming unit megakaryocyte (CFU_{MEG}); monocyte, dendritic cells and neutrophil, originating from the colony forming unit of granulocyte and monocyte (CFU_{GM}); basophil and eosinophil developing from CFU_B and CFU_{EO}. The lymphoid progenitor cells develop the B and T lymphocyte and natural killer cells, some differentiating to mature in the BM or thymus. Maintenance of this hierarchy is vital to production of blood cells. Image adapted from Morse and Kabrah, 2018.

HSCs oversees definitive haematopoiesis which is aided by their pluripotent capacity. This process is controlled by key genes such as runt-related transcription factor 1 (*Runx1*); which provides instructions for making of proteins (Jagannathan-Bogdan and Zon, 2013). The process starts from the embryo yolk sac with the first identifiable cell type called aorto-gonado-mesonephros (AGM), that transitions to the fetal liver and finally establishes the definitive blood production in the bone marrow and thymus (Ng and Alexander, 2017).

Despite the regulation of the blood production process, abnormal proliferation could lead to aberrant mitosis, affecting signalling pathways with stem cells as the initial targets. As such, long-lived stem cells are likely to acquire and accumulate initial transforming mutations, leading to malignancy through multiple self-renewal activities (Lobo *et al.*, 2007). Such transformed stem cells are referred to as cancer stem cells (CSCs) and are hypothesized to be responsible for tumour growth and its maintenance. Consequently, in a specific pathological state such as leukaemia, the mutated HSCs are referred to as leukaemic stem cells (LSCs), which occupy the BM endosteal and vascular niches, outnumbering the HSCs to convert the niches into a more hypoxic state necessary for its proliferation and survival (Nwajei and Konopleva, 2013). The exact mechanism underlying such leukaemic transformation is currently unknown, but certain genetic and metabolic changes play a role. This metabolic change is through the ability of LSCs to mirror the HSCs niche, thereby enabling the switch of normal oxidative mitochondria phosphorylation to glycolysis, potentiating their quiescent cell survival (Zhao *et al.*, 2010). While the hierarchy progenitor stem cells lead to production of descendant LSC, LSCs fate and survival is influenced by cross talk within the BM microenvironment.

Evidence to support the role of BM microenvironment in LSCs biology and leukaemia pathogenesis is under study. Some studies have revealed the potential cell types of the LSC niche within the BM microenvironment and their regulation within the niche (Figure 1.3). LSCs has been shown to express a counter receptor of the CXCL12 called CXCR4 using a mice model (Tavor *et al.*, 2004). Tavor and colleagues demonstrated that by using this counter receptor of CXCL12 (used to home HSCs secreted in the bone marrow into the blood circulation by chemokine attraction, as well as maintains the surface of the BM membrane), LSCs were able to block the normal CXCR4-CXCL12 function to allow homing of LSCs and leukaemia propagation.

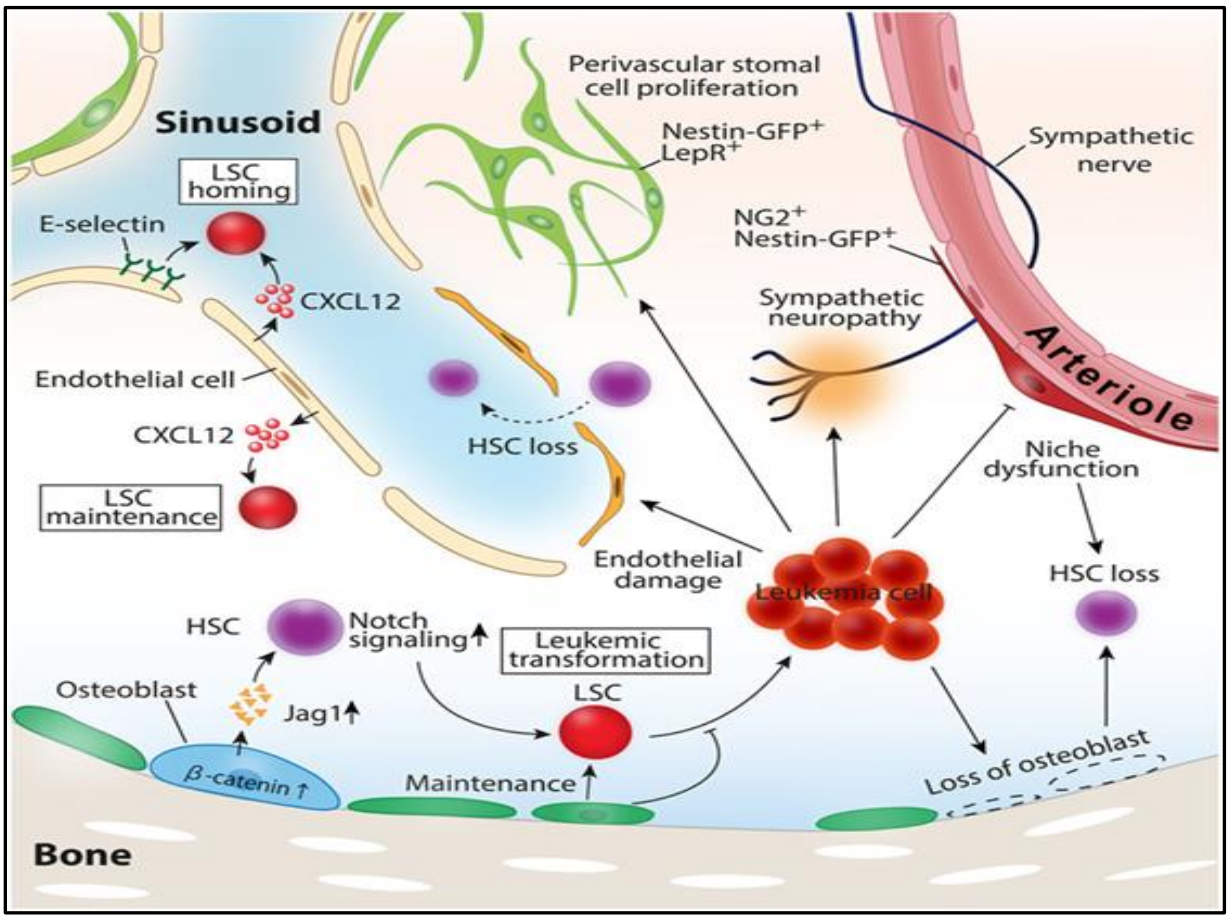

Figure 1.3: Influence of the BM microenvironment in leukaemia. Using a mice model, LSCs show the capacity to home and reside around the E-selectin and CXCL12, revealing crosstalk alteration and supportive role of vascular endothelium in LSCs expansion and maintenace.The activation of β-catenin stimulated by the expression of Notch ligand jagged 1 (Jag1) in osteoblasts leads to Notch signalling and an induced LSCs transformation. Transformed LSCs induces loss of osteoblast that maintains the endosteal HSCs leading to subsequent loss of the perivascular, endothelial and HSCs loss to prevent HSCs homing while propagating LSCs homing (aided by CXCL12 activation and the expression of E-selectin adhesion molecule). This figure is credited to Asada (2018) with permitted usage of the free creative common license.

LSCs are able to alter the BM normal dynamics through their expression of SCF, thus creating a new 'foster home' called the malignant niche. This alteration is achieved through the differentiation and self-renewal capacity of the LSCs, two features which are necessitated for tumour progression. Knowledge of the LSCs existence and quiescence has made researchers aware of the possible implications of this hierarchical cell population in cancer therapeutics. Most evidence of LSC have been accrued through mouse-models which have proved an invaluable tool

in most leukaemia studies. However, cautionary measures must be applied as some of the pathogenesis of leukaemia in these models may not be relevant in human, especially with the uncertainty of the genetic stimulations of disease in these models. Despite a few drawbacks, most genetically modified models closely mimic pathology in humans and has been pivotal to the milestones achieved in leukaemia research (Cook and Pardee, 2013). By providing this alternative home for the haemopoietic progenitor cells, they alter their migration pattern into the circulation, in the presence of granulocyte colony stimulating factor thereby altering normal cellular crosstalk between the HSCs and the BM stromal cells to secure survival (Colmone *et al*., 2008; Schmidt *et al.*, 2011). Most leukaemias occur due to a specific mutation, the LSCs also possess a long-term repopulation potential (enabled by the CSC unlimited differentiation capacity), and with some fractions evading chemotherapy, these attributes collectively contribute to relapse (Park *et al.*, 2012).

The molecular mechanism by which the BM microenvironment is altered is not fully elucidated but an understanding may likely provide a beneficial framework for creation of novel therapies (Nwajei and Konopleva, 2013). Some reported mechanisms include: a lack of retinoic acid receptor could cause myeloproliferative syndrome and the deletion of Dicer1 in osteo-progenitors can lead to myelodysplastic syndrome and AML (Boulais and Frenette, 2015). Notwithstanding, the process of leukaemogenesis still requires more investigations such as osteoblast factors (β-catenin and Notch ligand), fibroblast factors (CD147 and matrix metalloproteinases - MMPs), endothelial factors (E-selectin and CXCL12), CXCR4 and CD44 adhesion molecule; perivascular stromal cell factors (Nes GFP+ and NG2+) and the immune cells (Treg); all of which may likely contribute to the development of leukaemia. However, the extent of their contribution may vary with leukaemia subtype (Asada, 2018; Shafat *et al.*, 2017). Notably, these microenvironmental changes and survival of LSCs comes at the expense of other blood cells which are reduced in number.

1.3 Leukaemia

Leukaemia describes an uncontrolled progressive production of malignant blood cells, majorly the white blood cells of the BM (Abeloff *et al*., 2004). This malignancy occurs when there is an alteration in the normal regulatory process of blood production and it can affect both children and adults. Leukaemia is classified based on its disease characteristics as either acute (involving

immature cell types – 'blasts') or chronic (involving mature cell types – 'cytes'). Additionally, it is further classified based on the cellular lineage involved either as myeloid (monocytes, basophils, eosinophils and neutrophils) or lymphoid (T and B lymphocytes), hence giving rise to four major types: chronic lymphocytic leukaemia (CLL), chronic myeloid leukaemia (CML), acute lymphoblastic leukaemia (ALL), and acute myeloid leukaemia (AML) (Pokharel, 2012). Other types of leukaemia include hairy cell leukaemia (an uncommon chronic leukaemia), juvenile myelomonocytic leukaemia (JMML - myeloid leukaemia that occurs in children less than 6 years), chronic myelomonocytic leukaemia (CMML – develops specifically in monocytes), acute promyelocytic leukaemia (AML subtype) and large granular lymphocytic leukaemia (LGL – develops from lymphoid cells). While AML, CLL and CML are common in adults, ALL occurs in both adults and children but mostly children, with 53% of new cases occurring in persons less than 20 years (Davis *et al.*, 2014).

1.3.1 Epidemiology of leukaemia

The most recent data from Cancer Research UK (CRUK, 2015a) records leukaemia as the 12th most common cancer with 3% incidence of all new cancer cases, having a distribution of 59% and 41% respectively for male and females. Ten-year age-standardised net survival for leukaemia has increased from 7% (1971-1972) to 46% (2010-2011) in England and Wales, UK. The male population in the UK accounts for 3% (ranking 10th most common) of new male cancer cases, while females account for 2% of new female cancer cases, thus making it the 12th most common cancer in UK females. According to subtypes, no leukaemia subtypes are in the 20 most common cancers, as they are all less than 1% individually, however the distribution for males and females respectively is: ALL, 55% vs 45%; AML, 56% vs 44%; CLL, 63% vs 37%; CML 55% vs 45%. (CRUK, 2015b). In the context of this research study, the focus shall be on a de novo haematologic neoplasm called donor cell leukaemia (DCL – section 1.7) which develops majorly as acute leukaemia than chronic form of leukaemia.

Furthermore, the five-year survival rate of leukaemia is predicted at 54% (males) and 49% (females) in England and Wales, (2010 – 2011). While leukaemia is not the most common cancer type in adults, there has been a tremendous improvement as evidenced with the low 4% mortality rate (Figure 1.4a), of leukaemia compared to total cancer deaths in 2016 (UK cancer research). However, childhood cancer shows leukaemia as the most common cancer (Figure 1.4b), with a

rate of 31% compared to others, but this has also witnessed an improvement as five year overall survival rate of childhood leukaemia has a rate of 88%, with ALL (the most common) showing a five year survival of 92% (CCUK, 2019).

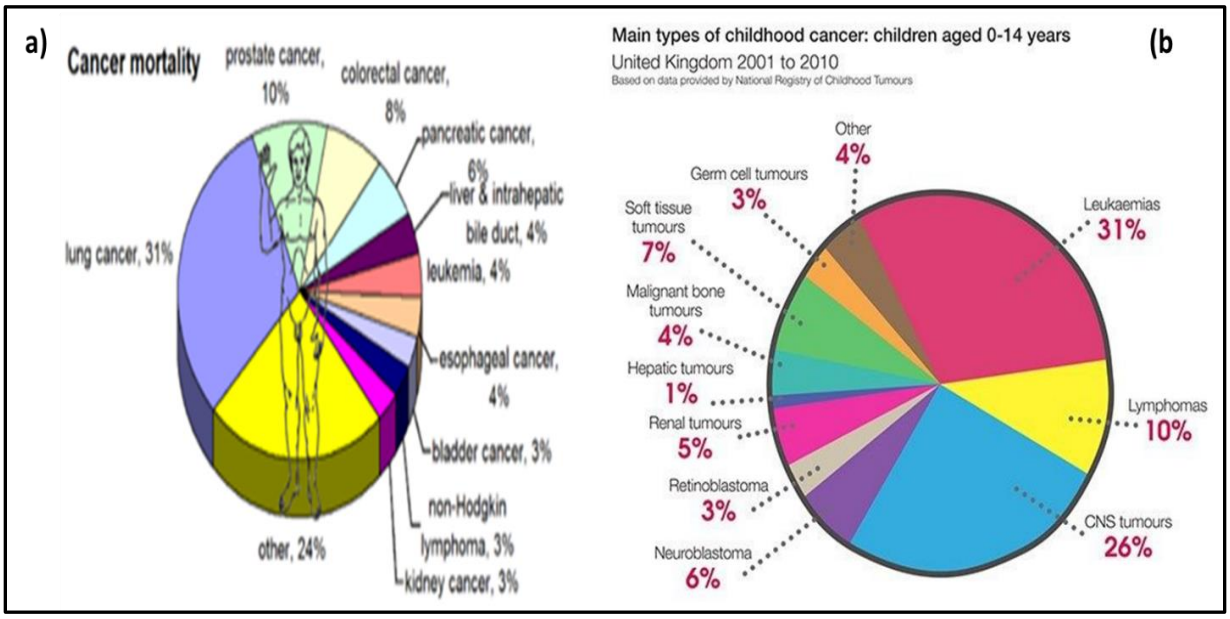

Figure 1.4: Cancer mortality rate and survival outcome. Childhood leukaemia is on the increase and represents the major type of cancer abundant in children. A) The number of deaths arising from adult leukaemia showing better disease outcome. B) Leukaemia is the most frequently occurring cancer in children followed by central nervous system tumours. Image credited to Cancer Research, UK (2010).

1.3.2 Aetiology and risk factors of Leukaemia

There is no single identified aetiology for leukaemia, rather it appears to have a combinatorial factor of genetics versus environmental interactions, alongside ionising irradiation and some chemicals. People exposed to ionising radiation as part of therapy, medical radiation staff or the survivors of atomic bombs show an increased risk for CML, AML and ALL (Kuznetsova *et al.*, 2016). There is little evidence to support viral transformation in acute leukaemia, but high penetrance germline mutations are implicated in about 5% of childhood leukaemia (Eden, 2010). Young people show increased leukaemia risk from radiation arising from computed tomography, while development of other leukaemia subtypes arise from previous haematologic malignancy history (Lichtman, 2010; Brenner and Hall, 2007). For instance, there can be increased AML from blood disorders such as myelodysplasia, polycythemia vera and primary thrombocythemia. Some

genetic disorders like Down syndrome, neurofibromatosis, Bloom syndrome, Fanconi anaemia, Klinefelter syndrome, ataxia-telangiectasia and increased exposure to household pesticides such as mosquito repellents or other insect pesticides do pose a higher risk for ALL and AML especially in children and during pregnancy (Maele-Fabry *et al.*, 2019 and Metayer *et al.*, 2013).

An established risk for some leukaemias (AML, ALL and CML) is exposure to certain environmental and occupational cytotoxicants (e.g. platinum agents, alkylating agents and topoisomerase inhibitors), as well as obesity and increased body mass index (Buffler *et al.*, 2005; Khalade *et al.*, 2010). According to Zeeb and Blettner (1998), some investigated and/or established risk factors for leukaemia are collated into three groups: environmental factors, therapy/medical related and genetic/familial causes. Environmental factors include: benzene (sources include: oil refineries, rubber industry, chemical plants, gasoline and shoe manufacturing plants), pesticides, ionizing and non-ionizing radiation, printing industry, occupational exposure such as leather, smoking and diets (Schuz and Erdmann, 2016). Therapy/medical related factors include: diagnostic radiology, chemotherapy, radiotherapy, viruses e.g. herpesvirus, human T-cell leukaemia/lymphoma virus (HTLV-1) and some medication such as chloramphenicol. Other risk factors include family history of leukaemia, age (AML and CML increases with age), race (increased risk in European descent and rare in Asian descent) and gender (more in men than women) (Purdie, 2017).

1.3.3 Leukaemia signs and symptoms

Clinically, leukaemia presents symptoms typical to that of BM failure such as frequent bruises due to fewer platelets, recurrent infections due to malfunctioning of white cells, anaemia (due to reduced red cell number), enlarged lymph nodes, liver and kidneys (Grigoropoulos, 2013; Hoffman, 2005). In addition, infrequent involvement of the central nervous system (CNS), meninges and cutaneous infiltration may occur, leading to headaches and gum swelling (Hoffbrand *et al.*, 2011). Classical symptoms however include: fever, night sweats, weight loss, fatigue, and malaise and bone/joint pains. Many diagnosed cases (75%) are through incidental diagnosis from asymptomatic patients (Pokharel, 2012).

Specifically, children with acute leukaemia present with fever, bleeding, lethargy, enlarged liver and spleen, lymphadenopathy, with 7% of CNS involvement. However, adults with acute

leukaemia show symptoms of fatigue, fever, weight loss, bone pain, shortness of breath, nose bleeds and excessive bruising. Furthermore, 50% of ALL adults present with enlarged spleen, enlarged liver and lymphadenopathy but these symptoms are not typical of AML. Conversely, chronic leukaemias are usually asymptomatic with 20% of CML and 50% of CLL patients discovered incidentally (Davis *et al.*, 2014). Classical symptoms are less common in chronic leukaemia but CLL show hepatosplenomegaly and lymphadenopathy, while CML commonly shows splenomegaly (Yee and O'Brien, 2006).

1.3.4 Staging and diagnosis of leukaemia

According to Cancer Treatment Centres of America (CTCA, 2019), staging refers to the act of determining the extent of spread of a cancer. Traditionally, most cancers are staged by a numbering system based on the tumour size and how far it has spread, but since leukaemia occurs in blood cells and by definition a systemic cancer, it is staged based on leukaemic cells accumulation in other organs (e.g. liver) and by blood cell count. This staging is a vital guide to the patient's general outlook and therapy options. Overall, factors to be considered for staging or prognosis include: age, history of a previous blood disorder, white cell and platelet counts, enlarged spleen or liver, bone damage or chromosomal abnormality. The various types of leukaemia are staged and classified according some existing systems (Table 1.1). Briefly, ALL does not form tumours, it develops in the BM and can spread to other organs before it is detected, and it's staged based on patient's age, and as the subtypes of B-cell ALL or T cell ALL. Conversely, AML also begins in the BM but is not detected until it spreads to other organs, and thus is staged based on cellular classification (number of healthy or leukemic cells, chromosome changes and genetic abnormality) using the French American British (FAB) system of M0 to M7 (CTCA, 2

Table 1.1: Leukaemia staging and diagnostic features. The classification of each leukaemia subtype based on the staging system and the characteristic distinguishing clinical features. ALL are based on cell type, AML uses the FAB system, CLL uses both Rai and Binet systems, and CML is staged by number of diseased cells. Features extracted from CTCA and WHO website.

Disease Type	Staging Type	Clinical features
ALL	B- Cell	ALL with hypodiploidy (Leukaemia cells have fewer than 44 chromosomes)
		ALL with hyperdiploidy (Leukaemia cells have more than 50 chromosomes)
		ALL with translocation between chromosomes 9 and 22 [t(9;22)] (the Philadelphia chromosome,creating the *BCR-ABL1* fusion gene)
		ALL with translocation between chromosome 11 and another chromosome
		ALL with translocation between chromosomes 12 and 21 t(12;21)
		ALL with a translocation between chromosomes 1 and 19 t(1;190
		ALL with a translocation between chromosomes 5 and 14 t(5;14)
		ALL with amplification (too many copies) of a portion of chromosome 21 (iAMP21).
		ALL with translocations involving certain tyrosine kinases or cytokine receptors (also known as "BCR-ABL1–like ALL" (B- cell receptor Abelson 1)
	T -Cell	**Pre-T cell ALL** - approxiamtely occur in 5 - 10% of ALL cases
		Mature T-cell - approximately occur in 15 - 20% of ALL cases
AML	French American British (FAB) classification	**M0** - Undifferentiated BM cells
		M1 - Myeloblastic leukaemia (signs of granulocyte differentiation)
		M2 - Myeloblastic leukaemia (early granulocyte maturation)
		M3 - Promyelocyte leukaemia (maturation between myeloblasts and myelocyte)
		M4 - Myelomonocytic leukaemia (variable monocyte and granulocyte eg eosinophil)
		M5 - Monocytic leukaemia (increased monoblasts, promonocytes and monocytes)
		M6 - Erythroleukaemia (abnormal nucleated red blood cells, over half the BM cells)
		M7 - Megakaryoblastic leukaemia (immature megakaryocytes with fibrous deposits)
CLL	Rai system	**Stage 0** - (Too many lymphocytes >10,000 and normal blood count for others).
		Stage I - (Too many lymphocytes, swollen lymph nodes; normal RBC and platelet).
		Stage II - (lymphocytosis, liver and spleen may be larger than normal)
		Stage III - (anaemia, may have swollen lymph nodes; > normal liver and spleen)
		Stage IV - (same as stage III as well as thrombocytopenia due to reduced platelets).
	Binet system	**Clinical Stage A** - (< 3 areas of lymphadenopathy)
		Clinical Stage B - (> 3 areas of lymphadenopathy)
		Clinical Stage C - (anaemia (<10 g/dl) ± thrombocytopenia)
CML	Based on number of diseased cells	**Chronic phase** - mild symptoms like fatigue (5-6 years)
		Accelerated phase - more aggressive symptoms/noticeable symptoms (6-9 months)
		Blast crisis - most aggressive stage; > 20% myeloblasts/lymph+B1:C31oblasts (3-6 months)

Two staging systems of CLL are Rai (American method) and Binet (mostly used in Europe) system. The Rai system (Rai *et al.*, 1975) depends on the number of lymphocytes, whether the lymph nodes, liver or spleen are enlarged and whether anaemia has developed. Thus, the system is classified as low (stage 0), medium (stages I and II) and high (stages III and IV). The Binet system on the other hand, evaluates the areas of the affected lymphoid tissue rather than blood count and are thus classed as clinical stage A (< three areas), B (> three areas) and C (anaemia and/or thrombocytopenia has developed). CML is majorly classified based on clinical symptoms and the number of affected cells and include: chronic (mild symptoms), accelerated (more aggressive or noticeable symptoms) and blastic (most aggressive with 20% myeloblasts or lymphoblasts) (Binet *et al.*, 1981). Use of two staging system for CLL was based on the recommendations of the International workshop on CLL as both systems correspondingly stages patients into three survival curves/groups, as CLL can be extremely variable with large survival times (ranging from 2-20years). Also, unlike other forms of leukaemia with easy staging based on tumour size, CLL does not usually form tumour but progressively starts from BM and spreads to other organs.

Leukaemia is diagnosed by performing a complete blood count and peripheral blood smear, to determine the number of blood cells, cell type and stage of development e.g. detection of blasts/cytes or auer rods (needle-like cytoplasmic inclusion bodies). A BM aspirate or biopsy is examined for haematopoietic cells with greater numbers than normal and for identification of chromosomal abnormalities such as loss or gain of chromosomes 7, 5, 11, 15, 17, 19, 21, 22 (Hamerschlak, 2008; Stieglitz and Loh, 2013). Depending on the leukaemia type, certain genetic markers such as *FLT3* (FMS3-like tyrosine kinase 3; mostly internal tandem duplication), *KIT* (tyrosine protein kinase KIT; point mutation) and nucleophosmin – a nucleocytoplasmic protein mutated in AML (Baldus *et al*., 2007) are examined. Also, by using fluorescent *in situ* hybridisation (FISH) or karyotyping, the *BCR-ABL1* fusion gene can be detected as well as the diagnosis of other subtypes of leukaemia.

More so, through the use of flow cytometry and immunophenotyping analysis, cloned lymphoid lineages can be sorted and counted, and some cell surface markers can specifically be identified (Craig and Foon, 2008). Molecular testing methods like polymerase chain reaction (PCR) can also be used to identify some mutations at the DNA level (Davis *et al.*, 2014). To assess for nodal

infiltration, lymph node biopsy and a spinal tap or lumbar puncture (in severe cases) can be examined (Dohner *et al.*, 2010; Pokharel, 2012). Specifically, AML and ALL are characterised by the blast cells on BM aspirate or peripheral blood smear and the presence of auer rods in AML. CLL features increased B lymphocytes and clonal expansion in peripheral blood, and CML is characterised by the Philadelphia chromosome (*BCR-ABL1* fusion gene) (Mondal *et al.*, 2006). Overall, with the vast diagnostic techniques for leukaemia, an initial diagnosis starts by checking the signs and symptoms and in case of bleeding for instance, a blood test is performed for the presence of abnormal white cells, which is suggestive of leukaemia. Confirmatory studies can be performed by needle biopsy and BM aspiration done to detect leukemic cells, alterations in chromosome and DNA markers. Other specific techniques are used as the need arises during specific leukaemia investigation.

1.3.5 Current leukaemia therapeutic regimens

Chemotherapy and/or radiotherapy is the mainstay treatment for leukaemia, and because they are DNA damaging agents, but they also attack other actively dividing cells. Treatment depends on the type or subtype of leukaemia and includes chemotherapy (Table 1.2), with/without radiotherapy, haematopoietic stem cell transplant (HSCT), use of targeted molecules (e.g. tyrosine kinase inhibitors like imatinib for CML), monoclonal antibodies such as rituximab for ALL (Jabbour *et al.*, 2015) and various immunotherapies (Hawkes, 2018). Treatment of acute leukaemia relies on the patient's condition, molecular findings and disease subtype. ALL therapy occurs in phases of one (starting with induction chemotherapy) to four (regular physical exams and laboratory testing to monitor remission) and any relapses are combatted with chemotherapy with some cases requiring stem cell transplant (SCT). SCT is a procedure for the replacement of damaged stem cells in the BM with healthy stem cells following use of chemotherapy and/or radiotherapy to get rid of damaged cells. AML treatment relies on overall wellbeing and blood cell levels, and similar o ALL it starts from induction therapy (first line of treatment eg surgery) to consolidation therapy (maintenance or intensification treatment utilised to sustain remission in patients) (Percival *et al.*, 2017).

Conversely, chronic leukaemia treatment is dependent on staging. In CLL, the patient's age, health and disease staging are considered, with initial stages requiring only close patient monitoring; stage I or II requiring further monitoring and final stages involving intensive chemotherapy and in

some cases HSCT. CML treatment involves targeted therapy with tyrosine kinase as a first choice approach, which controls the disease for long term but is not considered curative. Overall, a final or curative treatment option for cancer patients (leukaemia inclusive) involves HSCT which will always be preceded by conditioning therapy involving the use of chemotherapeutics (Davis *et al.*, 2014).

Table 1.2: Some examples of leukaemia chemotherapeutic regimens. Some of the classical chemotherapeutic agents used for the subtypes of leukaemia. Depending on the stage, age and disease subtype, an appropriate chemotherapeutic agent is used either alone or as a combination therapy, but may not be the first choice for therapy, depending on the subtype being treated.

Leukaemia Type	Chemotherapeutic Agent
ALL	Daunorubicin Hydrochloride
	Cytarabine (Ara-C)
	Doxorubicin Hydrochloride
	Methotrexate
	Vincristine Sulfate
AML	Cytarabine (Ara-C)
	Daunorubicin Hydrochloride
	Doxorubicin Hydrochloride
	Mitoxantrone
	Vincristine Sulfate
CLL	Chlorambucil
	Mechlorethamine Hydrochloride
CML	Cytarabine (Ara-C)
	Hydroxyurea
	Mechlorethamine Hydrochloride

1.4 Classes of chemotherapeutic agents and their mechanism of action

Chemotherapy agents are majorly classed into five groups. These agents are used in different forms of cancers as well as haematological malignancies including leukaemia. Depending on their mechanism of action and/or function, these classes include: alkylating agents, antimetabolites, topoisomerase inhibitors, antibiotics and plant alkaloids. Some classic examples of their activities

and mode of action either at cell cycle stage, DNA synthesis or other metabolic processes are illustrated below (Figure 1.5).

Briefly, the alkylating agents act directly on the cell genetic material (DNA) to interfere with cell reproduction. They act in all cell cycle phases and can cause long-term damage due to the destruction of the DNA. Examples include carmustine, melphalan, chlorambucil etc and are used in treatment of certain cancers such as leukaemia. Antimetabolites are known to mimic the DNA and RNA building blocks to interfere their growth, acting mainly on S phase of cell cycle. Examples include Ara-C, 5-FU, hydroxyurea, methotrexate etc and are used in leukaemia treatment and other cancers.

Furthermore, the anti-tumour antibiotics can be described as DNA intercalators, altering the DNA to prevent DNA synthesis and thus affecting reproduction. Some antibiotics include daunorubicin, doxorubicin, mitomycin-C and bleomycin etc. Topoisomerase inhibitors are enyzymes which enable the separation of DNA strands to enable the management of DNA tangles and supercoils. They type 1 enzyme cleave one DNA strand, passing on either a single or double strand break, while type II enzyme cleaves two DNA strands to pass on a double strand through the break. Examples include the etoposide, teniposide, mitoxantrone etc. The mitotic inhibitors are mostly plant alkaloids, including other compounds developed from natural produts. They inhibit the M phase of the cell cycle and has the ability to damage all phases by interfering with cell reproduction. These agents include the vincristine, vinblastine, taxane and docetaxel etc

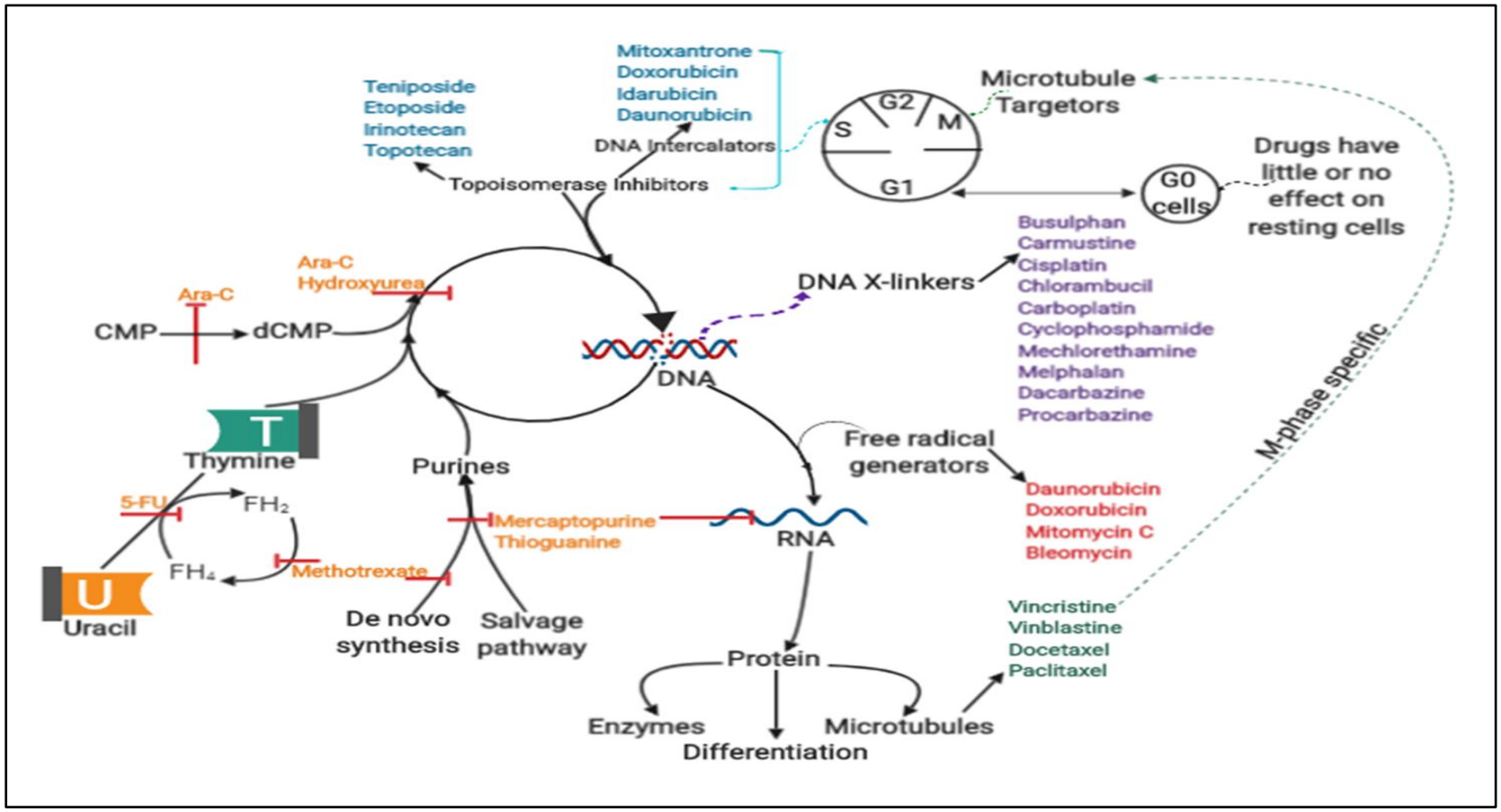

Figure 1.5: Classes of chemotherapeutic agents and functions. The chemotherapeutic agents used in this study are presented according to their five main classes and the functions they exert. These agents act on microtubules, during DNA synthesis (de novo and salvage pathways), as well as cause DNA damage to existing DNA strands through intercalation, crosslinking or via the generation of oxidative species. Blue = topoisomerase inhibitors and antibiotics; purple = alkylating agents; yellow = antimetabolites; green = plant alkaloids; red = antibiotics. Image drawn by the researcher.

1.4.1 Mechanism of action of the alkylating agents.

Alkylating agents covalently bind to alter the bases of the DNA, interfere with DNA replication and transcription (Huang and Li, 2013). Alkylating agents have three classical mechanisms: formation of crosslinks, mutations due to misrepair of nucleotides and DNA fragmentation due to activity of DNA repair enzymes (Ralhan and Kaur, 2007). These compounds exert their activity through a reactive alkyl group, which covalently binds to nucleophilic groups in DNA, attacking the N-1 and N-3 of adenine, N-3 of cytosine and particularly N-7 of guanine bases. These compounds are not cell cycle specific as they remain cytotoxic throughout the cell cycle process with the exception of the G0 phase. Subgroups include nitrosoureas e.g. carmustine which are lipid soluble and readily cross the blood-brain barrier and the nitrogen mustards e.g. chlorambucil, which were derived from the mustard gases, originally used as chemical warfare (Mangerich *et al.*, 2016). Note that in historic literature the platinum compounds e.g. cisplatin have been included as 'alkylating agents' as they possess similar crosslinking activity, however they do not contain an alkyl group (https://www.ncbi.nlm.nih.gov/books/NBK12772/). Following the preliminary findings of this research (see chapter 4), two main alkylating agents - carmustine and chlorambucil (Figure 1.6) were focused on for the latter part of the study (see chapter 5).

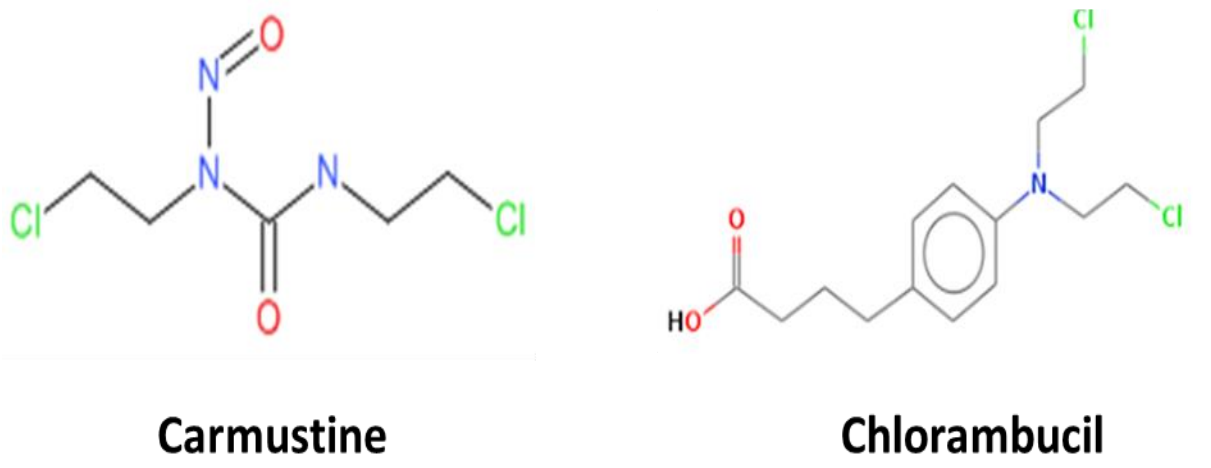

Figure 1.6: The chemical structure of carmustine and chlorambucil. Carmustine has a molecular weight of 214.05 g/mol with chemical formula of $C_5H_9Cl_2N_3O_2$**.** Chlorambucil has a chemical formula of $C_{14}H_{19}Cl_2NO_2$ with molar mass of 304.212 g/mol. N=Nitrogen, Cl=Chlorine, O=Oxygen. Images assessed from National Centre for Biotechnology Information, PubChem Database (Assessed Mar. 17 2020).

1.4.1.1 Carmustine

Carmustine (bis-chloroethylnitrosourea; BiCNU) belongs to the group of drugs known as the nitrosoureas, which are highly lipophilic with ability to cross the blood brain barrier. It undergoes hydrolysis *in vivo* to form reactive metabolites that cause alkylation, DNA and RNA crosslinking. Carmustine also inhibits DNA synthesis, DNA repair, RNA synthesis, RNA translation. BiCNU has been indicated for treatment of multiple myeloma, Hodgkins and non-Hodgkins lymphoma, gastrointestinal cancers and primary brain tumours (McEvoy, 2006). It alkylates DNA to cause inter and intra-strand crosslinks (Figure 1.7) and whilst they are rapidly taken up, they are easily degraded in the cells as well.

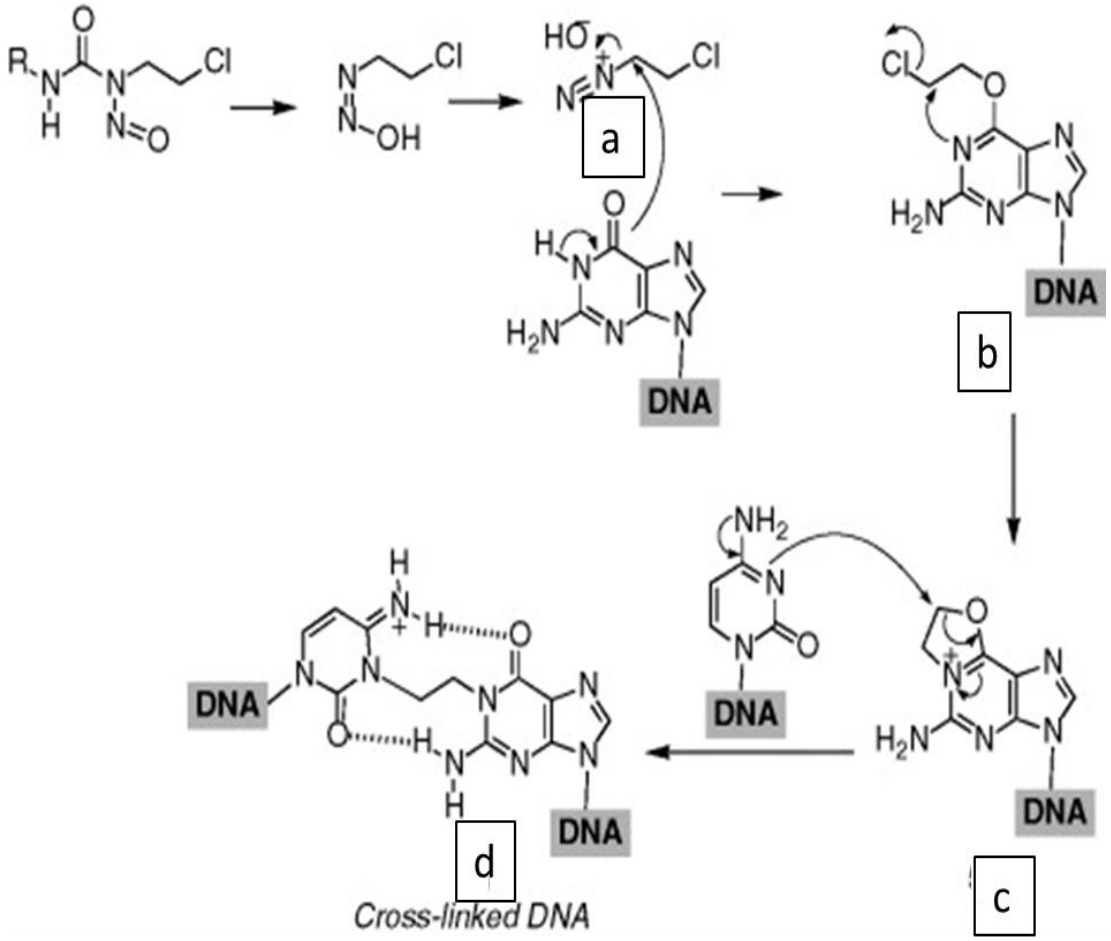

Figure 1.7: Mechanism of action of carmustine. Carmustine is able to cross link the DNA through the chloroethyl chain, which reacts with the electrohilic diazonium specie of the DNA at O-6 (a), giving a monoalkylated product (b), the monoalkylated product reacts with cytosine in the complementary DNA strand at N-3 through the assistance of guanines N-1 atom as an intermediate (c) to form the crosslinked DNA (d). Figure taken from Avendano and Menendez (2015).

1.4.1.2 Chlorambucil

Chlorambucil is a nitrogen mustard derivative and a cell cycle non-specific agent. It is a bifunctional alkylating agent acting through the formation of high reactive ethylenimonium radical which forms cross-linkage between two DNA strands to interfere with RNA, DNA and protein synthesis (McEvoy, 2006). Chlorambucil forms covalent interstrand and intrastrand adducts within the DNA double helix structure, particularly with the N7 of guanine to inhibit cell proliferation. While the intrastrand crosslinks are repaired by the nucleotide excision repair (NER) enzymes, interstrand crosslinks are toxic, forming double strand breaks thus inhibiting DNA replication. Chlorambucil is known to engage in off-target alkylation due to poor DNA recognition properties, but does affect its mechanism of action (Antonio *et al.*, 2014).

1.4.2 Mechanism of action of antimetabolites

These are analogues of the DNA building blocks and act to mimic the purines and pyrimidines. They become incorporated into the DNA molecule and inhibit the subsequent synthesis of DNA (Brana *et al*., 2001; Grem and Keith, 2005). They inhibit specific enzymes that utilize folic acid or the synthetic enzymes of purine and pyrimidine precursors, hence interfering with DNA synthesis at multiple levels (Payne and miles, 2008). Examples of antimetabolites include: cytosine arabinoside (Ara-C) which inhibits DNA polymerase; hydroxyurea which inhibits ribonucleotide reductase; 5-fluorouracil (5-FU) which inhibits thymidine monophosphate (TMP) synthesis by blocking the activity of thymidylate synthase and methotrexate which inhibits dihydrofolate reductase, blocking TMP and purine synthesis (Bhattacharjee, 2016).

1.4.3 Mechanism of action of anti-tumour antibiotics

The anti-tumour antibiotics are produced from natural products of microbial metabolism such as the *Streptomyces* species and are commonly referred to as anthracyclines. Generally, the anti-tumour antibiotics have many mechanisms which includes: intercalation of the DNA, free radical formation, direct membrane effects, inhibition of topoisomerase II and interference with DNA unwinding or strand separation (Szucs and Jones, 2016). They intercalate between adjacent nucleotides to form a tight DNA-drug interaction. Antibiotics inhibit enzymes involved in biosynthesis and interfere with DNA replication and transcription (Payne and Miles, 2008). They interfere with RNA and DNA synthesis, acting on multiple phases of the cell cycle, and thus are cell cycle non-specific.

Furthermore, they are capable of binding to the proteasome to inhibit cell growth (Bhattacharya and Mukherjee, 2015). They are used in the treatment of many human cancers such as leukaemia, neuroblastoma, lymphoma and sarcoma (Thirumaran *et al*., 2007). Some cause damage to DNA and prevent DNA repair (e.g. bleomycin), while others such as mitomycin C may act as a crosslinker (Bhattacharya and Mukherjee, 2015).

1.4.4 Mechanism of action of topoisomerase inhibitors

Topoisomerase inhibitors interfere with the topoisomerase enzymes responsible for regulating the DNA topology and are important for maintaining the integrity of genetic material during DNA transcription and replication process (Ziraldo *et al.,* 2019). There are two main types of topoisomerase enzymes: topoisomerase (Topo) I and topoisomerase II. Topoisomerase I cleaves and cuts one strand of the DNA helix to facilitate rotation and prevent supercoiling either side of the replication bubble, while Topoisomerase II cleaves both strands of the DNA complex in order to expedite the separation of the template and daughter strands post replication (Figure 1.8).

Topo II plays a vital role in transcription, replication and chromosomal segregation and its biological activity ensures the maintenance of genomic integrity (Nitiss, 2009). The topoisomerase inhibitors act to stabilize the DNA-topoisomerase cleavable complexes, hence inhibiting the religation step of the catalytic reaction (Lester, 2005; Yves *et al*., 2010) and can result in significant fragmentation of the DNA. As with the alkylating agents, two main topoisomerase inhibitors – etoposide and mitoxantrone (Figure 1.9) were also focused on in the latter part of this study (see chapter 5).

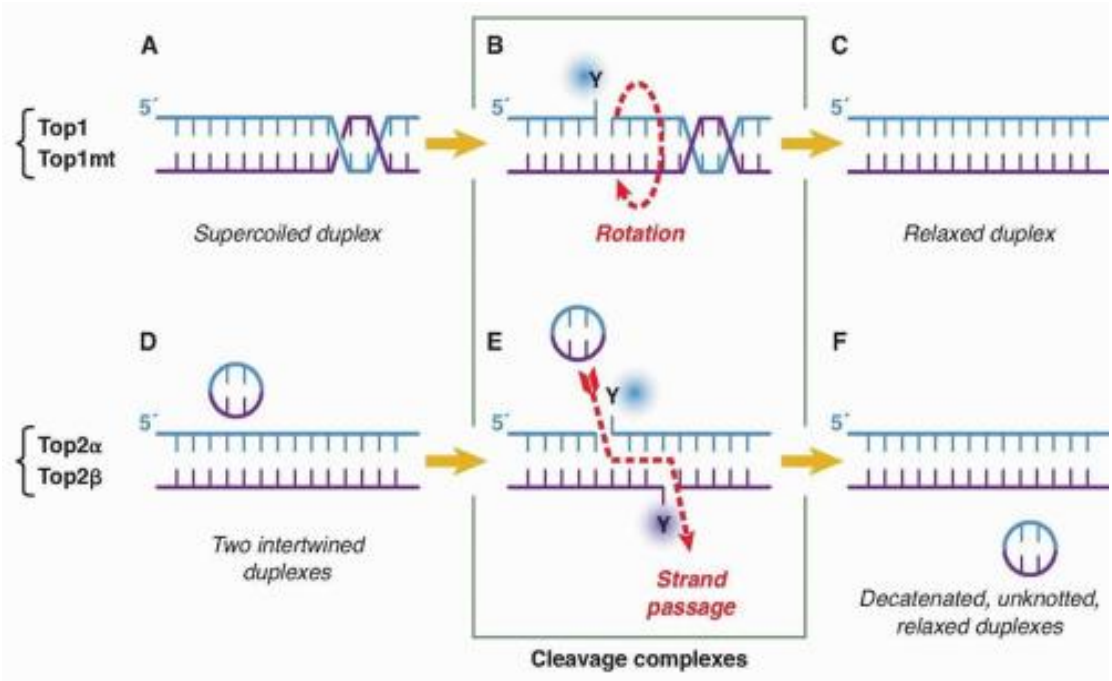

Figure 1.8: Mechanism of action of topoisomerase inhibitors. Topoisomerase I and topoisomerase II enzyme structure (a-c), and the activity of both enzymes (d-f). Topo I cleaves and cuts one strand of DNA segment to form covalent bond between the enzymes at 3' end, while Topo II act as homodimers, cleaving both strands and forming covalent bond at 5' end, to produce double strand breaks and inhibit recombination process. Topo 1 and II both engage in DNA relaxation. Image with creative common license and from Khanh *et al.*, *(*2010).

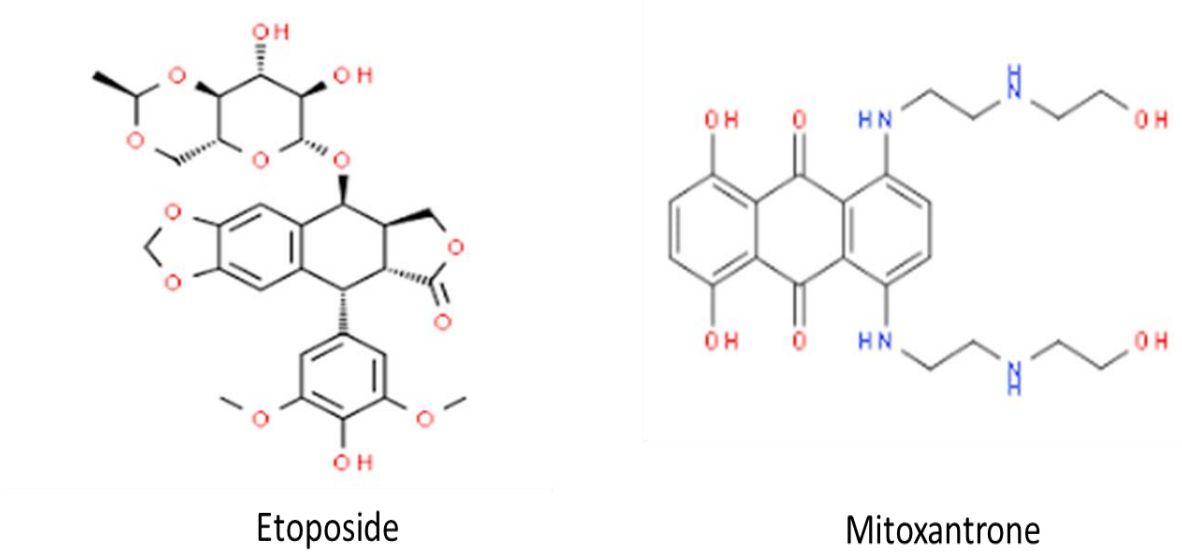

Figure 1.9: Chemical structures of etoposide and mitoxantrone.

Etoposide has a chemical formula of $C_{29}H_{32}O_{13}$ and molar mass of 588.557 g/mol and mitoxantrone has a molar mass of 444.481 g/mol, with a chemical formula of $C_{22}H_{28}N_4O_6$. O = oxygen, N = Nitrogen, H = Hydrogen. Images assessed from National Centre for Biotechnology Information, PubChem Database (Assessed Mar. 3, 2020).

1.4.4.1 Etoposide

Etoposide is an anti-tumour agent and an epipodophyllotoxin that is semi-synthetically obtained from podophyllotoxin (a toxin derived from American Mayapple) and is known as a topoisomerase II inhibitor. Etoposide forms a complex using tyrosine in the active site of topoisomerase II and the DNA phosphate backbone, thereby inhibiting DNA re-ligation. The complex induces a macromolecular effect by preventing repair through inducing single and double strand breaks into the DNA or the generation of free radicals (Kwok, Vincent and Gibson, 2017). The accumulated breaks prevents transition into the mitotic phase of cell cycle, and hence is cell cycle dependent and specific for the S and G2 phases. Two known isoforms exists: the alpha (α) and beta (β) isoforms and while inhibition of the α-isoform is associated with the anti-tumour effect, the β-isoform is associated with a carcinogenic effect (Azarova *et al*., 2007; Zhou *et al*., 2001). Etoposide is also known to inhibit microtubular assembly by binding tubulin (Newton, 2006).

1.4.4.2 Mitoxantrone

Mitoxantrone is a synthetic anthracenedione that inhibits topoisomerase II to interfere with the DNA synthesis. It intercalates DNA forming a stabilized DNA topoisomerase II cleavable complex to exert its cytotoxic activity, forming crosslinks and strand breaks (Parker *et al.*, 2004). Mitoxantrone decreases the secretion of proinflammatory cytokines e.g. interleukin 2 and tumour necrosis factor, producing a generalized immunosuppression (Vollmer *et al.*, 2009). Mitoxantrone is rapidly taken up by tissues, has a terminal half-life of 8.9 to 9 days and persists in the body for about 272 days (Fox, 2004). There is evidence that mitoxantrone may also exert its mechanism of action by the formation of drug-DNA adducts (Skladanowski and Konopa, 2000; Panousis *et al.*, 1995). Further studies suggest the oxidation of mitoxantrone into an active metabolite (naphthoquinoxaline) that covalently binds RNA, thereby contributing to its cytotoxic effect (Panousis *et al.*, 1995; Parker *et al.*, 2004). It is used in the treatment of prostate cancer, multiple sclerosis, melanoma, lymphoma and leukaemia (Dipaola *et al.*, 2001; Perez-Gracia *et al.*, 2001).

1.4.5 Mechanism of action of plant alkaloids

The plant alkaloids are largely microtubule inhibitors which prevent the formation of spindle fibres and disrupt the cytoskeleton of the cell, thereby inhibiting chromosome segregation and

consequently cell division (Nobili *et al*., 2009). Mitotic inhibitors act by binding to tubulin proteins, block the spindles and arrest mitosis, thus they are M-phase specific. Subgroups include: the vinca alkaloids, the taxanes and epipodophyllotoxins.

Taxanes are semi-synthetically prepared from yew needles upon harvest from the bark of the yew tree. They bind to the beta subunit of tubulin facilitating stabilization of the polymer complex. Vinca alkaloids are destabilizers, preventing the assembly of the mitotic spindles. Epipodophyllotoxins are natural substances occurring from the American mayapple plant.

1.5 Haematopoietic stem cell transplantation

Stem cells are primitive somatic cells with the capacity to self-renew (give rise to one/two daughter stem cells) and differentiate (develop into mature specialized cells). Conventional chemotherapy enables management of a patient's condition for longer term. The depletion of the leukaemia using chemotherapy can also lead to depletion of all of the bone marrow as chemotherapy is non-specific and so replacement with donor HSC can reconstitute the blood and help cure the leukaemia. Haematopoietic stem cell transplantation (HSCT) in most cases is considered the only potentially curative option for some haematological malignancies. Some consider HSCT a last resort treatment, but it is rather part of a component therapy involving use of high dose chemotherapy prior to HSCT, and is performed in an attempt to repopulate the BM. The two distinct types are autologous transplantation (self-donation) and allogeneic transplantation (non-self-donation). Autologous transplantation is used to treat lymphoma and multiple myeloma, but is less commonly utilised in leukaemia, because clinicians are generally concerned about a relapse possibly due to reinfusion of occult tumour cells. In allogeneic transplant, the goal is the creation of a strong donor-derived immune system that can not only reconstitute the blood system, but also lodge an immunologic attack upon recognition of mismatched leukaemic cells, thereby creating graft versus malignancy / graft versus leukaemia (GVL) effect.

HSCT occurs in three phases and includes: a conditioning phase, stem cell infusion and graft versus host disease prophylaxis (for allogeneic transplant). The conditioning regimen can be one or a combination of chemotherapy, radiotherapy or immunotherapy. Generally, both types of transplantation require high intensive conditioning (chemotherapy) which clears the bone marrow of both the leukaemic clones as well as the entire blood system – this is considered 'myeloablative'. However, allogeneic transplantation can also use reduced intensity conditioning in older and/or sicker patients who cannot tolerate myeloablative conditioning.

This procedure is considered as non-myeloablative, and the aim here is to create a 'mixed chimerism' between the host and donor lymphocytes; the consequent immune response resulting from the genetic mismatches is tipped in favour of the donor cells, by chasing the HSCT with donor leukocyte infusions and this promotes the GVL effect to kill the leukaemia. Such non-myeloablative or 'mini' transplants can be applied for diseases in remission or less severe cases, but has largely revolutionised the treatment of the elderly patients which make up the major proportion of leukaemic patients. This dual tumour kill effect in allogeneic SCT accounts for its higher risk of complications, most notably graft versus host (GVH) effect which can be life-threatening. However, the incidence of GVH is associated with producing GVL, and this provides the advantage of a low relapse rate unlike for autologous transplantation, and for these reasons the use of tissue type matched, but non-identical siblings is generally the preferred choice for HSCT treatment of leukaemia (Antin and Raley, 2009). Stem cells can be sourced from peripheral blood (mobilised from the BM), umbilical cord or BM or tissue type matched family member, or an unrelated fully matched donor in allogeneic transplant, while the peripheral blood or BM stem cells of the host is utilised in autologous transplant. Allogeneic HSCT can be used as an initial treatment depending on the treatment strategy and cancer type/stage. It is sometimes preferred over chemotherapy in patients with high risk of resistance (eg in intermediate to high risk AML in patients aged 40 and over) or relapse (eg a post-remission treatment in lymphoma patients) or recurrent/refractory disease (Yang *et al.*, 2018)

1.6 Side effects and complications of chemotherapy

Chemotherapy was originally thought to 'target' cancers, but they also target other dividing normal cells, thereby resulting in many side effects (Aslam *et al.*, 2014). A retrospective study conducted in emergency departments in the US found that out of 219,918 visits to the emergency department, 18% and 82% showed radiotherapy and chemotherapy side effects respectively (Jairam *et al.*, 2018). Some of these effects are detailed below (Table 1.3) and can be recognised as either short or longer-term complications. Subsequently, there are other major late complications that follow the use of chemotherapy and they include therapy related leukaemia and donor cell leukaemia. This study focused on the latter as a serious but rare pathology and shall be discussed in detail in the following sections.

Table 1.3: Chemotherapy side effects.

A summary of the varying early and late events that occur following chemotherapy. These events are classified as immediate, delayed and late depending on the site of activity for these agents and their classical presentation of effects.

Immediate	Delayed	Late
Allergic reactions	Hemorrhagic cystitis eg cyclophosphamide	Microdontia
Burning sensation	Infections	Crown hypoplasia eg missing enamel
Urine discoloration eg mitoxantrone - blue	Nutritional eg loss of apetite	Disturbed root formation eg in growing individuals
Acute emesis	Cytotoxic	Tooth agenesis
Fever & malaise eg Ara-C	Fatigue	Sexual dysfunction
	Diarrhea	Amenorrhea
	Metallic taste	Pulmonary fibrosis eg bleomycin, MTX
	Myelosupression eg daunorubicin	Cardiotoxicity eg anthracyclines
	Alopecia eg taxanes, doxorubicin	Myelodysplastic syndrome eg alkylating agents
	Nail discoloration	Leukaemia eg topo II inhibitors
	Fluid retention	Sterility
	Peripheral neuropathy eg taxanes, alkaloids, cisplatin	Liver toxicity eg MTX
	Mucositis (mouth sores)	

Key: MTX= mitoxantrone

1.7 Donor cell leukaemia

Amongst the major complications of allogeneic stem cell transplantation, like graft versus host disease and infections, disease relapse ranked highest in the cause of post-transplant mortality. Such relapse was originally thought a re-enactment of primary disease due to therapy evasion, particularly where the relapse was of the same subtype as the original. However, Fialkow *et al*., (1971) described a 16 female leukaemic patient who relapsed following HSCT donation from her matched brother, and the leukaemic clones were observed to be Y chromosome positive. This was the first description of the rare *de novo* haematological malignancy called donor cell leukaemia (DCL). DCL describes a form of leukaemia which is genetically proven to be of donor cell origin that develops in a recipient following transplantation of "healthy" donor cells. DCL has since been noted as a rare disorder but has gained greater insight in the last decade. The exact incidence of DCL is unknown but is reported to be between 0.12% and 0.13% for all relapsed leukaemia (Suarez-Gonzalez *et al.*, 2018). These reported cases can be

identified based on cytogenetic analysis in sex-mismatched cases (Hertenstein *et al*., 2005; Torra and Loeb, 2011). DCL incidence is arguably underdetected (e.g. in sex-matched cases) and underreported due to assumptions of disease relapse, as well as the uncertainty of neoplastic origin such as cases without clonal cytogenetic abnormality and overt leukaemia (McCann and Wright, 2003; Wang *et al*., 2011). However, the recognition of sex-mismatched transplant cases demonstrating donor cell origin made investigators aware of DCL and thus, formed the basis for the genetic determination of cell origin following SCT complication (Cooley *et al.*, 2000; Shiozaki *et al*., 2014; Torra and Loeb, 2011 and Ruiz-Arguelles *et al*., 2007). Nevertheless, care must be taken in identification of the malignant clone, utilising both cytogenetics and microsatellite analyses. The importance of this was demonstrated by Spinelli and co-workers (2000) who showed that a male patient with suggested DCL (XX clone) from his HLA-identical sister, subsequently was shown by microsatellite analyses to be of patient origin, and the explanation proposed to be a loss of Y chromosome, with duplication of the X chromosome (Spenelli *et al.*, 2000).

1.7.1 Aetiology and proposed mechanism of DCL

An understanding of the malignant transformation events of the donor stem cells provides an insight into deciphering the mechanisms involved in leukaemogenesis. However, studies into the aetiology of DCL have proved difficult due to its low incidence and difficulty in diagnosis. Most DCL cases present as an alteration of the homeostatic balance between the complex interactions of the growth factors, cells and cytokines within the BM microenvironment. This complex interaction and disturbance of the BM microenvironment is synonymous to the 'seed and soil' hypothesis of Paget in 1889, which according to Flynn and Kaufmann (2007) does serve as a model for understanding the possible events of leukaemic cell transformation in DCL. This opinion is further explained by the fact that the conditioning regimen markedly changes the BM microenvironment (the soil), thereby obstructing the usual homeostatic balance and cross talk between the BM cells, cytokines and the transplanted donor HSCs (the seed). However, this proposal is highly speculative and is further hampered by the scarce number of published works on DCL, thence resulting in no unifying model or specific aetiology for the pathology (Suarez-Gonzalez *et al.*, 2018).

Most reported cases to date have been unable to confirm one mechanism as the cause of DCL, rather its pathology appears to be a multifactorial (Ataergin *et al*., 2006; Gustafsson *et al*, 2012; Wiseman, 2011, Bobadilla-Morales *et al.*, 2015). Some of the hypothesized aetiologies (Figure

1.7) include the possibility of a transfer of malignant cells following solid organ or stem cell transplant, or the presence of inherited or acquired predisposing factors present in the donor. For example, there are evidence of accidental transmission of AML, CML and T-cell lymphoma from donor through peripheral and allogeneic stem cell transplantation (Baron *et al.*, 2003; Berg *et al.*, 2001).

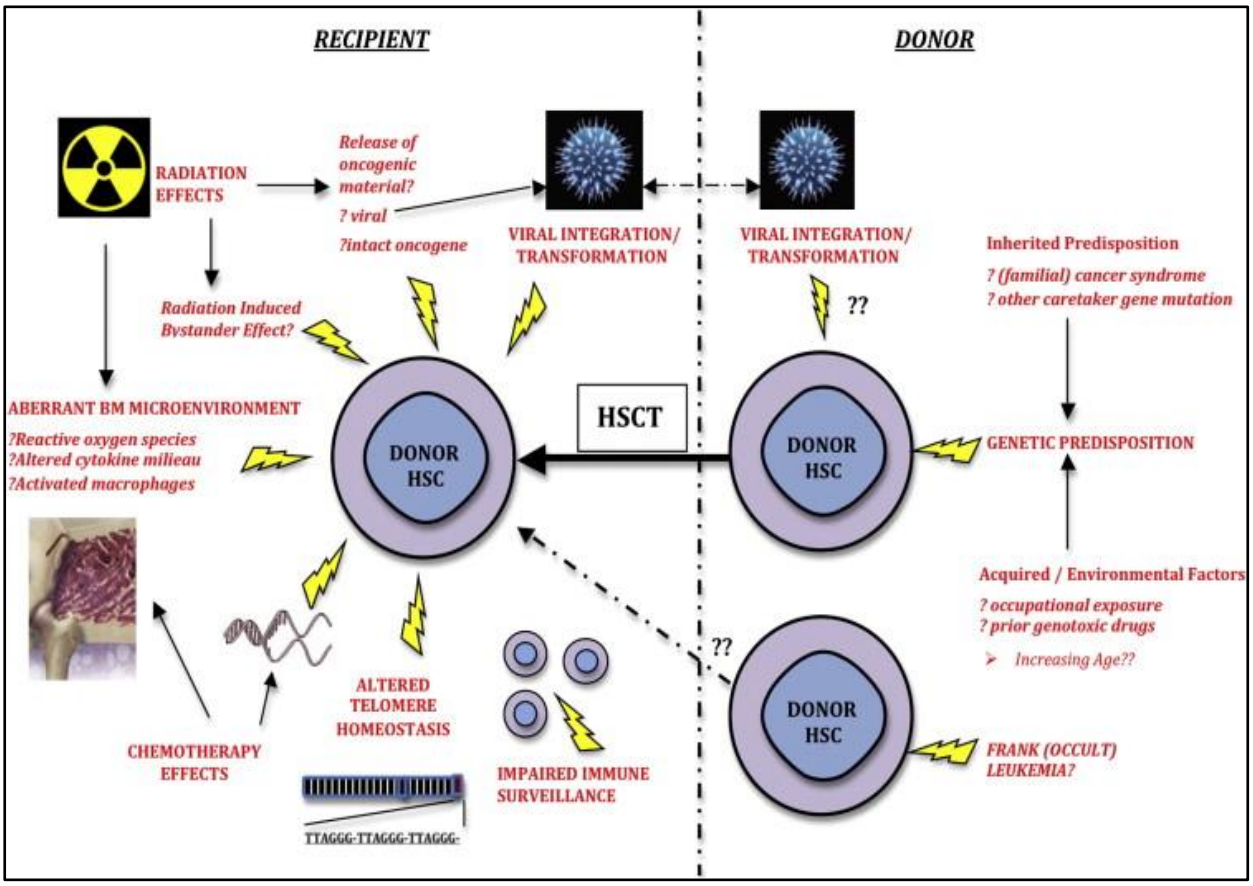

Figure 1.10: The proposed mechanisms involved in donor cell leukaemia. A multifactorial pathway has been predicted as possible aetiologies involved in DCL. These mechanisms can be either donor related or a recipient stimulated effects like some residual chemotherapy, homeostatic alteration, pre-leukaemic or occult factors of the donor origin. This figure is credited to Wiseman (2011) under the creative common license copyright.

These proposed mechanisms are best classified as the extrinsic and intrinsic factors that drive the fate of transplanted HSCs (Torra and Loeb, 2011) and they include:

a) Intrinsic donor factor:

Acquisition of an additional mutagenic ‘‘hit’’ of an already premalignant donor clone in the depleted recipient marrow (Hertenstein *et al*., 2005). This involves the oncogenic transformation of the potential ‘healthy’ donor cells following SCT.

b) Extrinsic host factors:

i) Chemotherapy-induced or inherent stromal abnormality; this is proposed for myeloid but not lymphoid DCL and could occur due to residual effects of cytotoxic agents (Wiseman, 2011; Ruiz-Arguelles *et al., 2*007).

ii) Sustained antigenic stimulation of donor cells in lymphoid DCL, when slight histocompatibility differences exist within the host (Witherspoon *et al*., 1985; Wang *et al*., 2011).

iii) Increased replicative stress, errors and mutation in transplanted donor cells in an attempt to repopulate the BM environment (Flynn and Kaufman, 2007; Gustafsson *et al*., 2012).

iv) Aberrant homeostasis (over/under expression or absence of receptors, ligands, transcription factors involved in cell signalling) could induce or enhance leukaemic transformation (Ruiz-Arguelles *et al., 2*007).

v) Impaired immune surveillance e.g. posttransplantation malignancy of Epstein-Barr virus-mediated post-transplant lymphoproliferative disorder (PTLD) and oncogenic transformation of material via communicable agents (Torra and Loeb, 2011; Nagamura-Inoue *et al*., 2007).

vi)Transfer of oncogenic material by fusion of residual host cells to donor cells (Bobadilla-Morales *et al.*, 2015).

vii) Radiation and/or chemotherapy-induced bystander effect (Wiseman, 2011).

1.7.2 Diagnosis, prognosis and treatment of DCL

DCL is identified upon an accurate detection of transformed leukaemic cells of the donor origin. Reliable molecular methods such as fluorescent *in situ* hybridization (FISH), YCS-PCR for detecting Y-specific chromosome sequence (YCS), mini-satellite or variable number tandem repeats (VNTRs), microsatellites or short tandem repeats (STRs), single nucleotide polymorphisms (SNPs), short inversion or deletion polymorphisms (SIDPs) and restriction fragment length polymorphisms (RFLPs) are used to investigate DCL (Thiede, 2004; Ruiz-Arguelles *et al*., 2007). The following relevant features are vital to the classification of DCL. They include: a proper documentation or identification of donor origin; recipient's sex and age; donor's age and sex (matched or mismatched, and related or unrelated), donor health status; primary haematological malignancy versus type of DCL malignancy; method used for chimerism analysis; type of conditioning regimen; stem cell source (cord blood, peripheral blood or BM) (Wiseman, 2011).

Based on the above descriptors, a recent systematic review (Suarez-Gonzalez *et al.*, 2018) for the reported DCL cases reveals as follows: median time to occurrence of DCL is 24 months (2 to 312 months) with some variation depending on the source of stem cells. Median recipient age at primary disease was 32 years and primary malignancies were AML (25%), ALL (23%), chronic myelogenous leukaemia-chronic phase (CML-CP, 16%), non-malignant haematological disorders (NMHD, 9%) and myelodysplastic syndrome (MDS, 8%). Children (less than 26 years) showed a median age of 6 years, representing 23% of reported cases. So far, there is no reported sexual preponderance between donor and recipient. Most frequent donor type include matched related (59%), cord blood (21%), matched unrelated (9%), mismatched related (6.5%), mismatched unrelated (3%) and haploidentical (1.5%). DCL cases were majorly gender mismatched (60%) with an increased rate of BM stem cell source (55%) and for people who received total body irradiation (67%). DCL types were mainly AML (50%), ALL (23%) and MDS (20%), which represent 93% of the reported cases.

In addition, most DCL cases show an abnormal karyotype (72%) which include balanced chromosomal translocations, deletions, chromosomal gains/losses, with frequent cytogenetic alterations including whole or partial loss of chromosome 5/7 and rearrangement of the 11q23 locus containing the *MLL* gene. As at the time of the cited report 85% of the donors were healthy, 12% developed haematological malignancy and 3% developed non-haematological malignancy.

DCL as a rare disorder has a very poor prognosis, hence the need for further studies. Treatment for DCL involves induction chemotherapy and stem cell transplant. Suarez-Gonzalez *et al.*, (2018) revealed that about 56% of identified cases had died at the time of the report, while 44% were alive. Mortalities were majorly due to severe cell depletion following chemotherapy or sepsis and other complications of SCT, and the time from DCL to death was about 10 months.

Largely, the heterogeneity of the DCL report prevents a recognizable risk factor, however it should be noted that whilst 574 non-duplicate papers were retrieved from database, meaning the report was based on only 137 documented cases. Yet, it is interesting to witness an increase in DCL reports owing to the impact of accurate diagnostic tools. There has also been a marked distinction between relapse and DCL, as DCL appears to be more of a late complication than the early events of most relapses, and DCL has shown ability to develop *de novo* neoplasms following either haematopoietic and/or solid organ transplantation. Relatively speaking, the better our understanding of DCL aetiology, the more efficient shall be the donor recruitment process, selection and patient outcome for SCT. Therefore, to investigate a likely aetiology of DCL, this study aimed to explore the concept of chemotherapy-induced bystander effect (CIBE).

1.8 Bystander effect

Ionizing radiations exert their effect on rapidly dividing cells and as such do not affect only the directly treated cells but also the unexposed/untargeted neighbouring compartments. When these non-treated cells show biological responses that mimic the direct effect, such a response is referred to as a 'bystander effect' (Marin *et al.*, 2014). The observed responses of bystander effect generally include: DNA strand breaks, gene mutations, altered protein and enzyme levels, micronucleation, increased apoptotic frequency, oncogenic transformation and reduced clonogenic efficiency (Hall, 2003). Bystander effect has been broadly studied in radiation rather than chemotherapy, with reports involving tissue culture experiments and a few *in vivo* studies. Bystander effect is a phenomenon usually associated with genomic instability (Wright, 2010), adaptive responses (Chaudhry, 2006) and abscopal effects (Stamell *et al*., 2013) (Figure 1.8). These effects may be as a result of factors released by the directly exposed cells into the surrounding medium and as such pose a vital clinical implication, both for improved cancer therapy and conversely as a health risk. This requires an in-depth understanding of the phenomenon, especially the aspect of its biological significance and associated non-targeted effects.

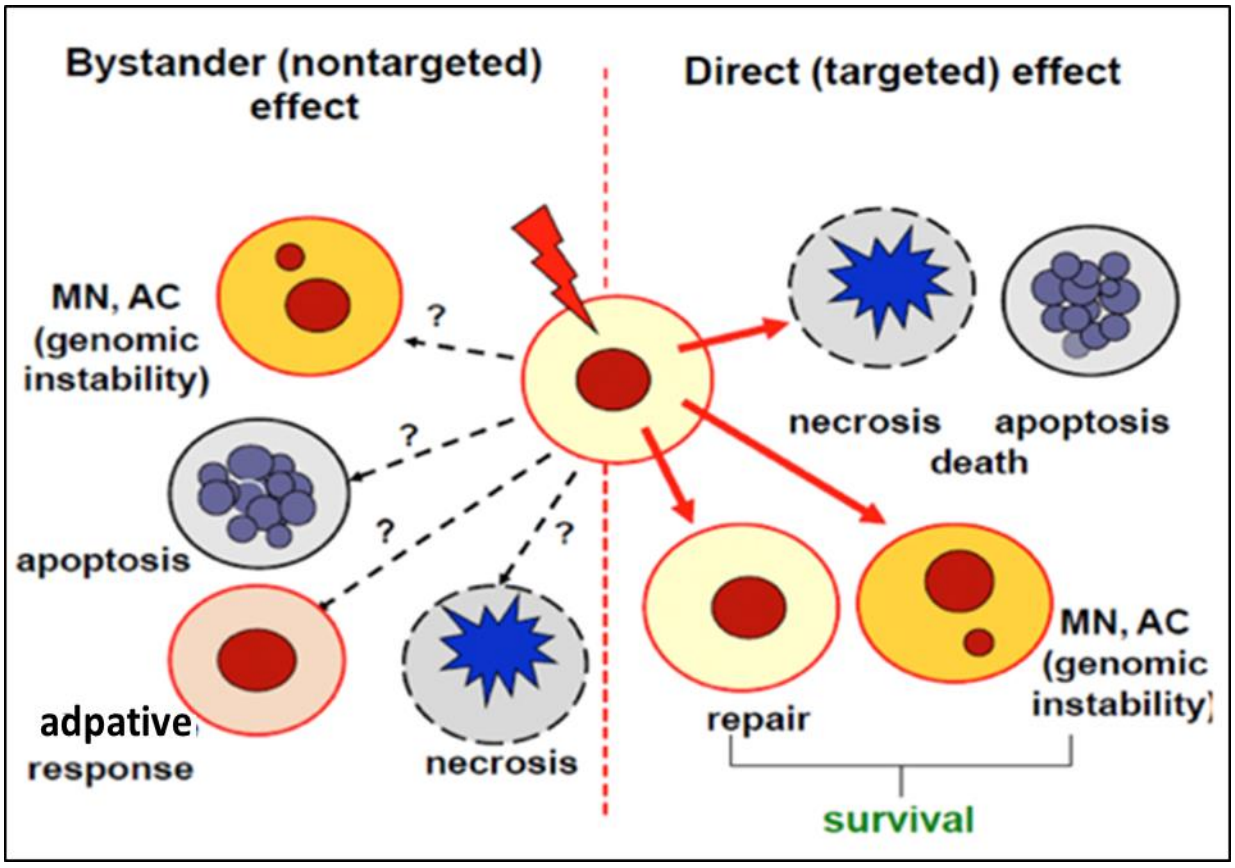

Figure 1.11: Cellular effects in targeted and non-targeted cells. Direct exposure of cells to radiation or chemicals result in secretion of molecular signals that induce changes in neighbouring cells and other distant cells that are away from the treated cells. The effects in directly targeted cells include micronuclei induction, necrosis, apoptosis and these may be the same in bystander cells. Adopted from Widel (2012).

1.8.1 Radiotherapy induced bystander effect

Radiation-induced bystander effect (RIBE), was first reported by Parson in 1954 through his observation that clastogenic factors from blood of irradiated patients caused damage to chromosomal structures (Seymour and Mothersill, 2004). RIBE is a phenomenon whereby damage from exposed cells is observed in neighbouring cells that were not exposed to ionising radiation; it is best described as post-exposure biological response to ionising radiation (Pinto *et al*., 2006). Biological effects such as DNA damage and chromosomal instability are observed in cells that were indirectly exposed to ionising radiation and due to failed repair attempts, would result in mutation and/or apoptosis. This ‘‘off target’’ indirect effect in unexposed cells was termed ‘radiation-induced bystander effect’ (Mothersill and Seymour, 2001; Marin *et al.,* 2014) and has been well characterised for *in vitro* and *in vivo* models of radiotherapy but not

for chemotherapy (Azzam and Little, 2004; Rzeszowska-Wolny *et al*., 2009; Prise and O'Sullivan, 2009; Chinnadurai *et al*., 2011). A highly recognised bystander mechanism for radiation involves oxidative stress from superoxide and nitric oxide radicals (McCann, 2003; Sawal *et al.*, 2017) although other mechanisms do exist.

RIBE has been observed in many different cell types despite the type or amount of radiation exposure, but it remains unclear the exact signal involved in mediating this effect. RIBE studies have demonstrated these effects *in vitro* and *in vivo* (Nagasawa and Little, 1999; Watson *et al*., 2000; Lorimore *et al.*, 2001; Azzam *et al.*, 2001). Potential mechanisms for RIBE include gap junction involvement, secreted factors in growth medium, cytokine production and secretion of apoptosis inducing factor (AIF) by mitochondria in response to oxidative stress (Snyder, 2004).

1.8.2 Chemotherapy-induced bystander effect

The concept of chemotherapy-induced bystander effect (CIBE) has struck the attention of researchers in recent times. Rugo and colleagues (2005) using wild type embryonic stem cells and fluorescent yellow direct repeat cells reported a hyper-recombination event in bystander cells following exposure to mitomycin C, and the ability of these bystander cells to further induce a sequence rearrangement in other neighbouring cells. CIBE was also observed for the chloroethylnitrosourea (CENU) agents, including carmustine, fotemustine, cystemustine and lomustine (Demidem *et al*., 2006; Merle *et al*., 2008). Demidem and colleagues (2006) demonstrated bystander capacity of these aforementioned agents *in vivo* and *in vitro* using a serum transfer experiment. In their study, *in vivo* cells showed cessation in tumour proliferation, metabolite alteration, reduced vessel formation and glutathione decrease. Cultured cells challenged with conditioned medium showed growth inhibition, metabolite alteration, cytoskeleton disorders with no reactive oxygen species (ROS) increase. Merle and his colleagues (2008) also used the same double tumour model as Demidem to show CENU agent's ability to induce a bystander response.

Alexandre *et al*., (2007) reported the ability of paclitaxel and vincristine but not doxorubicin and 5-fluorouracil to induce a bystander effect. They used two separate co-culture systems involving fluorescent and radioactive labelling to detect increased ROS in a treated breast cancer cell line (MCF7), human lung cancer cell lines (H1299) and human leukaemia cell line (HL60) with and without chemotherapeutic agent. Furthermore, the conditioned medium from phleomycin and mitomycin C treated human lymphoblast cell lines (GM15036 and 15510) was

shown to induce micronucleated cells in a cytochalasin B-blocked micronucleus assay (Asur *et al*., 2009).

Bleomycin and neocarzinostatin (Chinnadurai *et al*., 2011) were exposed to WI-38, hBMSCs, NCl-H23, A-549 cell lines and peripheral blood lymphocyte (PBL) cells in a co-culture system, and all cell lines showed bystander response using micronuclei induction as an endpoint after ruling out an effect from residual drug by HPLC. The same study demonstrated the involvement of ROS in a bleomycin-induced bystander effect. Subsequently, Jin *et al.,* (2011) were able to show the ability of actinomycin D to cause bystander effect, mediated through soluble factors in Chinese hamster V79 cells using chromosome aberration, ultrastructure and apoptosis rate as endpoints in the bystander cells.

Investigations at the cellular level for both RIBE and CIBE have demonstrated varying endpoints such as increased micronuclei, genomic instability, malignant cell line transformation, with abundant evidence for persisting chromosomal breakages and transferrable clastogenic factors (Mothersill *et al.,* 2017). How these damages occur is unclear, but is certainly not dependent on direct physical cell to cell contact; rather implicated factors include gap junctions, activity of ROS, various cytokines and possibly microRNAs (Wiseman, 2011), the latter two of which could be transferred via the medium directly or encapsulated within extracellular vesicles. Following the discovery of only a few studies on CIBE, with limited knowledge of mechanism of action, this study explored a panel of chemotherapeutic agents utilised mostly in haematology protocols to investigate this concept.

1.9 Oxidative stress and cellular response to chemotherapy-induced ROS

Oxidative stress reflects an imbalance between the systemic generation of reactive oxygen species (ROS) and the cellular ability to counteract and detoxify the reactive intermediates. Such imbalance has been implicated in neurodegeneration, carcinogenesis, aging and atherosclerosis (Choi and Tuveson, 2017). Most antineoplastic agents exert their effect through ROS mediated injuries and by oxidative stress induction in cancer cells. Oxidative stress is stress generated internally by the peroxisomes and enzymes (e.g. Nox family, xanthine oxidase) of the mitochondria, and external sources include chemical compounds, ultraviolet (UV) radiation and exercise. Oxidative stress alters and damages intracellular components such as lipids, DNA, RNA and proteins (Veskoukis *et al.,* 2012). ROS are generated through; activation of some oncogenes such as *Kras*, *Cmyc*, *BRCA1*, and alterations in signals associated

with tumorigenic transformation e.g. altered integrin and increased hypoxia in tumours (Weinberg *et al*., 2010; Azimi *et al.*, 2017 and Chiarugi *et al*., 2003).

Reactive species include ROS, reactive nitrogen species, reactive chloride species and reactive sulphur species, however, ROS are more abundantly generated. ROS collectively defines the partially reduced, unstable oxygen derived by-product of metabolism that plays various roles in biological processes. Low levels of ROS are tolerable by the cells and are vital to immune defence mechanisms, signal transduction, gene expression, enzyme activation, as well as acting as secondary messengers (Redza-Dutordoir and Averil-Bates, 2016). Cancer cells also use high ROS levels to maintain their high proliferative rate (Sosa *et al.,* 2013). Some examples of ROS include: singlet oxygen ($^1O_2$), ozone (O_3), hydrogen peroxide (H_2O_2), hydroxyl radical ($^{\cdot}OH$), superoxide anion (O_2^-), hypochlorous acid (HOCl), with the $^{\cdot}OH$ radical the most important as it is promutagenic and relatively easily formed through interaction with nucleobases of the DNA strand that leads to the formation of the biomarker 8-hydroxydeoxyguanosine (8-OHdG; Valavanidis *et al.*, 2009).

Most chemotherapeutic agents increase ROS levels intracellularly, alter the redox-homeostasis in cancer cells and exert their anticancer effect through oxidative stress induction, thus acting as a tumour suppressant (Roness *et al.,* 2014). Other evidence suggests that prolonged use of chemotherapeutics can reduce ROS in cancer cells and may potentially be the mechanism for drug resistance in chemotherapy (Yang *et al.,* 2018). Increased ROS generation during chemotherapy is due to mitochondrial ROS generation and the inhibition of antioxidant systems. Chemotherapy target the mitochondria affecting its membrane potential to cause inhibition of complex I and II, electron leakage and subsequent elevation in ROS. The antioxidant systems include some interacting enzymes such as superoxide dismutase, catalase and peroxidases and some low molecular mass antioxidants like reduced glutathione (GSH) and ascorbic acid (Apel and Hirt, 2004). The chemotherapeutic agents exhibit varying modes of production for ROS in a cell (Figure 1.10).

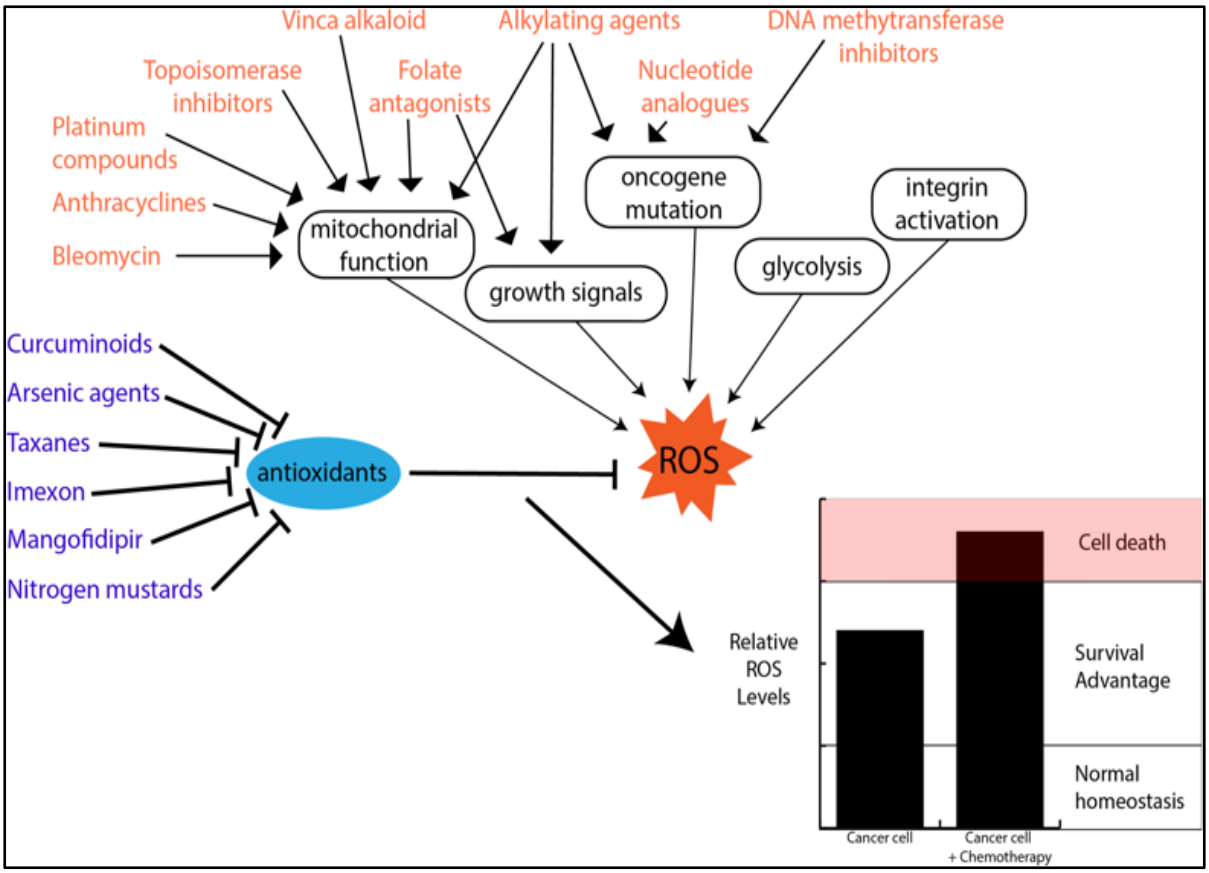

Figure 1.12: Chemotherapeutic agent's mechanism of action through ROS regulation. Chemotherapy elevate ROS levels. While some chemotherapeutic agents (orange) generate high levels of ROS in the cells, others (blue) regulate ROS by inhibition of cellular levels antioxidants. Treatment with chemotherapy increases the ROS levels and promotes cell death in tumours. Figure was adopted under the creative common license of an open access article credited to Yang *et al*., (2018).

The exact role of ROS in reference to chemotherapy has been a subject of debate. Whether ROS solely induces death in cancer cells or exerts other functions as chemotherapy side effect is being explored. For instance, some chemotherapeutic agents have been suggested to involve both ROS dependent and independent pathways and prolonged exposure to these chemotherapy-induced ROS is hypothesized to induce drug resistance (Sallymr *et al.*, 2008). ROS has also been implicated in RIBE as observed through experiments with ROS scavengers which reduced the bystander mediated genomic instability (Widal *et al.*, 2012; Harada *et al.*, 2008). Cellular response to chemotherapy-induced ROS is a reflection of the complex integration of the type of ROS involved, duration of the effect, cellular location and levels, hence depicting an involvement of a more diverse role than anticipated (Yang *et al*., 2018). Furthermore, cell response to oxidative stress is dependent on the cell type and level of stress

involved. These responses are in the form of increased level of free calcium, increased phosphorylation, an upregulation of repair systems, and activation of transcription factors that initiate adaptive response and in severe cases halt the cell cycle or initiate apoptosis (Halliwell, 2006).

For the roughly fifty trillion cells of the human body, there is an estimate of 10,000 oxidative hits per cell per day (Predi, 2014). Because DNA is the most significant biological target of oxidative stress, continual oxidative DNA damage is thought a major contributor to cancer and age related illnesses (Deavall *et al.*, 2012). Damaged DNA is repaired enzymatically under normal physiological conditions, but some unrepaired DNA lesions can persist or cause mutations that may lead to carcinogenesis. Free radical generation amongst others is a known mechanism for RIBE (Najafi *et al.*, 2014). Although ROS has been implicated in bleomycin CIBE (Jin *et al*., 2011), there is limited research (Chinnadurai *et al.*, 2012) on oxidative stress in CIBE for the vast majority of the chemotherapeutic agents utilised (Alexandre *et al.*, 2007), nor is there evidence of *in vitro* co-culture models in support of ROS involvement in CIBE, hence the need for this research.

1.10 Cell culture systems for genotoxicity evaluation

The development of plant cell and tissue culture dates back to the research publication of Haberlandt (1902) with a failed attempt at cell culture and the subsequent successful *in vitro* experiments of callus and suspension cultures using carrot and tobacco four decades later (Sussex, 2008; Giles and Songstad, 1990). Cell culture systems are widely used in tissue engineering, biomedical research, industrial practices as a tool to study the biophysical and biomolecular mechanisms of tissues or organs, and their functions and behaviours in health and diseases (Duval *et al.*, 2017, Ulrich and Pour, 2001). Traditionally, culture systems can be primary cell culture or cell line culture, each with its merits and limitations (Silicka, 2017).

Cell culture systems have been applied in genotoxicity testing for detecting the biological activity of test substances (Ekwall, 1990). On the other hand, co-culture systems (a culture set up of two or more differing cell populations but with some level of cell communication between them) have attracted research interest in recent times (Calvini *et al.*, 2013). Cole and Paul (1965) first co-cultured irradiated HeLa cells and murine embryo cells in an attempt to enhance the *in vitro* suboptimal media culture conditions. These systems were applied to the study of cellular interactions between populations; study of the complex multicellular synthetic systems or for improving cell culture success for some defined cell populations. There has been some

successful 2D co-cultures used in leukaemia studies (Dolen and Esendagli, 2013; Salman *et al.*, 2015) and genotoxicity assays (Hegarat *et al.*, 2012).

These successes are attributed to possible mechanisms like expression of growth factors (insulin-like growth factor, granulocyte-macrophage colony stimulating factor α and transforming growth factor α) and cytokines (interleukins 1, 6, 11 and leukaemia inhibitory factor) (Zeyneloglu, Kahraman and Pirkevi, 2011). Although, the concept of cells supporting cells has shown success with a few studies, there are a few inconsistencies with data acquired from co-culture systems in the literature. These variations as suggested by Kattal *et al.,* (2008) are due to the heterogeneity of cell lines and culture media. Co-cultures possess some distinct features over monocultures such as robustness, modularity, scalability and predictability (Rollie *et al.,* 2012), but requires a labour intensive *in vitro* characterization and optimisation of culture conditions to achieve this standard.

Whilst there are several studies in RIBE (Demidem *et al.,* 2006; Mothersill and Seymour, 2001) with monocultures and/or co-culture, only a few exist in CIBE. These CIBE studies exist as *in vivo* mice models (Merle, 2008) and some *in vitro* models either performed as separate monocultures and co-plated afterwards (Kumari *et al.,* 2009; Alexandre *et al.,* 2007) or investigated as medium transfer cultures and conditioned medium evaluated for its bystander killing on the effector cells (Singh *et al.,* 2015). Therefore, to attempt to represent the heterogeneity of the BM microenvironment and to provide the optimum standard culture conditions, that would elucidate the potential CIBE and its mechanism, a transwell co-culture system was developed in this study. This model would provide the soluble factors obtainable in a typical BM microenvironment. More so, the cell lines utilised in this study are of human origin and have been characterised separately, but nothing is known as to their functionality as a co-culture. Thus, this study would provide an insight into their characteristics in co-culture with or without chemotherapy. Finally, the assessment of the cytotoxic and genotoxic effects of these cell lines in the proposed optimised co-culture model would help inform about some cellular interaction within the BM microenvironment, as well as shed light into the pathology of CIBE and its possible mediators. Taken together, if the mechanism of bystander effect is determined, it could provide a whole new dimension in cancer chemotherapy as regards regimen choice, its dosage or the most efficient combination therapy required for the management of cancer patients. Furthermore, it will introduce interesting new perspectives on the scope of DNA damage induction, mutagenesis and carcinogenesis, when indirect

genotoxicity effects are taken into account during testing of novel and well described genotoxicants (section 6.1).

1.11 Hypothesis

Chemotherapy has the capacity to induce a bystander effect of cytotoxicity and genotoxicity in neighbouring unexposed cells, in a culture model of the human bone marrow. Disruption of redox status, and generation of reactive oxygen species represent a mechanism of action for induction of this bystander effect**.**

1.12 Aims:

1. **To develop a co-culture bystander model that will enable the study of the effect of chemotherapeutic agents on bystander cells**

    - Various culture conditions of the HS-5, TK6, AHH-1 and Kasumi-1 cell lines will be optimised to allow optimum growth conditions for all cell lines.

    - Optimisation will involve morphology and cell viability assessments.

2. **To explore the range of chemotherapeutic drugs that have the capacity to induce bystander effect**
    - The HS-5 cell line will be cultured in the presence and absence of a range of chemotherapeutic drugs, drugs washed away post exposure and will be co-cultured with the HS-5 cell line using either the lymphoblast cell lines (TK6 or AHH-1) or the myeloid cell line (Kasumi-1) for 24 hours. Bystander cells will be assessed for cell viability and genotoxicity post co-culture using established assays.

    - The alkylating agents, cytotoxic antibiotics, antimetabolites, topoisomerase inhibitors and plant alkaloids are the range of cytostatic agents used in cancer chemotherapy and in leukaemia; therefore a selection of different drugs from each group will be tested.

3. **To evaluate how long the bystander effect lasts**

    - Two drugs known to have high potency of bystander and two drugs with low potency will be selected to test for duration of effect, to determine if potency is long standing, or reduces over time.

- Cells will be co-cultured over the space of 5 days, with replacement of co-cultured cells each day and assessment for cytotoxicity and genotoxicity will be performed. This is to determine a safe duration for transplant.

4. **To evaluate the possible mechanisms of action of bystander effect**, a range of suspected mechanisms may be explored. These will be chosen based on the outcomes of the genotoxicity assays which will provide clues to possible bystander molecules/mechanisms.
    - **Simple drug elution**; conditioned medium and the final medium wash off from HS-5 treated cells will be utilised to evaluate for transfer of toxic signals into the bystander cells. Also an attempt will be made to develop a liquid chromatography and mass spectrometry (LCMS/MS) method that will be used to assess drug elution in the bystander cells and measure drug metabolites in bystander cells (if any).

    - **Free radicals**; these will be determined using co-cultures supplemented with reagents that scavenger or that promote free radicals. Also, co-cultures will be assessed with antioxidant enzymes for specific free radicals (e.g. catalase, superoxide dismutase and thioredoxin).

5. **To explore if the bystander effect can induce mutagenesis; possibly relevant to donor cell and therapy related leukaemia**
    - Using an established protocol for the HPRT mutation assay, this assay will be validated in house for TK6 and AHH-1 cells, the bystander cells will be grown in co-culture and evaluated for mutant cell colonies.

Chapter 2

Materials and Methods

2.1 Materials

All reagents that were used in this research were purchased from Sigma Aldrich (Dorset, UK) except where otherwise stated. All protocols were performed accordingly and supported by the use of appropriate control of substances hazardous to health (COSHH) regulations, which encompasses all risk assessments and control measures for the use of chemicals and fumes involved in this study.

2.1.1 Cell lines

Detailed description of the cell lines are shown in table 2.1 and were confirmed mycoplasma free for the purpose of this study. Four cell lines were used in this study and they include the HS-5, TK6, AHH-1 and Kasumi-1 cell line. The choice of these cell lines for any individual assay are explained in the appropriate result sections but overall, the use of these cell lines in an *in vitro* model serve to mimic the BM compartment and its cellular crosstalk as closely as possible. The BM typically consist of the mesenchymal stromal cells (HS-5) and the haemopoietic stem cells (TK6 or AHH-1 or Kasumi-1). Also, a combination of both the lymphoid (TK6 and AHH-1) and myeloid (Kasumi-1) cell lineages, aided a good representation of the leukaemia pathology – a focus of this study.

2.1.1.1 Stromal cell line

HS-5 is the fifth of the twenty-seven designated immortalised cell clones derived from long-term bone marrow culture. HS-5 expresses similar genes to a typical bone marrow and secretes cytokines that support growth and proliferation of committed haemopoietic cells when co-cultured in serum-deprived media (Rocklein and Torok-Storb, 1995; Graf *et al.*, 2002). Genes expressed include G-CSF, M-CSF, Kit Ligand; macrophage-inhibitory protein-1 alpha; interleukin-1 (IL-1α, IL-1β, IL-1RA, IL-6, IL-8, IL-11 and leukaemia inhibitory factor. Short tandem repeat (STR) profile includes: Amelogenin - X,Y; D16S539 - 10,11; CSF1PO - 10,11; D5S818 - 12; D7S820 - 12; D13S317 - 11; TH01 - 7,9; TPOX - 8; vWA - 18, 19.

2.1.1.2 Lymphoblast cell lines

TK6 is a thymidine kinase heterozygote cell line obtained from the HH4 cell line which was derived from the WIL-2 cell line (Levy *et al*., 1968; Levy *et al*., 1971; Skopek *et al*., 1978). The STR profile includes: Amelogenin - X,Y; D16S539 - 11,12; CSF1PO - 11,12; D13S317 - 11; D5S818 - 12,13; D7S820 - 9,11; TH01 - 8,9; TPOX - 8,11; vWA - 17,20. TK6 cells express positive cell surface markers for CD19, CD20 and CD22 and is reported negative for bovine viral diarrhoea virus (BVDV). They grow as suspension cultures in conventional Roswell Park Memorial Institute (RPMI) 1640 culture medium.

AHH-1 (aryl hydrocarbon hydroxylase) cell line was derived from RPMI 1788 lymphoblast cell line and is highly metabolically competent (can activate nitrosamines, mycotoxins, polycyclic aromatic hydrocarbons) and exhibits cytochrome P450 activity (Freedman *et al*., 1979; Crespi and Thilly, 1984). The human cytochrome P450 gene was transfected into AHH-1 cell line using pHEBo vector and hygromycin selection (Crespi *et al.,* 1989). The AHH-1 STR profile includes: Amelogenin - X,Y; D16S539 - 10; CSF1PO - 10; D13S317 - 11,13; D16S539 - 10; D5S818 - 12,13; D7S820 - 10,11; TH01 - 6,9; TPOX - 8,9; vWA - 18,19. AHH-1 shows high levels of oxidative activity and is sensitive to killing by benzo(α)pyrene. The cell line contains herpes virus, carries endogenous Epstein-Barr virus genome and positive nuclear antigen called Epstein barr nuclear antigen 1 (Crespi *et al.,* 1993).

2.1.1.3 Myeloid cell line

Kasumi-1 cell line possesses a t(8;21) chromosome translocation, which juxtaposes acute myeloid leukaemia 1 (*AML1)* and eight twenty one (*ETO)* genes to create a *AML1-ETO* fusion gene which produces a chimeric AML1-ETO fusion protein. Kasumi-1 stain positive for myeloperoxidase and respond to IL-3, IL-6, G-CSF in proliferation assay cultures, but not IL-1 or IL-5. Addition of phorbol ester to culture results in the production of macrophage-like cells, hence, Kasumi-1 is of both myeloid and macrophage lineages (Asou *et al*., 1991). The STR profile includes: Amelogenin - X; CSF1PO - 10,12; D13S317 - 11,13; D5S818 - 9,11; D7S820 - 8,11; TH01 - 6,9; TPOX - 8,9; vWA - 14, D16S539 - 9,12.

Table 2.1: Cell lines investigated in this study.

The source of the cell line, seeding density, gender, morphology and other vital details are indicated. The cell lines investigated were the bone marrow cell line (HS-5), the lymphoblast cell lines (TK6 and AHH-1) and the myeloid cell line (Kasumi-1). TK6 was a kind gift from Professor Ann Doherty and other cell lines were purchased from the American type culture collection (ATCC).

ATCC	HS-5	Homo Sapiens (human)	Bone marrow stroma	HPV-16 E6/E7 transformed	Fibroblast	Normal	30yrs	Male (Caucasian)	60 - 72 hrs	2 x 10^5 cell/cm^2
Donated by Dr Ann Doherty, AstraZeneca, UK	TK6	Homo Sapiens (human)	Spleen	Lymphoblast	Lymphoblast	Hereditary Spherocytosis	5yrs	Male	12 - 16 hrs	3 x 10^5 cells/ml
	AHH-1	Homo Sapiens (human)	Peripheral blood	B-Lymphocyte	Lymphoblast	Unreported	33yrs	Male (Caucasian)	16 -19 hrs	1 x 10^5 cells/ml
ATCC	Kasumi-1	Homo Sapiens (human)	Blood	Myeloblast	Myeloblast	Acute Myeloid leukaemia	7yrs	Male (Japanese)	40 - 45 hrs	3 x 10^5 cells/ml

2.2 Cell culture

All the cell culture procedures were carried out in a class II biosafety cabinet working with aseptic technique to prevent cell culture contamination, guided by the use of an appropriate COSHH assessment.

2.2.1 Standard culture conditions of BM and lymphoblast cell lines

HS-5 was cultured in a 'complete' culture medium consisting of its basal medium (Dulbecco's Modified Eagles medium {DMEM} either with high glucose (DMEM/HG) or low glucose (DMEM/LG) or F12 (DMEM/F12)) supplemented with 10% heat inactivated foetal bovine serum (HI-FBS), L-glutamine (2 mM), penicillin (100 U/ml) and streptomycin (100 µg/ml). Cells were maintained 37 ^{0}C and 5% CO_2 until log growth phase with replacement of fresh complete medium every 3 days until it reached about 70-80% confluence and then sub-cultured by trypsinisation (see 2.2.4). Cell viability was performed using trypan blue assay (see 2.2.6) and viable cells reseeded as a 1:3 split at a density of 2 x 10^5 cells/cm^2 using the tissue culture treated Corning flask (Fisher Scientific).

TK6, AHH-1 and Kasumi-1 cell lines were cultured in RPMI 1640 (basal medium) with a few modifications in their supplementation for a 'complete' culture medium. TK6 was supplemented with 2 mM L-glutamine, 100 IU/ml penicillin, 100 µg/ml streptomycin and 10% HI-FBS. AHH-1 was supplemented with 2 mM L-glutamine, 1.5 g/L sodium bicarbonate, 4.5 g/L glucose, 10 mM HEPES, 1.0 mM sodium pyruvate and 10% horse serum. Kasumi-1 was supplemented the same as TK6 except for use of 20% HI-FBS. Cells were maintained in culture at 37^{o}C with 5% CO_2 using these complete culture medium. Cells were seeded at the appropriate seeding density (Table 2.1) and maintained in culture until about 70-80% confluent. They were sub-cultured (passaged) by centrifugation at 230 x g for 5 minutes using a Hettich Universal 320 centrifuge and replacement of medium every 2 days.

2.2.2 Thawing of cryopreserved cell lines

Cells were transferred from liquid nitrogen and rapidly thawed by agitation in a 37 ^{0}C bead bath. Just before the ice completely melts, the vial is fully thawed by adding a thaw medium (20% HI-FBS in basal medium) in a dropwise manner with mixing to fill the vial. The contents of the cryovial were transferred into a 15 ml tube and made up to the 10 ml mark by addition of thaw medium in 1 ml aliquots with mixing over about a 10 minute period. The thawed cells

were then centrifuged (5 minutes; 230 x g). The thaw medium and centrifugation step ensures removal of dimethylsulphoxide (DMSO) from the cells. The cells were washed again with thaw medium before seeding cells at the required density.

2.2.3 Cryopreservation of cell lines

Cryopreservation aims to maintain a master stock at early passage and a large batch of stock cells for repeat of experimental research at the same passage. This will avoid long maintenance of cell lines in culture and avoid the risk of microbial and cross contamination with other cell lines.

All cell lines were slow freezed using 25% FBS, 10% DMSO and 65% cell line basal medium at a concentration of 30 x 10^5 cells/ml for TK6 and 10 x 10^5 cells/ml for Kasumi-1 cell line and 15 x 10^5 cells/ml for HS-5 cell line. DMSO acts as a cryoprotectant through a partial solubilisation of the cell membrane thereby making it less prone to puncture and by hindering the formation of intra and extracellular ice (formed as suspension of cell freezes) crystals (Berz *et al*., 2007). The ice cold cryopreservation solution (10% DMSO, 25% HI-FBS and 65% basal medium) were added dropwise into pelleted cells on ice, mixed and aliquoted into cryovials at 1 ml per vial. They were placed into ‘‘Mr Frosty’’ (a chamber containing isopropanol which holds cryovials; Sigma) which enables a slow temperature reduction of cells at -1 ^{0}C per minute (achieved in the -80 ^{0}C freezer over about 3-4 hours) and then transferred to vapour phase liquid nitrogen.

2.2.4 Detachment of adherent HS-5 cells

HS-5 cells that had grown to about 70% confluence were passaged by trypsinization. Working solution (1x) contained 0.25% trypsin and 1 mM ethylenediaminetetraacetic acid (EDTA). Cell culture medium was first decanted and cells were washed with phosphate buffered saline (1x PBS at a concentration of 10 mM PO_4^{3-}, 137 mM NaCl, and 2.7 mM KCl). This was followed by addition of trypsin (2 ml per T25 cm^2 flask), incubated for 5 minutes at 37 °C, 5% CO_2. A gentle tap facilitated the detachment process and trypsin activity was inhibited by addition of FBS in basal growth medium (1:9 v/v). Cells were spun at 300 x g for 10 minutes, the wash step repeated, then cells were reconstituted, counted and seeded at the correct density.

2.2.5 Trypan blue exclusion assay; manual cell counting

Cell suspensions were harvested and centrifuged at 230 x g for 5 minutes, the supernatant was discarded and cells re-suspended in complete culture medium (volume dependent size of cell pellet). Upon uniform resuspension, a 20 µl aliquot was mixed with an equal volume of 0.4% trypan blue in a microcentrifuge tube and allowed to sit for at least 1 minute at room temperature. The trypan blue/cell mixture was applied to a Neubauer haemocytometer and a count of unstained (viable) and stained (non-viable) was made and percentage viability calculated.

2.2.6 Cytotoxicity by fluorescent image-based automated cell counter

The trypan blue exclusion assay was made more robust through the use LUNA (Labtech, UK) fluorescent automated cell counter, thus minimising possible error from manual cell count. To do this, a 1:10 dilution of cell suspension and AO/PI (50 µg/ml) was made and 20 µl representative sample loaded on to the disposable haemocytometer. Protocols were set into the counter specifically accommodating the ranges of cell line size used in this study. The machine analyses this sample to produce values of total, viable and dead cells within seconds and a visual mark up of live versus dead cells is also produced.

2.3 Chemotherapeutics agents

Twenty-two different chemotherapeutic agents (Table 2.2) were utilised in this study for an initial screen of drugs able to produce a bystander effect, with later focus on four major drugs which were carmustine, chlorambucil, etoposide and mitoxantrone.

2.3.1 Treatment protocol

The chemotherapeutic agent stocks were made up in recommended solvents at a 100x concentrates, stored in small aliquots and frozen at -80^{o}C. Working concentrations were prepared fresh on the day of the assay, with dilutions made in culture medium. Cells were treated at clinically relevant dose concentrations for one hour at 37 ^{0}C with 5% CO_2. After one hour these agents were washed off the cells twice in PBS with a further wash with culture medium.

Table 2.2: Plasma concentrations of chemotherapeutic agents.

The literature was searched for the peak plasma concentrations of these agents; ranges of which determined the concentrations that were used in the present study.

Groups	Drug names	Solubility	Conc. (This study)	Peak plasma Concentration (Literature)	Clinically relevant dose/ Route	References
Alkylating agents	Carmustine	Ethanol	7.8 µM	7.8 µM	300-750 mg/m^2	Henner *et al*., 1986
	Chlorambucil	Ethanol	4 µM	2-6 µM	0.6 mg/kg	Hong *et al*., 2010
	Cisplatin	Water	20 µM	16 µM 12 µM 40 µM	Toxic conc. 100 mg/m^2 100 mg/m^2	Charlie *et al*., 2004 Oldfield *et al*., 1985 Vermorken *et al*., 1984
	Mechlorethamine	Water	50 µM	5 ng/ml	0.01-0.04% (topical)	Lubin and Bullock, 2013
	Melphalan	Methanol or	32.8 µM	4-13 µmol/L	0.6 mg/kg (IV)	Hong *et al*., 2010

		DMSO				
Antimetabolites	Cytarabine (Ara-C)	Water	25 µM	0.2 µM 103 ng/ml 10.8 µg/ml	100-300 mg/m^2 20 mg/m^2/day (IV) 3 g/m^2 (IV)	Hande *et al.*, 1982 Tsutsumi *et al.*, 1995 DeAngelis *et al.*, 1992
	Fluorouracil (5-FU)	Water or DMSO	1 µg/ml	10 µM	1750 mg/m^2/day (IV)	Tachimto *et al.*, 1999
	Hydroxyurea	Water	5mM	0.54-2.48 mM 0.9-6.4 mM	500-800 mg/m^2 (IV) 8-40 g/m^2 (IV)	Belt *et al.*, 1980 Gandhi *et al.*, 1998
	Methotrexate	DMSO DMF	5 µM	>5-10 µM (at 24 hours)	Not stated	Widemann and Adamson, 2006
Antibiotics	Bleomycin	Water	150 ng/ml	150 ng/ml	30 units 3-5 days (IV)	Gillman *et al.*, 1980
	Daunorubicin	Water	50 µg/ml	16-227 ng/ml	45 mg/m^2	Estling, 2000
	Doxorubicin	Water	50 ng/ml	1640 ng/ml	30 mg/m^2	Estling, 2000

				2.6-36.89 µM	400 mg/ m^2 (IV)	Rahman *et al*., 1990
	Mitomycin C	Water DMSO	0.1 µM	0.002 µM 1.2-5.9 µg/L	10 to 20 mg/m^2 20 mg/50ml	Hartigh *et al*., 1983 Paroni *et al*.,1997
Topoisomerase inhibitors	Etoposide	DMSO	15 µM	10-20 µM 14 µM	100 mg/m^2 (Oral) 100 mg/day for 8-15 days (Oral)	Clark *et al*., 1994 Millward *et al*., 1995
	Irinotecan	DMSO	2 µg/ml	1.97 µg/ml	150 mg/m^2 (IV)	Barakat *et al*., 2013
	Mitoxantrone	Ethanol or PBS	500 ng/ml	500 ng/ml	12 mg/m^2 (IV)	Smyth *et al*., 1986; Van Belle *et al*., 1986
	Teniposide	DMSO (10 mg/ml)	8 µg/ml	4-12 µg/ml 4-13 µg/ml	150 mg/m^2 (IV) 450 mg/m^2 (IV)	D'Incalci *et al*., 1985 Rodmann *et al*.,1987
	Topotecan	Water or	3.6 ng/ml	10.6±4.4 ng/ml	Not stated	Herben *et al*., 1999

		DMSO		4.7-11.7 nm	Not stated	Catimel *et al*.,1995
Mitotic Inhibitors	Docetaxel	DMSO	3.12µg/ml	3.7 µg/ml	100 mg/m2	Data sheet Medsafe (2016)
	Paclitaxel	DMSO	0.125 µM	0.05-0.2 µM	175 mg/m^2	Joerger *et al*., 2007
	Vinblastine	DMSO	4.8 ng/ml	3.2-6.3 ng/ml	3 mg/m^2 (IV)	Links *et al*., 1999
	Vincristine	Water	0.1 µM	1-2 nm <10nm	Not stated 1.0 mg/m^2	Estling, 2000. Hoffman *et al*., 2013

2.4 Bystander co-culture model

HS-5 cells were seeded at a density of 2.5 x 10^4 cells/cm^2 into a 12 well plate containing 1ml of complete medium per well. This density was sufficient to allow adequate proliferation before and during the experiment to avoid induction of apoptosis or necrosis. Upon confluence (usually 72 hours), HS-5 cells were treated with clinically relevant doses of chemotherapeutic agents (table 2.2) incubated at 37 ^{0}C and 5% CO_2 for 1h, upon a platform shaker (to ensure uniform distribution of the drug) gently rocking at 40rpm. Cells were washed three times in warm PBS to ensure removal of the drug and each well in the plate containing adherent cells was filled with 1 ml of complete DMEM/HG. Using sterile forceps, 0.4 µm polyethylene terephthalate (PET) hanging culture inserts (Merck Millipore, UK) were transferred into the wells and an additional 1 ml of medium added for resuspension of lymphoblast cell lines within the culture insert. Cells were co-cultured (Figure 2.1) for 24 hours and samples were harvested, counted and aliquots taken for analysis of toxicity, genotoxicity assays and other bystander assays in this study. All bystander experiments for this research were performed using the HS-5 cell line as a treatment compartment with TK6/AHH-1/Kasumi-1 cell lines as bystander cells.

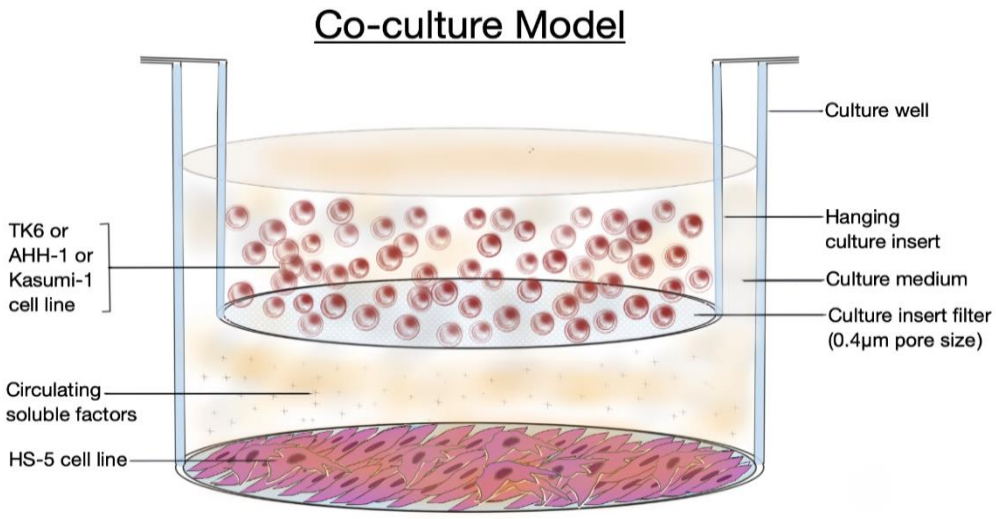

Figure 2.1: Representation of the co-culture model to determine bystander effect. HS-5 cells were seeded into the base of the well and initially exposed for 1h to drugs, then washed free of drug treatment, followed by addition of either TK6 or AHH-1 or Kasumi-1 into the well via a culture insert. Bystander cell lines were co-cultured with HS-5 and incubated at 37^{0}C at 5% CO_2 for 24 hours. Figure sketched by author, with some help from Sultan (colleague).

Co-culture experiments were set up in different culture medium to establish an optimal culture medium, which efficiently supported co-culture of HS-5 together with TK6, AHH-1 and Kasumi-1. Co-culture conditions using 2 x 10^4 cells/cm^2 seeding density for HS-5 and 5 x 10^5 cells/ml for bystander cells was established and the optimal culture medium for all cell lines was determined as DMEM/HG (section 3.2.1).

2.5 Genotoxicity assays

2.5.1 *In vitro* micronucleus assay

After determination of at least 50% viability, harvested bystander cells (2 x 10^4 per slide) were pipetted into microcentrifuge tubes and centrifuged (MicroCentaur SANYO) at 200 x g for 5 minutes. The supernatant was decanted and the pellet resuspended in 150 µl of PBS. Cell suspensions were dispensed into Shandon cytofunnels attached onto a clean grease free microscope slides (cleansed by soaking in 100% methanol and wiped dry with tissue) and centrifuged (Cytospin 4 from ThermoScientific) at 300 x g for 8 minutes. Microscope slides were carefully removed from the cytospin and the slides were air dried. To avoid detachment of cells from the slide, they were fixed using 90% methanol for 10 minutes.

Slides were stained with 12% (w/v) acridine orange in phosphate buffer for 45 seconds after brief rehydration in freshly prepared phosphate buffer (0.66% w/v potassium monobasic + 0.32% w/v sodium phosphate dibasic; pH 6.4) and further destained in two washes of fresh phosphate buffer (15 and 10 minutes respectively). Slides were air dried and stored in the dark to avoid fading until scoring.

Slides were analysed by a wet mount with phosphate buffer and visualization using a fluorescent microscope (Nikon Eclipse 80i) at x 40 magnification using triple band pass (standard excitation and emission wavelength range of 435-660nm for DAPI, FITC and Texas Red filters). Images were visualised with NIS Elements software and captured with a Nikon Digital Sight DSF1 camera (Nikon Instruments Europe). Aberrant cells were identified through the distinctive properties of acridine orange where the cytoplasm stains orange and nuclear material (including micronuclei) appear green. Slides were scored for mononucleated cells (normal), mononucleated/binucleated and multinucleated cells with or without micronuclei, lobed cells, apoptotic and necrotic cells (Figure. 2.2). A total of 2000 cells were scored per treatment. The criteria for scoring the MN are: a) must be about 1/16th to 1/3rd of the main

nucleus, (b) must be distinct from artefact and non-refractile, (c) must have same staining intensity as the main nuclei and (d) can touch the main nuclei but must not be linked or overlap it (Fenech, 2000).

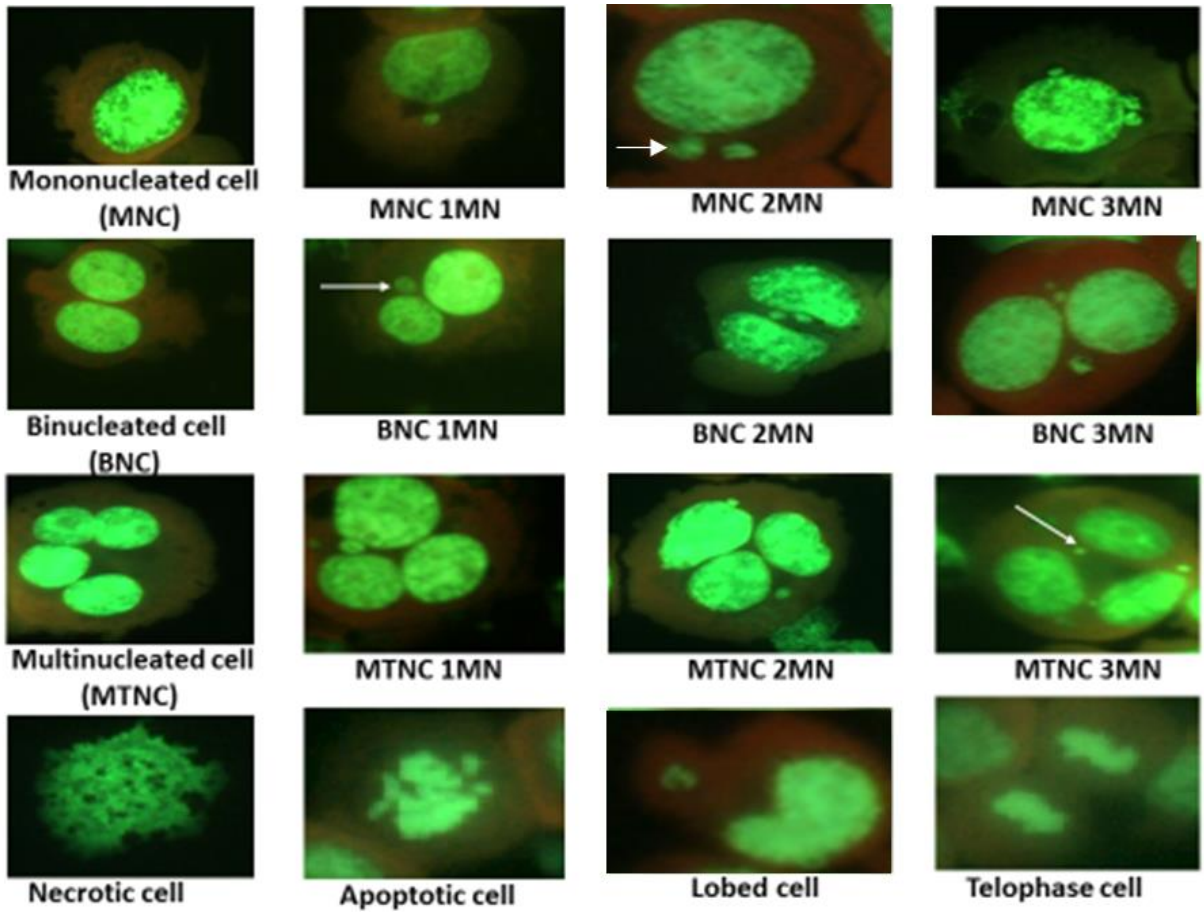

Figure 2.2: Scoring of micronucleus assay.

Micronuclei (MN) extruded during mitosis as a result of nuclear damage and are stained green (indicated with white arrows) against an orange cytoplasmic background. These different parameters were observed under the fluorescence microscope and MN scored according to recommended criteria of size ($1/16^{th}$ to $1/3^{rd}$ of main nuclei), appearance and similar staining intensity with main nuclei. Figure put together from the researcher's study.

2.5.2 Fluorescence *in situ* hybridisation (FISH) using pancentromeric probes

The MN assay is limited by its inability to differentiate the type of damage detected, whether due to clastogenicity (loss of DNA fragment) or aneugenicity (loss of whole chromosome), hence the need to label the cells. Reagents to prepare are as follows:

- 3:1 methanol and acetic acid (45ml methanol + 15 ml acetic acid, vol:vol).
- Formaldehyde fixative (1% formaldehyde + 1x PBS + 50 mm MgCl; store cold).

- 10% Pepsin stock (0.1 g per ml of distilled water, pre warm at 37 ^{0}C, aliquot and freeze).
- 0.005% pepsin working solution (25 µl of 10% stock + 49.5ml of distilled water + 0.5 ml of 1M HCl).
- RNase solution (dissolve 20mg/ml of RNase in sterile water, boil for 15 minutes, cool and freeze).
- 20x sodium saline citrate (SSC; 3M NaCl + 0.03 M NaCitrate)
- 2x SSC and 0.4x SSC (both prepared from 20x stock).
- 70% and 85% ethanol (in a 100 ml jar, add 30 and 15ml of water respectively).

2.5.2.1 FISH slide preparation

This involved two steps of denaturation and hybridisation (labelling). Harvested bystander cells was cytospinned at 300 x g for 8 minutes and fixed in 3:1 methanol and acetic acid for 15 minutes and stored in a warm (30 ^{0}C) incubator. Prior to the actual assay, slides were air dried for at least 24 hours overnight. Slides were incubated in 0.005% pepsin solution (pre-warmed to 37 ^{0}C) for 8 minutes and were then washed twice in 2x SSC in a coplin jar for 1 minute each. Slides were fixed in formaldehyde fixative solution at room temperature for 5 minutes followed by two washes in 2x SSC, 1 minute each time. The slides were dehydrated in ascending grades of ethanol (70%, 85 and 100%); and warmed at 45^{0}C for 5 minutes. Then a 7 µl of the ready to use FITC labelled probe (Star FISH human chromosome pan-centromeric – Cambio, UK) was added to the slide, cover-slipped and edges sealed using the rubber cement glue which was allowed to air dry completely in the dark. Once the glue was dried, slides were loaded onto the ThermoBrite system (Leica Biosystems) which automates the denaturation and hybridisation steps. Denaturation was carried out at 73^{0}C for 5 minutes and hybridisation was performed at 42^{0}C for 24 hours, whilst minimising light interference as much as possible. Once hybridisation was completed, the rubber seal was gently removed and slides were agitated for 2 seconds in 0.4x SSC (0.06 M NaCl and 0.006 M Na Citrate, pH 7.0) with 0.3% Tween 20 heated at 73 ^{0}C and further left undisturbed for 1 minute. Slides were then treated with 2 x SSC with 0.1% Tween 20 for 2 minutes. Slides were retained in the post wash until they were hydrated in descending grades of alcohol, counter stained and mounted.

2.5.2.2 Slide mounting and analysis:

Slides were counter stained using a drop of the Vectashield antifade mounting medium with DAPI (Vector Laboratories, UK) and cover-slipped (22 x 22cm). The mountant was evenly spread across the slide whilst layering over the coverslip avoiding air bubbles. Slides were visualized using a fluorescent microscope (Nikon Eclipse 80i) at x40 magnification using a DAPI (standard excitation and emission wavelength range of 435-660nm) and FITC (465-495nm) single filters and images were merged with the aid of Fiji - ImageJ analysis software.

2.6 *In vitro* alkaline comet assay

The comet assay was used to assess DNA damage in bystander samples as described in McNamee *et al*., (2000).

2.6.1 Slide preparation

Harvested lymphoblast cell lines were centrifuged (MicroCentaur SANYO) at 200 x g for 5 minutes and pelleted cells were resuspended and counted and determined viable. Cells (2 x 10^4) were resuspended in 40µl of low melting agarose (LMA; 0.5% w/v in PBS, 4^0C) and were placed onto gel bond film (Lonza) and cover slipped (22 x 22 mm).

2.6.2 Unwinding and electrophoresis

For each treatment, two gels were prepared and films were placed in at 2-8 ^{0}C to allow the LMA to set for about 30 minutes. All gels had their cover slips removed and were lysed overnight in a light proof box containing pre-cooled freshly prepared complete lysis solution (178ml of incomplete lysis solution [100 mM ethylenediaminetetraacetic acid {EDTA}, 2.5 M sodium chloride and 10 mM Tris base adjusted to pH 10.0 using 10 M sodium hydroxide {NaOH}], 1% Triton X-100 and 10% DMSO). Lysis removes the cell membranes and the nuclear proteins, leaving just the supercoiled DNA structure as a nucleoid in the gel. A positive control slide was prepared (cells treated with 50 µM hydrogen peroxide (H_2O_2) for 5 minutes at 4 ^{0}C) prior to complete lysis. Exposed DNA following lysis were relaxed and unwound for 20 minutes by soaking gels in a pre-cooled alkaline electrophoresis buffer (200 mM NaOH, 1 mM EDTA, pH 13). The gel bond placed in an electrophoresis tank kept cool at 4^0C using a

recirculating water bath (Grant Instruments, UK), gels were then electrophoresed at 0.7 V/cm and 300 mA for 20 minutes in alkaline electrophoresis buffer.

2.6.3 Neutralisation and staining

Slides were neutralised in three changes of neutralisation buffer (0.4 M tris-HCl (hydroxymethyl aminomethane hydrochloric acid, pH7.5) for 5 minutes each wash, all in a light proof box and the film left in the last wash and stored at 2-8 ºC until analysed.

2.6.4 Analysis of comets

Slides were analysed by staining with 40 µl of 20 µg/ml propidium iodide per slide using a fluorescent microscope (Nikon Eclipse TE300 with FITC excitation (465 – 495nm) and barrier (515-555nm) filters, at 20x magnification) linked to a computer with installed comet assay IV software (Perceptive instruments). A total of 150 comet images (Figure 2.3) taken with Nikon Digital Sight DSFI 1 camera and NIS element software (Nikon Instruments Europe) were scored per treatment, for all three biological repeats, analysing the percentage tail intensity.

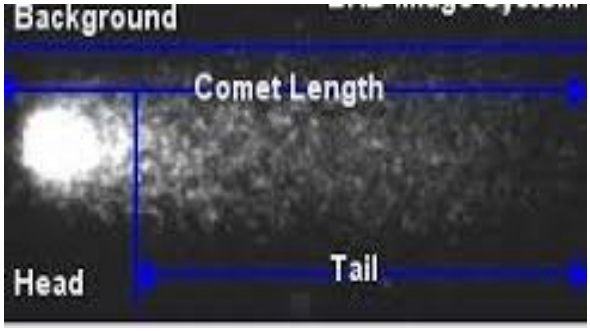

Figure 2.3 Representative comet image.

DNA fragmented in a cell under alkaline electrophoresis condition migrates towards the anode forming a comet image with a ‘head’ and ‘tail’. Fragmentation was measured using the percent DNA in the tail.

2.6.5 Modified enzyme linked comet assay

The modified comet assay is advantageous for increased sensitivity and specificity for the recognition of specific types of DNA damage/lesions. This assay makes use of lesion specific endonucleases which when incubated with nucleoids creates additional breaks upon

recognition of damaged bases. Endonucleases used were human 8-hydroxyguanine DNA-glycosylase (hOGG1) and Fpg (formamidopyrimidine DNA-glycosylase). Whilst both Fpg and hOGG1 recognizes oxidized purines {4,6-diamino-5-formamidopyrimidine (FaPyAde), 8-oxo-7,8-dihydroguanine (8-oxoGua), 2,6-diamino - 4 - hydroxyl – 5 - formamidopyrimidine (FaPyGua)}, use of hOGG1 is reported to be more specific than FPG which recognises damages due to alkylation (Smith *et al.*, 2006).

In this study, the hOGG1 (catalogue no. M0241S) and Fpg (catalogue no. M0240S) enzymes were purchased from New England Biolabs (NEB). Following complete lysis (section 2.6.2), slides were immersed in two different changes of enzyme buffer (40 mM HEPES, 100 mM KCL, 0.5 mM EDTA and 0.2% BSA; pH 8.0) for 5 minutes at room temperature. Initially, varying enzyme concentrations were titrated against 2 mM $KBrO_3$ and the optimised amount of enzyme (hOGG1 – 0.15U and FPG – 0.2U per gel) used subsequently. These enzymes were added to the gel in 50 µl of enzyme buffer, cover slipped and incubated in a humidified chamber for 30 minutes at 37 ^{0}C. The coverslips were detached and placed in the electrophoresis chamber and further steps were the same as previously described (section 2.6).

2.7 DCFDA assay

DCFDA is a non-fluorescent molecule 2', 7'- dichlorofluorescein diacetate, which has the ability to fluoresce when oxidised. Thus, the assay is based on the detection of any ROS released during oxidative stress rather than determination of specific ROS (Hempel *et al.*, 1999; Halliwell and Whiteman, 2004; Eruslanov and Kusmartsev, 2010). The assay was initially optimised with varying concentrations of H_2O_2 (50 - 1600 µM) and $KBrO_3$ (3.12 to 400 mm) with and without N-acetylcysteine (NAC – 0.1 to 5mM) or diethylmaleate (DEM – 0.1 to 5 mm); over a range of DCFDA concentrations (1 to 25 µM) which was made in anhydrous N'N-dimethylformamide (DMF). Optimised concentrations (section 3.2.5) for DCFDA (1 µM), DEM (2.5 mM), and NAC (0.5 mM) were used for final the assay. In a black clear bottom 96 well plate (BMG Lab technologies, UK), the perimeter wells were loaded with 100µl of PBS to avoid drying out of the wells. The remaining wells were further loaded with varying concentrations of $KBrO_3$, chemotherapy agents (carmustine, chlorambucil, etoposide and mitoxantrone), and untreated controls with or without DEM and NAC.

To stain the cells, HS-5 (2 x 10^4 cells/200 µl) were seeded overnight to adhere, exposed to chemotherapeutic agents the next day. After treatments, they were washed in complete culture medium (DMEM/HG without phenol red and serum) and DCFDA final concentration in 2 x 10^4 cells per well was 1 µM. Plates were sealed with biofilm to protect the aseptic environment, wrapped in foil and incubated at 37^0C, 5% CO_2 in the dark. The DCFDA diffuses into the cell and intracellular esterases hydrolyse the acetate group of DCFDA to produce a non-fluorescent cell-impermeable compound 2', 7'- dichlorofluorescin (DCFH) which further reacts with intracellular oxidants to produce a cell permeable fluorescent compound dichlorofluorescein (DCF).

The evaluation of the produced DCF fluorescent compound was detected using a microplate reader (BMG Fluostar optima) with 488nm excitation and 525nm emission filters. Fluorescent intensities of plates was measured at different time points up to 24 hours. The measured drug absorbances were analysed against the standard curve concentrations.

2.7.1 DCFDA bystander cells evaluation by flow cytometry

The bystander cells (5 x 10^5 cells/ml) were fixed in 4% PFA on ice for 10 minutes; washed twice in DPBS (Dulbecco's phosphate buffered saline – 8g NaCl, 0.2g KCl, 0.2g monobasic potassium phosphate KH_2PO_4, 1.15g sodium phosphate Na_2HPO_4) at 130 x g for 5 minutes and incubated with DCFDA (1 µM) in the dark for 45 minutes. Cells were washed as above, resuspended in 300 µl PBS and 10,000 cells measured using the BD accuri flow cytometry with excitation and emission filters of 488nm and 530/30nm respectively. Three biological repeats were analysed using the FL1 channel against an untreated control.

2.8 8-hydroxy-2'-deoxyguanosine (8-OHdG) antibody ROS evaluation

8-OHdG antibody (Abcam ab183393) is an anti-DNA/RNA oxidative damage antibody, which detects lesions excised from DNA in intact cells. It serves as a marker for DNA damage, detecting lesions in DNA caused by oxidative stress with high specificity and affinity to oxo8dG (8-hydroxy-2'-deoxyguanosine), oxo8Gua (8-oxo-7,8-dihydroguanine), and oxo8G (8-oxo-7,8-dihydroguanosine) present in biological fluids.

2.8.1 Cell Preparation/fixing/permeabilisation

Bystander cells (1 x 10^6 cells/ml) were harvested post co-culture and cell pellets fixed in 4% paraformaldehyde (PFA) with 0.1% Triton X-100 for 10 minutes on ice. At the end of 10 minutes, the fixative were layered over the cells, hence aspirated off and the wash buffer containing PBS/ 0.1% Tween-20/ 0.05% sodium azide (PBST) was added slowly along the sides of the tube and cells spun down at 130 x g for 5 minutes. Cells were washed twice in wash buffer and subsequently permeabilised in 0.1% Triton X-100 in PBS for 10 minutes on ice and underwent a further two washes in PBST.

2.8.2 Staining/analysis

Cells were first blocked for one hour at room temperature on a rocker using 3% BSA in PBST. A 1 µg/ml of the 8-OHdG antibody and 1 µg/ml of the untreated isotype, a concentration chosen after optimisation (section 3.2.4) of different ranges of concentrations (0 – 10 µg/ml), was used to stain the cells overnight at 4ºC while in the dark. The unbound antibody were washed twice in wash buffer and cells were resuspended in 300µl of PBS and both the unstained untreated, untreated isotype control (ab18427, Abcam UK) and treated samples were evaluated using the FL1 channel on the flow cytometry with excitation and emission filters of 488nm and 530/30nm respectively. Data were analysed against an untreated stained (FITC antibody) control sample.

2.8.3 Confocal microscopy

Localisation of 8-OHdG antibody to the nucleus was optimised (3.2.3) prior to quantification by flow cytometry. Using the established protocol (section 2.8), varying concentrations of KBrO3 (12.5 mM and 25 mM) and H_2O_2 (50 and 100 µm) direct treatments were qualitatively assessed to ascertain localisation and antibody penetration of the nucleus. Optimal antibody concentration was ascertained to be 1 µg/ml and cells were counterstained with 4',6-diamidine-2'-phenylindole (DAPI; 1µg/ml) for 15 minutes at room temperature. Cells were spun onto a slide using the cytospin and slides mounted with vectashield antifade mounting medium (H-1000) and tile scans or Z stack images acquired with the confocal microscope (Leica TCS SP8 – Leica microsystems, UK) using the LAS X acquisition software.

2.9 Liquid chromatography mass spectrometry (LC-MS) assay

This is a high-pressure liquid chromatography system for separation of compounds within a mixture, and connected to a triple quadrupole mass spectrometer equipped with an electrospray ionization source, which produces a spectrum corresponding to analytes mass to charge ratio. A method for each drug and sample extraction was optimised (section 3.2.6). The instrument was equilibrated to ensure steady binary pump pressure whilst the mobile phases flowed through. Samples were identified in a worksheet to analyse as three separate measurements for each sample followed by a blank that is also ran in same way as a sample, with an automated needle wash after every sample injection. The separated compounds were detected using a tandem mass spectrometer operated with an electrospray ionisation (ESI) interface in positive ionisation mode for most drugs, under the optimised ionization conditions. The high performance liquid chromatography (HPLC) conditions and target compounds were analysed using the multiple reaction monitoring (MRM) mode scanning for transitions of the mass to charge ratios. Data acquisition, qualitative and quantitative analysis, as well as generation of report analysis was performed using the Agilent LCMS/MS MassHunter software.

2.10 Seahorse XF mitochondria (mito) stress test

Oxidative phosphorylation in mitochondria and glycolysis in the cytosol are the major ATP production mechanisms in cells (Plessis *et al*., 2015). Therefore, measurements of oxygen consumption rate (OCR) and extracellular acidification rate (ECAR) are vital parameters for assessing mitochondrial energy metabolism. This metabolism involves production of reactive oxygen species (ROS), a possible mechanism for bystander effect (chapter 5). For this assay, the Seahorse extracellular (XFe) 24 analyser (Agilent technologies, UK) was used.

A sensor cartridge was hydrated overnight by pipetting 500 µl of XF calibrant solution into each well and incubating at 37^0C in a non-CO_2 incubator. Seahorse utility plates were coated with poly-l-lysine (50 µg/ml) for 1h, washed three times in PBS and left to air dry in the fume hood, stored overnight at room temperature before seeding the correct cell density (25 x 10^4 cells/well). Cells were allowed to adhere properly overnight in 500 µl of complete culture medium. Prior to measurement of OCR and ECAR, the complete culture medium was removed from the microplate, leaving roughly 30 to 40 µl to cover the cells. Cells were washed three times with culture medium and finally incubated in serum free seahorse XF culture medium containing DMEM with 10 mM glucose, 2 mM L-glutamine and 1 mM fresh sodium pyruvate

pH (7.5) for 1h at 37 ^{0}C in a non-CO_2 incubator. The assay solvents in their respective concentrations: oligomycin (1 µm), FCCP (1 µm) and rotenone/actinomycin A (0.5 µm) were injected into ports A, B and C respectively for analysis of a normal seahorse mitochondria test and port D (injection of target compound) utilised if running an acute seahorse mitochondria test. The wave software was opened and mitochondria stress test protocol chosen, key identifiers like name, test date, treatments (colour coded individually) were set up. The calibration plate was used to calibrate the machine for 20 minutes and the culture plate was inserted afterwards for evaluation. Data was analysed using the automatic Seahorse XF mitochondria stress generator spreadsheet whilst normalizing each well to cell number.

2.11 Western Blotting

A western blot cocktail antibody (Abcam, ab179843) for assessment of the oxidative stress defence system of a cell was used as detailed below.

The following reagents were prepared and they include:

- 2x laemmli loading buffer – (4% SDS, 20% glycerol, 0.004% bromophenol blue, 0.125 M Tris-HCl, 10% 2-mercaptoethanol, pH 6.8).
- Resolving buffer – 18.67g Tris-HCl (1.5 M) in 100 ml distilled water, pH 8.8
- Stacking buffer – 12.5 g Tris-HCl (1M) in 100 ml distilled water, pH 6.8
- 10% APS – 0.1g APS in 1ml water
- 1x migration buffer - Tris – 25 mM, glycine - 1.92 mM, 0.1% SDS, in 1 litre distilled water, pH 8.3
- Resolving gel – 12% (29:1 acrylamide:bis-acrylamide – 30% stock), 0.375 M tris-HCl pH 8.8, 0.1% SDS, 0.1% APS (ammonium persulfate) and 0.4% TEMED (N,N,N′,N′-Tetramethylethylenediamine).
- Stacking gel – 4% (29:1 acrylamide:bis-acrylamide – 30% stock), 0.0125M Tris-HCl pH 6.8, 0.1% SDS, 0.1% APS and 0.4% TEMED.
- 10x Transfer buffer – 30.29g Tris (250 mM), 142.63g glycine (1.9M) in 1 litre distilled water, pH 8.3.
- 1x transfer buffer – 50ml of 10x transfer buffer pH 8.3, 750ml of distilled water and 20% methanol. NB: This was the working transfer buffer referred henceforth as transfer buffer.

- 1x wash buffer – phosphate buffered saline and tween-20 (PBST- 950ml of 1X PBS and 500µl Tween-20).
- Radioimmunoprecipitation assay (RIPA) buffer - 150 mM NaCl, 0.1% Triton X-100 , 0.5% sodium deoxycholate , 0.1% sodium dodecyl sulphate , 50 mM Tris-HCl pH 8.0

2.11.1 Isolation of proteins

Cells were harvested, washed with ice cold PBS and concentrated pellets in a microcentrifuge were placed on ice (minimizes high temperature effect thereby avoiding proteolysis). An addition of 500µl RIPA buffer and a freshly added protease inhibitor (Thermo Scientific Pierce protease inhibitor mini tablets) with gentle pipetting up and down, lysed the cells to release the proteins. Initial experiment utilised three cycles of freeze thawing samples, with a 30 seconds vortex each time to enable adequate cell lysis. Subsequently, for fast and higher protein yield, samples were sonicated for two cycles of 15 seconds at 45% amplitude and intermittent placing on ice for 30 seconds. Cell lysates were subsequently centrifuged at 24,192 x g for 15 minutes at 4^0C. The supernatant containing the protein was transferred to a new tube and quantified using the BCA assay (section 2.11.2). Aliquots were made and tubes stored at -80^0C.

2.11.2 Quantification of proteins:

To confirm the presence of protein, as well as maintain uniform load of protein sample onto the gel to ensure comparable equivalents for downstream analysis, the total protein was quantified against known concentrations of bovine serum albumin (BSA) standard using the bicinchoninic acid (BCA) assay. BCA has high sensitivity (0.5 µg/ml) and it shows a strong linear absorbance with increasing amount of protein. It is based on the biuret principle of reducing cupric ion to cuprous ions to form a faint blue colour, which upon chelation of BCA with cuprous ion forms a water soluble purple coloured complex measurable at 562 nm (Olson, 2016). Briefly, BSA standards are prepared making eight serial dilutions from a stock of 2 mg/ml. BCA working reagent is made by a mixture of 50:1 reagents A:B from Sigma BCA protein assay kit (BCA1). A 96 well microplate was prepared with 25 µl negative control (cell lysis buffer and/or water), 25 µl BSA concentrations (0.2 mg/ml, 0.4 mg/ml, 0.6 mg/ml, 0.8 mg/ml and 1.0 mg/ml) and 25 µl protein sample, all in duplicates, with a final addition of 200

µl of BCA working reagent to each well. The plate was incubated at 37^0C for 30 minutes, a further 5 minutes at room temperature and read at 562 nm on a plate reader.

2.11.3 Sodium dodecyl sulphate polyacrylamide gel electrophoresis (SDS-PAGE)

The SDS-PAGE technique is used to separate proteins according to their molecular weight in the presence of anionic SDS detergent. As described in the tris-glycine system of Laemmli (1970), this study achieved protein separation at high pH in a discontinuous buffer system (done by layering of a non-restrictive large pore stacking gel over a thin pore resolving gel). To do this, a protein sample (15 µg/ml) preparation was made in 2 x Laemmli loading buffer in a 1:1 ratio, pre-heated at 95^0C for 5 minutes, then placed on ice until ready for use. A 4% stacking gel and 12% resolving gel was cast to evaluate the protein of interest using a mini-protean III system (Bio-rad). Resolving gel was gently poured in between the gel rig vertical plates, leaving approximately 1cm mark from on top where the stacking gel was subsequently layered over and an adequate comb (mini-protean 10-well, for 1.0mM, glass plates, 40µl) fitted. After the gel polymerised, combs were gently removed and samples were loaded in parallel to a colour-coded pre-stained protein marker (11-250 kDa, NEB 14208S). The gel cassettes was sandwiched into the module assembly and the inner and outer chambers were filled with 1x migration buffer. The stacking gel concentrates the proteins into a sharp band just as they resolve by isotachophoresis (same speed migration achieved by differences in the pH of the stacking gel, resolving gel and electrophoresis buffer) at 70V for about 30 minutes. This time was enough to allow samples to travel through the stacking gel and align horizontally just above the resolving gel) and then the proteins were separated in the resolving gel at 100V for about 1.5 hours. Optionally, gels or membrane blot were stained after separation to check for uniform migration and efficiency of transfer respectively. Staining was done in Coomassie blue (0.25% w/v), water, methanol and glacial acetic acid (50:40:10) and destained in solution of glacial acetic acid, water and methanol (10:70:20).

2.11.4 Wet transfer (blotting) of proteins to a polyvinylidine difluoride (PVDF) membrane

The separated proteins were transferred onto a solid matrix support with great protein binding affinity and retention capacity. The 0.45µm PVDF membrane (GE Healthcare Amersham

Hybond –XL Membranes via Fisher Scientific) was activated by soaking in methanol for 2 minutes and further rinsed in ice cold transfer buffer. The protein is transferred by sandwiching the gel in the format of figure 2.4, using 4x Whatmann's paper cut into suitable sizes, gel and PVDF membrane (both previously soaked in ice cold transfer buffer). The membrane was placed between the gel and filter paper closest to the positive electrode to aid transfer of the negatively charged protein onto the membrane. It was layered carefully to avoid air bubbles. The transfer assembly was put into a tank filled with transfer buffer and electrophoresed at 70 V for 4.5 to 5 hours at 4^0C.

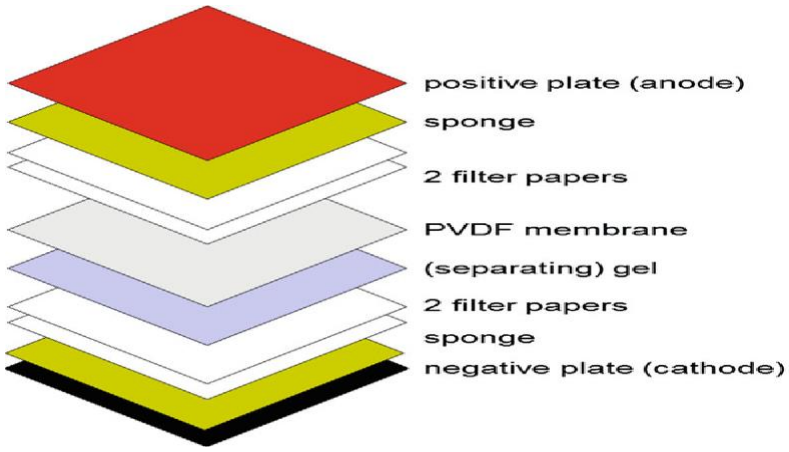

Figure 2.4: Stacking of western blot membrane.

Representation of the order of layers in a western blot transfer assembly copied with creative common licence from Landsberger and Brinkmeier (2018).

2.11.5 Detection of target protein:

The blot was blocked using 5% skimmed milk powder in PBST for 1h at room temperature on a rocker. After blocking, the blot was transferred into the primary antibody solution (1:1000 in blocking solution), incubated overnight at 4^0C on a rocker at a speed of 70 rpm. The primary antibody is a cocktail of four antibodies: superoxide dismutase 1 (SOD1; 16 kDa), catalase (CAT; 60 kDa), thioredoxin (TRX; 12 kDa) and smooth muscle actin (β-actin; 42 kDa). Subsequently, the membrane was washed three times for 5 minutes each in PBST on a rocker at room temperature. The anti-rabbit IgG horseradish peroxidase (HRP) linked secondary antibody (1:5000 in blocking solution) from NEB (Cat no-7074P2) was added and the membrane incubated for 2 hours at room temperature on a rocker, followed by a further three washes as stated earlier.

The membrane was detected by visualizing the blot on the Li-Cor Odyssey. Its principle is based on the fact that addition of a chemical substrate (GE Healthcare Amersham ECL Prime Western Blotting Detection Reagent) to the HRP enzyme conjugated secondary antibody generate a light signal. This was done with the excitation channel (600nm) for 30 seconds and final detection with the chemiluminescence channel, which detects visible wavelengths emissions.

2.11.6 Data analysis (western blot)

The data was normalized using the β-actin housekeeping protein internal control. The LiCor Odyssey enables densitometry quantification, through automatic or manual drawing of a rectangle at the band location. Once the target (SOD1, CAT and TRX) bands were identified by an alignment to a molecular weight marker, its signal intensities were compared to the signal intensity of the corresponding lane of the β-actin. The analysed data for the normalized abundances were represented.

2.12 HPRT gene mutation assay

Material required include:

- 50x sodium hypoxanthine (5 mM), aminopterin (20 μm) and thymidine (0.8 mM) - HAT supplement (21060017; ThermoFisher scientific, UK).
- 100x HT supplement – sodium hypoxanthine (10 mM) and thymidine (1.6 mM) – (11067030; ThermoFisher scientific, UK).

The HPRT assay was performed as described in Adams *et al.*, (2013). Briefly, background mutants were removed from the TK6 and AHH-1 cells (5 x 10^5 cells/ml) by cleansing them in culture medium (HAT medium - consisting of hypoxanthine (2 x 10^{-4} mol/l), aminopterin (8 x 10^{-7} mol/l) thymidine (3.5 x 10^{-5} mol/l); diluted to these final concentration with complete culture medium) for 3 days. The cells were washed off in complete culture medium, followed by a further 24 hours growth in HT medium diluted in complete culture medium to a final concentration of 2 X 10^{-4} mol/l (hypoxanthine) and 3.5 x 10^{-5} mol/l (thymidine), and were again washed and grown in complete culture medium for three days. The cells were either directly treated with different doses (0.0025 - 0.075 μg/ml) of methylnitrosoureas (MNU; positive control) for 24 hours in a 10 ml culture at 5 x 10^5 cells/ml or used as bystander cells

for co-culture as described in section 2.2.5. Cells were washed and resuspended in fresh medium to culture for thirteen days. Subsequently, medium containing 0.6 µg/ml of 6-thioguanine (6-TG; prepared from a 600 µg/ml stock dissolved in 1M NaOH; Alfa Aesar, Fisher Scientific) was used to select for HPRT forward mutation, by seeding cells at 4 x 10^4 cells per well. A non-selective medium (without 6-TG) was used to determine plating efficiency by seeding at 20 cells per well; four plates were seeded per treatment/dose. Colonies (single clone of >20 cells) were scored and assessment of mutation frequency was determined as described by Georg *et al.,* (2012).

2.13 Enzyme-linked immunosorbent assay (ELISA)

ELISA was developed to assess the possible role of cytokines (IL-1β, TNFα) in chemotherapy-induced bystander effect. Both antibodies were purchased from BD biosciences, UK. To prepare the plate, 2 µg/ml of TNFα and 3 µg/ml of IL-1β capture antibodies prepared in bicarbonate buffer (pH 9.6) were used to coat a clear 96 well Nunc immunosorbent plate (ThermoScientific, UK). Following a gentle tapping of the plates for even spread, they were allowed to incubate overnight at 4^0C. The next day, the wells were washed twice with PBS/0.1% Tween-20 (tween wash), twice with PBS and blocked in 200 µl of PBS/1% BSA incubating at 37^0C for 1 hr. Plates were washed twice with tween wash and a further twice with PBS, whilst preventing drying of the plate at any step. The top standards for TNFα recombinant antibody was 30 ng/ml while IL-1β was 20 ng/ml. Their quality control samples were: TNFα (1500 pg/ml; 500 pg/ml) and IL-1β (1000 pg/ml; 500 pg/ml) for their respective high and low concentrations. These top standards prepared in PBS/1% BSA were pipetted into the first well of the top two rows of the plate. The remaining wells of these rows was filled with 50 µl of PBS.

Using a multichannel pipette, 50 µl was removed from the first two wells and double diluted across the plate; discarding the final 50 µl removed from the last wells. Equal amount (50 µl) of the QCs, blank (PBS/1% BSA) and samples were added in duplicates to their respective wells. Plates were incubated for 2 hours at room temperature, washed twice each in tween wash and PBS, patting dry over a wad of tissue. Equal volume (50 µl) of the biotinylated detection antibodies: TNFα (15 µg/ml); IL-1β (0.25 µg/ml), prepared in PBS/1% BSA were added as quickly as possible using a multichannel pipette. Plates were incubated for 1h at room temperature, washed twice with tween wash, then twice with PBS. Streptavidin peroxidase (50

µl of 0.5 µg/ml; Pierce, Fisher Scientific UK) diluted in PBS/BSA was added to all wells and incubated for 30 minutes at room temperature. The plate was washed twice with the tween wash and twice with PBS and 100 µl of substrate (0.1 mg/ml 3,3',5,5' – tetramethylbenzidine (TMB) in 0.1 M phosphate/citrate buffer with 0.03% H_2O_2) was added to the plates. When the blue colour developed in the penultimate standard, 50 µl of 2M sulphuric acid (H_2SO_4) was added to stop the reaction and plates were read on a Fluostar Optima spectrophotometer (BMG Labtech, UK) at 450nm.

2.14 Statistical analysis

Except for where otherwise stated, the mean, standard deviation and standard error of the mean were calculated using the Graphpad prism 7.04 software and were tested for normality using both D'Agostino-Pearson omnibus and Shapiro-Wilk normality test in Graphpad. The unpaired Student t-test was used to determine direct significance between treated and untreated (control) samples, while two-way ANOVA was used for group comparisons followed by a Dunnett's post-hoc multiple comparison test. All analysis are representative of three biological repeats unless otherwise stated. Statistical significance of the presented graphs were identified as (*) for $p \leq 0.05$, (**) for $p \leq 0.01$, (***) for $p \leq 0.001$ and (****) for $p \leq 0.0001$.

CHAPTER 3

Method Development

3.1 Introduction

Mammalian cell culture technology in recent times has become an essential tool for the study of cellular activity in a controlled environment, because of the advantage that cell behaviour *in vitro* transcends its behaviour *in vivo.* It has been used to study cell and tissue physiology or pathophysiology outside the organism (Joseph *et al.*, 2018). Cell culture has been widely applied in the life sciences and general medicine for assessment of drug efficacy and toxicity, reproductive technology, and production of vaccines and biopharmaceuticals. However, challenges with the interpretation of the *in vitro* data persist due to effects of hyperoxic conditions of cell culture or improper mechanical environment (Yao and Asayama, 2017). Thus, optimising cell conditions ensures the maintenance of experimental reproducibility.

The essential requirements for cells to grow optimally include provision of substrate for cell attachment, a good incubator that provides the correct pH and osmolality, a controlled temperature system and the choice of an adequate growth medium. Of these essential factors, investigators suggest that for the maintenance of cell culture quality and generation of a good research outcome, it mainly relies on the quality of the culture medium, hence medium selection has become the most crucial aspect of cell culture (Arora, 2013). In order to investigate the hypothesis of this study, development of an *in vitro* co-culture model was required. This development implied a provision of an enabling environmental condition for the optimum growth of all cell lines proposed for this study within a co-culture setting. To this effect, various media were chosen and optimised relative to all cell lines. This was to maintain same culture conditions, generate robust data and to serve as a good quality control measurement.

Furthermore, following the optimisation of the co-culture model and the later acquisition of genotoxic evidence (chapter 4) of chemotherapy-induced bystander effect (CIBE), there became a need to investigate the potential cause of CIBE with a focus on the role of reactive oxygen species (ROS) and potentially drug elution or cytokines. This required the development of other functional assays that would potentially aid in determining ROS as a part of the CIBE

mechanism. These assays include: enzyme-modified comet assay, 8-OHdG antibody assay, 7,8-dichlorofluorescein diacetate (DCFDA) assay, Agilent Seahorse XF mito stress test, liquid chromatography and dual mass spectrometer (LCMS/MS).

This chapter describes the development an *in vitro* co-culture model for the BM cell line HS-5, with the myeloid (Kasumi-1) and lymphoblast (TK6 and AHH-1) bystander cell lines. It further describes the development and validation of the aforementioned functional assays that will aid in the investigation of the various mechanisms such as ROS involvement (Seahorse assay and enzyme modified comet assay) or drug elution (LCMS/MS) in CIBE.

3.2 Methods

3.2.1 Cell culture medium optimisation

The media employed in this study were DMEM/LG, DMEM/HG, DMEM/F12 and RPMI 1640 with varying supplementations (section 2.2.1). All cell culture procedures were performed as discussed in section 2.2. Cell line viability for the different culture media was determined using the trypan blue exclusion assay and automated LUNA cell counter (section 2.2.6).

3.2.2 Enyzme-modified comet assay

To assess the impact of oxidative stress on the co-cultured cells following indirect chemotherapeutic agents exposure, the traditional comet assay (section 2.6) was modified using the specific endonucleases, human 8-hydroxyguanine DNA-glycosylase (hOGG1) and Fpg (formamidopyrimidine DNA-glycosylase). Optimisation involved a titration based assay for a range of enzyme concentrations (0.05 units, 0.1 units, 0.15 units and 0.2 units) by titrating them against cells treated with potassium bromate (2 mM) as positive control. Comet analysis was performed as described in section 2.6.4 and full details of the enzyme modified comet assay are as detailed in section 2.6.5.

3.2.3 Antibody optimisation for 8-OHdG

The antibody (mouse monoclonal to DNA/RNA damage; Abcam) was optimised using the method described in section 2.8 with a few modifications. Cells which were directly exposed to the toxicants hydrogen peroxide (H_2O_2) and potassium bromate ($KBrO_3$), were titrated

against varying antibody concentrations (0 - 1µg/ml) for 1h and assessed by flow cytometry in comparison to untreated cells. Both the anti-DNA/RNA 8-OHdG antibody and the accompanying mouse antibody isotype control (ab18427; Abcam, UK) were optimised for high signal to background ratio, as well as appropriate penetration into the cells on a slide. The best fixative (methanol or 4% paraformaldehyde (PFA)) for immunofluorescence were also assessed. Different staining techniques (room temperature and at 4^0C; competitive binding assessed by applying both FITC 8-OHdG antibody and 4',6-diamidino-2-phenylindole (DAPI) counterstain at the same; and use of slides polished with and without 100% methanol) were applied. Images were acquired using the Nikon eclipse fluorescent microscope, whilst co-localisation of both the 8-OHdG and isotype control antibodies binding to the nucleus; counterstained with dapi was determined through acquisition of Z stack images on the confocal microscope as described in section 2.8.3.

3.2.4 DCFDA assay optimisation

Details of this assay are as described in section 2.7. This part of the study optimised a working concentration for the DCFDA dye, as well as produced a standard curve that would be used to extrapolate the data from the treated samples. To do this, varying concentrations (1 - 25µM) of the DCFDA fluorescent dye dissolved in DMF (N,N-dimethylformamide; 10mM stock) was used to incubate the cells in the dark for 45 minutes, washed and analysed by flow cytometry. Also, the DCFDA was tested with of DEM (diethylmaleate) and NAC (N-acetylcytesteine) to ascertain their capacities to inducer or scavenge ROS.

3.2.5 Agilent Seahorse XF mito stress test assay

To measure in real time the oxygen consumption rate (OCR) and extracellular acidification rate (ECAR) parameters as a function of the mitochondrial activity in the treated HS-5 cell line, it required an optimisation for a correct cell seeding density and a determination of the optimal concentration for the fluoro carbonyl cyanide-p-trifluoromethoxy phenyl-hydrazon (FCCP) solvent. Using the seahorse extracellular flux 24 (XFe24) microwell plate with surface area of 0.275cm^2, various cell seeding densities of the HS-5 cell line ranging between 2.5 x 10^4 - 30 x 10^4 were seeded, with and without the use of poly-l-lysine (50 µg/ml). Cell densities were analysed using the manufacturer's instructions for the Seahorse phenotype test assay. After the establishment of the appropriate cell seeding density, an assessment of the FCCP maximum

concentration for the cell line (HS-5) was performed, whilst adhering to the established mitochondria stress test protocol of the Seahorse assay (section 2.10). Upon completion of the program cycle, an automated report was generated and data analysed using Graphpad prism.

3.2.6 Liquid chromatography and tandem mass spectrometry (LCMS/MS)

3.2.6.1 Materials

- LC-MS grade acetonitrile (Fisher scientific, UK)
- LC-MS grade 0.1% formic acid in water (Fisher scientific, UK)
- LC-MS grade methanol (Fisher scientific, UK)
- LC-MS grade ethanol (Fisher scientific, UK)
- LC-MS grade formic acid (Fisher scientific, UK)
- LC-MS grade water (Fisher scientific, UK)
- 2ml amber screw top vials and blue screw cap (Agilent, UK)
- Agilent poroshell C18 column (2.7 µM; 3.0 x 50 mM)

3.2.6.2 Method

This method was optimised for chlorambucil with melphalan as internal standard and lidocaine as instrument standard. The drug choice was following the initial assessment of the above agents and other chemotherapeutic agents such as carmustine, etoposide, daunorubicin, teniposide, mitoxantrone, with theophylline as instrument standard.

3.2.6.2.1 Preparation of samples

All stock concentrations were prepared in acidified acetonitrile for chlorambucil (acidified with 0.1% v/v of hydrochloric acid), acidified methanol for melphalan (acidified with 0.1% v/v of formic acid) and in acidified acetonitrile for LID (acidified with 0.01% v/v of formic acid). All stock solutions were prepared to a concentration of 5 mg/ml and stored at -20^0C. The stock solution at 5mg/ml was a high concentration used for the initial double mass spectrometry (MS2) scan and was reduced to 1 mg/ml when the method was developed.

3.2.6.2.2 Instrumentation

This assay was optimised using the Agilent 1260 liquid chromatography series, interfaced to the Agilent 6460 triple quad LCMS/MS detector, equipped with a jet stream technology that

use the electrospray ionisation (ESI) to separate compounds. The instrument was coupled to a nitrogen gas source.

3.2.6.2.3 LC-MS conditions

Mobile phase A (80% volume of 0.1% formic acid in water) and B (20% volume of 0.1% formic acid in acetonitrile) were run for about 15 minutes each time to stabilise the binary pump pressure. The initial scan of the stock preparations was performed without the column for quick elution as there was no knowledge of the elution times for these agents, this allowed for setting of the detection parameters of the drugs. Subsequent assays utilised the C18 column maintained at 25^0C for separation of the drugs, and aliquots of 20 µl sample were injected onto the column. Samples were eluted with the optimised gradient for the respective mobile phases (0 -2 minutes at a ratio of 80:20 for 0-2 minutes; 60:40 for 2 – 6 minutes and 30:70 for 6 – 8 minutes) delivered at 0.6 ml/ml, and sample flow rate of 0.2 ml/min, with a post run time of 5 minutes. The triple quadrupole mass spectrometer was utilised for analyte detection as performed in the positive ESI in multiple reaction mode (MRM).

3.2.6.2.4 MS2 scan

A 200 µl volume of the stock preparations was loaded into the Agilent amber vial and 10 µl injected onto the column. The instrument was set to MS2 mode and detection mode of ESI with a run time of 1 minute (this was adequate as no column was used and the analyte eluted quickly). The molecular weight and formula of the analyte was input into the optimizer software and all the other settings were by default. Following the MS2 scan, an MRM method was set up, using the ion abundances detected by the MS2 scan. Two ion transitions (product and precursor ion) was input for each analyte. Various mobile phase phases, internal standards and different mobile phase gradients were attempted, starting with no end time initial runs, until the optimal method was determined.

3.2.6.2.5 Preparations of standards

Following the optimised parameters for these agents, various concentrations of CHL were prepared ranging from (0.1 – 10 µM), while MEL and LID were 500 µg/L and 20 µg/L respectively. Standards were prepared in an intermediate solution containing 50% of (80% mobile phase A; 20% mobile phase B) and 50% of (acetonitrile acidified with 0.1% HCL).

Samples were vortexed briefly and stored in the fridge until analysis. Standards were optimised at room temperature, between 2 to 8^0C and also on ice (all samples were prepared at the same time, placed into an ice box with well fitted cover and placed in a refrigerator). Samples were run in triplicates including a mobile phase blank, whilst enabling needle wash on the instrument after each sample injection. The intermediate solution served as the sample solution preparation solution for all other assay.

3.2.6.2.6 Extraction efficiency

Chlorambucil (2 and 10 µM) and melphalan (500 µg/ml) were spiked into culture medium and various solvents explored for their extraction. These solvents include diethylether: dichloromethane (3:2 v/v); ethylacetate; and ethylacetate: hexane (1:1). Samples were pipetted into the falcon tubes and solvents added, vortexed and freezed at -20^0C for 30 minutes, after which the aqueous layer was separated and dried under a stream of nitrogen gas. Upon adding the intermediate solution (section 3.2.6.2.5), vials were vigorously shaken and refrigerated on ice prior to analysis. A blank sample of just mobile phase was added to the run and each vial analysed in triplicate with a wash (intermediate solution) run after each solvent.

3.2.7 Statistical Analysis

Data presented are that of mean ± SD for three independent biological repeats. Results were analysed using on the Microsoft excel, computing the average, standard deviations and statistical significance (p values) between untreated control and treated within a group and statistical significance was considered as $p < 0.05$. These direct comparisons was analysed using the Student t-test.

3.3 Results

3.3.1 Evaluation of optimum culture conditions for cell lines

The cell lines used in this study were cultured in different culture medium and growth monitored until about 80-90% confluent. The culture medium that propagated the best healthy cell growth and proliferation for all cells lines was used in the *in vitro* co-culture model. HS-5, TK6, AHH-1 and Kasumi-1 cells were grown in different culture medium over 72 hours (closest to HS-5 doubling time). Photographs of the HS-5 cell morphology were taken and cell viability was assessed for all the cell lines at 24, 48 and 72 hours.

3.3.1.1 HS-5 cell line

HS-5 cell line maintained a typical BM tissue culture plastic adherence and showed a fibroblast-like morphology for all the culture media tested except for its appearance in RPMI 1640 supplemented as the conventional AHH-1 growth medium, where it appeared to lose its plasticity and morphology (Figure 3.1). Qualitatively, in comparison to a typical primary MSC morphology (Figure 3.1), the fibroblast morphological projections appeared most closely aligned with the cells grown in standard RPMI 1640 medium, whereas the other media demonstrated morphology closer to endothelial cells, even for DMEM/HG which is its recommended medium. At 24 hours all cells thrived very well with some adhering to the culture flask except for the AHH-1 medium which floated in colonies. Whilst all other cells increased to cover the culture flask surface area as the cells proliferated and divided, the RPMI supp. medium rather decreased in cell number as observed at 48 and 72 hours. At 72 hours, all other media showed cell confluence, with growth consistency and the vast majority of the cells appeared massively populated in DMEM/HG, although its fibroblast projections were of length compared to the others.

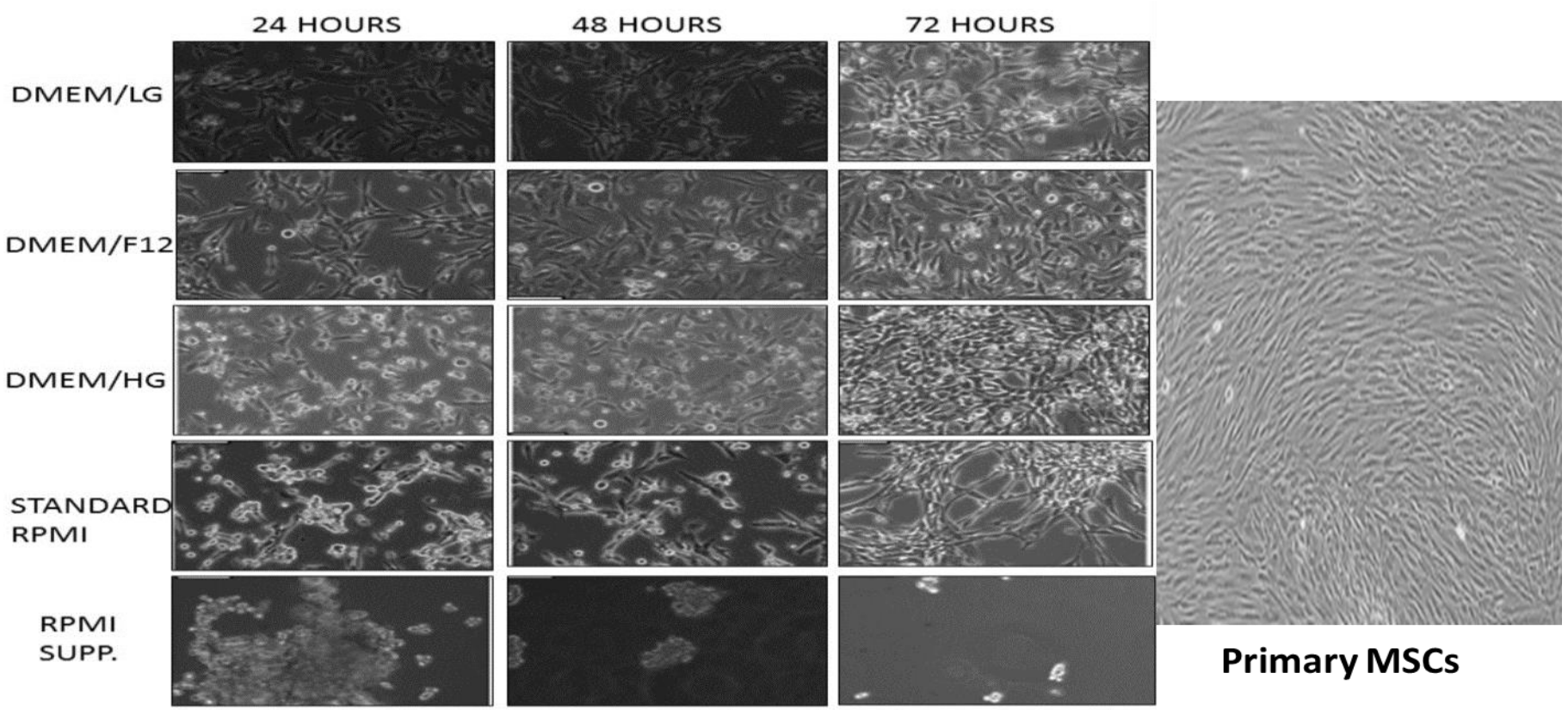

Figure 3.1: Morphology of HS-5 in different culture media. Representative photomicrographs of HS-5 cells cultured in DMEM/LG, DMEM/F12, DMEM/HG, RPMI and RPMI supplemented with horse serum, (a composition for AHH-I cells culture; RPMI SUPP.). Cells were seeded at 2.5 x 10^4 per cm^2 in a 12 well plate and images were taken with an inverted light microscope every 24 hours over 72 hours at x10 magnification. Primary MSCs (Cyagen Biosciences, US) are also depicted to show comparison of morphology to the HS-5 cell line. HS-5 cells showed gradual adherence, dividing and multiplying to cover the cell surface area and showing good cell growth of the HS-5 cells over 24, 48 and 72 hours with exception of cells grown in RPMI SUPP.

Quantitatively, all cultures were assessed for total cell numbers (not shown), total live cell numbers (Figure 3.2a) and viability for the culture (Figure 3.2b). Data show better cell growth and viability in DMEM-HG thereby validating the manufacturers recommended culture medium. DMEM/LG at 60% cell viability was just a bit more viable than RPMI 1640 which had a cell viability at about 55%. DMEM/HG as expected had both the highest total cell number ($1x10^6$cell/ml/72hrs) and best cell viability (70%).

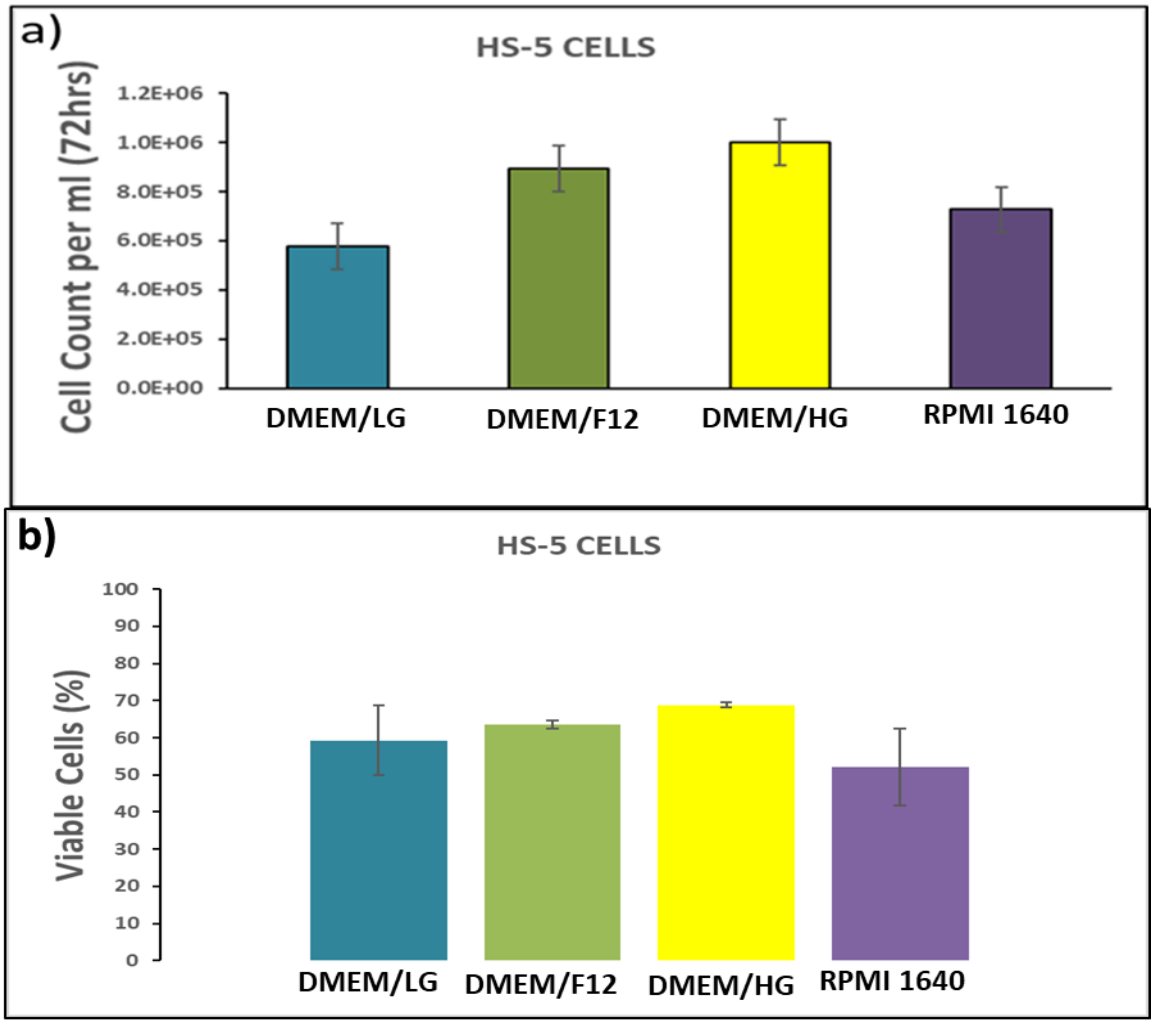

Figure 3.2: HS-5 total live cells and percentage viability. Cells seeded at 2.5 x 10^4 per cm^2 were trypsinised after 72 hours, estimated for total live cells (a) and percentage viability (b) by trypan blue exclusion assay. Data presented are for mean ± SD of three biological repeats. Cells generally show good cell viability in all. DMEM/LG=Dulbecco's Modified Eagle Medium in low glucose, F12=Hams F12 nutrient mixture, HG=high glucose, RPMI 1640=Rosewell Park Memorial Institute medium.

3.3.1.2 TK 6 cell line

Using an initial cell seeding density of 3 x 10^5 cells/ml, the TK6 cells were quantified for their total number of live cells and percentage viabilities in the four different culture media and at different time points (Figure 3.3), as described for the HS-5 cell line. At 24 hours, the TK6 cell in various culture media showed good cell numbers at about 5 x 10^5 cells/ml for all media. While there was increased growth in DMEM/HG, DMEM/F12 and RPMI 1640 at 48 hours, the DMEM/LG stayed relatively the same.

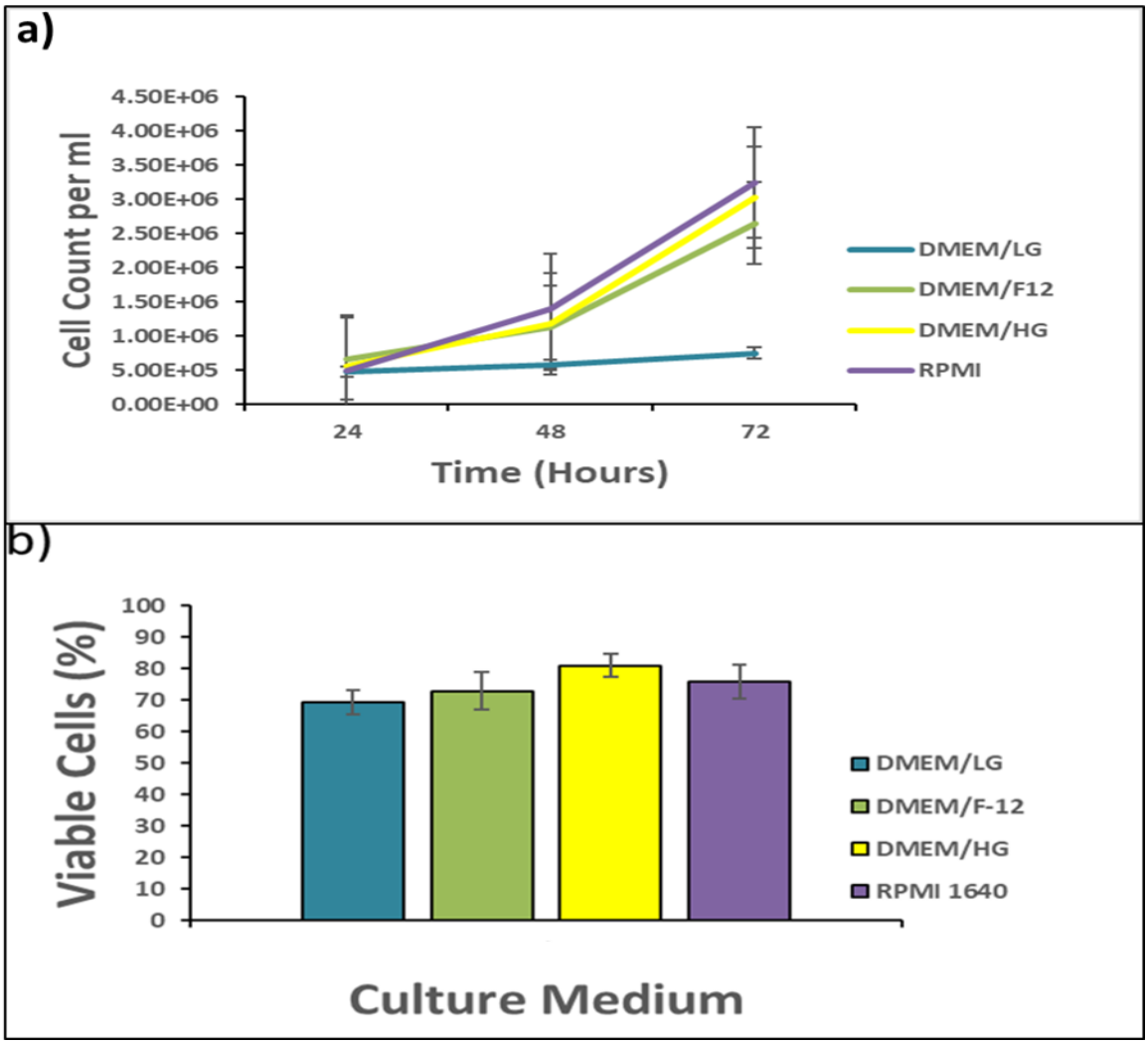

Figure 3.3: Total live cells of TK6 in different culture media. TK6 Cells were seeded at a density of 3 x 10^5 cells/ml and total cell count per ml (a) was determined every 24 hours for 3 days in T25cm^2 flask and cell viability measured at 72 hours (b). Data is represented as mean ± SD (n=3). DMEM/LG show low cell count, but media cell viabilities are >60%. DMEM/LG=Dulbecco's Modified Eagle Medium in low glucose, F12=Hams F12 nutrient mixture, HG=high glucose, RPMI 1640=Rosewell Park Memorial Institute medium.

All media except the DMEM/LG doubled in cell population every 24 hours to reach estimated cell numbers of 2 x10^6 cells/ml for both DMEM/HG and DMEM/F12, while RPMI 1640 was at 3 x 10^6 cells/ml at 72 hours. Their corresponding cell viability assessed at 72 hours revealed DMEM/HG with the best cell viability in comparison to other media. While the cell viability of DMEM/HG was at 80%, RPMI 1640 showed 75% cell viability, with DMEM/F12 at 70%. As observed with the total cell counts per ml, DMEM/LG showed the least cell viability (65%).

3.3.1.3 AHH-1 cell line

AHH-1 cells data (Figure 3.4) was grown in same culture medium as with TK6 (section 3.3.1.2) with the addition of its conventional growth (RPMI supp.), which unsurprisingly was the best of all media since it is the recommended culture medium supplementation. It showed a total cell number of 3 x 10^6 cells/ml at 72 hours, while the second best medium (RPMI 1640) had a total cell number of 2.5 x 10^6 cell/ml at 72 hours.

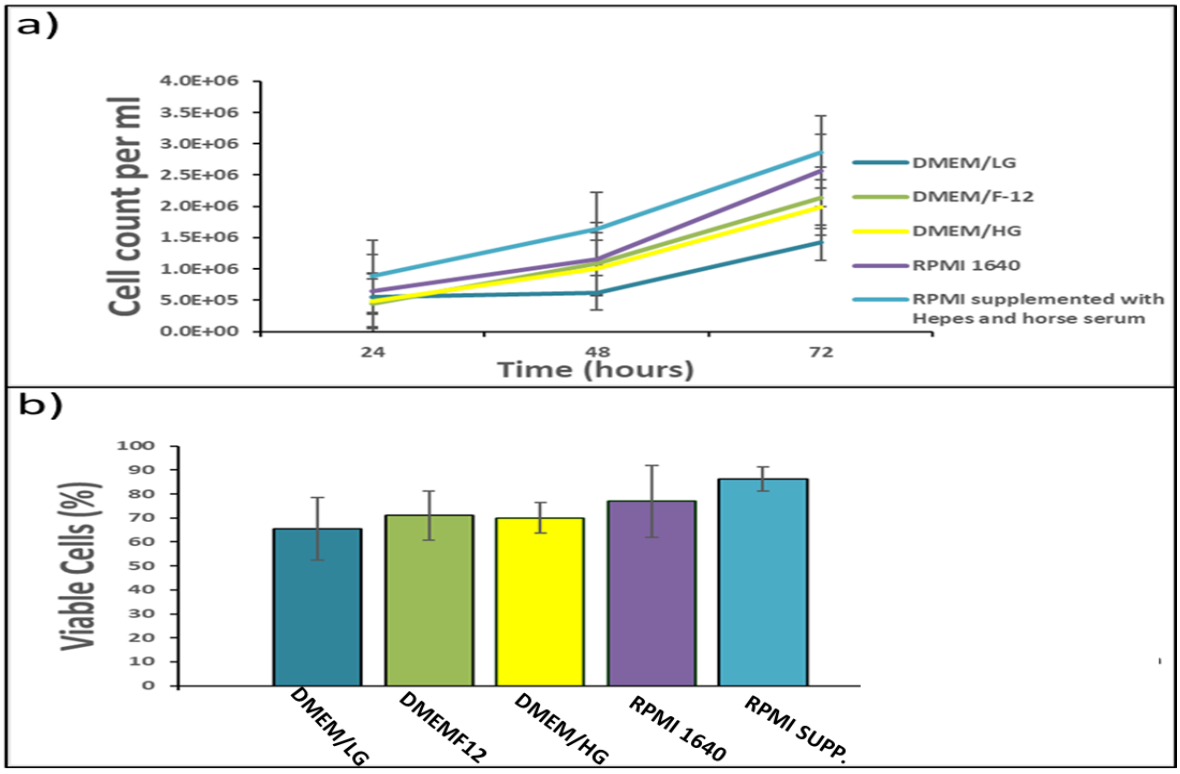

Figure 3.4: AHH-1 cells in different culture media. Cells seeded at 3 x 10^5 cells/ml were estimated for the total number of cells/ml (a) and percentage cell viability (b) count at 72hours. Percentage counts were plotted as mean ± SD for three separate repeats. DMEM/LG=Dulbecco's Modified Eagle Medium in low glucose, F12=Hams F12 nutrient mixture, HG=high glucose, RPMI 1640=Rosewell Park Memorial Institute medium. Recommended media (RPMI supplemented with hepes/horse serum) had better cell growth in all.

DMEM/HG and DMEM/F12 showed similar cell viabilities at 24 and 48 hours, although the DMEM/F12 revealed an increase above the DMEM/HG at 72 hours. DMEM/LG was increased and higher than both DMEM/F12 and DMEM/HG at 24 hours. However, it witnessed a decrease in cell viability at 48 hours, but this decline recovered at 72 hours to reveal a total cell number of 1 x 10^6 cells/ml. All cell viabilities were good for every medium, with RPMI supplemented medium at 80%, showing the highest just above the RPMI 1640 at 75%. DMEM/F12 and DMEM/HG were about the same level at 70% cell viability while DMEM/LG showed a 60% cell viability. These data collectively suggest good cell growth and cell viability for all media, but compared to the HS-5 data and in an attempt to select one best culture medium, DMEM/HG appeared to support all cell types most successfully.

3.3.1.4 Kasumi-1 cell line

Kasumi-1 cells data (Figure 3.5) was grown in same culture medium as other bystander cells (section 3.3.1.2 and 3.3.1.3) and as with these other cell lines it showed better cell count cell viability in the recommended media (RPMI; which was supplemented 20% FBS). All cell were seeded at 3 x 10^5 cells/ml and cell counts estimated every 2 hours over 3 days. DMEM/LG did not do well over all as it showed just 50% cell viability at 72 hours, with no major cell growth and witnessed a decrease in cell number at 24 hours 1.5 x 10^5 cells/ml, slight increase at 48 hours but a further decline at 72 hours (1.5 x 10^5 cells/ml). DMEM/F12 had some increase in cell population almost twice its original cell number. Overall, there was a total cell number between 4 x 10^5 to 6 x 10^5 cells/ml from 24 to 72 hours, with cell viability of about 70%. DMEM/HG also showed good turn over, rating the second best. It had cell numbers increasing from 5 x 10^5 at 24 hours to 7 x 10^5 at 72 hours, showing same cell viability (70%) as DMEM/F12. RPMI was the best and of course the manufacturers recommended cell culture medium. At 24 hours cell numbers were at 5 x 10^5 cells/ml, to double at 48 hours (6 x 10^5 cells/ml) and a further increase (9.5 x 10^5) at 72 hours. RPMI also had the best cell viability (75%) overall.

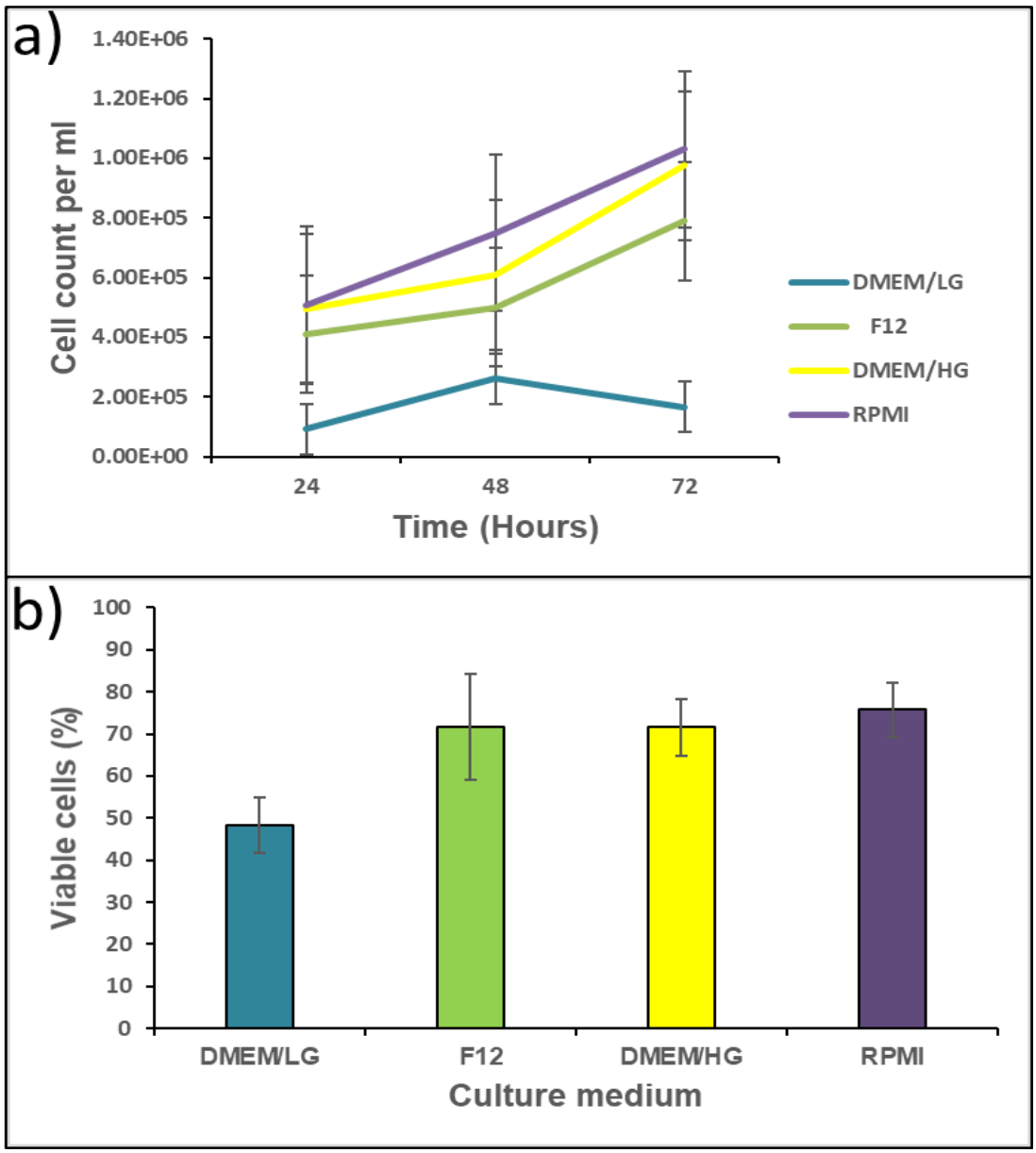

Figure 3.5: Total live cells of Kasumi-1 in different culture media. Kasumi-1 cells were seeded at a density of 3 x 10^5 cells/ml and total cell count (a) was determined every 24 hours for 3 days in T25cm^2 flask and cell viability measured at 72 hours (b). Data is represented as mean ± SD (n=3). DMEM/LG show the lowest cell count, with cell viabilities at 50%. DMEM/HG, F12 and RPMI had great cell viabilities at >70%. DMEM/LG=Dulbecco's Modified Eagle Medium in low glucose, F12=Hams F12 nutrient mixture, HG=high glucose, RPMI 1640=Rosewell Park Memorial Institute medium.

3.3.2 Optimisation of the enzyme modified comet analysis

Evidence from this study (Figure 3.6) showed the capacity of these two enzymes to detect oxidative lesions in the DNA. The hOGG1 had a relatively stable control (4%) value at all incubation times, whereas the Fpg, which showed a continual increase at all-time points measured, rising from about 5% at 10 minutes to 20% DNA tail intensity at 40 minutes. This suggests that fewer non-specific cuts occur with hOGG1 than with Fpg.

Whilst hOGG1 was very stable for the untreated control and did not introduce non-specific cuts over the various incubation times, Fpg was non-specific and cuts increased dramatically with increased incubation time which is cause for concern. However, Fpg demonstrated a dose response in its ability to induce strand breaks with increasing number of enzyme units, whereas hOGG1 exhibited an efficient strand break induction, but no dose response observed with increasing enzyme units. While an increased strand break induction was observed with enzyme units 0.1, 0.15 or 0.2U over all incubation times, 0.2U was not as efficient as the lowest enzyme units. Use of hOGG1 at 0.05U did not appear suitable, as overall low tail intensity was detected and this did not improve with incubation time.

Overall Fpg created more DNA fragmentation, represented by increased comet tails, but this must be taken with caution given the observation of the untreated control. In summary, because of the ability of hOGG1 and Fpg to recognise different lesions, both enzymes were used in the final assay, but Fpg was used at 0.2U and hOGG1 was used at 0.15U, both for a 30 minutes incubation time.

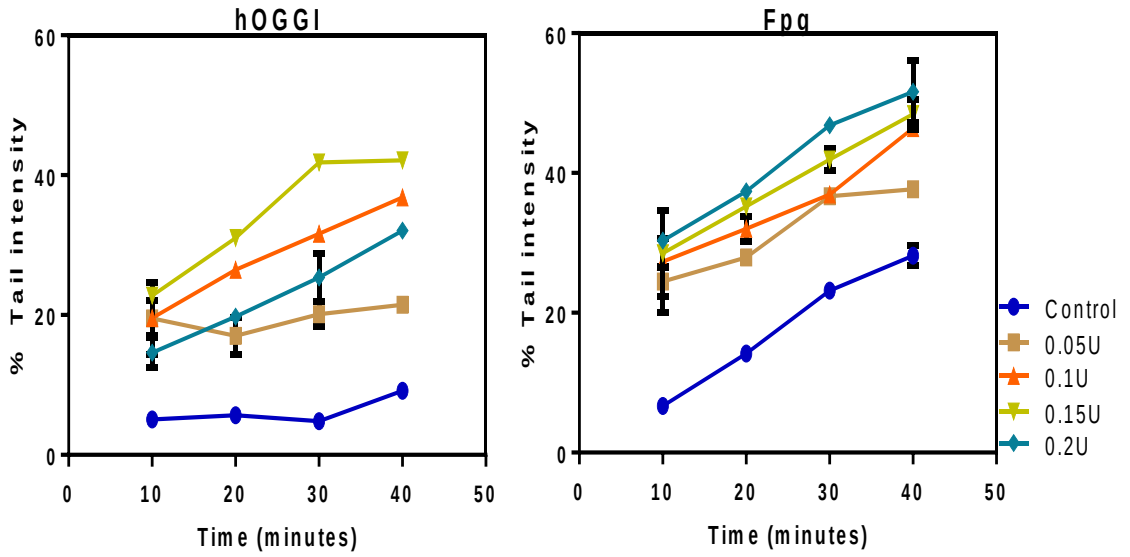

Figure 3.6: The detection of DNA fragmentation in TK6 using DNA endonucleases. TK6 cells were exposed to $KBrO_3$ (2 mM) as a positive control, analysed with hOGG1 and Fpg endonucleases, to detect oxidative lesions induced in the DNA. Following toxicant ($KBrO_3$) exposure, cells were treated with different enzymes units, using the enzyme modified comet assay method of Smith *et al.,* (2006). Data is shown for mean and SD of three separate repeats (n=3) and reveal 0.15 units were better for the hOGG1 while 0.2 units was better for Fpg.

3.3.3 Oxidative damage detection using the anti-DNA/RNA damage antibody with 8-OHdG specificity

The median fluorescent intensities (MFI) determined for the mouse monoclonal to DNA/RNA damage responded well when tested for the basal level of detection with untreated TK6 cells.

Whilst there was a clear dose response increase in both MFI and percent positive cells in the untreated sample after about 2 µg/ml for the anti-DNA/RNA damage antibody (Figure 3.7; 2a), conversely there was little response from the isotype control (Figure 3.7; 1a) with only a subtle rise after about 4-8 µg/ml. It would be expected to have baseline oxidative damage even in untreated cells, but the rise in binding for both antibodies suggests non-specific binding at these higher concentrations, however there generally is low non-specific binding by the isotype control. Corresponding histogram on the FITC channel for the antibody responses are depicted for isotype (Figure 3.7; 1b-c) and 8-OHdG detection antibody (Figure 3.7; 2b-c).

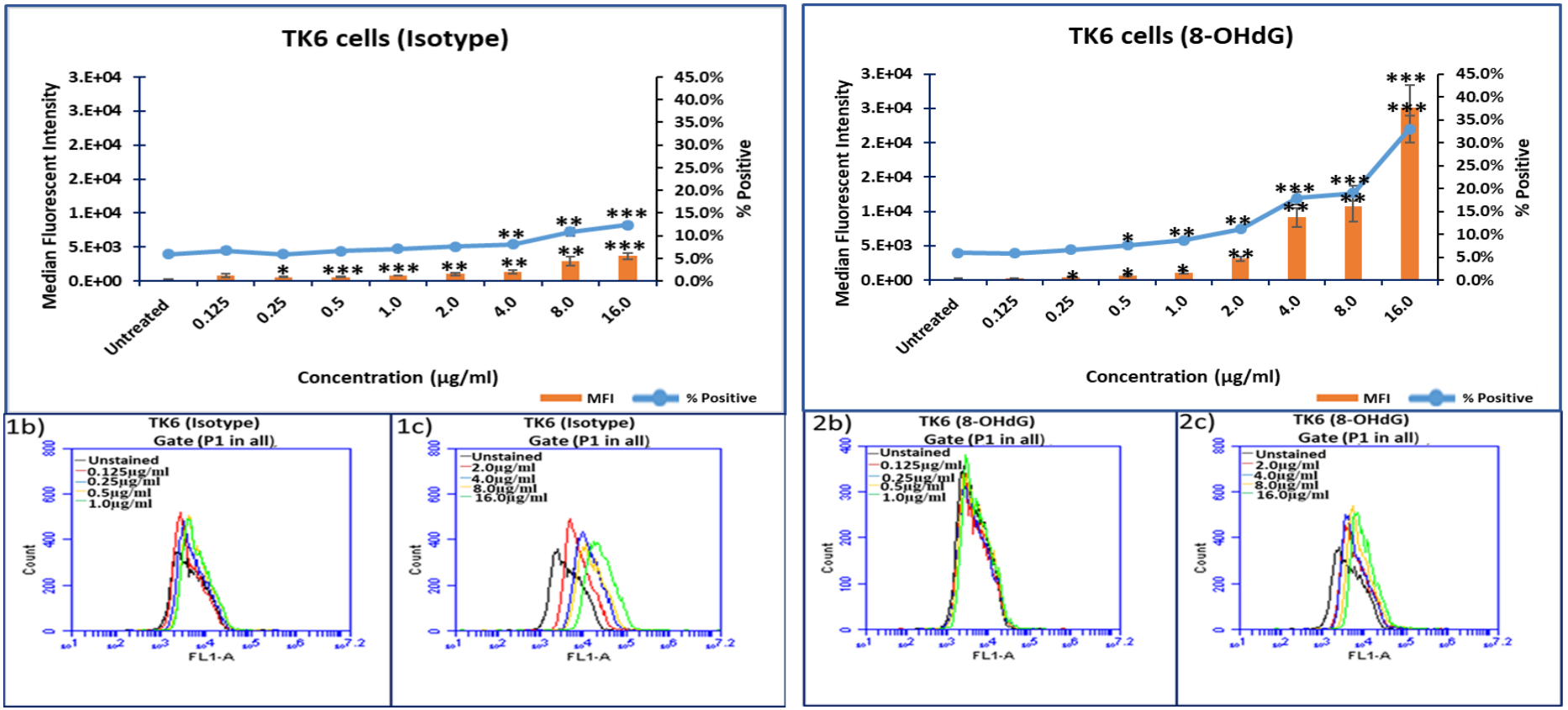

Figure 3.7: The median fluorescent intensity in TK6 cells using the anti-DNA/RNA 8-OHdG and isotype antibodies. The titration levels of these antibodies were determined in cells after fixation in 4% PFA on ice for 10 minutes. Cells were washed in PBS mixed in 0.1% triton X and sodium citrate, blocked with 0.01% bovine serum albumin in PBS for 1h. Data show the MFI and percent positive cells (1a), with representative histograms (1b and 1c) for the isotype antibody control. Also shown is the MFI and % positive cell evidence (2a) and the representative histograms (2b and 2c) of 8-OHdG range of concentrations (0.125 – 16 µg/ml) tested. Data is presented for three individual experiments n=3 and statistical significance shown for *$p \leq 0.05$, **$p \leq 0.01$, ***$p \leq 0.001$ as analysed using student T-test.

Following the initial titration with the untreated controls, the positive controls were analysed and presented in figure 3.8a (peroxide) and figure 3.8b (potassium bromate).

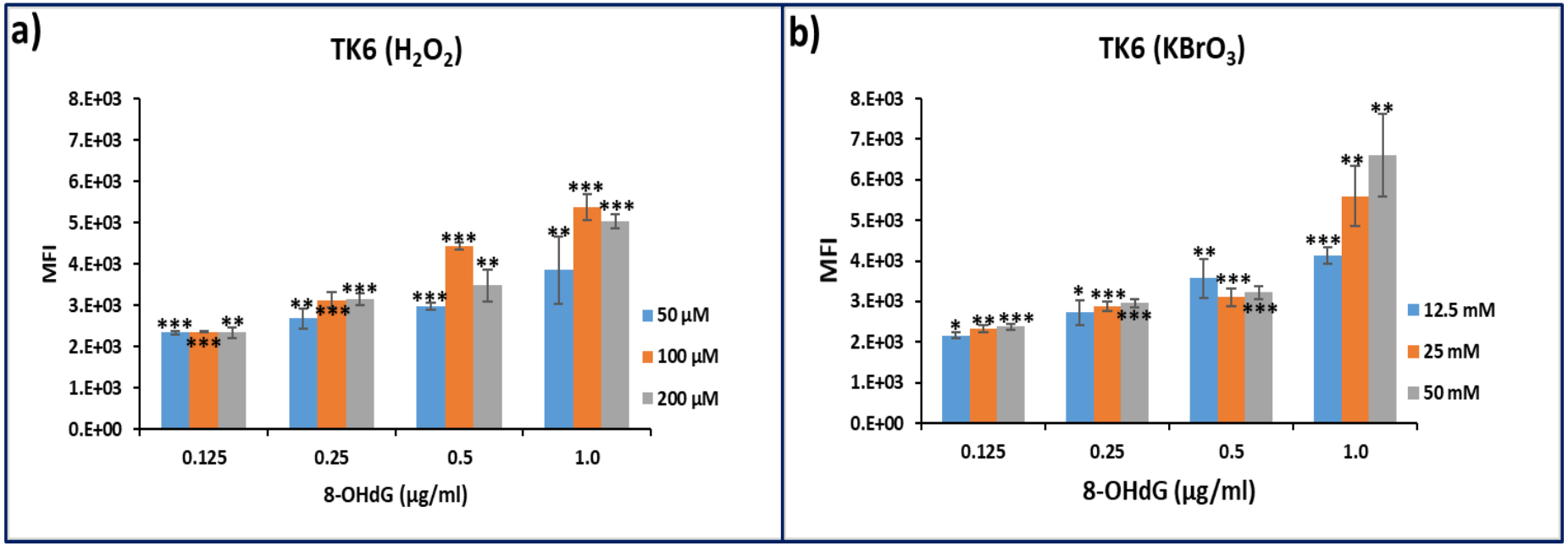

Figure 3.8: 8-OHdG detection in H_2O_2 and $KBrO_3$ treated TK6 cells. Cells were treated with H_2O_2 (figure a) and $KBrO_3$ (figure b) for 1 and 3 hours respectively. After fixation in 4% PFA and blocking in 1% BSA/PBST, cells were incubated with the antibody in the dark for 1h and evaluated with flow cytometry following three washes in PBS. Data represents three separate experiments (n=3) with statistical significance shown as *$p \leq 0.05$, **$p \leq 0.01$, ***$p \leq 0.001$. Overall, the detection with 1 µg/ml seemed appropriate for both treated conditions.

For the positive controls data, the accrued TK6 data (Figure 3.8a-b), show the effect of both toxicants on the cells. While 50 µM gave the lowest oxidative damage amongst the H_2O_2; the 100 µM showed higher damage induction than the 200 µM, which may reflect some cell death at the higher dose. The H_2O_2 showed increased MFI from 2 x 10^3 of the lowest concentration to 5 x 10^3 at 1 µg/ml (highest dose). Apart from the decreased MFI observed for 200 µM at 0.5 µg/ml, it showed a comparable MFI levels with the cells at 100 µM peroxide. $KBrO_3$ on the other hand, witnessed similar strength in activity for the lowest concentrations (0.125 – 0.5 µg/ml) to show an MFI of 2.7 x 10^3 at 0.5µg/ml. Except for the lowest $KBrO_3$ concentration (12.5 mM), all other concentrations showed differences with the 1 µg/ml concentration. Both H_2O_2 and $KBrO_3$ showed a rise in the MFI, corresponding to 5 x 10^3 and 6 x 10^3 respectively. Thus, the data suggests better detection with 1 µg/ml for both treatments.

Following the positive controls evaluation, slides were prepared for a positive evaluation of localisation of the antibodies to the DNA/RNA. This posed some difficulties, e.g. evidence of artefacts and low fluorescence of the FITC signal for the 8-OHdG antibody. Therefore, some troubleshooting was performed such as robust polishing of the slides with methanol (Figure 3.9) and wiping dry with tissue to assess if the tissues or unpolished slides produced the artefact

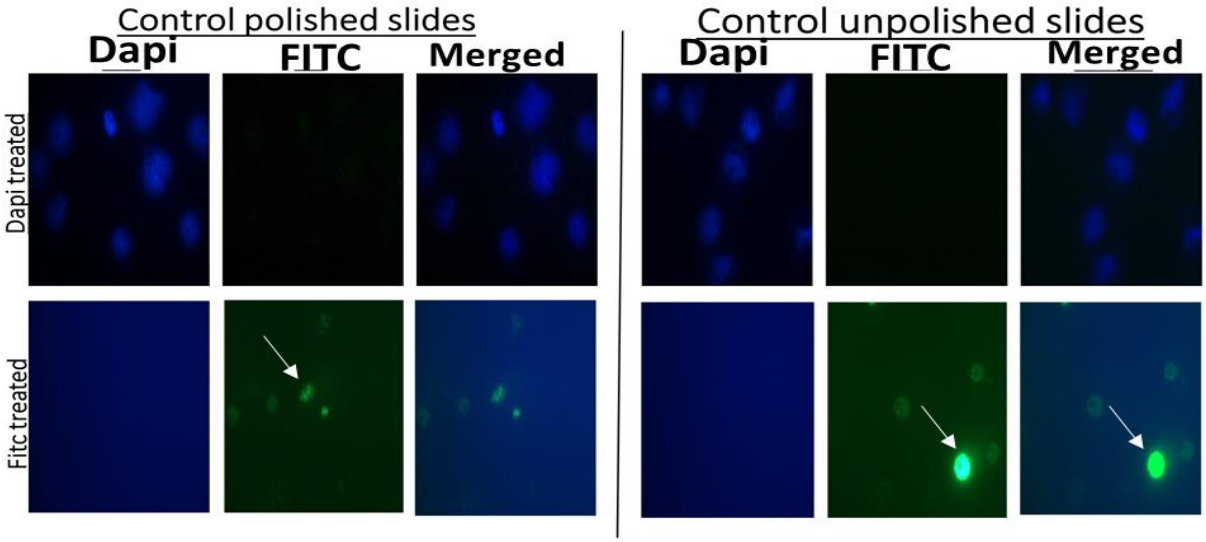

Figure 3.9: Assessing the effect of polishing slides with methanol for possible artefacts. Slides were ensured grease free using 100% methanol. This experiment compared the single DAPI treated cells with the FITC stained cells with and without slide polishing. There was no observable differences between the two conditions, there was still presence of artefact in both cases for the FITC filter. White arrows describe artefacts; Images (20x).

Analysis of the slide polishing effect (Figure 3.9) on cells did not improve the slide quality and if anything, both the polished and unpolished showed artefacts in the FITC filter. The DAPI filter showed clear images, suggesting artefacts were from something else. Thus, an assessment of methanol fixative, was determined. At the same time, stain uptake was determined.

The methanol fixed samples (Figure 3.10) show good stain penetrations for the individual filters, but there were some artefacts on the FITC filter for the chemotherapeutic agents used. The merged filters for the untreated cells show the DAPI centrally placed in the nucleus, and some FITC appeared in the cytoplasm, which was not unexpected, as this antibody also should detect RNA and mitochondrial DNA damage. The carmustine and chlorambucil direct treatments showed good stain uptake but also revealed increased background staining which may be possible cell membrane damage, but this did not appear on the control slide, although it could be more visible if labelled.

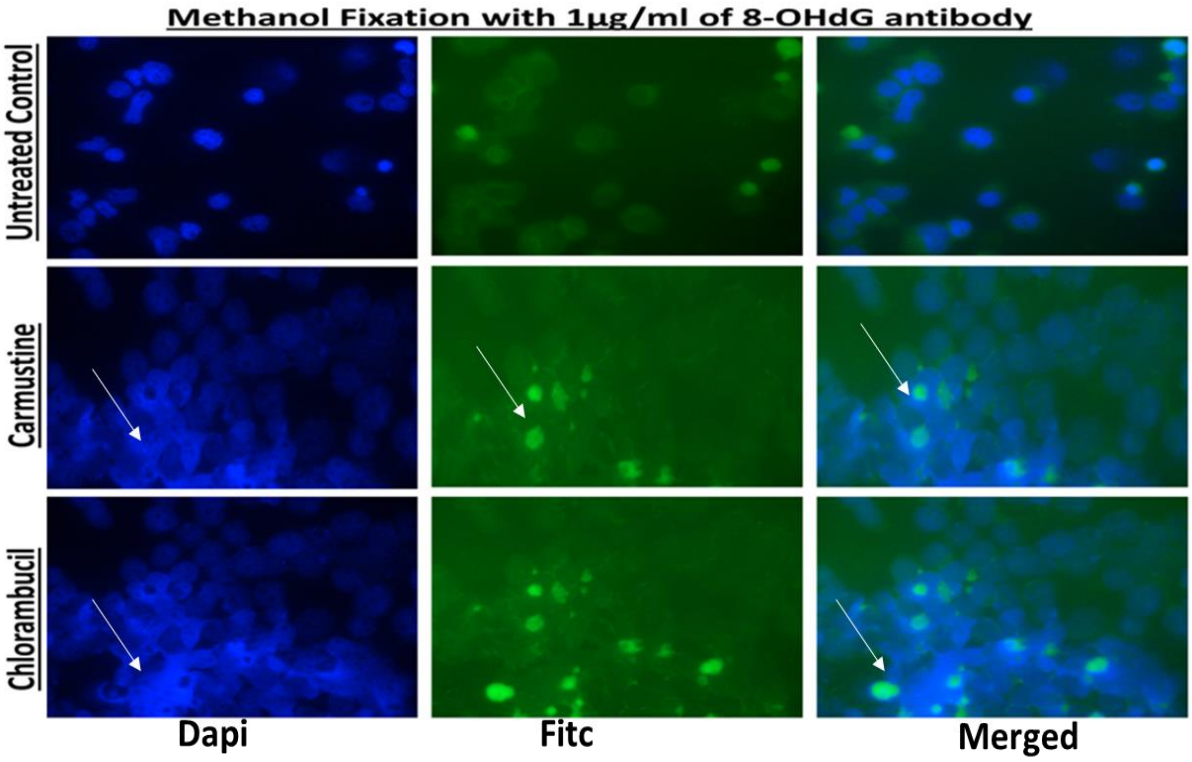

Figure 3.10: Assessment of methanol as a fixative for the cells. Tk6 cells were used to assess methanol fixing capacity after 1h direct treatment with clinical relevant doses of carmustine (8 µM) and chlorambucil (4 µM), with an untreated control. Cells were harvested and fixed on ice for 10 minutes, blocked and stained with the 8-OHdG antibody. Cellular morphology appeared acceptable with 10 minutes incubation on ice for methanol. White arrows show the increase of background stain uptake in the form of artefact.

With the observation that carmustine and chlorambucil appeared to have higher background staining, 4% PFA was assessed for use as an alternative fixative to determine if PFA gave better resolution and less background, whilst also ensuring the stain uptake by performing an overnight incubation at 4^0C. The data for the fixative assessment (Figure 3.11) using the isotype and 8-OHdG antibodies in untreated cells revealed good stain uptake for the two stain concentrations (0.5 – 1 µg/ml). All the fluorescence signals were visible and well stained, except for the few artefacts observed in 8-OHdG with FITC. This showed that 4% PFA was a preferable fixative with these antibodies, based on low artefact detection.

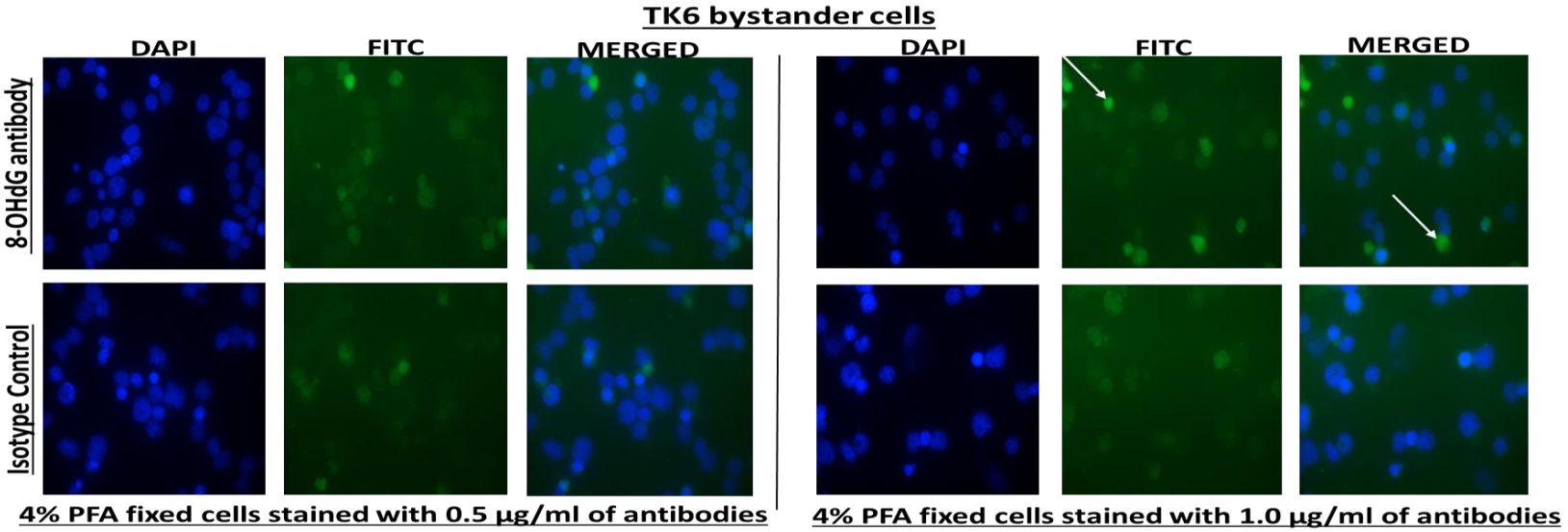

Figure 3.11: Assessment of 4% paraformaldehyde (PFA) as a fixative for 8-OHdG antibody. PFA (4%) was used to treat the cells for 10 minutes on ice, and fixative were gently aspirated following incubation. No further centrifugation steps were performed after cell washes, a method which was found not to distort the cellular morphology. DAPI filter gave a better resolution than FITC. Generally, results show good fixing for the cells investigated and no morphological distortion. Images were taken using the x20 magnification and white arrow describes spots of background staining or artefact.

Due to the improvement in signal and background, the confocal microscope was used for ascertaining the localisation of the antibody within the cells, which was expected to stain DNA in the nucleus, RNA and mitochondria in the cytoplasm. The assessment using confocal microscopy demonstrates the sectional images and direction of the antibody body staining for both the axial Z (show depth and optical plane) and lateral Y (specimen plane) direction. The data analysis in the untreated TK6 cells (Figure 3.12) for the cross sectional depths of the cells, show the presence of both stains in the cell (nucleus and cytoplasm).

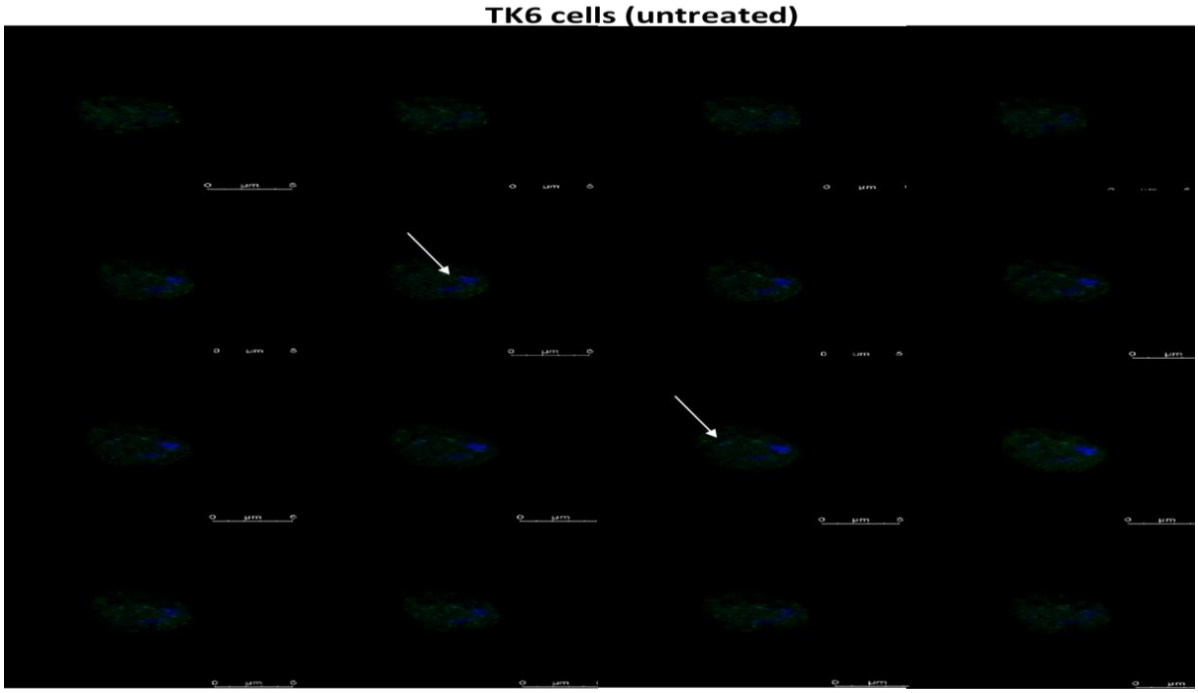

Figure 3.12: Representative image of the localisation of anti-DNA/RNA detection antibody. Cells were prepared in 4% PFA and after blocking with 1% BSA/PBST, cells were stained overnight at 4^0C. The confocal microscope was utilised to take 40 Z-stack images of cell nuclei DAPI (Blue) and 8-OHdG antibody FITC stain (Green). Images show the baseline detection of 8-OHdG in TK6 cells and localisation to both nucleus and cytoplasm, as this antibody detects RNA damage as well as 8-OHdG in the mitochondria.

A positive control slide using 50 µM H_2O_2 was determined in Kasumi-1 (Figure 3.13). The data shows co-localised images of both the FITC and the DAPI, with an observation of some FITC within the cytoplasm, surrounding the nucleus, suggestive of oxidative damage staining in the mitochondria. These data showed a good stain uptake and antibody penetration and because different cell lines were used the method was thus optimised for 1 µg/ml antibody using 4% PFA as fixative and overnight antibody staining at 4 ^{0}C.

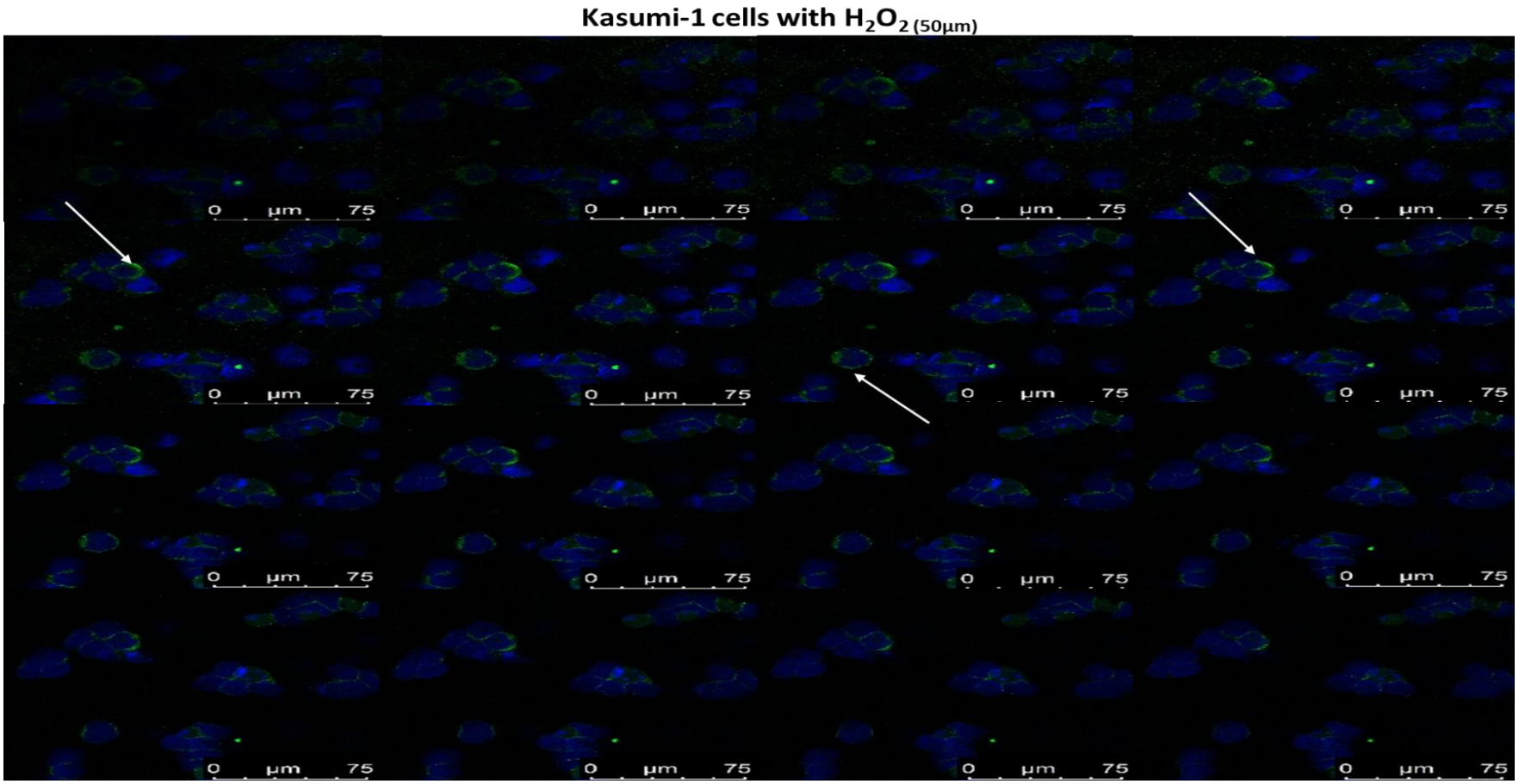

Figure 3.13: Representative image of the localisation assessment using 50 µM of H_2O_2. . Slides were treated with peroxide to assess the localisation of the 8-OHdG (FITC, green) antibody, counterstained with DAPI (blue). The image shows localisation to the nucleus, but also demonstrates the presence of some damage detected within the cytoplasm, possibly of RNA or mitochondrial origin. Images were taken using 40x magnification and a scale 75 µM. Treatment with H_2O_2 was used in validation of the assay.

3.3.4 DCFDA evaluation

The DCFDA assay was used to determine the presence of intracellular ROS in the HS-5 cells and the method was optimised for the concentration required to differentiate ROS levels in the cells. The HS-5 untreated cells data (Figure 3.14a) shows increased MFI detected with increased concentration of DCFDA ranging from 1 x10^6 to 7 x 10^6 from lowest to highest. This increase was statistically significant (*p≤ 0.05) for the two highest concentrations (20 µM and 25 µM) when compared to the unstained untreated control.

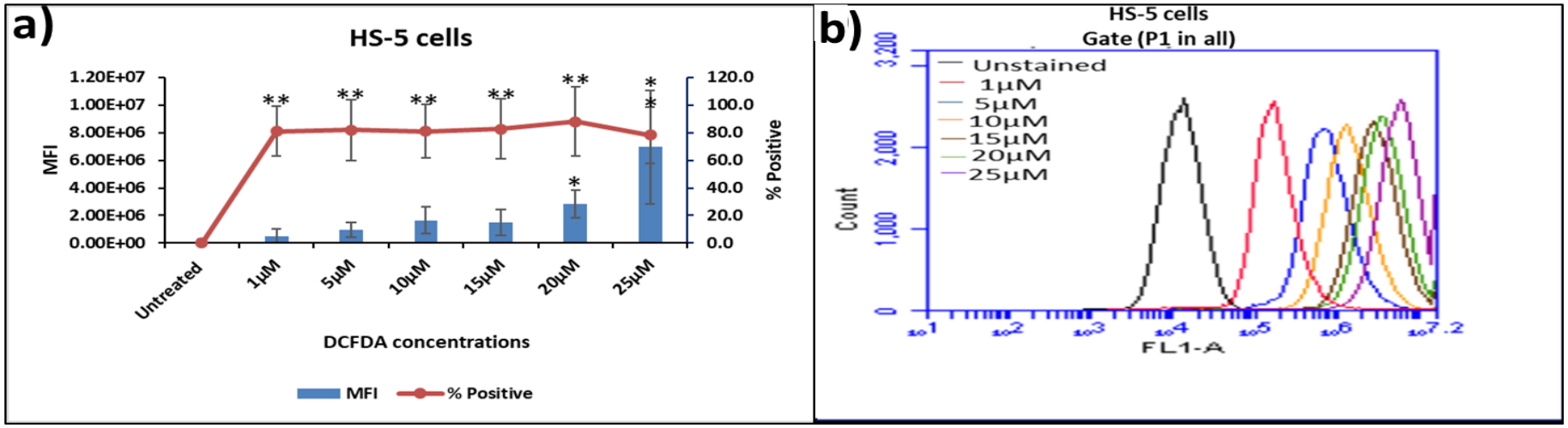

Figure 3.14: The DCFDA fluorescent dye optimisation in HS-5 cells. Cells were stained with varying concentrations of the DCFDA dye in the dark for 45 minutes after fixing in 4 % PFA for 10 minutes and permeabilised with a solution of 1% triton X and sodium citrate. Cells were washed 3 times with PBS and analysed by flow cytometry. Figure 3.14a shows the MFI (blue bars) and % positive cells (red line). The cells were analysed against an DCFDA untreated control sample. Figure 3.14b show the histogram plot of the analysed concentrations and their varying strengths shown as colour coded. Results show 1 µM to be effective and less toxic to the cells. Data is shown for three separate experiments (n=3), where statistical significance is stated as *p ≤ 0.05 and ** p ≤ 0.01, analysed using student T-test.

The percent positive cells (Figure 3.14a) were statistically significant (*p≤ 0.05) at 80% for all these concentrations (1 – 20 µM), but showed a slightly decreased value (70%) for the final concentration, with statistical significance of *p≤ 0.05. The FITC peaks distribution (Figure 3.14b) for the positive cells shows a shift towards the right as the DCFDA dye concentration was increased with the lowest 1 µM closest to the untreated unstained control.

Furthermore, a standard curve (Figure 3.15) was generated using different $KBrO_3$ concentrations from 3 to 400 mM. A baseline MFI of 5 x 10^3 was observed with $KBrO_3$ 3.12 mM to 25 mM concentrations, which had same MFI with both the untreated unstained control and DCFDA treated control. The initial measurements from 0 to1h did not have any effect detect but started to rise to detectable levels at 3 hours. However, at 6 hours, concentrations of 50 to 400 mM revealed an increased fluorescence with a dose response for each concentration up to the 24 hour time point. All the lowest concentrations (3.12 – 25 mM) stayed relatively same as the untreated control, showing no oxidative damage detection for all measured time points.

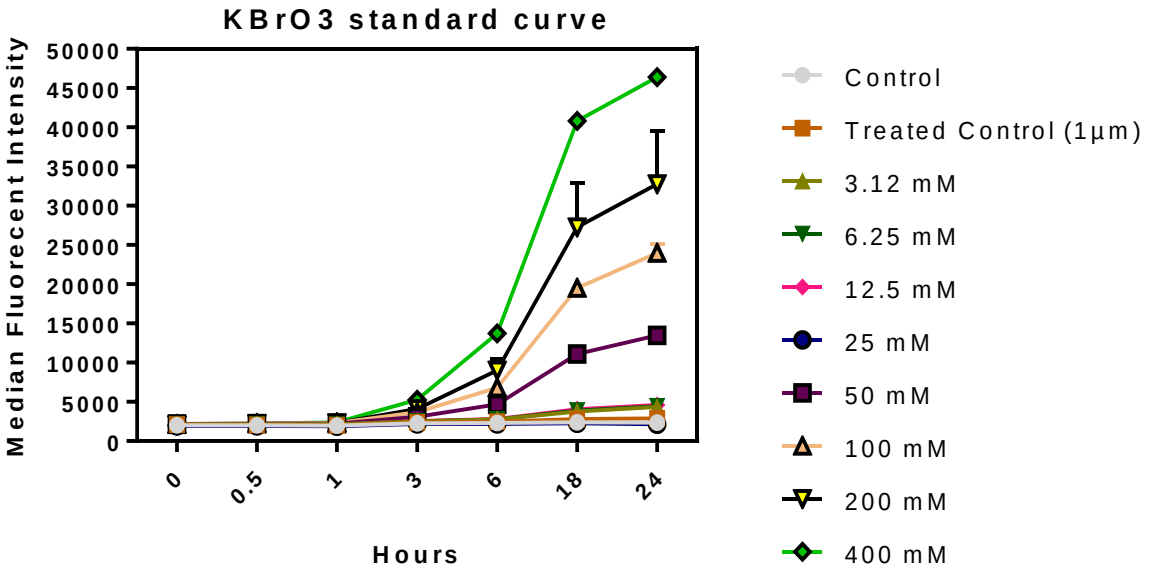

Figure 3.15: DCFDA standard curve using KBrO3. HS-5 **c**ells at about 80% confluence, were exposed to varying concentrations of $KBrO_3$ (3 to 400 mM) for 3 hours and was further stained with 1 µM of DCFDA, incubated for 45 minutes in the dark. Varying time points (0 -24 hours) were measured to estimate the level of oxidative stress and possible release of ROS. Data is presented for n=3 separate biological repeats.

Following the generation of a standard curve, an assessment of oxidative stress induction and reduction capacity was investigated using the NAC, an antioxidant reported with the capacity to reduce oxidative stress (Qanugo *et al.*, 2004*;* Aldini *et al.*, 2018) and DEM, reported as an oxidative stress inducer (Kaur *et al.*, 2006). While NAC is supposed to reduce the oxidative stress induced in the cells by the $KBrO_3$, DEM was supposed to evidence increased oxidative stress by inhibiting glutathione. The data analysis shows the inability of DEM to increase oxidative stress in a dose dependent manner (Figure 3.16), with no obvious increase from 1 to 24 hours.

However, in comparison to the $KBrO_3$ standard curve it is apparent that an increase in MFI did not occur until about 3-6 hours after DCFDA addition, whereas with DEM, this increase began at about 1h. Increments of DEM did not exacerbate this observation however. MFI was at baseline for 0 and 30 minutes, with an increased MFI of 10×10^3 from 1h for all concentrations. While the final two concentrations (200 mM and 400 mM) showed increases up to 40×10^3 and 60×10^3 MFI respectively, all the other concentrations did not increase except for 50 mM and 100mM that ranged between 15×10^3 - 25×10^3 at 24 hours. This high range MFI at 24 hours is a measure of accumulated fluorescence, thus the increased value.

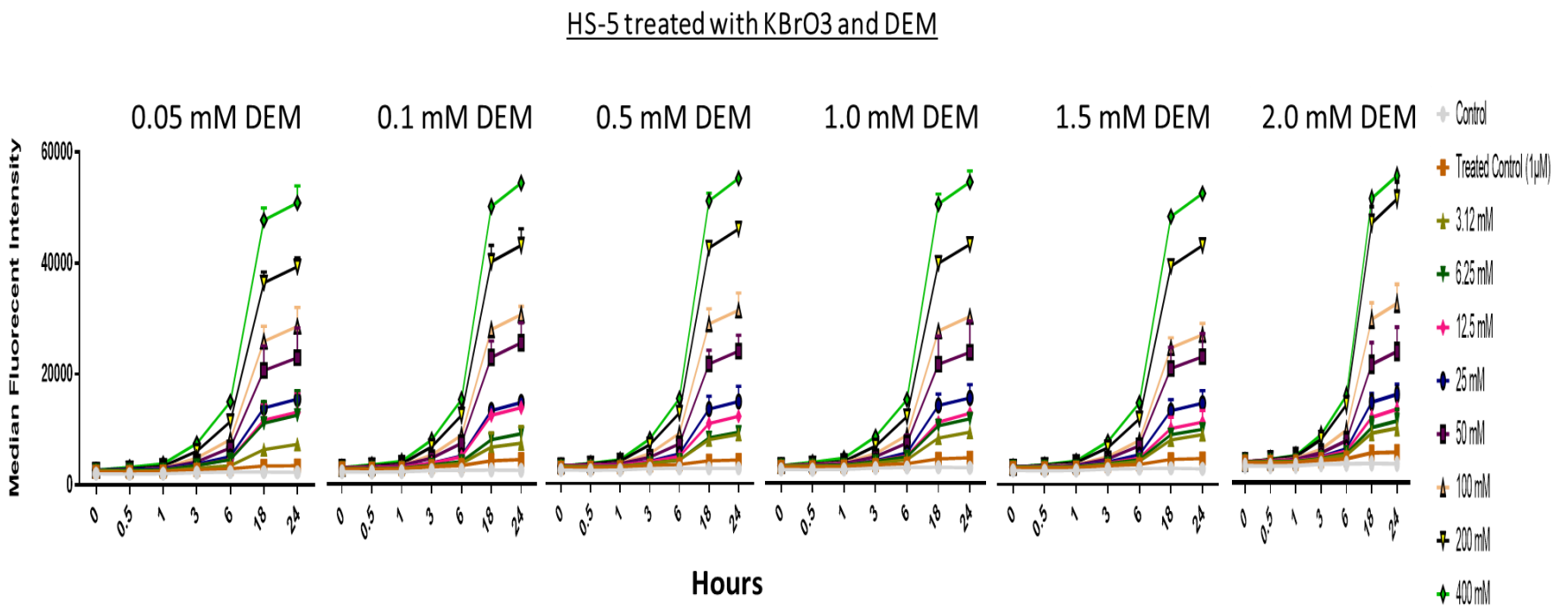

Figure 3.16: HS-5 optimisation with diethylmaleate (DEM) using $KBrO_3$ as oxidant. HS-5 cells were used to optimise the DCFDA assay in treated cells using 1 µM of the DCFDA dye. Cells were treated for 3 hours with $KBrO_3$ in a 96 well clear bottom plate and pre-incubated with DEM for 30 minutes. The edges of the plate were sealed with parafilm and plates covered in foil to avoid light influence. Different time points were measured upon addition of the DCFDA from 0 to 24 hours using the spectrophotometer at absorbance with excitation and emission wavelengths of 488 and 565nm respectively. The assay is represented for n=3 different assay repeats. There was no obvious increase in oxidative stress with any of the DEM concentrations, although an increase in fluorescence appeared earlier than for the standard curve without DEM.

NAC (Figure 3.17) showed similar trend as DEM and did not reveal any capacity to scavenge ROS induction. All MFI for 3mM to 25 mM remained at 10 x 10^3, while 50 and 100 mM MFI was 20 x 10^3 - 25 x 10^3. The highest concentrations 200 mM and 400 mM showed MFI of 40 x 10^3 and 45 x 10^3 at 24 hours, which were slightly lower than the MFI for DEM, but similar to DEM, increments of NAC did not produce an expected dose response. This data showed that as the $KBrO_3$ doses increased there was increase in MFI, with no reduction for any of the NAC doses uses. This suggests that NAC is not a potent antioxidant for HS-5 cell line at the doses tested in this study.

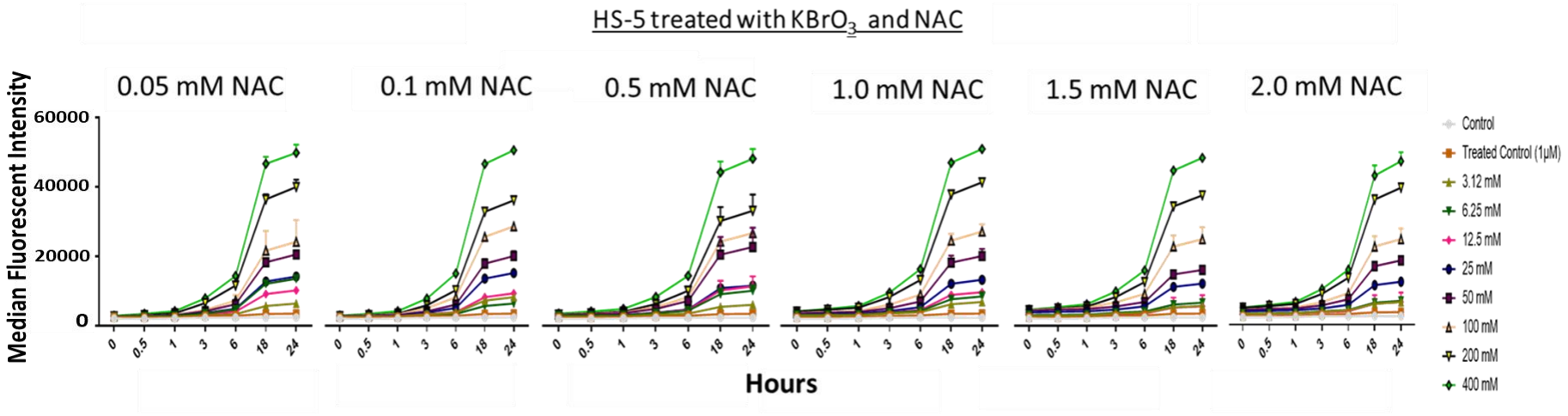

Figure 3.17: The assessment of the anti-oxidative property of NAC in HS-5 cells. Cells were pre-incubated for 30 minutes with varying NAC concentrations (0.05 to 2.0 mM) before exposure to different concentrations of $KBrO_3$ (3 – 400 mM). DCFDA (1 µM) dye was added and incubated for 45 minutes in the dark, with parafilm sealed edges and absorbances were measured at different time points with the spectrophotometer at 488 and 565nm excitation and emission wavelenghts. Rather than the expected antioxidant property of NAC with ranges tested, there was an increase in fluorescence over time, which correlates with the increased doses of $KBrO_3$. Data is shown for three different experiment (n=3).

Evidence from the DEM and NAC (Figures 3.16 & 3.17) when compared to the standard curve (Figure 3.15) were not different. All three individual biological repeats had continual fluorescence and gave an accumulated MFI at 24 hours, in a range of $50 \times 10^3 – 60 \times 10^3$. The outcome did not matter if either plates was pre-treated with an inhibitor or an inducer. Thus, this study required further troubleshooting to ascertain why the two agents used did not have effects on the cells as predicted and a further investigation to understand if the measured fluorescence was an actual reflection of the $KBrO_3$ induced by ROS in the cells was also explored. On this note, to determine that the measured fluorescence was solely due to the cells, an assay without the cells was to be set up, using only spiked culture medium. Furthermore, a parafilm sealing for the edges of the 96 well plates is done once the DCFDA was added and during all measurements. This was solely to avoid the interference of air which would cause oxidation of the measured ROS. More so, NAC is a non-hygroscopic substance which oxidizes in air and thus for any interference; the HS-5 was used for this part of the study to measure ROS with the BM compartment which would normally be hypoxic. Thus sealing the plates edges slightly met these criterion. However, based on the unexpected data, it was thought on one hand that possibly the increase was due to hypoxia and so measurement with the sealant, would confirm that. If on the other hand the increased fluorescence was due to increased ROS from the cells, then we expect a reduction in fluorescence in the experiment without the cells. Thus, these assays were set up in spiked culture medium with and without the parafilm and in culture medium alone.

Results of the parafilm and no parafilm sealing (Figure 3.18) revealed differences between the sealed and unsealed plates. The unsealed plates witnessed a sharp rise at 1h but plateaued at 6 hours and showed a static fluorescence with both $KBrO_3$ and H_2O_2. The sealed plates however measured with a continual rise in MFI. There was no difference in the final accumulated differences for all plates except the sealed H_2O_2 plate. While the spiked and sealed H_2O_2 plate peaked at 6×10^4, the peaked $KBrO_3$ was at 8×10^3. This outcome evidenced that measured fluorescence was not due to the cells. The unsealed plates with immediate increases in MFI suggested the influence of atmospheric air which quickly oxidized these substances. To measure ROS by spectrophotometer was not feasible at this time, and would require further optimisation of various concentrations and conditions.

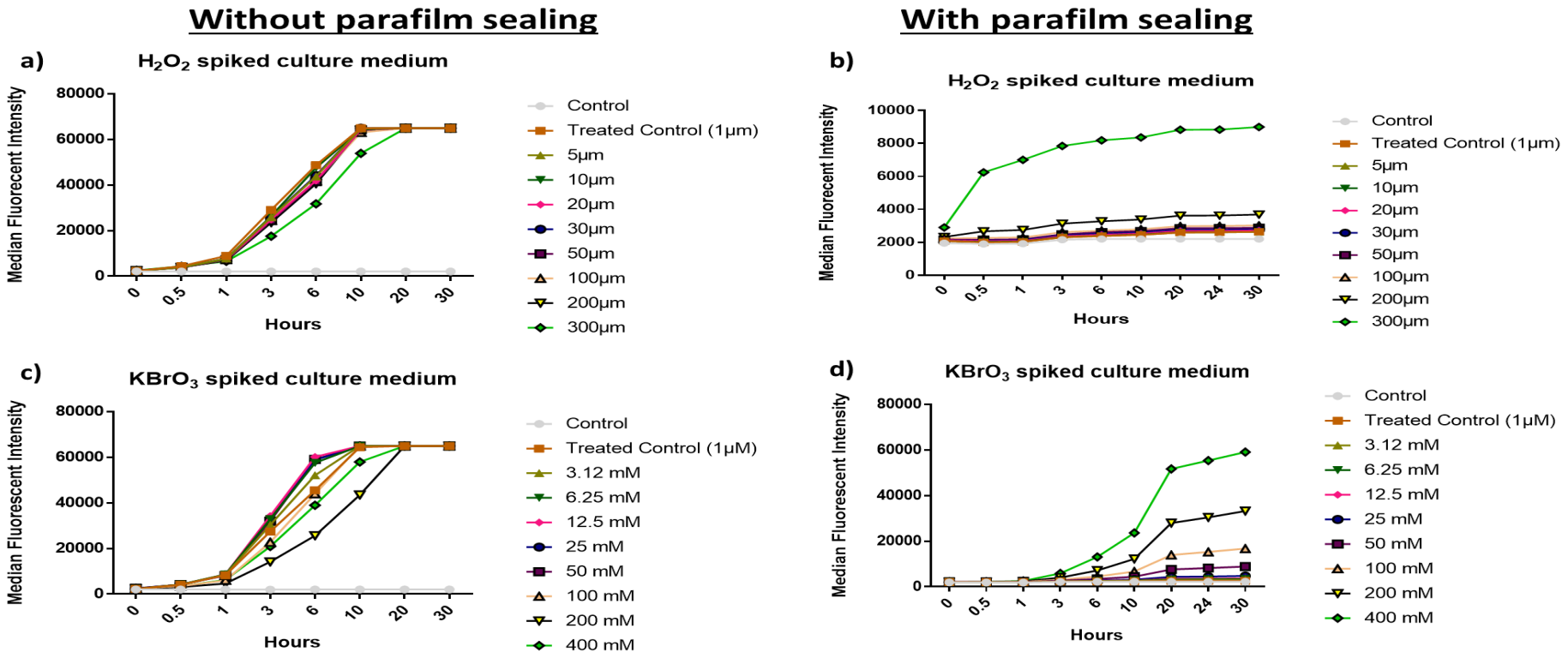

Figure 3.18: H_2O_2 and $KBrO_3$ spiked culture medium assessment by DCFDA assay. The culture medium was plated as a normal culture with 200 µl total volume. Drugs were added in their varying concentrations, ranging from 0 – 300 µM for H_2O_2 and 3 to 400 mM for $KBrO_3$. While some plates were sealed with the parafilm, others were not. They were measured for their fluorescent intensities at different time points (0 – 30 hours) at 488 and 565nm excitation and emission wavelengths respectively. Data is shown for three separate biological repeats and except for H_2O_2 with parafilm, all concentrations were statistically significant (***$p \leq 0.001$) from 3 to 24 hours.

3.3.5 Seahorse XF mito stress test

This assay was performed to determine the effect of chemotherapeutic agents on the functionality of the mitochondria (chapter 5). However, it required an optimisation of the stressor compound (FCCP) utilised in the assay, as well as the optimisation of an optimum cell seeding density of the HS-5 cell line. The latter was necessitated, so that the cell density was not too confluent in such a manner that it will affect oxygen circulation within the microwell plate, which would result to false positive measurement of the oxygen consumption level in the cell.

Various seeding densities of HS-5 ranged from $10 \times 10^4 – 30 \times 10^4$ and evidence from the assay (Figure 3.19) showed that 30×10^4 was adequate to seed the culture plates overnight ready for assay next day. This number were sufficiently confluent as it gave the manufacturers recommended OCR of 200 pmol/min and ECAR range of 80 to 100 mpH/min. OCR estimation in necessary to measure as a way of establishing varying mitochondria parameters. It is measured before and after addition of any inhibitor. A baseline respiration is measured by subtracting the non-mitochondrial respiration from the basal OCR and after addition of the complex V inhibitor (oligomycin), a resulting OCR is used to derive both proton leak respiration and ATP-linked respiration.

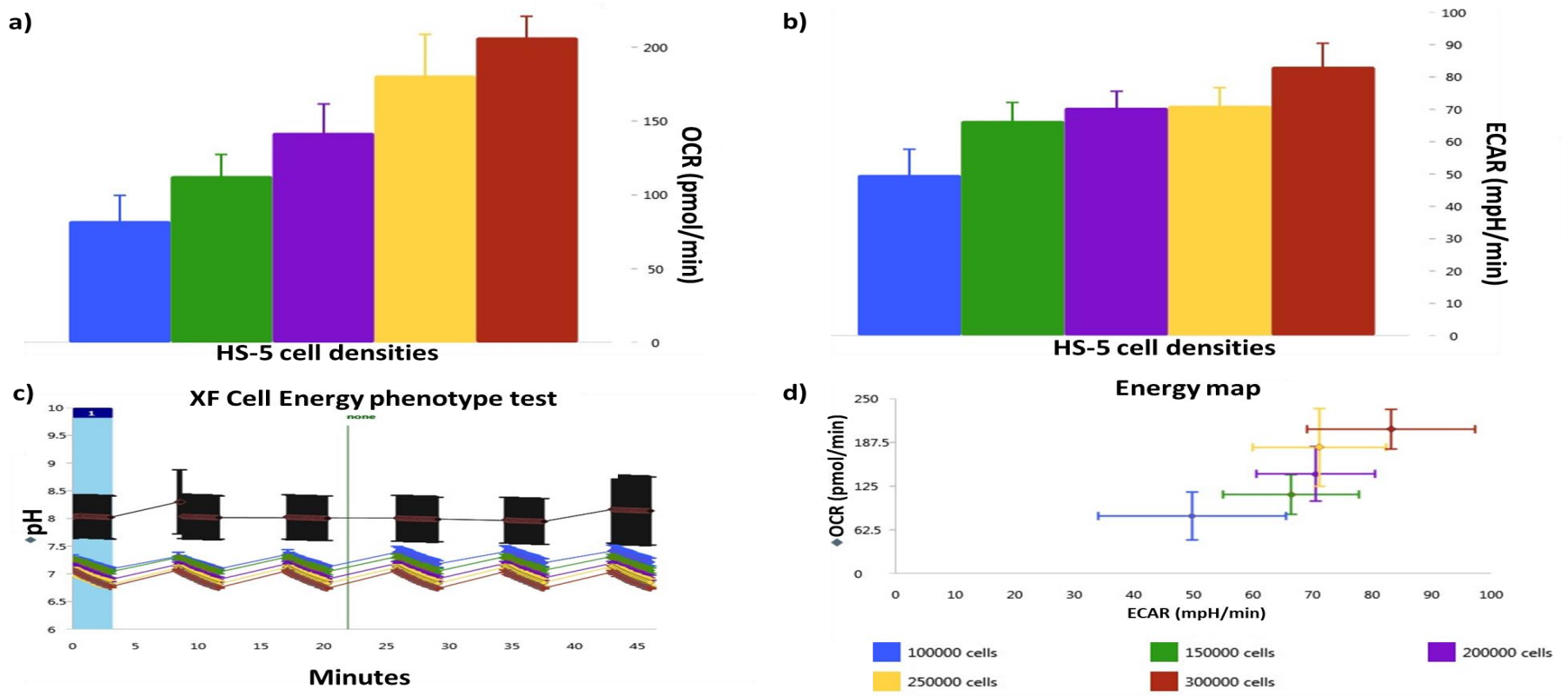

Figure 3.19: Assessed parameters for the optimisation of cell seeding density in the Seahorse XF mito stress test. Various cell densities of HS-5 cells were seeded into seahorse 12 well plate and using the seahorse phenotype test OCR and ECAR (a and b) measurements were taken over 50 minutes. This test was utilised to decide on cell seeding density to use for the study, whilst maintaining the assay condition at required pH 7.4 (c) for a valid assessment. The energy map (d) indicates the energy levels in the cells, another vital parameter of seahorse assay. All the above parameters were compared based on the requirement to have at least 200 OCR and between 80 and 100 ECAR, pH of 7.4. Depicted above are representative images of pH and energy map; and mean values of OCR and ECAR for three different biological repeats.

HS-5 cells from 10 x 10^4 to 20 x 10^4 seeding densities had an OCR at about 100 pmol/min, increasing to 150 pmol/min with 25 x 10^4 cell density and at 200 pmol/min for 30 x 10^4 . With the exception of 30 x 10^4 all the other cell seeding densities had an ECAR rate below 80 mpH/min. Also, the energy phenotype of cell densities of 20 x 10^4 and above were quiet energetic and others below. Energy phenotype helps with an understanding of the role of energy in metabolism, thus enabling a better picture of any pathology.

The FCCP titration (Figure 3.20) showed that 1 µM was sufficient with HS-5 cell line amongst other concentrations. FCCP is a protonophore which when added to the cells collapses the inner membrane gradient, allowing the electron transport chain to function at its maximal respiratory capacity. Although 0.5 µM FCCP concentration appeared to show a higher OCR (250 pmol/min) as well as 2.0 µM with 200 OCR, the choice of 1 µM appeared more stable in real time and based on a combination of a good ECAR of 120 mpH/min and just an adequate OCR, both of which were close to the manufacturers recommended. Both ECAR and OCR data were all accessed while also taking into consideration the maintenance of the recommended pH of 7.4 units for the cells through the assay duration, as fluctuation impacts on the OCR and ECAR.

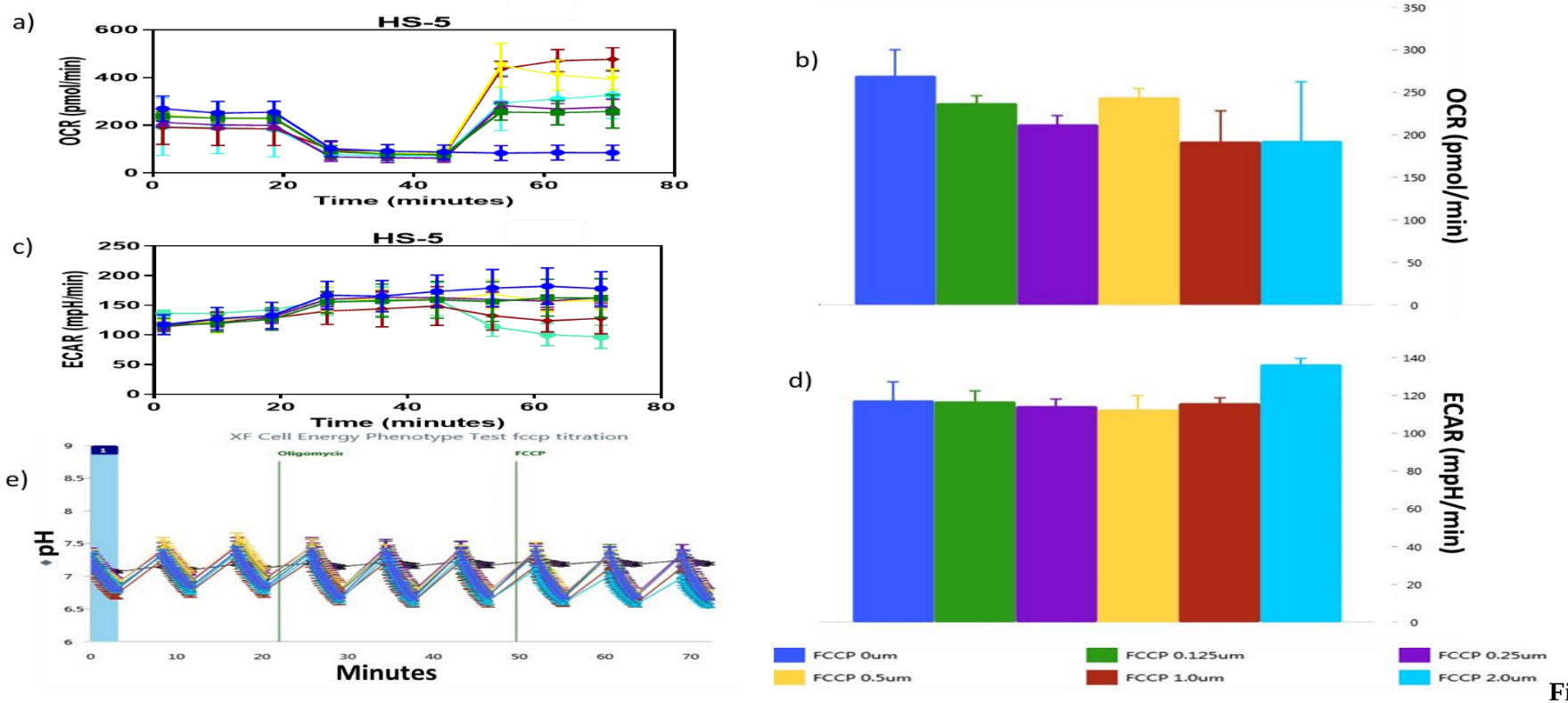

Figure 3.20: Seahorse assay FCCP concentration determination for the HS-5 cell line. The FCCP for the mito stress test assay was prepared using varying concentrations (0 – 2 µM) and injected into the confluent cells as determined by the seeding density. The assay was performed using the manufacturer's protocol and allowed to run until its end time (80minutes). The data was analysed and a decision for the chosen FCCP (1µM) concentration was based on the cells having at least 200 OCR, ECAR range between 80 and 100 ECAR, pH at 7.4. Assay was performed three separate times and representative images (a= OCR, b=ECAR and e=pH) and mean of three repeats (b and d) are depicted.

3.3.6 LC-MS/MS analysis

To optimise this experiment, a range of chemotherapeutic agents were chosen initially in order to determine first the capacity of the detector to detect the analytes and then couple of mobile phases combinations at different gradient combinations, internal standards were tried (data not shown). Presented in this section are some analysis that were performed before the method of choice was selected. Figure 3.21 describes the initial trial with different agents (carmustine, chlorambucil, etoposide, daunorubicin, melphalan and mitoxantrone). These were randomly chosen from study agents to confirm detection of the drugs and their molecular weights on the instrument, and since they were all trials, they were performed with no column for quick elution assessment prior to the main assay. This initial step was a confirmation that these drugs could be detected using the LCMS instrument available.

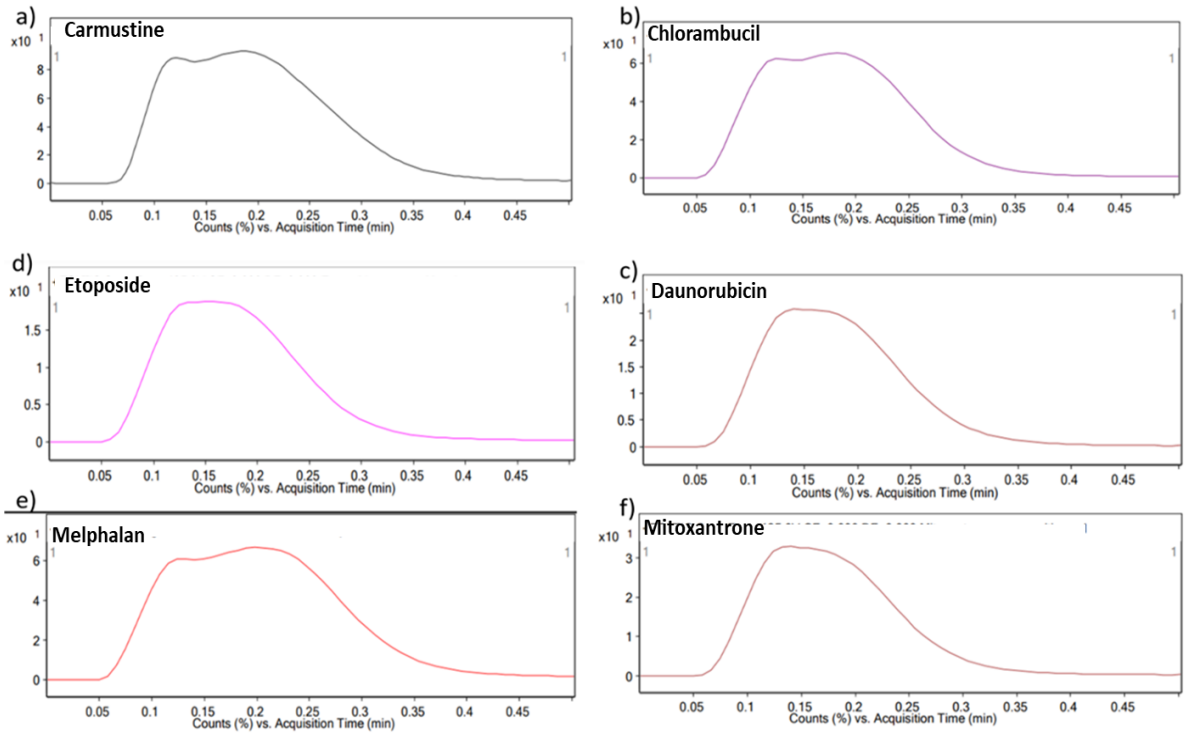

Figure 3.21: LC-MS mass spectrometry scan of various chemotherapeutic agents. The drugs were prepared in intermediate solution for this study, scanned without the use of a column for quick elution of any molecule and the spectra relative to its molecular weight was produced by the MS. Agents used were carmustine (a), chlorambucil (b) etoposide (c) daunorubicin (d) melphalan (e) and mitoxantrone (f). Detection was positive in a positive ion scan mode. All agents eluted off quickly in less than half a minute. Drug elution indicated presence of the agents and ability of the detector to recognise the analytes and spectras correspondent to molecular weights.

Two agents were chosen for instrument standards (theophylline and lidocaine), based on their similarity in chemical structures and molecular weight. Different combinations of drug and instrument standard was assessed to determine compatibility with any possible internal standard. Using the two instrument standards, they were compared either against chlorambucil (304.212 g/mol) and melphalan (305.2g/mol) or daunorubicin (527.52g/mol) and mitoxantrone (444.481g/mol). The elution properties of these agents with the two instrument standards was assessed (Figure 3.22). The instrument standard assesses the functionality of the instrument during data acquisition and lidocaine was considered most appropriate, giving better peaks at all times. Theophylline combinations were not reproducible, whereas lidocaine in combination with chlorambucil and melphalan was steadily reproducible using 80:20 gradient combination of mobile phases A and B. The various drug combinations and different gradients made the analytes elute at different times and with various peak sizes. This assay sort to have a method for eluting analytes at the shortest time possible and separate times, but distinct peak sizes.

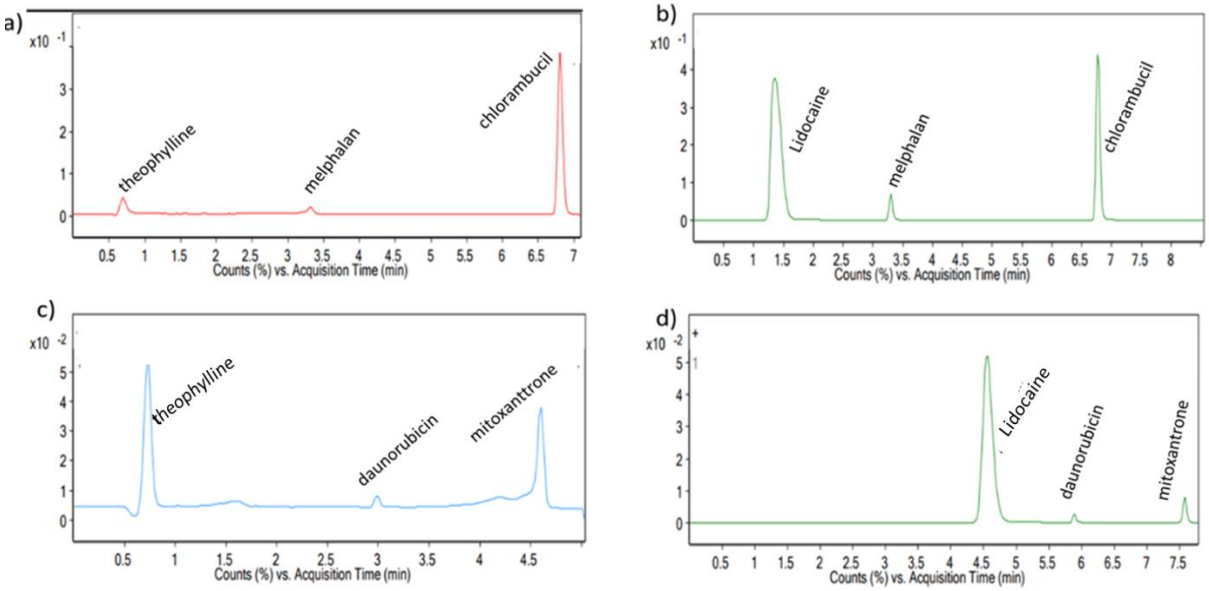

Figure 3.22: The optimisation of internal and instrument standards: Theophylline (A and C) and lidocaine (B and D) were tested as instrument standards at varying gradients of mobile phases and conditions for different agents. (A) chlorambucil was optimised with melphalan using theophylline as instrument standard (B) chlorambucil, was optimised with melphalan (internal standard) and lidocaine as instrument standard (C) mitoxantrone was optimised using daunorubicin (internal standard) and theophylline as instrument standard (D) mitoxantrone and daunorubicin were optimised with lidocaine as instrument standard. The final mobile phase ratio of choice was 80 (0.1% formic acid in water):20 (acetonitrile) for 0 – 2 minutes, 60:40 for 2 – 6 minutes and 30:70 for 6 – 8 minutes.

Since this study evidenced the possibility of progressing with chlorambucil combined with melphalan and lidocaine, production of a quality standard curve that will aid the extrapolation of the analytes concentration/levels became apparent. Figure 3.23(a-d) showed the various standard curves generated. Initially no linear curve was produced and following searches in literature and realization of cold temperature for stability, other curves was produced. Figure 3.23a and "b" are same assay, while the "a" depicted the lower ranges detected in the instrument, it shows its sensitivity but with a linear graph "b" it appeared 1 µM was its lowest detection limit for a linear graph. Next was the curves performed by storing samples in the fridge (c) versus at -20^{0}C. These samples were all prepared on ice, stored in various conditions, and analysed overnight one at a time. Data show the better stability at 2 to 8 degrees but best stability with the -20^{0}C samples. Thus suggesting the effect of storing at cold degrees.

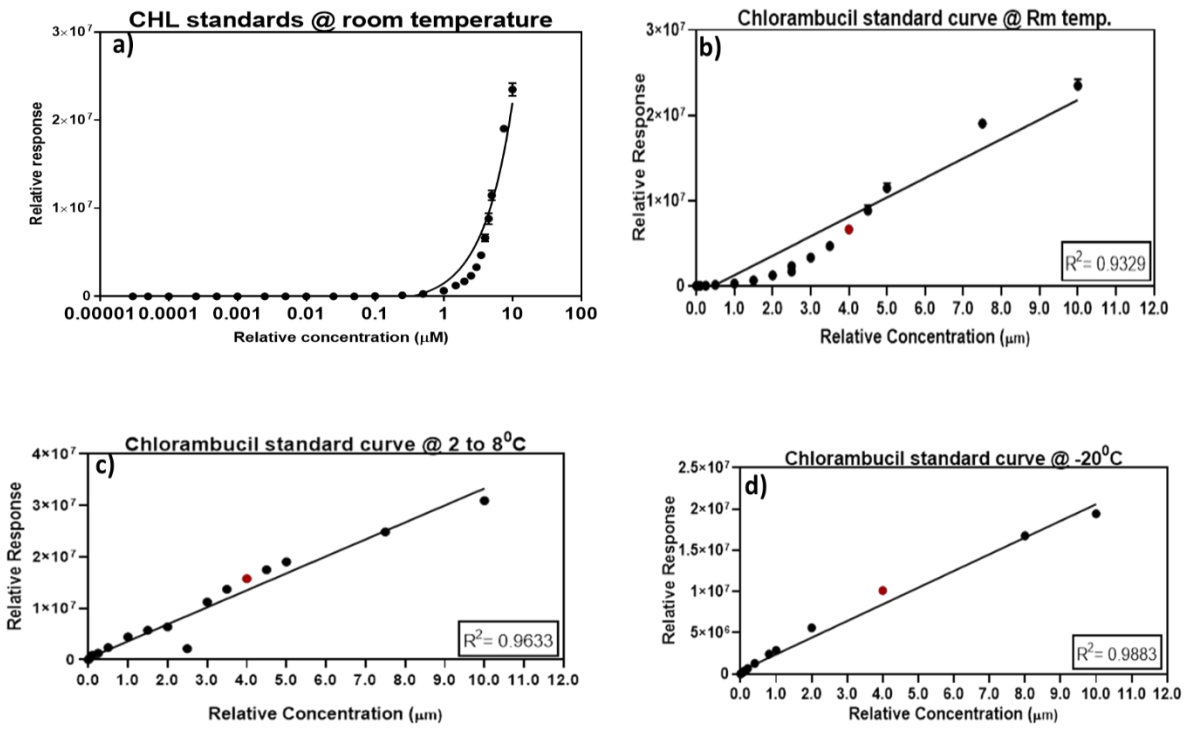

Figure 3.23: Standard curves analysis of chlorambucil in different solvents and temperatures using LCMS: Samples (a & b) were prepared in 50:50 of 0.1% formic acid in water and acetonitrile; and all analysis at room temperature. (a) A logarithmic plot of the lowest detectable ranges and their linear ranges (b). (c) Samples prepared in 50:50 of 0.1% formic acid in water and acetonitrile refrigerated prior to analysis. d) Samples prepared with acidified (0.1% HCL) acetonitrile, freezed in an ice box (-20^{0}C), stored in the fridge (2-8^{0}C), then analysed one at a time. These varying conditions show the effect of cooling and acidification on the samples; as linearity was achieved with the samples stored on ice. The red dot is chlorambucil (4µM) clinical relevant dose.

Prior to the determination of a final standard curve, a stability assay was performed to ascertain the reason for the interferences observed in the generation of a linear standard curve. To do this, a chlorambucil concentration of 2.5 µM was chosen and compared with melphalan (500 µg/L) over 0-600 minutes time point. All vials were set up at room temperature and loaded onto the instrument to analyse overnight and the generated relative responses graphically represented (Figure 3.24). Data show a rapid deterioration of these agents at room temperature particularly for chlorambucil. Chlorambucil response showed a relative degradation from 2.5 x 10^7 to 2 x 10^6, while melphalan deteriorated from 2 x 10^6 to 8 x 10^5 over the measured time points. This evidence revealed the instability of chlorambucil and melphalan at room temperature and other options were explored, such as the addition of a tinge of hydrochloric acid into the stock and working sample preparations, which was found to stabilise them.

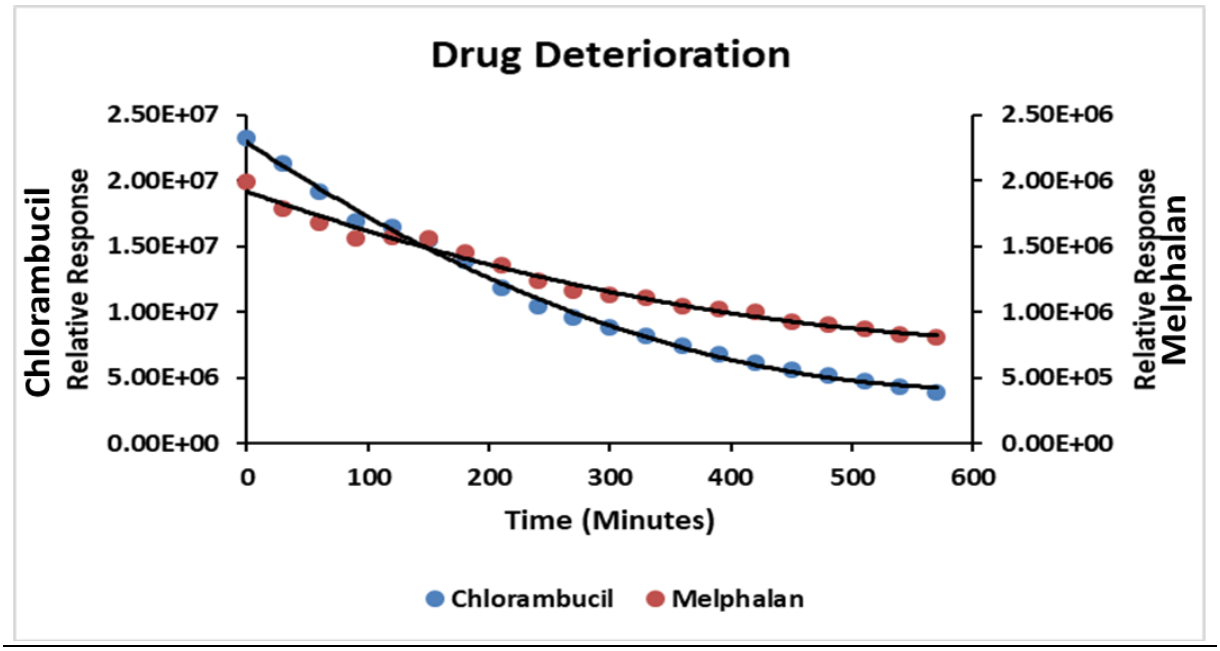

Figure 3.24: Drug deterioration analysis of chlorambucil and melphalan using the LCMS: These chemotherapeutic agents were analysed for their stability at room temperature. Drugs were prepared in 50:50 solution of 0.1% formic acid in acidified (0.01% HCl) acetonitrile and 0.1% formic acid in water. Samples were prepared and loaded on the instrument to run overnight at 30 minutes intervals, for a total of 600 minutes, with n=3 replicates for chlorambucil 2.5 µM concentration.and 500 µg/L melphalan. This analysis was performed for these agents based on initial data (figure 3.23a-c), due to the inability to generate a good standard curve. The data shows a rapid degradation of both drugs and thus they are unstable at room temperature over the time points analysed.

Subsequently, this study explored a range of solvents for the successful extraction of melphalan and chlorambucil, one that would show good percentage recoveries for both, before proceeding to evaluate them in the bystander co-culture model. Figure 3.25 describes some of the solvents evaluated and show their variabilities. Assay was set up for two chlorambucil concentrations; 2 µM (Figure 3.25b) and 10 µM (Figure 3.25a), using 500 µg/L of melphalan and 20 µg/L of lidocaine.

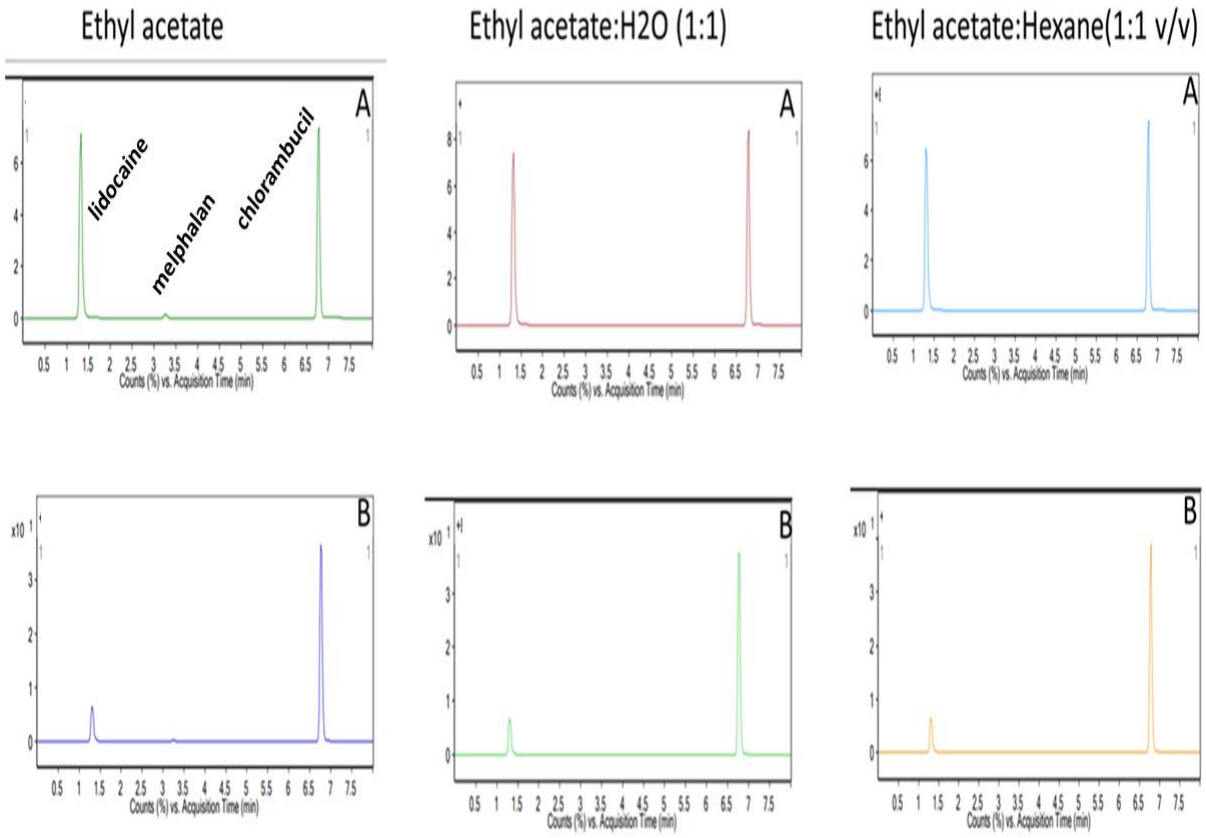

Figure 3.25: LCMS extraction solvents tested in this study. Drugs spiked in culture medium samples were mixed into a total of 5ml of each solvent, vortexed thoroughly, and freezed at -80^{0}C. After 30 minutes tubes were separated into different layers, the aqueous layer aspirated and dried under a stream of nitrogen gas. Vials were reconstituted in mobile phases identified in this study and analysed. Data shows good chlorambucil extraction in all conditions but not melpahlan and lidocaine. Image are depicted for "b" (2µM of chlorambucil) and "a" (10 µM of chlorambucil), while 500 µg/L melphalan concentration was used.

For the two different concentrations of chlorambucil (2µM and 10 µM), they showed good solubility and sizeable peak heights for all solvents (ethylacetate, ethylacetate and water-1:1,

and ethylacetate and hexane-1:1). Lidocaine also showed a similarly good extraction efficiency whereas none of these solvents was able to extract melphalan adequately. Overall, the lesser concentrations seem to be recovered more than the higher concentrations.

Additionally, use of acidified acetonitrile (acidified with 0.1% v/v of hydrochloric acid) gave the best extraction efficiency so far in the study. It was found that chlorambucil produced 80 – 90% efficiency (Figure 3.26). Acetonitrile alone also produced good recovery at 60 and 80% for 2 µM and 10µM respectively. Melphalan produced about 50% extraction in acidified acetonitrile with lower results (25-30%) in acetonitrile alone. Therefore, this study required another agent that can efficiently extract both agents to a larger degree in other to be apply in the bystander effect model.

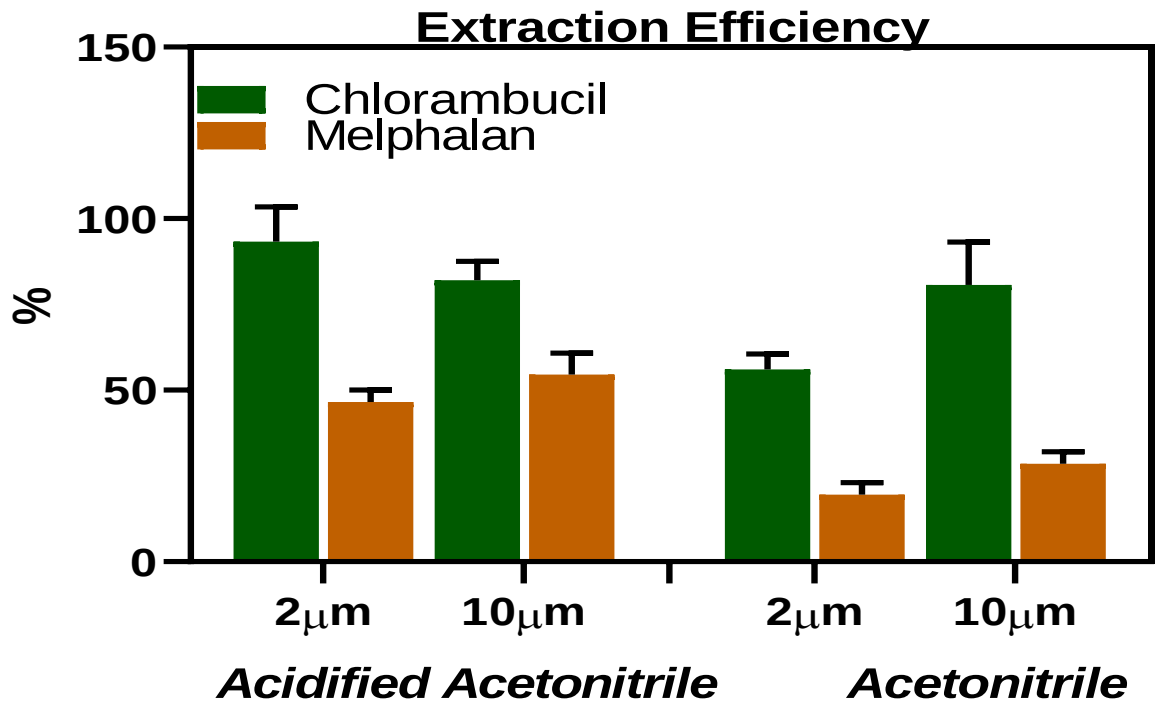

Figure 3.26: The extraction efficiency of chlorambucil and melphalan. These agents were spiked into culture medium and various solvents (Acidified acetonitrile and acetonitrile) tested for extraction efficiency. Cells were extracted, solvents added, shaken and rapidly vortexed for homogeneous mixture. Tubes were freezed at -80^{0}C for 30 minutes and once thawed the separated layers were visible and the aqueous portion separated. These extracts were dried under a stream of nitrogen gas and re-suspended in mobile phase for analysis. Data show the acidified acetonitrile with better recovery of both agents compared to just acetonitrile although Melphalan (500 µg/L in all) recovery was only 50%.

3.4 Discussion

3.4.1 Cell culture medium

In this study, cell culture conditions were considered a vital factor as the overall outcome of the study would be irrelevant without the use of standard conditions that will provide the basic requirements for growth of the cell lines investigated, as they were needed to be in co-culture. Generally, the practice of good cell culture technique is by itself a sophisticated process due to the demands for routine maintenance of the various cells in their optimum growing conditions. More so, due to some inconsistent data produced both for intra- laboratory and inter-laboratory experiments (Baker *et al.*, 2016), in order to ensure accuracy, reliability and reproducibility of assay outcomes, it is imperative that all laboratory experiments are standardised.

In an attempt to address the hypothesis in this study, an optimisation of the individual cell lines in different culture media was assessed. Although these immortalised cell lines generally proliferate and thrive well in different culture conditions, so far there is no development of a culture medium suitable for all cell types. However, this study was based on co-culturing investigations and so there was a requirement to culture each cell line using the identified (section 2.2.1) four conventional media across all cell lines and to determine a 'common denominator' beneficial to all cell types.

The media used in this study include the DMEM/LG, DMEM/HG, DMEM/F12/ RPMI 1640 and RPMI supplemented in horse serum, which were the conventional medium for the cell lines and from this study, DMEM/HG showed to be the best for all parameters assessed, in terms of total number of cells and percentage viability. The HS-5 BM stromal cell line has been utilised in a lot of leukaemia and biomedical research. Recently, Guan *et al.*, (2018) used HS-5 cells alongside HL60 cells in a co-culture study using RPMI 1640 supplemented with 10% foetal calf serum (FCS). In another recent co-culture model study, the HS-5 live characteristic parameters were studied using flow cytometry for a hypoxia co-culture model with Kasumi-1, K562, HL60 and LAMA-84 leukaemia cell lines with the co-cultured medium as RPMI 1640 supplemented with 2mM l-glutamine and 10% FCS (Podszywalow-Bartnicka *et al.*, 2018). The Kasumi-1 cell is considered a model for acute leukaemia investigation and has been applied widely in other leukaemia research (Vladimir *et al.*, 2011 and Larizza *et al.*, 2005). TK6 has

also been applied in a co-culture study with Caco-2 adherent cell line. In their study (Hegarat *et al.*, 2012), the cells were maintained in different culture medium and prior to the experiment they were co-cultured in RPMI 1640 with glutamax and supplemented with 5% FCS. Although not described in co-culture studies, the AHH-1 cell line has also demonstrated good functionality as a model in mutation research and is traditionally grown in RPMI 1640 with some supplements such as horse serum (Yang *et al.*, 2015 and Bruasehafer, *et al.*, 2016).

The results of this study showed that DMEM/HG was the best medium for all cell lines in this study (section 3.3.1). Culture conditions were unfavourable for the DMEM/LG in general and this study observed no growth of HS-5 in the AHH-1 conventional culture medium. This may be explained by the cell line differences as AHH-1 is known to be metabolically competent but not HS-5 cells. This is an interesting outcome warranting further exploration. Another outcome of this study was the presence of fibroblast morphology typical of BM cell lines, an observation more like an endothelial structure was observed in all medium except RPMI which was more fibroblast-Iike. The HS-5 variable morphology can be explained by the possibility of precursor types as reported by Nombela-Arrieta *et al.*, (2012). This was not an issue in this study, as the HS-5 have previously demonstrated MSC characteristics including differentiation capacity into osteoblast, adipocytes and chondrocytes within the research group. In summary, this study has been able to demonstrate DMEM/HG medium as the medium of choice for cell growth and viability for the cell lines used for this study.

3.4.2 The evaluation of oxidative damage and cellular stress

This study was able to optimise an enzyme unit concentration required to detect oxidative lesions in the cells using the enzyme modified comet assay (Figure 3.6). Smith *et al.*, (2006), used 0.08 enzyme units of hOGG1, Fpg unit not reported; but found the production % DNA tail intensity of about 39% using a range of 0 – 2.5mM of KBrO3. This was comparable to the outcome of 0.15 enzyme units used both hOGG1 and Fpg with 2mM $KBrO_3$ of this study, which also produced %DNA tail intensity in the range of 39 to 42%. Therefore, 0.15U was utilised to take the assay forward (chapter 3). Also, Smith e*t al.*, (2006) reported hOGG1 endonuclease enzyme as a more specific detection of oxidative damage than Fpg, since Fpg

also detect alkyl damage and could explain why this study observed bigger tails with Fpg in most cases than hOGG1.

The optimisation of the 8-OHdG anti-DNA/RNA damage detection antibody did not reveal any differences by using the 100% methanol polished slides or unpolished slides. This study found the use of 1 µg/ml of the 8-OHdG antibody and isotype sufficient to detect oxidative damage in the cells, which was found to be effective using the H_2O_2 and $KBrO_3$ positive control (Figure 3.9). This outcome was supported with the co-localisation studies where the antibody was found to detect the oxidative damage impacted by 50 µM of H_2O_2 (Figure 3.14).

The data for the optimisation of the DCFDA reagent (section 3.3.4) suggested that use of 1 µM was sufficient to detect intracellular ROS in the cells (Figure 3.15). However, the evidence using the suggested 2mM KBrO3 (Qanugo *et al*., 2004) as ROS inducer, neither the DEM (a potent oxidative stress inducer; Kaur *et al.,* 2006), nor the NAC (a reported antioxidant; Aldini *et al*., 2018) gave the expected outcome. However, Podszywalow-Bartnicka *et al.,* (2018), recently reported the capability of NAC to reduce ROS produced in HS-5 cells co-cultures using 5 mM NAC. This study only utilised ranges up to 2 mM and so in the future it may be worth exploring a higher NAC concentration and potentially same for DEM.

3.4.3 LC-MS/MS analysis

The use of LCMS has been widely applied in metabolomics and biomarker studies (Zhao *et al.,* 2016) due to its characteristic feature to detect molecules in trace amounts, especially those with very low limits of detection whilst supporting the generation of qualitative and quantitative data. LCMS is a fundamental separation technique applied in life sciences and other related chemistry fields for the separation of organic compounds to include small drug metabolites, peptides and proteins (Wang *et al.,* 2016).

This study attempted to develop a method to analyse the chlorambucil using melphalan as an internal standard. Initially, the method optimisation was based on a few reports for some of these agents such as carmustine, chlorambucil, and mitoanxtrone (Dhakane *et al.,* 2012; Davies *et al.,* 1999; Kate *et al.,* 2010 and Zhang *et al.,* 2010), which coincidentally were among the key agents of this study. However, the reported methods were impractical in this study, possibly

due to the variations of this study from the reported LCMS instrument. The main complexity in developing this assay was the instability of the drugs at room temperature. The drug instability reported in this study, was also seen by Alberts *et al.*, (1980) who observed the unstable nature of nitrogen mustards. Davies *et al.*, (1993) also reported the same for carmustine. This study outcome was also supported by Negreira *et al.*, (2013) who found that chlorambucil amongst 21 cytostatic agents tested, was very quick to deteriorate in aqueous solution at room temperature. Knowledge of this outcome was vital to this study as it was relevant to modify the handling (storage and usage) of these agents at room temperature, especially during cell culture. Furthermore, outcome was vital, as this study originally planned to spike HS-5 cells with drug and monitor any release into the medium over timescales. Thus, if there were detectable levels in a culture medium, study would ascertain further if these levels might align with genotoxicity or cytotoxicity generated by directly exposing the cells to those concentrations *in vitro,* data which would support a role for drug elution in the bystander effect. However, the fact the drugs were so unstable, even at room temperature implied it was impossible to measure them as planned, especially as the cells were at 37^0C which was likely to make them more unstable according to the data procured at lower temperatures, since stability was only better in cold degrees.

The lack of this study was frustrating in this capacity that we couldn't perform this analysis, but on the contrary, it then indirectly supported the notion that simple drug elution could not be the main or sole mechanism for bystander as the drugs were not stable to produce the outcomes we saw. Coupled with the observed outcomes in the genotox (chapter 4) data where lesions did not necessarily agree with the known modes of action, accrued evidence so far, point to a different mechanism other than simple drug elution.

3.5 Conclusion

This chapter has emphasized the importance of assay development, optimisation and revalidation of test protocols for every experiment. This would support the generation of reproducible data in the laboratory. An *in vitro* bystander co-culture model was developed in the course of this study, to provide a good culture conditions for the four cell lines used in co-culture. A protocol was developed with the use of the 8-OHdG antibody for the detection of oxidative damage in the cells, a relevant hypothesis in the bystander model. An LCMS method was developed for analysis of chlorambucil and melphalan, and can be applied in the bystander model or other biomedical research. This data generated has supported the idea that drug elution was unlikely a major player in the generation of the bystander effect. This assertion requires a confirmation using other agents. While there were some failed attempts in the optimisation steps, this has reiterated the inaccuracies with some published works based on the non-reproducibility of some of the methods and concentrations recommended. Developed methods has provided initial data that can be used for comparability studies in the future, when the assay has been fully optimised. Whilst the failed attempts in this study, the need for validation of test protocol cannot be over-emphasised and as such it is recommended for the execution of assays with consistency, to avoid unnecessary trends and bias.

Chapter 4

Genotoxicity evaluation for the *in vitro* bystander co-culture model

4.1 Background

The maintenance of genomic integrity is an essential part of an organism's survival and vital to the transfer of hereditary traits to an offspring. However, genomic instability can arise due to DNA damage through exposure to genotoxic substances, radiation, endogenous active metabolites and oxidative stress. Such lesions can further impair the DNA replicative processes, transcription or translation and coupled with uncontrolled cell division processes that can lead to various mutations including DNA strand breaks (clastogenicity), point mutations and numerical chromosomal aberrations (aneugenicity). These events can occur endogenously or exogenously and DNA damage requires adequate control mechanisms (i.e. DNA damage response and DNA repair pathways) to protect the genome (Tubbs and Nussenzweig, 2017). All activities that disrupt genomic integrity are known as genotoxicity and are widely implicated in carcinogenesis (Langie *et al.*, 2015).

Chemotherapeutic agents mainly target the DNA, with the actively dividing cells mostly affected (section 1.4); even the normal cells are damaged as demonstrated by hair loss, immunosuppression and gastrointestinal disturbances in patients (Woods and Turchi, 2013). Today, one high contributor of exogenous genotoxicity is chemotherapy and while the body is able to initiate effective DNA damage response and control measures, there is no doubt that damage still occurs following cancer chemotherapy and other occupational exposure (Cheung-Ong *et al*., 2013). The cellular responses to external toxic stimuli such as chemotherapy can activate various signalling molecules, including cytokines and ROS, potentially causing DNA damage or cell death (Rugo, 2005). Whether DNA damage happens or not, it is known that the resulting signalling processes from the exposed cell may affect the cell itself or alternatively affect its neighbouring cells (Demidem *et al*., 2006). Currently, one emerging issue is the impact of genotoxic substances to bone marrow microenvironment and its capacity to cause secondary malignancies such as donor cell leukaemia (section 1.7) following chemotherapy (Bolt *et al*., 2004; Neuman, 2009 and Wiseman, 2011). It is therefore important to understand the activities and genotoxic potential of anticancer drugs, as well as explore the genotoxic

potential of these agents in bystander cells; the potential mechanism of some secondary malignancies including leukaemia. Whilst there is limited evidence of chemotherapy-induced bystander effect (CIBE), this chapter aims to screen a panel of widely used chemotherapeutic agents to determine which one can or cannot produce bystander effect.

Using appropriate cell lines in the laboratory to mimic the bone marrow microenvironment, several approaches can be used for evidence of DNA damage. Such investigation involves a battery of test protocols as no single assay can detect all mutagenic outcomes (Kirkland *et al.*, 2011). A good assessment of genotoxic damage can be made using the micronucleus and comet assay and some point mutation assays (Nagarathna *et al.*, 2013). Such combinatory investigation facilitates a confirmation of a genotoxic agent capacity (OECD, 1987; OECD, 2015). Bystander effects are predicted to occur either through cell-to-cell communication or through secretion of soluble factors and a lot of these factors are predicted to be either short-lived such as ROS or long-lived factors such as proteins of unknown nature (Asur *et al.*, 2010; Iyer *et al.*, 2000 and Shao *et al.*, 2008). Short-lived factors could lead to DNA damage which could potentially be repaired and hence a short bystander effect. Whereas long-lived factors may cause mutations which are stable and propagated in bystander cells. Based on these variable factors predicted in bystander effect, it therefore requires varied investigations using different techniques. In this study, in order to do a broad assessment of genotoxicity from bystander model, various assays were used. Comet assay was used to determine structural changes in the cell DNA; micronucleus assay with or without FISH analysis was used to evaluate structural and numerical aberrations, while HPRT mutation assay was used to measure point mutation.

4.2 Methods

4.2.1 Cytotoxicity assessment

The trypan blue exclusion assay was used to assess the viability of both pre-seeded and postharvested bystander cells, prior to determination of genotoxicity. This assay was performed as detailed in sections 2.2.6 and 2.2.7. Cytotoxicity was determined for both the directly exposed HS-5 cell line, as well as the bystander cells post co-culture. Using the clinically relevant doses of 18 chemotherapeutic agents cell viability of HS-5 was assessed at different time points (Figure 4.1). Also HS-5 cell line was used to assess cell viability of four key drugs (carmustine, chlorambucil, etoposide and mitoxantrone) at different time points and using a selected range of doses (Figure 4.2). The cytotoxicity evaluation of TK6 and AHH-1 bystander cell lines following co-culture with HS-5 was assessed for all the clinically relevant doses of 22 chemotherapeutic agents (Figure 4.3).

4.2.2 Alkaline comet assay

The comet assay, which was developed for measurement of DNA fragmentation in single eukaryotic cells, was used to detect genotoxic damage of lymphoblastic cell lines following 24 hours co-culture with the HS-5 cell line previously exposed to the clinically relevant doses of 22 selected chemotherapeutic agents (section 2.3) for 1h. All comet assays were conducted as described in 2.4.2.

4.2.3 Micronucleus assay

The micronucleus assay was used as a multi-target genotoxic endpoint to screen 22 potential genotoxic chemotherapeutic agents (section 2.3). Twenty-four hours post co-culture with the bone marrow cell line HS-5, bystander cells were harvested, measured for viability and cells scored for the presence of micronuclei. The entire micronucleus assay was executed as earlier described in section 2.4.1.

4.2.4 Pan-centromeric labelling of bystander lymphoblast cell lines

To establish the pattern of damage identified by the micronucleus assay (which detects both chromosomal breakages and loss of whole chromosome), the lymphoblast cells following co-culture were fixed, hybridised and labelled with a pan-centromeric fluorescent probe, and

evaluated using a fluorescent microscope with individual DAPI and FITC filters, and a triple band pass. Slides were scored for a hundred micronuclei for treatment groups and two thousand cells scored for control slides with low MN induction, whilst estimating presence or absence of centromere (section 2.6). Scoring criteria utilises the detection of a centromere signal in the micronuclei as an indication of whole chromosome as opposed to chromosome fragments (Fenech *et al.,* 2011).

4.2.5 Bystander longevity assay

To determine the probable time for the bystander effect to induce cytotoxicity or genotoxicity in cells, a modification of the co-culture was applied. Briefly, HS-5 cells were exposed as stated in section 2.4 and co-cultured with lymphoblast cells for 24 hours. After 24 hours, the initial bystander cells were removed from co-culture for genotoxicity assessment and replaced with fresh culture inserts and bystander cells. This modification allowed a five-day experimental assessment of lymphoblast cells with daily replacement of culture inserts with new lymphoblast cells; cells were harvested 24 hours after the commencement of co-culture and evaluated for viability and genotoxicity. The endpoints used were MN induction using micronucleus assay (section 2.4.2) and single/double strand breaks detection using the comet assay (section 2.4.1).

4.2.6 Residual drug detection assay

In order to investigate a possible mechanism of the observed bystander effect, an assessment for residual drug effect within the HS-5 bone marrow compartment was evaluated. Briefly, the clinically relevant doses of carmustine, chlorambucil, etoposide and mitoxantrone were used to directly treat TK6 for an hour, cell viability was determined and TK6 cells were assessed for genotoxicity using the micronucleus assay. This direct bystander data was compared to the previously generated bystander effect data of TK6 cell line (Figure 4.15), as well as genotoxicity data of two different conditioned media (medium from the final (third) wash of the HS-5 cell line after 1h of drug exposure and the 24 hours conditioned medium of HS-5 cell line post exposure to chemotherapeutic agents). Under these conditions, TK6 cell line was assessed for the mechanism of simple or residual drug elution within the culture microenvironment, as well as the capacity to release other soluble factors that may induce damage in other unexposed cells within the vicinity.

4.2.7 Forward mutation assay

Using the hypoxanthine phosphoribosyl transferase (*HPRT*) assay as described in section 3.2, AHH-1 and TK6 (cell lines with heterozygosity for the thymidine kinase (*TK*) locus were used to evaluate the possible involvement of point mutation in chemotherapy-induced bystander effect. Briefly, cells were first made void of any background mutants, allowed to recover in complete culture for four days and then directly exposed to varying doses of methylnitrosourea (a highly potent mutagen) to validate the assay. The assay was then further utilised in the *in vitro* bystander co-culture model experiment for carmustine, chlorambucil, etoposide and mitoxantrone at clinically relevant doses, and thereafter plated with 6-TG (a toxic analogue) to positively select for mutants as well as a duplicate non-selective plating wells for assessing plating efficiency. A comparative analysis was made between the two cell lines.

4.2.8 Statistical analysis

Data presented are that of mean ± SD for three independent biological repeats, some including at least two individual experimental repeats. Results were analysed using the Graphpad Prism software to perform two-way ANOVA, employing multiple comparisons and Dunnett's post hoc test to determine statistical difference between treated and untreated in a group and statistical significance with p value was considered as $p < 0.05$. For any direct comparison between a treated agent and a control, this study utilised the Student t-test following data compilation on Microsoft excel spreadsheet.

4.3 Results

4.3.1 Cytotoxicity

According to the Organisation for Economic Co-operation and Development (OECD) guidelines, the cell viability is vital to making a good genotoxic assessment, as cell viability should be at least 50% ± 5% (Honma, 2011). Its evaluation permits a determination of the lethal dose of a chemotherapeutic agent, which upon genotoxicity testing, detects its likely capacity to induce DNA damage. The trypan blue assay was used to determine cytotoxicity in the bystander cells based on its speedy procedure and the ability to exclude non-viable cells through their characteristic blue colour uptake and the capacity to exclude both apoptotic and necrotic cells (Peter, 2011). Using the trypan blue assay, harvested cells were analysed for viability, and in some cases acridine orange and propidium iodide were used and cells determined for total, live, dead and percentage viability parameters using the automated LUNA counter, which maximised accuracy and reproducibility. Following 24 hours co-culture of TK6 and AHH-1 cell lines with HS-5, cell viability determined (Figure 4.1). Genotoxicity was then assessed when cytotoxicity was found to meet OECD guidelines.

4.3.2 HS-5 cytotoxicity assessment

For this study, the bone marrow cell line (HS-5) which was constantly the 'drug treated compartment' for the bystander model, was assessed for cytotoxicity. Briefly, HS-5 cells (1 x 10^4 /cm^2) were treated with different chemotherapeutic agents for 1h (section 2.4), resuspended in fresh medium and sampled for cytotoxicity at different time points. Eighteen (Figure 4.1) of these agents were used at clinically relevant doses to treat HS-5 cells and cells were evaluated at 1, 6, 24 and 48 hours post drug exposure.

At 1h (Figure 4.1a) all agents were above the 50% recommended threshold with exception of mechlorethamine, hydroxyurea and daunorubicin, which some witnessing a recovery to almost 50% 6 hours later. At 6 hours (Figure 4.1b), cells treated with these agents appeared stably viable with only a few exceptions, but overall viability ranged from 43% to about 80%. There was a few decrease in cell viability for some agents (cisplatin, 5-FU and methotrexate), but not beyond 50%. Hydroxyurea and daunorubicin showed a recovery in cell viability to 50%. Interestingly, at 24 hours (Figure 4.1c) the viability of these cells were all above 60%, indicating a good viability of the treated BM compartment 24 hours post chemotherapeutic

agent exposure, a time which coincides with harvesting of the bystander cells post co-culture. Mechlorethamine treated cells had recovered and the cells that witnessed a decrease at 6 hours also increased their cell viability. Of note, the topoisomerase inhibitors, plant alkaloids, melphalan, Ara-C and some antibiotics (bleomycin, doxorubicin, mitomycin C) maintained good cell viability throughout the assessed time points. At 48 hours, all cells treated with these 18 agents showed a very good recovery in percentage cell viability (Figure 4.1d).

As the focus of this study was to explore a possible role of ROS to cause bystander effect, this study avoided the generation of data that are not true bystander effect. This is following the possibility of a direct ROS release from HS-5 treated cells due to cellular lysis and death. Thus, cytotoxicity was determined for the HS-5 cells in a single culture using varying doses that included clinically relevant dose and accrued data assumed to replicate the situation when cells were in co-cultured with bystander cells. Demonstration of good viability of HS-5 over the 24 hour period suggests that any ROS arising from HS-5 cells would be as a result of a bystander effect and not cell death. To investigate this further cytotoxocity, the four key drugs: Carmustine, chlorambucil, etoposide and mitoxantrone (Section 1.4) were evaluated for their toxicity with the HS-5 cell line using a range of doses and at different time points. The choice of the doses spanned below and above the clinically relevant doses (Table 2.2) and the essence of this was to establish that the cells of the BM compartment remained viable during co-culture and that genotoxic effects observed in the bystander cells were not related to factors released from the HS-5 following cell death and lysis. These drug choices were made to serve as a representation of low and high micronuclei induction (selected from the result of the initially screened 22 agents of this study). Also, they were chosen based on their relevance with treatment of haematological malignancies (Spurgeon *et al.,* 2012; Oliver and Palanca, 2014) and link to the induction of TRL (Kayser *et al.,* 2011 and Morrison *et al.,* 2002).

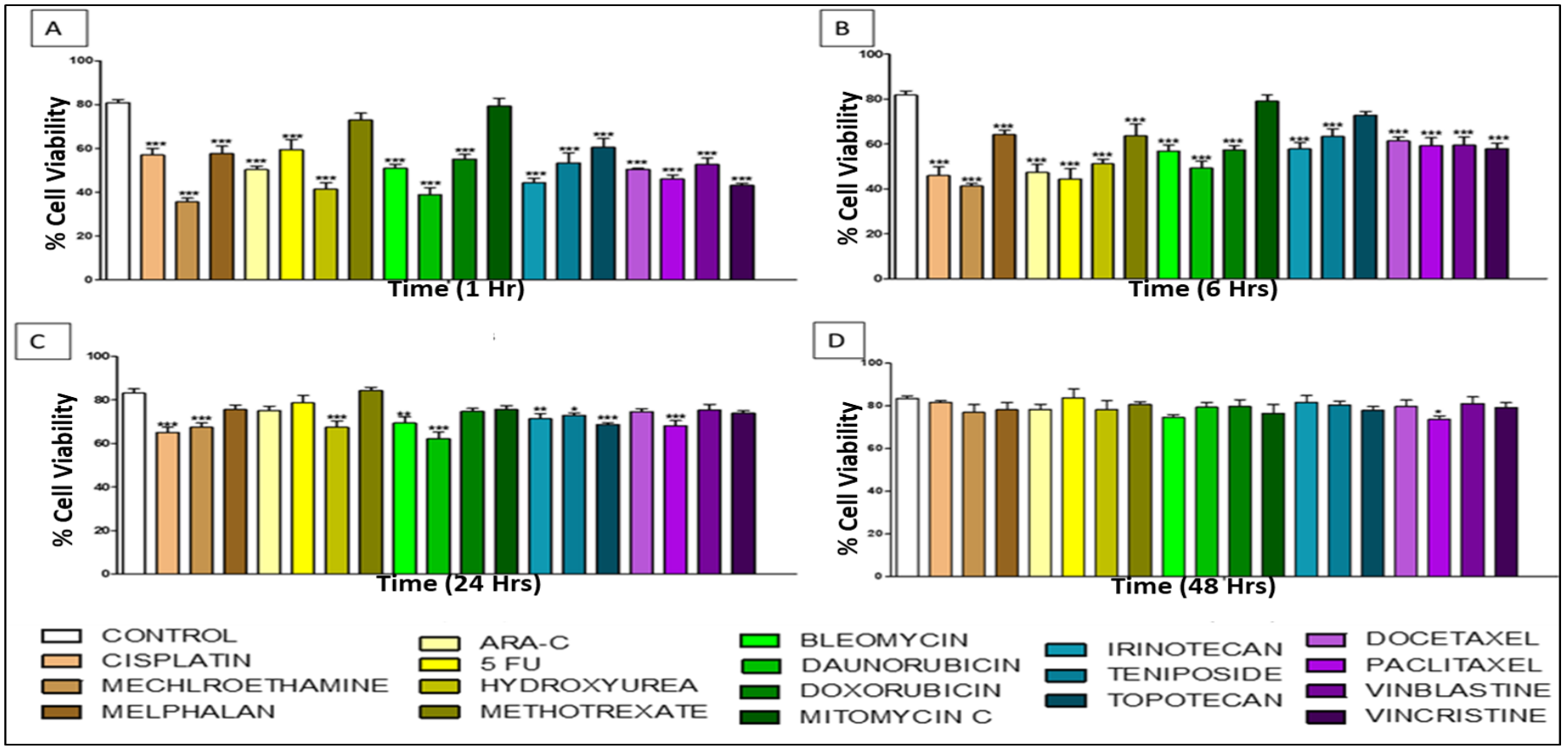

Figure 4.1: Cytotoxicity of HS-5 cells post treatment. HS-5 cells were exposed to the clinically relevant doses of eighteen chemotherapeutic agents for one hour, drugs were washed off and cells resuspended in complete culture medium and sampled at the indicated times. Colour codes are for drug class: alkylating agents (brown shades – column 1), antimetabolites (yellow green shades- column 2, antibiotics (green shades – column 3), topoisomerase inhibitors (blue shades – column 4) and mitotic inhibitors (purple shades – column 5). Cells were trypsinized and assessed for viability at 1 (figure A), 6 (figure B), 24 (figure C) and 48 (figure D) hours. Data represents the mean ± SD of three biological repeats, with statistical significance for $*p \leq 0.05$, $**p \leq 0.01$, $***p \leq 0.001$ as analysed using two way ANOVA.

Similar to the eighteen agents initially assessed, these agents were used to treat HS-5 cells for 1h, trypsinized and sampled at 1, 3, 6, 24, 48 and 72 hours, a period which will enable at least one population doubling time for the HS-5 cell line. Therefore, it was expected that an increased dose would increase cytotoxicity for the same 1h exposure time. For all five doses (with clinically relevant dose as the middle dose), these agents (Figure 4.2) demonstrated at least 50% cell viability and the lowest cytotoxicity was not always the highest dose. All agents were relatively viable with chlorambucil and etoposide witnessing a decline for their lowest doses at 48 hours. Chlorambucil showed decreased cell viability (about 50%) for doses 3 to 6 µm, including the clinically relevant doses at 48 hours, but recovered at 72 hours.

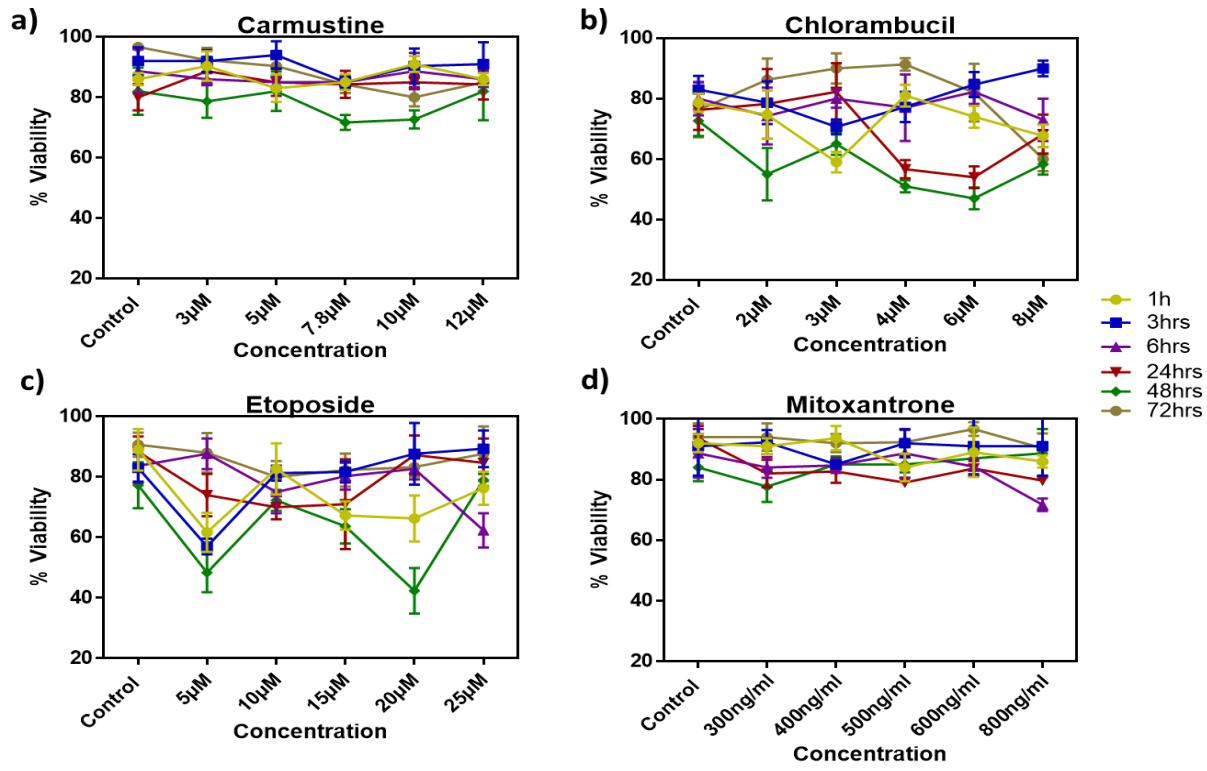

Figure 4.2: Cell viability assessment for the four chemotherapeutic agents of interest in HS-5. HS-5 cell line was exposed to (a) carmustine, (B) chlorambucil, (c) etoposide and (d) mitoxantrone at varying doses ranging from low to high, including their clinically relevant doses (the middle doses in the figure) for 1h. Aliquots were taken post treatment to determine the cell viability at 1, 3, 6, 24, 48 and 72 hours. The mean ± SD is presented and data is representative of three different biological experiments. All agents show cell viabilities above 50% for all the measured time points, no dosage effect was observed and the clinically relative doses were generally stable. Data suggest the possibility of chemoresistance in HS-5 cells. These four agents became a study focus due to their implications in haematological malignancies.

The above data show no dosage effect for the evaluated concentrations, as the highest doses were relatively viable for all time, except for the observed decline to about 50 % in etoposide and mitoxantrone. The middle concentrations represent the clinically relevant doses and they show good cell viability above 70% for all time points, except for the observed decrease in cell viability for chlorambucil at 24 and 48 hours to about 50%. However, there was an increased cell viability back at 72 hours. Furthermore, the morphological appearance of the treated HS-5 cells (Figure 4.2a) after 1h was observed by doing a circular mark-up of the culture plate, which was focused and image taken prior to cell treatment and same field taken after 1h. This data reveal an alteration in the adherence and plasticity of the cell lines following cell treatment. The cells appear to have more spaces in between with most appearing circular and lifted off the cell surface. In comparison with the untreated control compartment, one can observe a clear separation of the originally adhered cells from the culture plate.

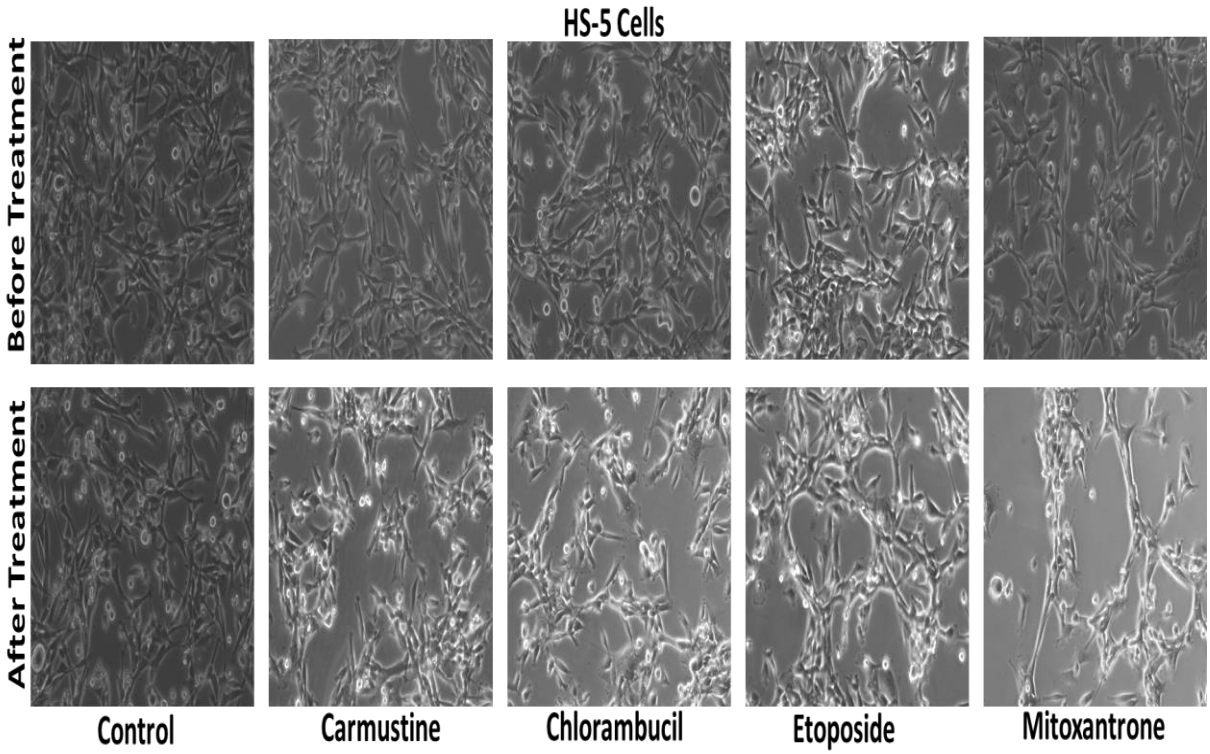

Figure 4.2a: The HS-5 morphological appearance after chemotherapeutic agent exposure. Prior to cells treatment, the individual wells for these agents were marked and representative images of the marked compartment taken upon focusing under an inverted light microscope at 10x magnification, pictures were taken before and after treatment for comparative assessment. Image suggests that the treated wells was morphologically altered (but not viability) unlike the untreated wells, evidence suggestive of drugs (carmustine, chlorambucil, etoposide and mitoxantrone) penetration into HS-5 cells in the bystander co-culture model.

TK6 bystander cells co-cultured with treated HS-5 cells for 24 hrs, generally showed good cell viability of about 65% and above for most chemotherapeutic agents with a few exceptions like the daunorubicin, docetaxel and vincristine, which were almost at a 50% borderline (Figure 4.3). The alkylating agents resulted in good viability with carmustine as most at 70% and chlorambucil at 55% with the least viability. The plant alkaloids were similar to alkylating agents except for docetaxel which produced viability of 52%. The antibiotics cell viabilities ranged between 60 to 75%, with daunorubicin as the lowest and mitomycin C as the highest. The antimetabolites were within the range of 50 to 76% viability, topoisomerase inhibitors ranged between 52% (irinotecan) to 67% (etoposide) and the plant alkaloids ranged between 51 % (docetaxel) to 73% (vinblastine), all showing a good viability across board.

The mean percentage viability data of the AHH-1 (Figure 4.3) for all the chemotherapeutic agents showed good cell viability, which was non-significantly higher than for TK6 cells. Whilst the AHH-1 bystander cells showed viability from 83% (cisplatin) to 91% (mechlorethamine) for alkylating agents following co-culture with treated HS-5, the antibiotics produced viabilities between 67% (daunorubicin) to 82% (mitomycin c). Additionally, the antimetabolites produced viabilities between 77% to 85%; the topoisomerase inhibitors ranged from 73% to 89%, and the plant alkaloids were at about 73% to 83%. The sets of data represent mean values of three different repeats and give a good indication of cytotoxicity evaluation of the cells. Overall, whilst there is little difference between the control data for TK6 (83%) and AHH-1 (86%), the metabolically competent AHH-1 cell line appears to have better viability than TK6 for all agents tested.

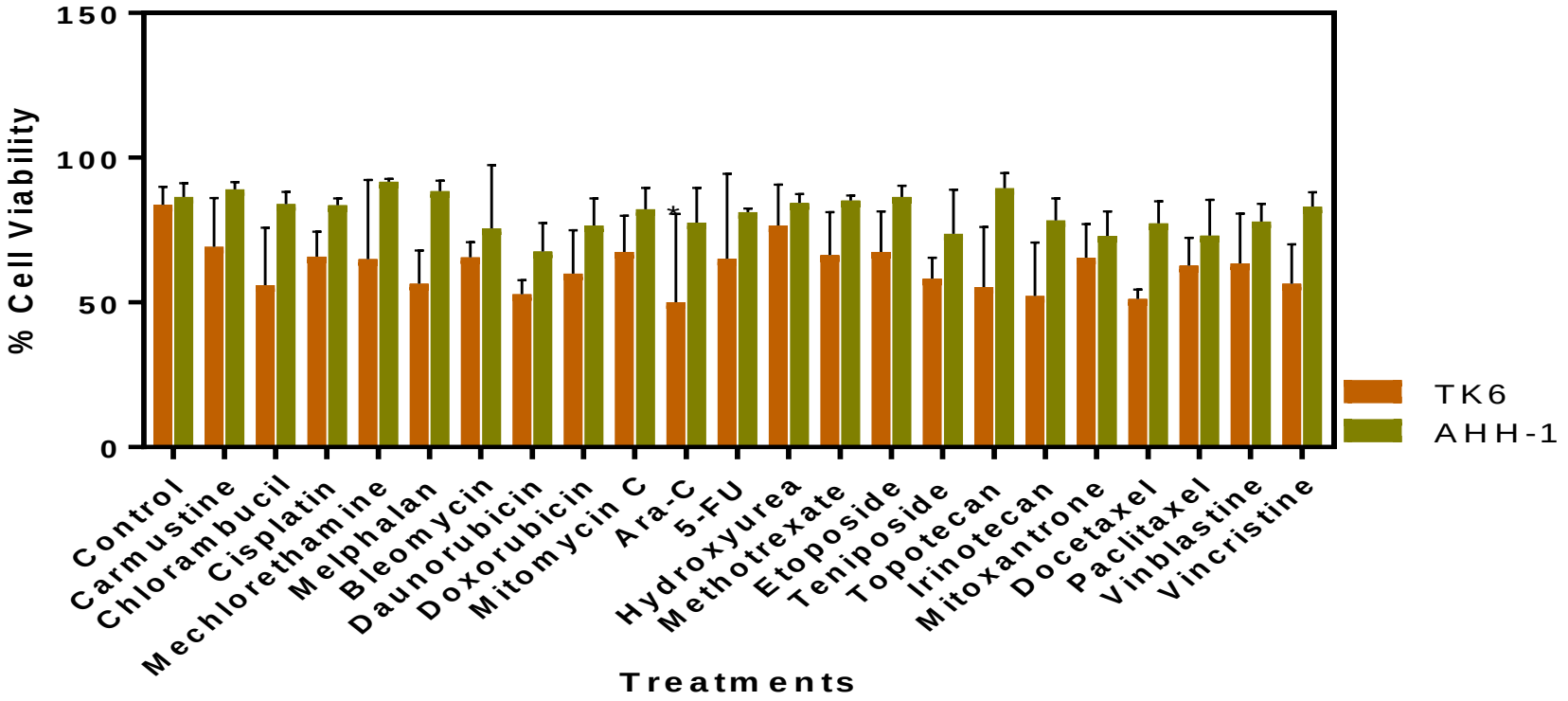

Figure 4.3 Percentage viability of the lymphoblastic cell lines (TK6 and AHH-1) after co-culture. Prior to genotoxicity assessment post co-culture, the harvested cells was evaluated for cell viability by the trypan blue exclusion assay using three separate representative samples and analysed automatically with the LUNA cell counter. Data is representative of three separate repeats for each chemotherapeutic agent indicated and presented as mean ± SD. Both TK6 (orange) and AHH-1 (green) bystander cells show a reasonably good cell viability of 50% and above when compared to the approximate 85% cell viability of control for both cell lines and showing a statistical significance of $*p \leq 0.05$ (analysed using two-way ANOVA) for carmustine in TK6 cells.

It is of note that whilst haematopoietic cells typically succumb to these levels of dosing, instead where the HS-5 are treated, and then co-cultured (free of drug) with the TK6/AHH-1 bystander cells, that the latter have largely excellent viability, and certainly within acceptable toxicity ranges for evaluation of genotoxicity assessment according to OECD guidelines. Thus if genotoxicity is present in bystander cells following such co-culture, good viability infers that any mutagenic events are 'real' and of concern when the cell remains viable.

4.3.2 Genotoxicity evaluation

In order to detect the genotoxic capacity of the 22 chemotherapeutic agents, various genotoxic end points were assessed. The alkaline comet assay enables the assessment of single and double strand breaks, DNA base damage, DNA repair and alkali labile lesions in individual cells; thus a clinically relevant biomarker to detect exposure to genotoxic agent (Calini *et al.*, 2002). The micronucleus assay is a well-established technique that is used as a genotoxicity endpoint owing to its capacity to detect chromosomal mutation transmitted to daughter cells during cell division (Hintzsche *et al*., 2017 and Kirsch-Volders *et al*., 2011). MN frequency gives an indication of the capacity of a chemical to induce damage either as clastogen or aneugen (Norppa and Falck, 2009). It also serves as a biomarker for assessing chromosomal damage due to genotoxicity testing and for biomonitoring studies following genotoxic exposures in humans (Fenech, 2000 and Schwarzbacherova *et al.*, 2016). Based on the established potentials of these assays, they were utilised in this study.

4.3.2.1 Comet Assay

In this study, the alkaline comet assay was used to detect the induction of DNA fragmentation to TK6 and AHH-1 cells as bystander cells. Following exposure of HS-5 cells to the 22 chemotherapeutic agents at clinically relevant doses (Table 2.2), bystander cells were co-cultured with the treated HS-5 and harvested 24 hours later; 150 comets were analysed per treatment (OECD guidelines of 2014 for testing of chemicals). The assay was validated using a positive control slide of hydrogen peroxide (section 2.4.2.1). Several parameters (tail length, tail moment and percentage tail intensity) for scoring the comets exist, with no parameter superior to the other rather justifies reason for choice of any.

TK6 bystander cells (Figure 4.4), show varying degrees of sensitivity to the different classes of drugs tested. There were no obvious trends in sensitivity when comparing agents within or between the classes of chemotherapeutics. When screening all the drugs, 8 drugs significantly increased the DNA in the tail, whereas 14 did not. In comparison with the control sample, mechlorethamine ($p \leq 0.0001$), bleomycin ($p \leq 0.01$), Ara-C ($p \leq 0.0001$), hydroxyurea ($p \leq 0.05$), teniposide and mitoxantrone ($p \leq 0.0001$) and vincristine ($p \leq 0.001$) show a significant increase in percent DNA in the tail. DNA damage for most of the other agents was below 7%, and whilst most of these drugs (carmustine, cisplatin, docetaxel, irinotecan and vinblastine) were of similar range to the control (6%), chlorambucil, etoposide and topotecan were slightly above the control in the rang e of 7%. Two antimetabolites (5-FU and methotrexate) show non-significant tail retardation relative to the control, suggesting reduced DNA damage in the range of 5%.

Furthermore, mechlorethamine depicted the highest level of damage among the alkylating agents ($p<0.0001$) whereas carmustine, chlorambucil, melphalan and cisplatin (platinum compound) showed a non-significant increase in damage. More so, within the anti-tumour antibiotics, all agents appear to be about the level of 9% to 10% DNA damage with significant effects for bleomycin ($p \leq 0.001$) and mitomycin C ($p \leq 0.05$). The plant alkaloids level of damage for all agents fall within the range of 6% to 12%, but with a significant increase ($p \leq 0.0001$) observed only for vincristine at a DNA damage level of 12%. There was a significant increase ($p \leq 0.001$) in DNA damage observed for topoisomerase inhibitors (teniposide and mitoxantrone) drug class in the TK6 cells, while etoposide and topotecan show non-significant increase.

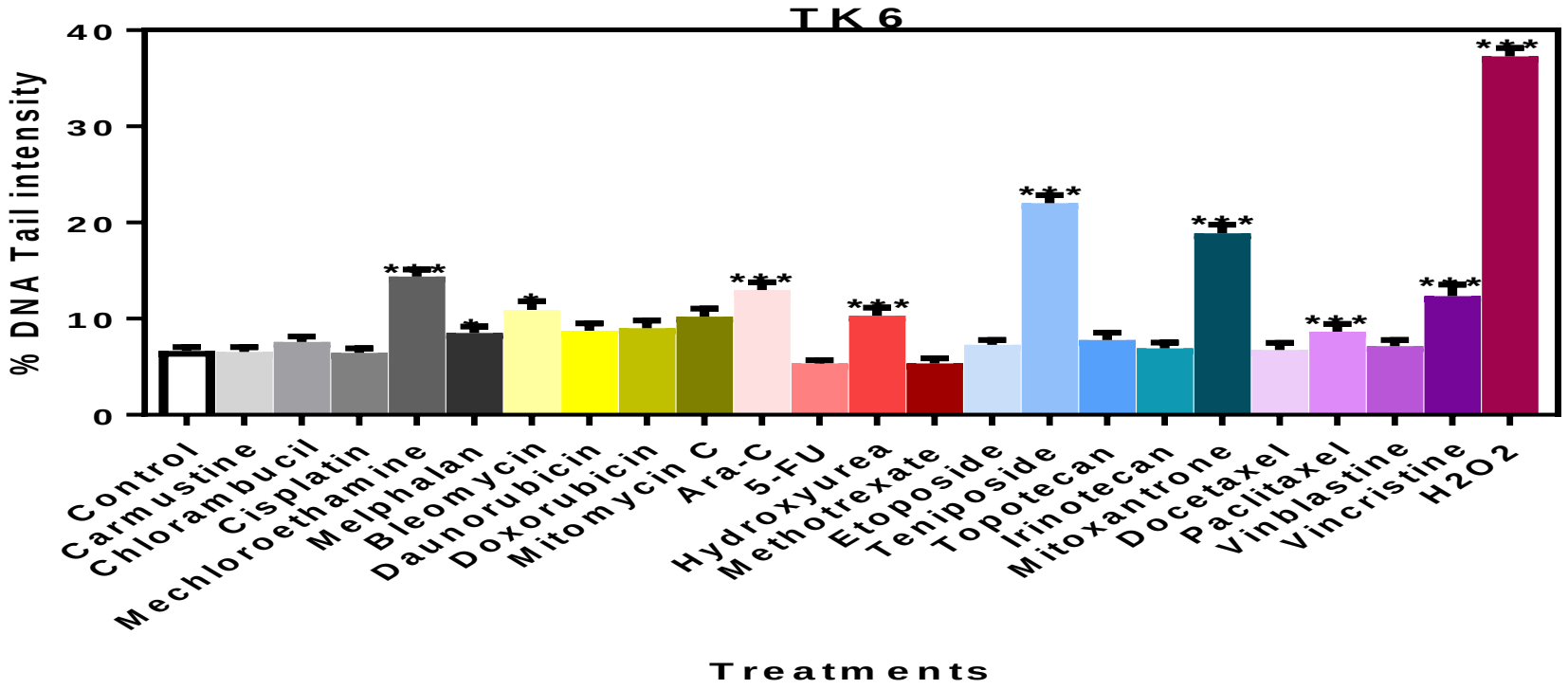

Figure 4.4 The percentage DNA tail intensity of TK6 bystander cells following co-culture with HS-5. TK6 cells were assessed using the alkaline comet assay and evaluated for DNA strand breaks indirectly induced by the chosen chemotherapeutic agent at clinically relevant doses. The figure shows no significant difference for 14 of the 22 drugs, with two drugs significant to the $p \leq 0.05$, 1 drug significant to the $p \leq 0.001$ level and 6 highly significantly increasing the percent DNA in the tail. Mean ± SD are presented for three independent repeats for the five classes of chemotherapeutic agents colour coded as gradients of black (alkylating agents), yellow green (antibiotics), red (antimetabolites), blue (topoisomerase inhibitors) and purple (mitotic inhibitors). Statistical significance for each data are shown as *$p \leq 0.05$, **** $p \leq 0.0001$, estimated using two-way ANOVA and Dunnett's post hoc analysis.

Collectively, all groups of drugs demonstrated at least one drug that was able to significantly increase the DNA in the tail. However, the measurements were highly variable across the drugs in each group, with no clear pattern of reactivity. Of all the drugs, teniposide produced the largest increase in percent DNA in the tail, closely followed by mitoxantrone; both of which belonged to the group of topoisomerase inhibitors (2 out of 5 drugs). The 'least' reactive group arguably was the alkylating agents, with only mechlorethamine able to significantly ($p \leq 0.0001$) increase the DNA in the tail (1 out of 5 drugs). Of the other groups, 2 out of 4 antibiotics, 2 out of 4 antimetabolites, and 1 out of 4 plant alkaloids were able to significantly increase the percent DNA in the tail. The assay was validated, and the data was supported, by an increase in tail intensity to almost 40% for the peroxide treated TK6 cells (positive control).

AHH-1 cell line (Figure 4.5) appears to have high levels of damaged DNA. It showed a more substantial level of DNA damage with most of the drugs tested in comparison to the TK6 cell line, with more drugs capable of inducing a significant increase in percent DNA in the tail (13 out of 22). The alkylating agents including the crosslinking agent (cisplatin) showed a non-significant increase in DNA damage with exception of melphalan ($p \leq 0.0001$). More so, the anti-tumour antibiotics (bleomycin, daunorubicin, doxorubicin and mitomycin C) show the highest level of DNA damage among all the classes, showing an increased DNA damage to range between 11% to 20% and all drugs were statistically significant ($p \leq 0.001$). Whilst etoposide ($p \leq 0.05$); teniposide and topotecan ($p \leq 0.0001$) and irinotecan ($p \leq 0.01$) show a significant level of DNA damage within the topoisomerase inhibitors, mitoxantrone was surprisingly reduced in comparison to the TK6 results, to show a non-significant DNA damage level at about 6.7% in comparison to the control.

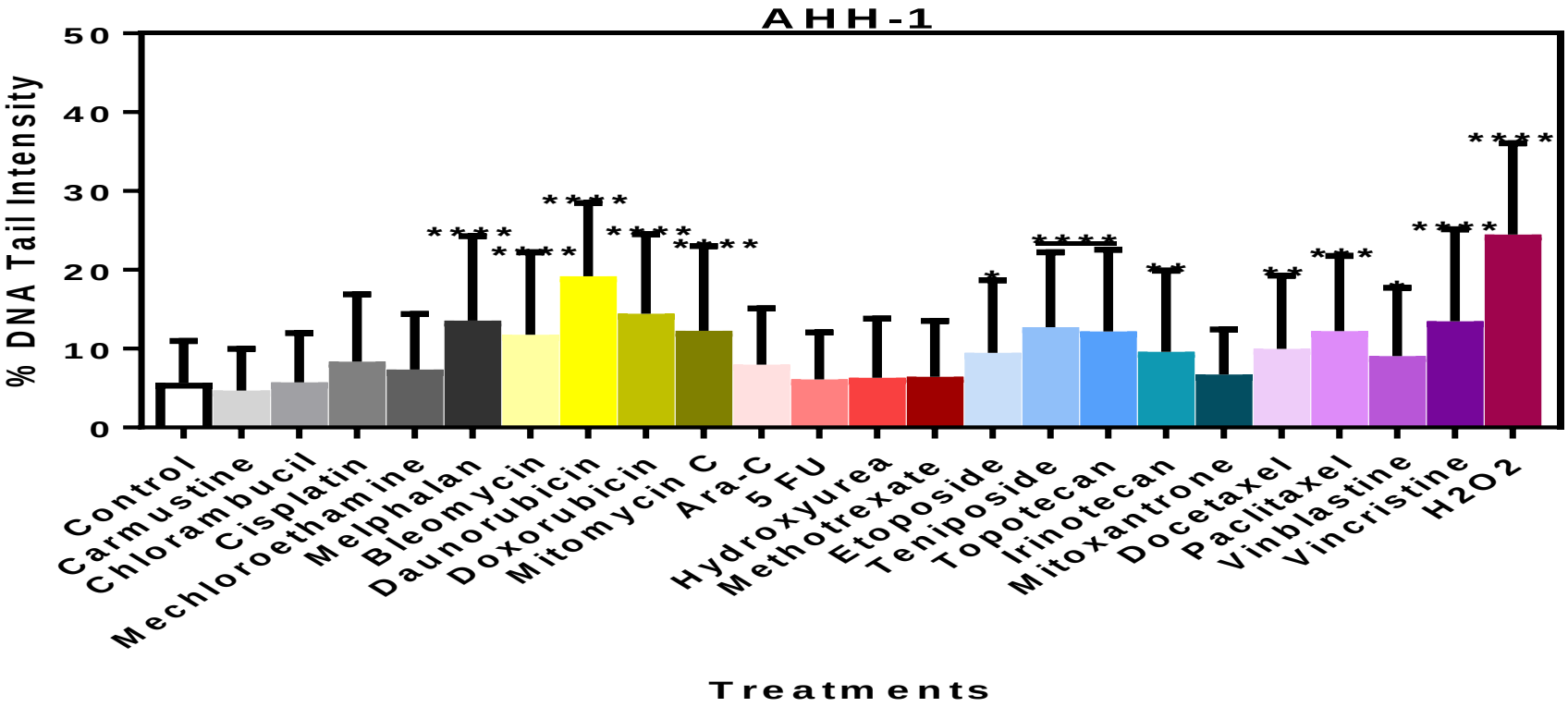

Figure 4.5 The percentage DNA tail intensity of AHH-1 bystander cells. The AHH-1 bystander cells was assessed by the alkaline comet assay to determine the percentage DNA tail intensities, following co-culture with previously treated HS-5 cells. Data is presented for the mean ± SD for the five classes of chemotherapeutic agents separated by the different colours: alkylating agents (black), anti-tumour antibiotics (yellow green), antimetabolites (red), topoisomerase inhibitors (blue) and plant alkaloids (purple). The statistical significant levels for each data are indicated as *$p \leq 0.05$, **$p \leq 0.01$, ***$p \leq 0.001$, ****$p \leq 0.0001$, analysed using two-way ANOVA and Dunnett's multiple comparison test.

This suggests that the metabolic capability of the AHH-1 cells can counteract the toxicity of the mechanism of bystander effect induced specifically by mitoxantrone. The antimetabolites (5-FU, hydroxyurea, and methotrexate) were all non-significant and did not increase comet tails The vinblastine ($p \leq 0.05$), docetaxel ($p \leq 0.01$), paclitaxel ($p \leq 0.001$) and vincristine ($p \leq 0.0001$), all within the plant alkaloids show a significant DNA damage level above the control to range between 9% to 13.5%. No particular trend was observed between TK6 and AHH-1 cell lines. However, some agents were significant in both cell lines and these included the antibiotics (bleomycin and mitomycin-c), topoisomerase inhibitors (teniposide) and the plant alkaloids (vincristine). While mechlorethamine, ara-c, hydroxyurea, bleomycin and mitoxantrone were increased in only TK6, these agents (melphalan, daunorubicin, doxorubicin, etoposide, topotecan, irinotecan, paclitaxel, docetaxel and vinblastine) showed specific increase for AHH-1 cell line. The negative controls in both cell lines were approximately the same at about 6%, and similarly the positive hydrogen peroxide (H_2O_2) controls reveal high levels of DNA fragmentation, as expected corresponding to high percentage tail intensity and these were raised over and above all the other chemotherapeutic agents. However, percent DNA in the tail was slightly reduced in AHH-1 (25%) compared to the TK6 (38%), but both peroxide controls confirmed a working assay technique.

4.3.2.2 Micronucleus Assay

In this study, the ability of the 22 chemotherapeutic agents to induce bystander effect was assessed by micronucleus assay which detects the induction of chromosomal damage. Because the comet assay does not detect chromosomal damage, the micronucleus (MN) assay another genotoxic endpoint detection assay was used in order to determine DNA damage (if any); which would help inform on the phenomenon of CIBE. As with the comet assay, two cell lines (TK6 and AHH-1) was used for the MN assay. TK6 was chosen for its wide usage and application in genotoxicity testing and following the outlined advantages and recommendations of Lorge *et al.,* (2016). TK6 has an active tumour protein gene (p53) which regulates the cell cycle, thus important in tumour suppression. The AHH-1 cell line is considered a metabolically competent cell line based on the expression of cytochrome p450, an enzyme produced by the cytochrome p450 genes, which are involved in the synthesis and metabolism of various chemicals within the cells. Thus, in addition to their advantages for use in genotoxicity testing, both cell lines are also representative of the lymphoid BM compartment; a vital representation of the bystander model. TK6 (Figure 4.6) data show an increase in the number of micronuclei scored for all chemotherapeutic agents. While the increase in some of these agents was significant (12 out of 22 drugs), the others were not significant. The alkylating agents show an increased number of MN ranging from 84 to 111 MN per 2000 cells scored. Amongst this class, only mechlorethamine showed a significant ($p \leq 0.05$) increase compared with the control whereas carmustine, chlorambucil, cisplatin and melphalan were increased but not statistically significant. The antibiotics show MN induction ranging from 72 to 104 with significant levels detected for daunorubicin ($p \leq 0.001$) and mitomycin C ($p \leq 0.05$), whereas others were non-significant. The antimetabolites' MN frequencies varied between 88 to 141 and for all agents (hydroxyurea, 5-FU and methotrexate) MN were significantly raised ($p \leq 0.05$), except for Ara-C with a non-significant MN frequency of 92. Also, the topoisomerase inhibitors were remarkably increased showing an MN induction that ranged from 82 for topotecan and irinotecan up to 149 for mitoxantrone. Whilst etoposide ($p \leq 0.05$) and teniposide ($p \leq 0.01$) were significant, mitoxantrone even though it possess the highest number of micronuclei both within and between the groups was however non-significant. Also significantly ($p \leq 0.05$) increased were the plant alkaloids (docetaxel, paclitaxel, docetaxel and vinblastine) and they had the highest MN induction across all tested agents, ranging from low (103) to high (141).

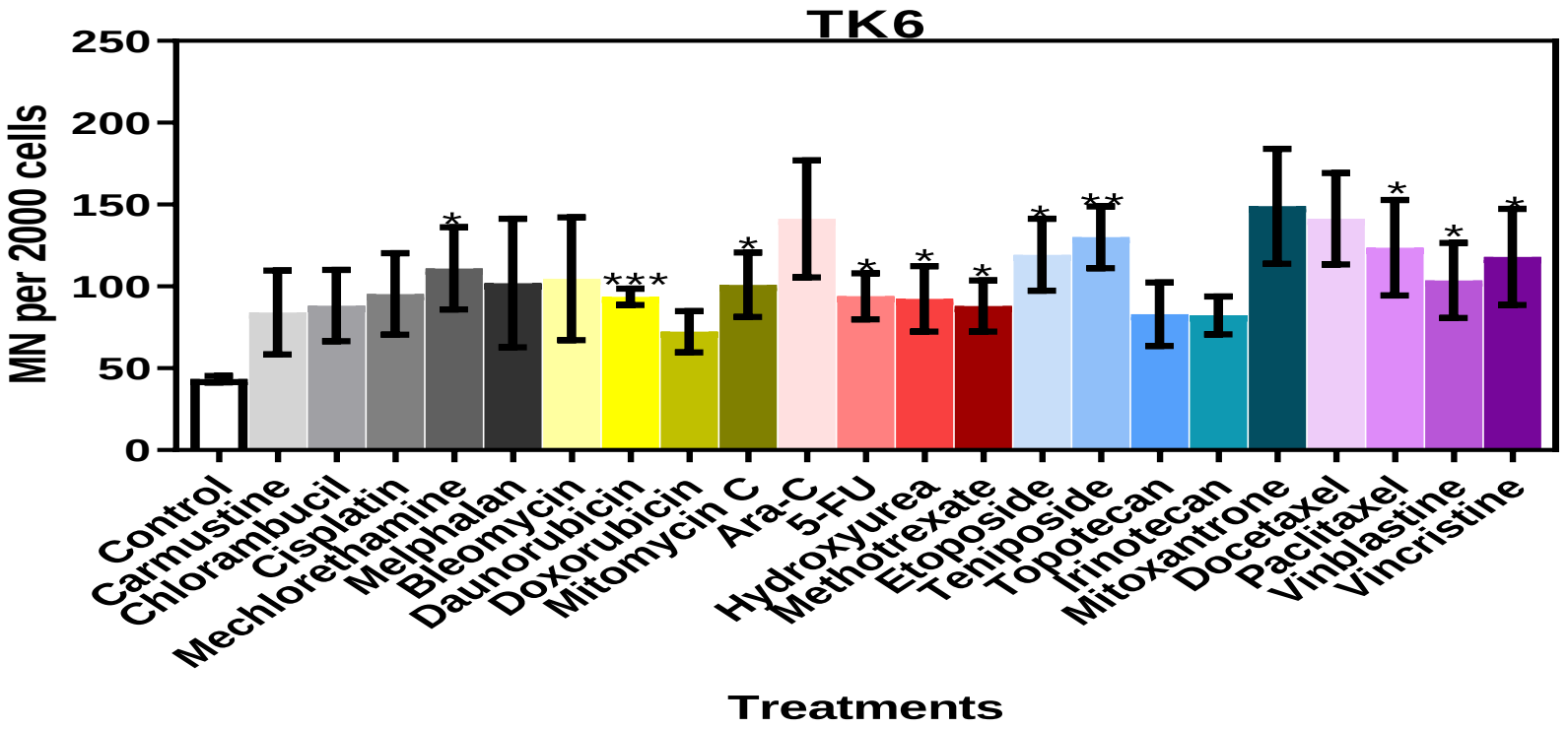

Figure 4.6: The induction of micronuclei in TK6 bystander cells for a panel of chemotherapeutic agents. TK6 cells post 24 hours co-culture were harvested and evaluated for chromosomal damage by scoring the number of micronuclei (MN) present. The total of all MN for mononucleated, binucleated and multinucleated cells are presented for Mean ± SD for all the chemotherapeutic agents analysed and significant difference shown as $*p \leq 0.05$, $**p \leq 0.01$ and $***p \leq 0.001$, as analysed used two-way ANOVA and Dunnett's post hoc multiple comparison test. The data presented show control as colourless, alkylating agents (shades of black), antibiotics (shades of yellow green), antimetabolites (shades of red), topoisomerase inhibitors (shades of blue) and mitotic inhibitors (purple shades). Data show the mitotic inhibitors with the highest MN induction before the alkylating agents; while the other classes were similar.

In contrast to TK6 cells, the AHH-1 cell line (Figure 4.7) MN induction frequency increased substantially for all the chemotherapeutic agents. Generally, the number of MN induced by the alkylating agents (153 to 187) and antibiotics (147 to 197) appear almost identical as shown by their total MN range, whereas there was large variation within and across the group of antimetabolites, topoisomerase inhibitors and plant alkaloids. The alkylating agents were all significant (cisplatin; $p \leq 0.01$, mechlorethamine and melphalan; $p \leq 0.05$) except carmustine and chlorambucil, although it had an increased MN of 178. The antibiotics show an MN induction ranging from 147 to 197, which show significance (bleomycin; $p \leq 0.05$), doxorubicin and mitomycin C; $p \leq 0.001$) for all agents except daunorubicin. The antimetabolites were all significant (Ara-C; $p \leq 0.001$, hydroxyurea; $p \leq 0.01$ and methotrexate $p \leq 0.05$) except for 5-FU with an MN induction of 114. More so, the topoisomerase inhibitors' MN frequencies were shown to be between the lower MN inductions of 98 (topotecan) to a higher level of 195 (etoposide). Whilst etoposide ($p<0.01$) and mitoxantrone ($p<0.05$) were statistically significant, teniposide, topotecan and irinotecan were non-significant. Of note were the plant alkaloids which all show a good statistical significance with an increased micronuclei frequency ranging from 108 (docetaxel; $p<0.01$) to 211 (paclitaxel; $p<0.001$).

As seen with the comet assay, the AHH-1 levels of genotoxicity in the form of MN were higher in comparison with TK6. MN induction of each group in AHH-1 cells were raised compared with their TK6 counterpart as evidenced in Figure 4.7. Agents that were significant in both cell lines include mechlorethamine (alkylating agent), mitomycin C (antibiotic), hydroxyurea and methotrexate (antimetabolites), etoposide (topoisomerase inhibitors), as well as all plant alkaloids except docetaxel. There was an observation of similar background levels of MN for both cell lines (TK6; 2.15% and AHH-1; 3.25%) which in comparison to the treated data are considerably low.

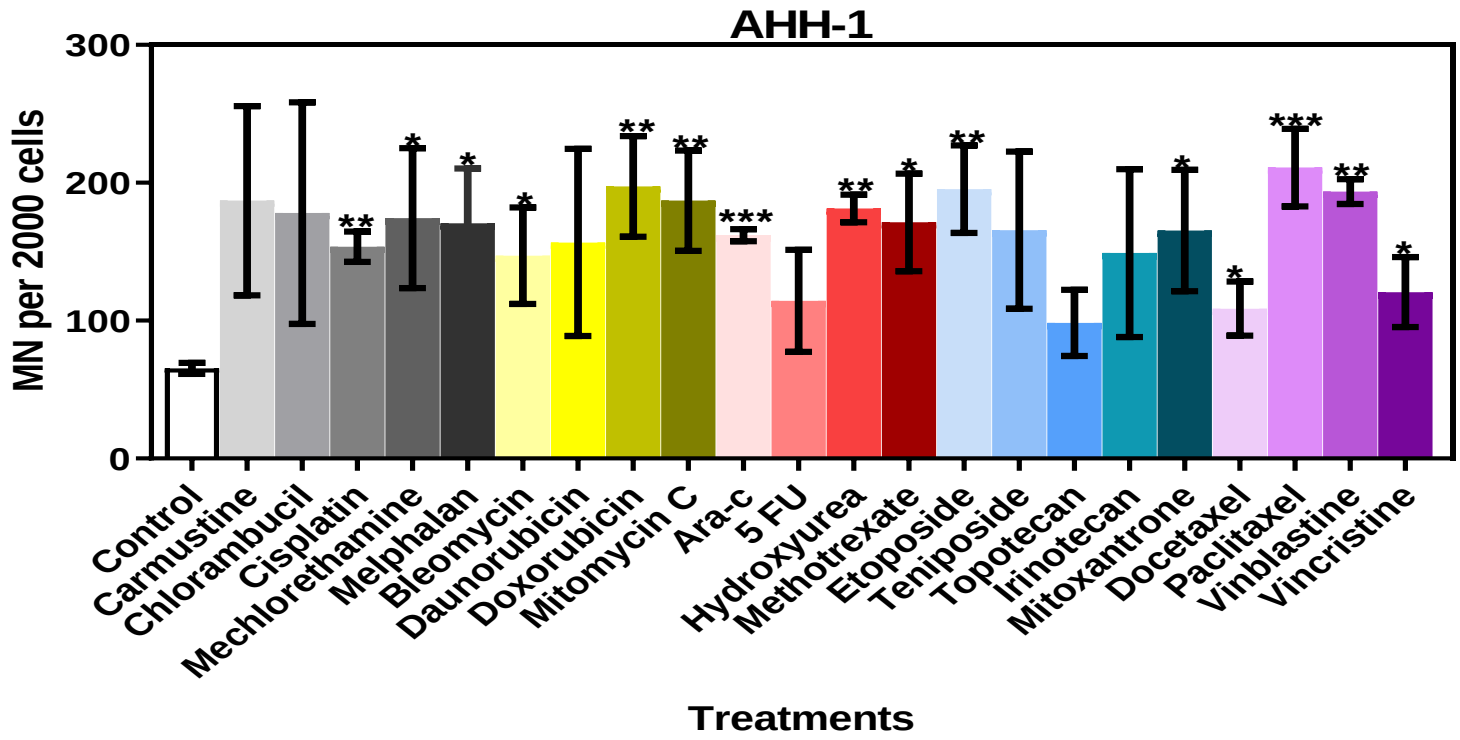

Figure 4.7 The micronuclei induction in AHH-1 bystander cells for some chemotherapeutic agents. AHH-1 cells were scored based on observation of micronuclei induction. Data is presented for the mean ± SD of 2000 cells scored and the statistical significance level represented with asterisks on the respective bars as $*p \leq 0.05$, $**p \leq 0.01$ and $***p \leq 0.001$ analysed using two-way ANOVA and Dunnett's test of multiple comparison, as shown for three independent experiments (n=3). Data show differences in the MN induction within each class as colour coded: alkylating agents (shades of black), antibiotics (shades of yellow green), antimetabolites (shades of red), topoisomerase inhibitors (shades of blue) and mitotic inhibitors (purple shades). All the classes investigated for this cell line show a very high MN induction in the range of 80 to 200 with vast number showing statistical significance.

Following the accrued data for the initial screen of the 22 chemotherapeutic agents, other assays focused on the four key drugs to help establish possible mechanism for CIBE and provide further clarity to the outcome of the earlier genotoxic assay.

4.3.2.3 Human pan-centromere labelling

In this study, FISH labelling of centromeres (section 2.6) was used to analyse the bystander cells to investigate the type of MN observed within the micronucleus assay. Identification of the origin of MN is necessary for genotoxicity testing or in biomonitoring studies as exposure to a chemical majorly induces a particular type of damage (Norppa and Falck, 2003). To assess this mutation assay, presence of a centromere signal in the MN infers loss of a whole chromosome (aneugenicity) whereas absence of centromere signal in the MN infers chromosomal breakage (clastogenicity).

Figure 3.5 shows the data for the evaluation of the fraction of centromere positive and centromere negative MN scored for the TK6 and Kasumi-1 cells. TK6 was utilised for the reasons in section 4.3.2.2. As the study evolved the Kasumi-1 cell line (a myeloid cell line) was added to complete the typical BM compartments, which also evidenced an increase in MN induction in the duration assay (Figure 4.14). Thus, in an attempt of the *in vitro* bystander model to mimic the *in vivo* BM as a proper representation of the DCL study, FISH analysis was performed for these lymphoid and myeloid cell lines. Overall, a total MN in 2000 cells were scored per slide for the control sample and 100 MN assessed for each treated sample; the data was averaged for the three repeats. The TK6 cells data showed that most agents could induce centromeric signal in MN (Figure 4.8) with all drugs having roughly equivalent centromere positive to negative MN. All drugs showed a slight 'preference' to centromere positive, except for mitoxantrone. The alkylating agents (carmustine and chlorambucil) exhibited an equal number of centromere positive and centromere negative MN frequency, shown as 59 and 41 respectively and these were statistically significant ($p \leq 0.01$, $^{***}p \leq 0.001$) relative to the control. Whilst etoposide scored 55 for centromere positive, mitoxantrone was slightly less at 46. Also, etoposide scored 45 centromere negative but mitoxantrone scored 54. This assay was analysed based on the scoring that MN less than or equal to 50% are representative of a mixed events whereas aneugenic event would predominantly be above 70%. It is of interest that there is approximately equal centromere positive to negative MN for the topoisomerase inhibitors, as these are known clastogens. This suggests that the mechanism for

genotoxicity in bystander cells is unlikely due to drug elution from treated cells. These data indicate that carmustine, chlorambucil and etoposide MN induction are of mixed mode of action for the TK6 cell line.

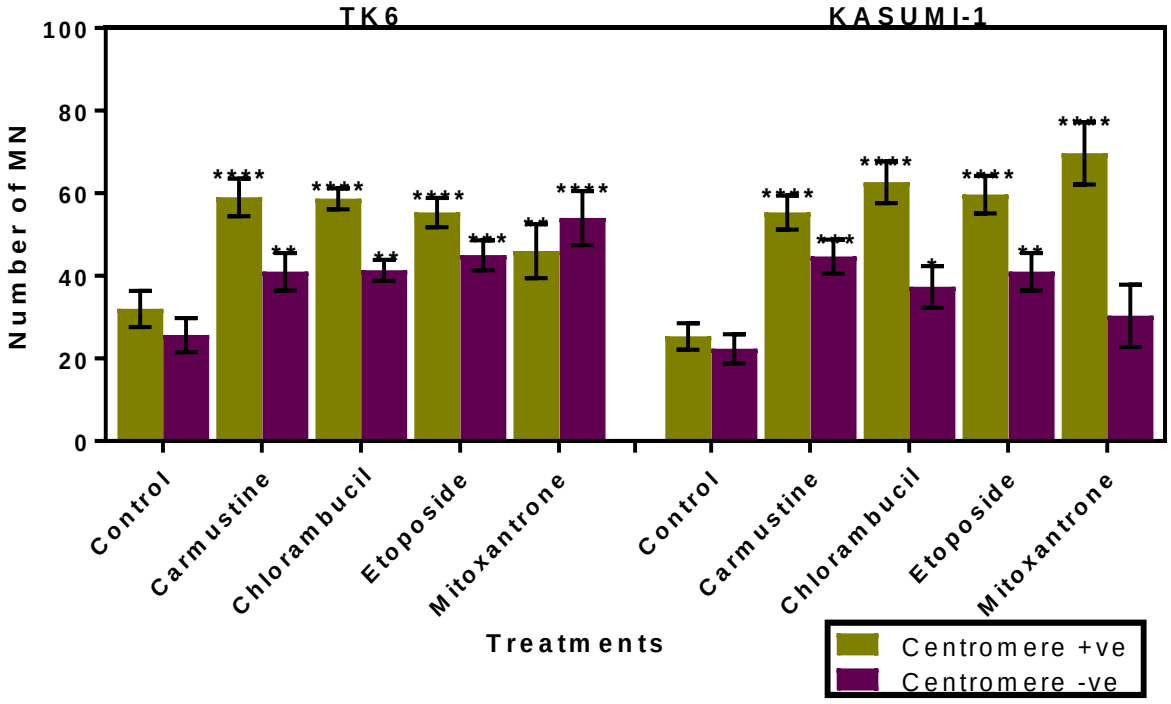

Figure 4.8 Comparative assessment of aneugenicity and clastogenicity in MN of bystander cells using pancentromeric probe. The number of MN obtained in the bystander co-culture model for the TK6 and Kasumi-1 cells following HS-5 exposure to the clinically relevant doses of carmustine, chlorambucil, etoposide and mitoxantrone. Data represents the mean ± SD for three biological repeats (n=3) of the induced MN in bystander cells. Significance levels of $*p \leq 0.05$, $**p \leq 0.01$, $***p \leq 0.001$ and $****p \leq 0.0001$ (analysed using student T-test relative to individual controls) are indicated on the bars as compared to their respective control values. The MN induction in control data were scored for a total of 2000 cells, whereas treated samples were scored as centromere positive or negative per 100 micronucleated cells.

Contrary to the TK6 cells, the Kasumi-1 cell line showed evidence that all tested agents possess a MN frequency with a higher number of centromere positive signals (Figure 4.9). Only carmustine had lower centromere positive MN than in TK6, but still showed a preference towards aneugenic events. The number of MN with centromeric signals that were scored for Kasumi-1 are as follows: 55 (carmustine), 63 (chlorambucil), 58 (etoposide) and 70 (mitoxantrone), whereas the number of MN with no centromere signals were 45 (carmustine), 37 (chlorambucil), 41 (etoposide) and 30 (mitoxantrone). These data were the average of three independent assessments. Whilst carmustine, chlorambucil and etoposide could still be

considered of 'mixed mode of action' in producing a cytogenetic bystander effect with Kasumi-1 cells, conversely mitoxantrone could be considered primarily aneugenic (70% of events were centromere positive). This is in contrast to its known mode of action of being a clastogen during direct exposure to cells. This again supports the idea that the drug is not simply eluting from the HS-5 treated cells, but some other mechanism is at play. Furthermore, the variation in the outcomes for TK6 and Kasumi-1 with pancentromeric labelling, as well as the differences in data for comet and micronuclei between TK6 and AHH-1, strongly suggest that the bystander cells themselves have an influence on the outcome toxicity, given they were all co-cultured with the same treated HS-5 cell line.

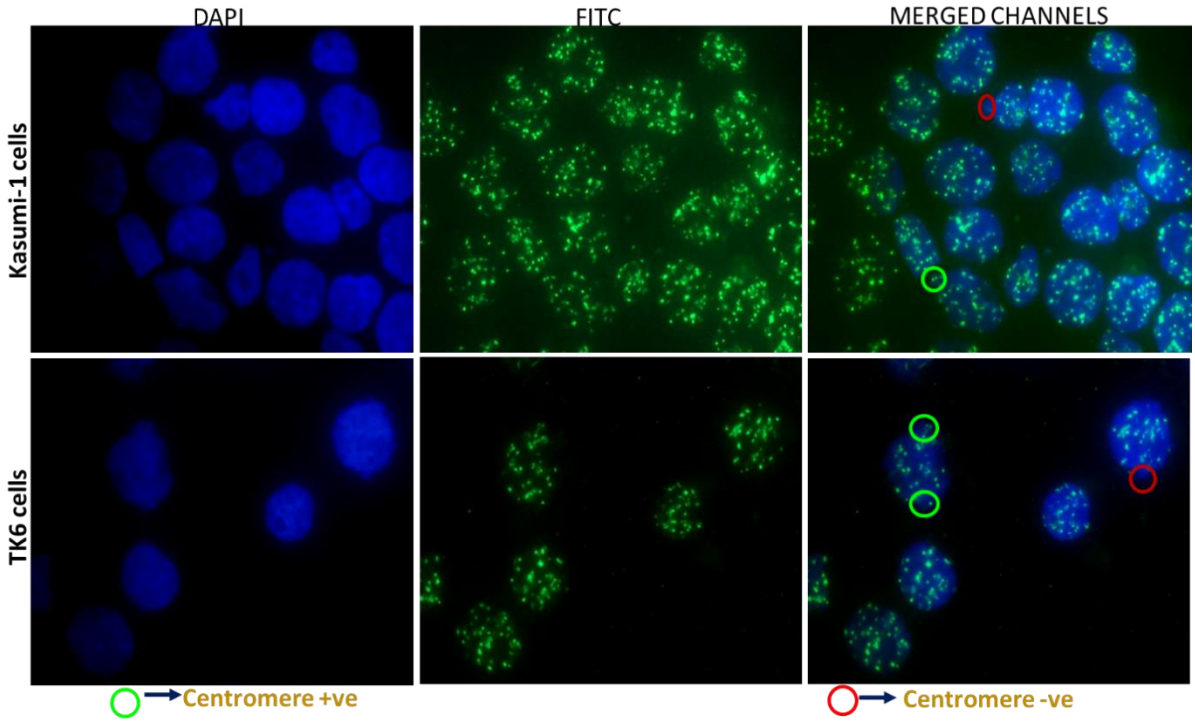

Figure 4.9: Fluorescent in situ hybridisation of the bystander cells. TK6 and Kasumi-1 cells following the *in vitro* co-culture experiment were harvested, evaluated for cytotoxicity and slides prepared for micronucleus assay. Slides were painted with the ready to use FITC labelled human pan-centromeric probe (Cambio, UK) using the in-house FISH technique optimised. Slides were visualised with separate channels of Dapi, FITC and merged on the ImageJ software. Images (40x magnification) are representative of how the centromere positive chromosome or centromere negative micronuclei was scored in both cell lines.

Since MN can arise from various sources including chromatid fragments, whole loss of chromosome or a combination, using the FISH technique to quantify MN induction enables an assessment of the fraction of clastogens and/or aneugens (Figure 4.9). It should be mentioned

that according to guidelines (Doherty, 2011), a total of 100MN should normally be scored for treated cells for this type of technique, but for uniformity and comparative analysis between agents especially for cases with low MN induction like control sample, a total of 2000 cells were scored as recommended. Such comparison between controls indicate that 10.95% of TK6 show a centromere signal and about 9.05% show no centromeric signal. Additionally, about 12.3% (centromeric positive) and 7.62% (centromeric negative) of the total cells scored for Kasumi-1 cells indicates similarity with the TK6 control.

4.3.2.4 Hypoxanthine phosphoribosyl transferase (HPRT) mutation assay

Mutations are those changes caused by mutagenic chemicals, radiation, viruses, transposons and errors in cell division or DNA replication thereby resulting in a change in the DNA sequence of a cell (Nagarathna *et al*., 2013). These mutations could be structural aberration, genome mutation or single gene point mutation. The HPRT assay was designed as part of the battery of tests needed in combination with bacterial gene mutation and chromosomal aberrations for the specific detection of mutation caused by certain chemicals or toxic substances in mammals. The HPRT assay is advantageous for its gene specificity, response to a large mutagen spectrum and capacity of testing on human derived cell lines. The human lymphoblastoid cell lines such as AHH-1, TK6 and MCL-5 were the preferred cell line of choice as they are male cell lines with heterozygous sex chromosomes, thereby allowing loss of function selection for the target gene on X chromosome.

To investigate the possible involvement of mutants point mutations in CIBE, the HPRT assay was applied to the *in vitro* bystander co-culture (section 2.2). Four 96 well plates per treatment/dose containing 0.6 µg/ml of 6-TG for the positive selection was prepared, filling the inner wells ($4x10^4$cell/well) per plate and leaving the outermost wells to avoid desiccation. Another four 96 well plate containing only 20 cells per well was plated per treatment for the plating efficiency evaluation. This method was adapted from Thomas *et al*., (2013) and Doak *et al*., (2007). On the 13th day, live colonies ($HPRT^-$) were scored and analysed as in Johnson (2012). Methylnitrosoureas (MNU - positive control) doses (0.0025 µg/ml, 0.01 µg/ml, 0.025 µg/ml and 0.075 µg/ml) on AHH-1 cells showed mutant frequencies (MF) just under 2×10^{-5} for the two lower doses and about 3×10^{-5} for 0.025 µg/ml and 5×10^{-5} for 0.075 µg/ml doses (Figure 4.10A). The bystander data for AHH-1 shows carmustine MF as just under 1×10^{-5}, chlorambucil with 1.7×10^{-5}, etoposide as 2.7×10^{-5} and mitoxantrone as 4.2×10^{-5}. For MNU

and other agents used, only the highest dose and mitoxantrone respectively were statistically significant ($p \leq 0.05$) compared with the controls. The MF of mitoxantrone in AHH-1 bystander cells corresponds to that of the highest dose of MNU investigated at 5×10^{-5}. The relative plating efficiencies were plotted against the increasing MNU doses and other chemotherapeutic agents used (Figure 4.10 A&C). The MNU plating efficiency showed no dosage trend, but the lowest and highest dose appeared lower than other doses. Significant to the control were the 0.025 µg/ml dose for MNU ($p \leq 0.001$), and etoposide ($p \leq 0.05$) of the bystander cells. The MNU data was a proof of concept that the assay was valid and functional as the mean data of three repeats were comparable to that of Thomas *et al. (*2013).

Contrarily, the TK6 cells with same MNU doses (Figure 4.10 B&D) showed no change in MF for the lowest dose compared with the control, but a dose dependent increase for the next two doses, and plateau between the final two doses. MNU revealed an increased MF corresponding to increased dosage, but this was not a linear response. Only dose 0.075 µg/ml was significantly different ($p \leq 0.001$) to the control. The bystander TK6 cells revealed a significant value for etoposide ($p \leq 0.05$) as the highest MF, to be more potent than carmustine which showed a non-significant MF of 3×10^{5}, and both agents were the most decreased of the plating efficiencies at 60%. Etoposide MF was above the highest MNU dose, showing statistical significance for both plating efficiency ($p \leq 0.01$) and the MF ($p \leq 0.001$). Whilst mitoxantrone was raised, chlorambucil was almost the same as the control and neither of these agents was statistically significant. Parallel to the increasing doses of MNU were the relative plating frequencies of these agents for both the positive control and bystander cells. These data is a representation of the plating efficiency and viability assessment for three biological repeat experiments. The relative plating efficiencies performed as part of the post assay analysis were good, with the highest dose of MNU at 100% and TK6 cells significant at 60% ($p \leq 0.01$). The bystander cells plating efficiencies were above 80% in AHH-1 cells with etoposide significantly higher than untreated control at 110% ($p \leq 0.05$), while the cell viability of TK6 cells reduced at about 50% for carmustine and etoposide compared with the untreated control, but these were still within the acceptable 50% limit (OECD, 1997).

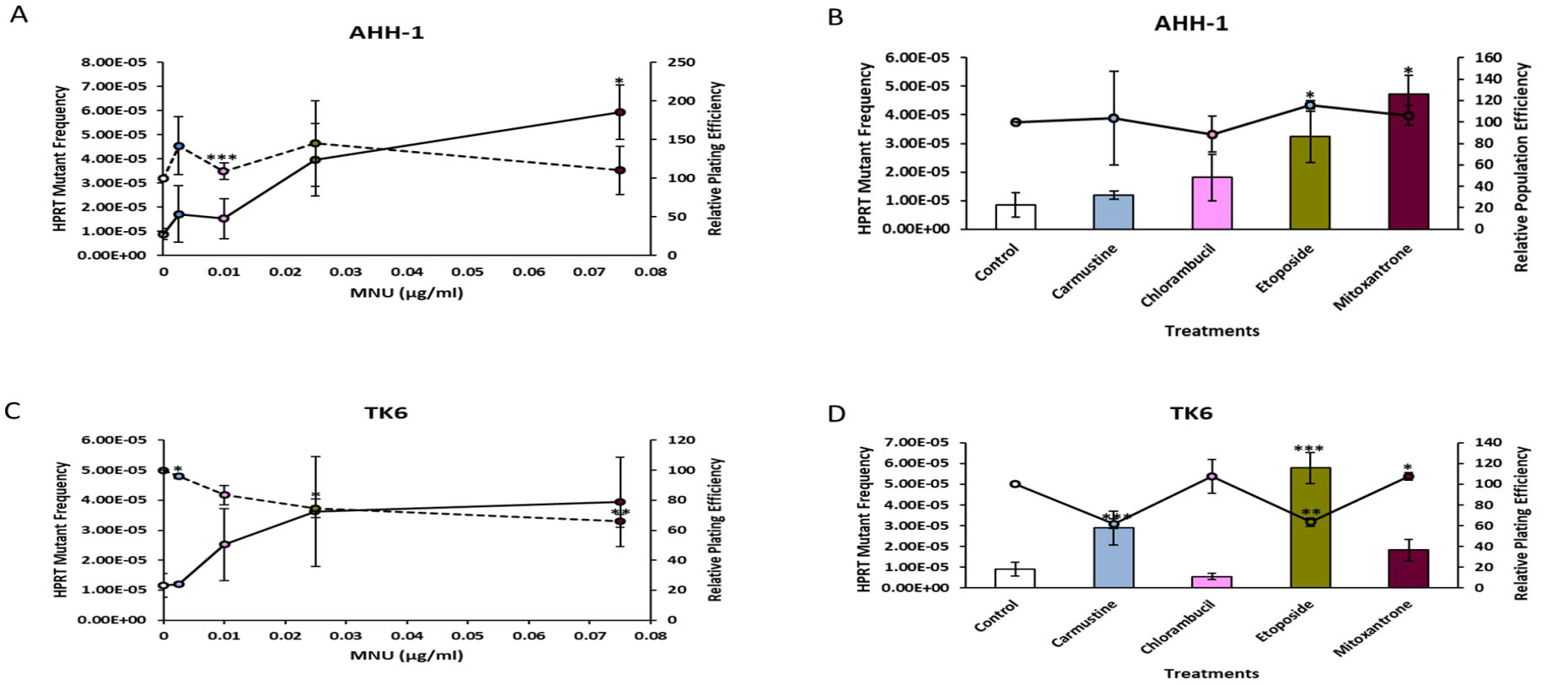

Figure 4.10 HPRT dose response to MNU of AHH-1 and TK6 and their bystander mutant frequencies. Various doses of MNU were used to determine a dose response of directly treated (straight line) AHH-1 (A) and TK6 (C). HPRT mutant frequencies for the bystander cells (bar charts) are shown for AHH-1 (B) and TK6 (D) cells. The data represents the mean ± SD for three biological repeats of AHH-1 cells but two repeats of TK6 cells are shown. The plating efficiencies of MNU are depicted in dotted lines (A&C) and that of the bystander cells as a straight line (B&D). While MNU showed a non-linear dose response, etoposide consistently revealed evidence of point mutation in both cell lines. Statistical representation are shown for $*p \leq 0.05$, $**p \leq 0.01$ and $***p \leq 0.001$.

All cells were evaluated for cytotoxicity following exposure to treatments. Cells were assessed by trypan blue exclusion following exposure to treatments in HAT and HT media. Also at pre and post MNU/chemotherapeutic agents exposure, cell viability was estmated before cells were seeded in 96 well plates for mutant frequency estimation. Data (Figure 4.11) show a relatively good cell viability, with minimum of 60% overall. Whilst the untreated control showed an almost 100% cell viability, there was an observation of a significant (*$p \leq 0.05$ and ***$p \leq 0.001$) decrease for the treated agents especially in all MNU doses (0.0025 to 0.075µg/ml) of both cell lines. Only carmustine treatment in TK6 cells showed a significant (*$p \leq 0.05$) decrease from the control.

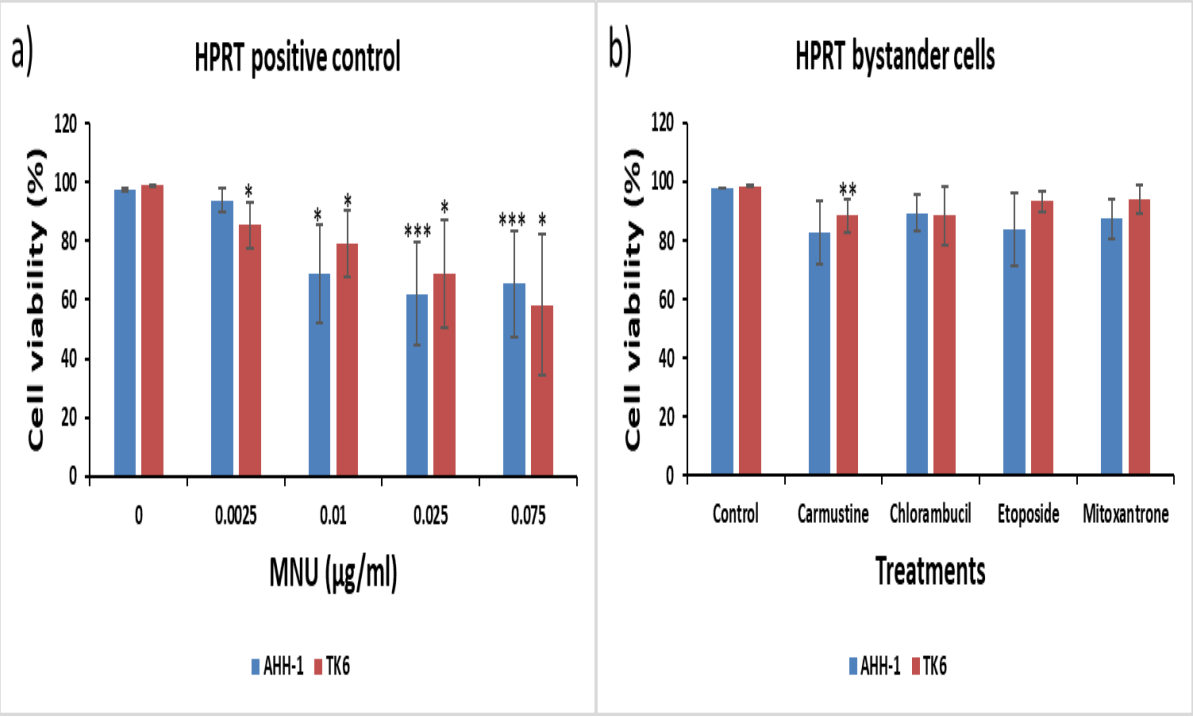

Figure 4.11: The cell viabilities of AHH-1 and TK6 cells used to assess the HPRT point mutation. Following removing of background mutants from the cell lines, AHH- and TK6 cell were directly exposed to concentrations of MNU as positive control (A) and some were used in the co-culture model as bystander cells (B). After treatments, the cell lines were allowed to recover, proliferate and increase in cell number. Cytotoxicity was assessed and cells plated in four repeats for MF assessment and same number for plating efficiency determination. Cell viability was assessed by trypan blue exclusion. Presented data are for n=3 in AHH-1 and n=2 for TK6 bystander. Both cell lines show good cell recovery with cell viabilities above 70%, with statistical significance shown for *$p \leq 0.05$, **$p \leq 0.01$ and ***$p \leq 0.001$.

Both AHH-1 and TK6 bystander cells showed independent specific mutation induction. Whilst they show similar evidence of a non-linear dose response for MNU, their plating efficiencies were different and so was the bystander outcome. Taken together, although these cell lines showed different outcomes with different agents, it would be logical to argue that except for chlorambucil, all agents exhibit a capacity for single point mutation within the bystander assay, but the outcome appeared to be dependent on the bystander cell and the agent used. This suggest that the incoming donor/bystander cell may play an important role in the outcome for genotoxicity.

4.3.4 Bystander duration determination

This study investigated the longevity of the bystander effect over a five-day period. As described in section 4.2.5, the HS-5 cell line was exposed for 1h at clinically relevant doses of carmustine, chlorambucil, etoposide and mitoxantrone. Post-exposure, cells were harvested 24 hours later to assess for viability and genotoxicity. Each day of the assay witnessed a harvest and replacement of the bystander culture insert with new lymphoblastic cells. Such daily replacement was to enable a specific detection of the exact day for the induced DNA damage.

4.3.4.1 Cytotoxicity of bystander duration cells

Cell viability was analysed daily using the dual staining acridine orange and propidium iodide stain (50 µg/ml stock) and read using the Luna counter fluorescence reader. Three readings were taken for each sample using different field of view and the mean value presented.

Analysis of the cytotoxicity (Figure 4.12) data generally depicts an overall population of viable cells throughout the five days. In comparison with the control, all four agents showed viability between 60 to 80 % over the entire duration of the experiment. In the TK6 cells the viability of day 1 was the lowest, but still above the 50% threshold required by OECD guidelines. Viability gradually improved for all four drugs over the 5 days, and none was significantly lower in comparison with the control. Therefore, although the greatest toxicity appeared to be on day one, there is little difference in viability of TK6 between each day for all drugs, though viability was consistently lower than the control.

Furthermore, the Kasumi-1 cell line showed a very good viability in the range of 70 – 85 for the entire duration. Chlorambucil viability was almost steady at about 75% with a slight rise on the final day to about 80%. Etoposide revealed a decline in viability (~60%) for days two

and three and returned to 80% on days four and five. Mitoxantrone did show an almost steady percentage viability for the whole five days, ranging from 70% to 80%. In some cases the mean viability for the cells, non-significantly exceeded that of the controls.

The very good viability of both cell lines with all agents achieving the accepted viability limit supports the criteria for evaluation of genotoxicity in these cells. It is of note that bystander cells showed consistently good viability through the range of assays performed in this thesis, suggesting that this could be problematic if the same occurred *in vivo*. Specifically, low cell death with concomitant genotoxicity could propagate mutagenic events, and this is particularly relevant when considering the data and duration of viability for Kasumi-1, where proliferation and viability appeared occasionally to exceed that of the untreated controls.

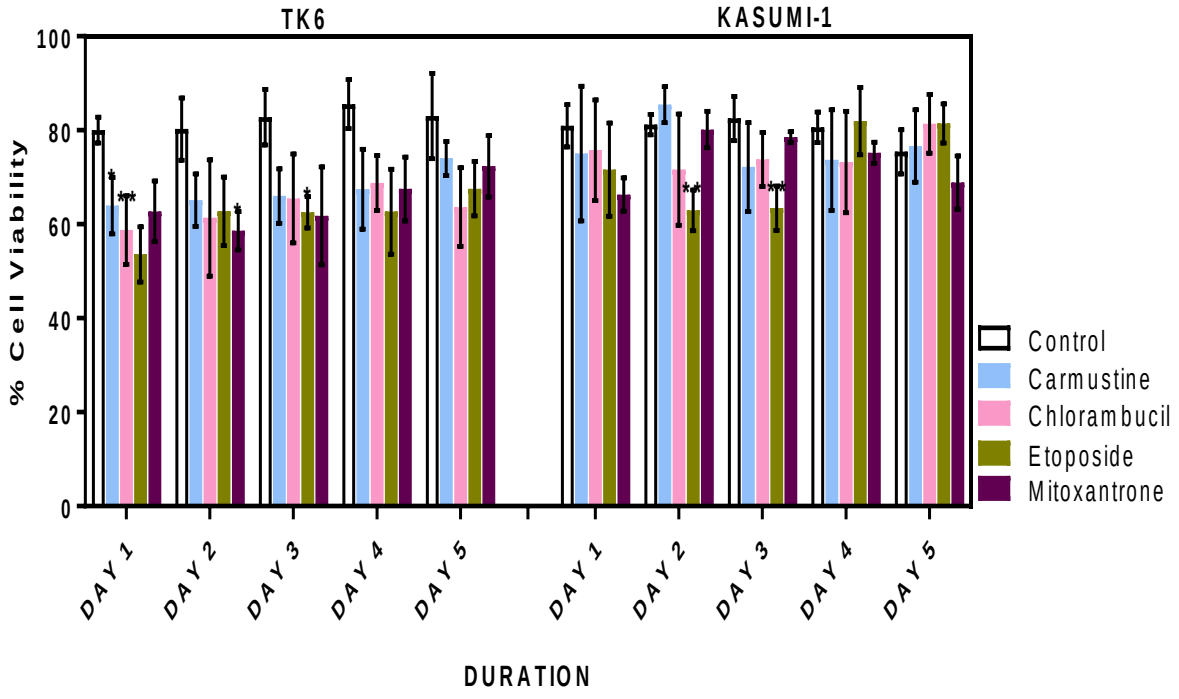

Figure 4.12 Comparative percentage viability of lymphoblastic TK6 and myeloblastic Kasumi-1 over a five-day period assessed in the bystander co-culture model for the four key chemotherapeutic agents. Twenty-four hours post co-culture, cells were harvested and cell viability evaluated using the acridine orange/propidium iodide stain and automatic cell viability evaluation by LUNA counter. Data is presented for three independent biological experiments and mean ± SD are indicated. All cells show at least 60% cell viability for all days and statistical significance is shown for $*p \leq 0.05$ and $**p \leq 0.01$ as performed with two way ANOVA and Tukey's multiple comparison test.

4.3.4.2 Comet assay evaluation of bystander duration

Assessment of DNA strand breaks was investigated in TK6 and Kasumi-1 cells for each day of the 5-day co-culture. Once cell viability was determined (Figure 4.12), 2.5 x 10^4 cells/ml was mixed with a low melting agarose, allowed to set on a gel bond and once comet electrophoresis was completed, cells were scored immediately using the comet IV software.

All values were compared with the untreated control on their respective days. The TK6 cells (Figure 4.13) showed no evidence of DNA damage with the tested agents on any day over the five period. Carmustine showed a trajectory increase from day 1 to 4 and rapid decline on day 5. Chlorambucil showed a similar pattern to carmustine with exception of a slight decrease on day 3 to below 10% and a further rise and decline on days 4 and 5 respectively. There was increase observed for either the topoisomerase inhibitors (etoposide and mitoxantrone) relative to the control, however they both slightly declined on day 5. All the tested agents showed a non-significant difference between each day and within each day. Only the values for the assessed positive control was highly significant ($p \leq 0.0001$), thereby indicating that the assay worked, but there was just no significant DNA damage detected in the cells over the five day period. Whilst there appeared to be a slight rise in DNA in the tail on day 4, this was also observed for the control, and no statistical differences were noted.

The Kasumi-1 (Figure 4.13) cell line evaluation showed no difference for all agents on day one in comparison with the control. Carmustine and chlorambucil did show a very minimal raise on day three, but on the other days tended to be the same as, or lower than the control. However, etoposide and mitoxantrone showed an indication of DNA fragmentation in comparison with the control on day 2, returning to basal levels by day 4 and 5. Increases in DNA fragmentation for these drugs, was however, not significant. Only the H_2O_2 positive controls were statistically significant. When all the bystander duration comet data is considered, it indicates no DNA strand breaks were induced in the bystander cells by these agents at any time. Whilst TK6 cells appears to peak at day four, Kasumi-1 peaks around day 2, with no further effects observed in the other days. Considering the initial screen of 22 drugs, and the focus here of four drugs over 5 days, it appears that little DNA fragmentation is caused in bystander cells. This may offer insights into the type of signalling molecules that potentially released from the HS-5 cells in response to the chemotherapy treatments.

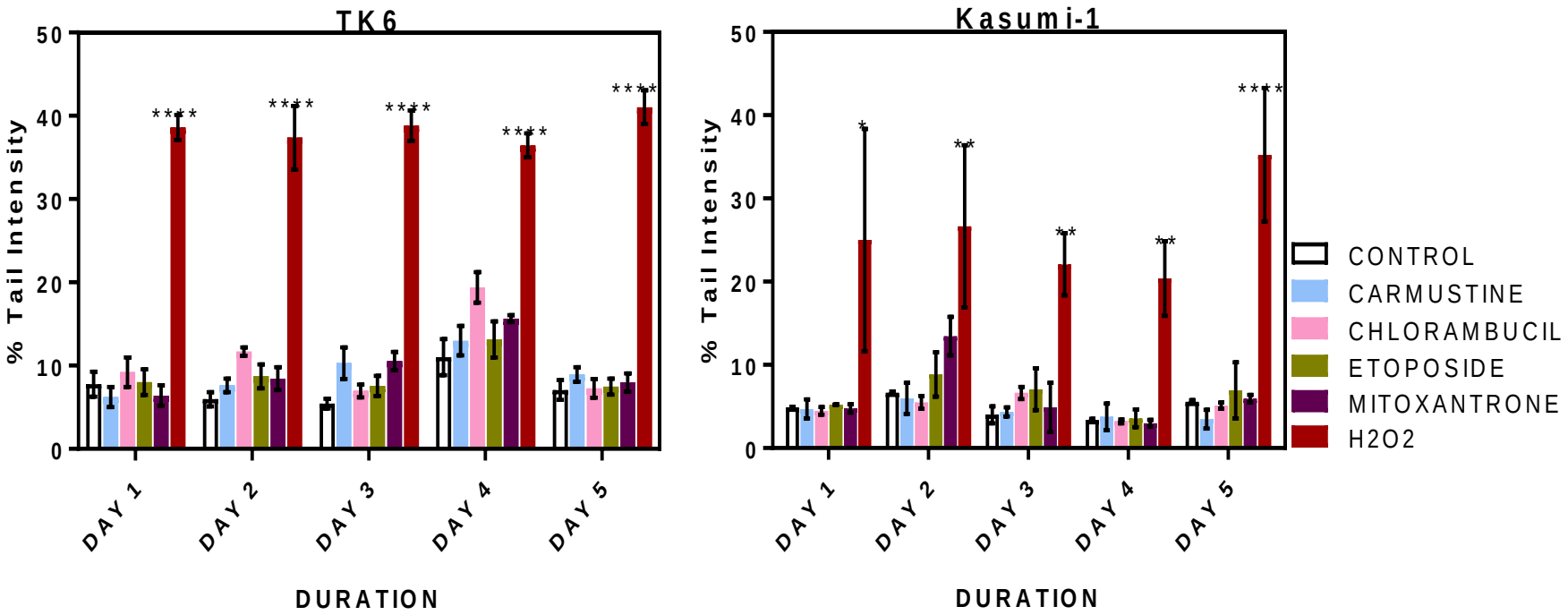

Figure 4.13 Comet assay assessment of TK6 and Kasumi-1 over a five-day period assessed for the four key chemotherapeutic agents. The percentage DNA tail intensity of TK6 and Kasumi-1 cells post co-culture was evaluated using the alkaline comet assay with hydrogen peroxide as positive control (an indication that the assay is sensitive). There was a daily replacement of cells and each bar represents the mean ± SD as analysed for three different biological experiments. Only the H_2O_2 in both cells show statistical significance for *$p \leq 0.05$, **$p \leq 0.01$ and ****$p \leq 0.0001$, as estimated using two-way ANOVA and Dunnett's multiple comparison test. None of increases evidence were not statistically different from the treated cells for none of the days, as estimated to their respective control data.

4.3.4.3 Micronucleus assay evaluation of bystander duration

Further to the initial MN assessment of the 22 screened chemotherapeutic agents, the ability to induce MN over a five-day period was assessed.

The TK6 cells (Figure 4.14) showed evidence for increased micronuclei over the five days assessed. There was high rate of DNA damage evidenced in TK6 over a 24 hour period for day 1 and a continual rise up to day 3 for all four agents. Carmustine demonstrated a steady increase in MN, peaking at day 3, but then declined over days 4 and 5; except for day 2, all its changes were significantly ($p \leq 0.01$; $p \leq 0.0001$) increased relative to the control. Chlorambucil also showed a steady rise in the number of micronuclei, similarly peaking at day 3, after which there was a continual decline up to day 5; however, chlorambucil was significantly ($p \leq 0.01$; $p \leq 0.0001$) different to the control on every day, except day 1. Etoposide was almost identical in numbers of micronuclei and trends as described for chlorambucil whereas mitoxantrone appeared to peak twice, on days 2 and 4, with a return to basal levels on day 5. In comparison with the controls of the individual days, for days 1 to 4, all agents were statistically significant for all days except the carmustine in day 2 as well as the mitoxantrone of day 3. All agents of day 5 were reduced and were statistically relevant ($p \leq 0.01$) except for etoposide.

Furthermore, in the Kasumi-1 cells (Figure 4.14) carmustine evidenced almost similar micronuclei induction on days 1, 4 and 5 but with an increase on days 2 and 3. Chlorambucil witnessed an increase in MN induction on days 2, 3 and 4 with a return to basal level (as day 1) on day 5. Etoposide show continual increase on day 2, to peak on day 3 with decline on days 4 and 5. Mitoxantrone had same trend as etoposide, increasing up to day 3, reaching its peak at day 4 and a further decline on day 5. Notably, all these agents demonstrated significant ($p \leq 0.0001$) differences on each day relative to the control of individual days and as in TK6 cells, show a general increase on days 2 up to 4, but on day 5 witnessed a decline. In contrast to TK6 all the decline on day 5 appeared to show similar level of MN induction as day 1.

Collectively, this continual induction of micronuclei over three days after initial exposure is highly suggestive of a possible long-lasting effect of the signal transduction or other potentiating factors, like stress, occurring with the cells in co-culture. Given the clinical observation that stem cells are usually infused around day 2 post-conditioning therapy, and day 5 is considered the latest day that infusion could take place, it is possible that there is never a

'safe time' to infuse stem cells to avoid the occurrence of a bystander effect, and possible induction of DCL.

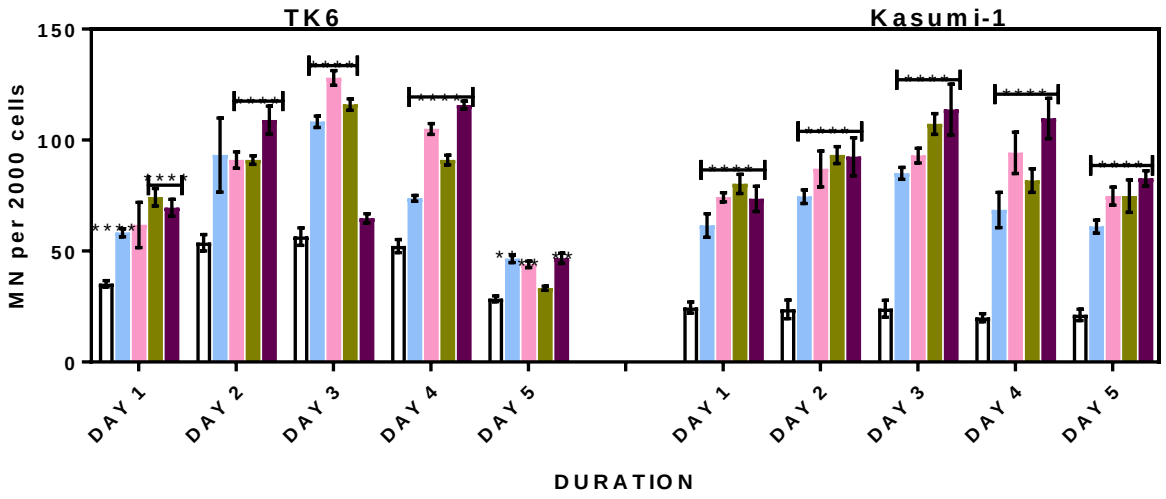

Figure 4.14: Micronucleus assessment for the duration of bystander effect in TK6 and Kasumi-1 cell lines. After an initial 1h exposure of BM cell line to chemotherapeutic agents, they were washed three times in culture medium and co-cultured for 24 hours with TK6 and Kasumi-1 cell lines. TK6 and Kasumi-1 cells were harvested post-co-culture and analysed for genotoxicity by micronucleus assay. This evaluation was performed over a five- day period, with daily replacement of fresh lymphoblast cells and then cell harvest 24 hours post co-culture for MN genotoxicity evaluation. Mean ± SD are represented in each bar (days 1 to 5) for three separate experiments (n=3) and statistical significance shown for $^{**}p \leq 0.01$ and $^{****}p \leq 0.0001$ in both cell lines as analysed with two way ANOVA and Tukey's multiple comparison test.

4.3.4.4 Medium transfer experiment

The bystander effect results in the damage of cells that were not originally exposed to any damaging agent such as chemotherapy or radiotherapy. It has been reported that medium from irradiated cells was able to transfer cytotoxic factors to cells in co-culture which were not directly exposed to irradiation (Shao *et al*., 2001; Lyng *et al.*, 2002). Some authors of RIBE reported the ability of treated cells to transfer genotoxic signals to bystander cells through their conditioned medium experiment. They noted that all cells were not capable of producing this transferable cytotoxic factors and some cells do not also have the capacity to receive the transmitted signals and hence concluded the mechanism of signal transduction through soluble factors as bystander mechanism and not through cell contact (Prise *et al.*, 2003; Lyer *et al.*, 2000).

To investigate the possibility for the transfer of cytotoxic signals to bystander cells, a conditioned medium experiment was set up. Also, based on the increased MN induction observed in this study, an investigation into the mechanism of drug elution was carried out through conditioning the cells with medium from the final wash and by LCMS (chapter 3) as well. Thus, this study compared the MN induction generated from a direct exposure of TK6 cells using the clinically relevant doses of carmustine, chlorambucil, etoposide and mitoxantrone with the MN induction frequency of two conditioned medium (final wash of treated cells and 24 hours conditioned medium from previously exposed cells). These various conditions were estimated as described in section 4.2.6.

As described earlier for this study, 2000 cells (Figure 4.15) were scored per experiment and a total of 6000 cells were evaluated per treatment, per condition and all cell viability was assessed (Figure 4.16). Direct treatment indicates a high induction of MN ranging from the least with 165 (mitoxantrone) to the highest with 222 (chlorambucil) and all agents were statistically significant compared with the control. Direct exposure in comparison with the bystander data for all four agents (with a slight exception of mitoxantrone) far exceeded the number of MN induced in the bystander cells. The conditioned medium was comparable to the duration bystander data indicating an effect over time, but the final wash medium was not comparable. The final wash medium was expected to produce low levels of MN as a potential indication that all traces of drug were removed from the HS-5 cells. Only mitoxantrone showed similar MN induced by the final wash in comparison with the conditioned medium and bystander cells. All the other drugs demonstrated little difference in MN induction compared with the control for the final wash. For all drugs, the MN outcomes were virtually the same for both conditioned medium and bystander cells, although there was more variation in the bystander data, evidenced by the large error bars.

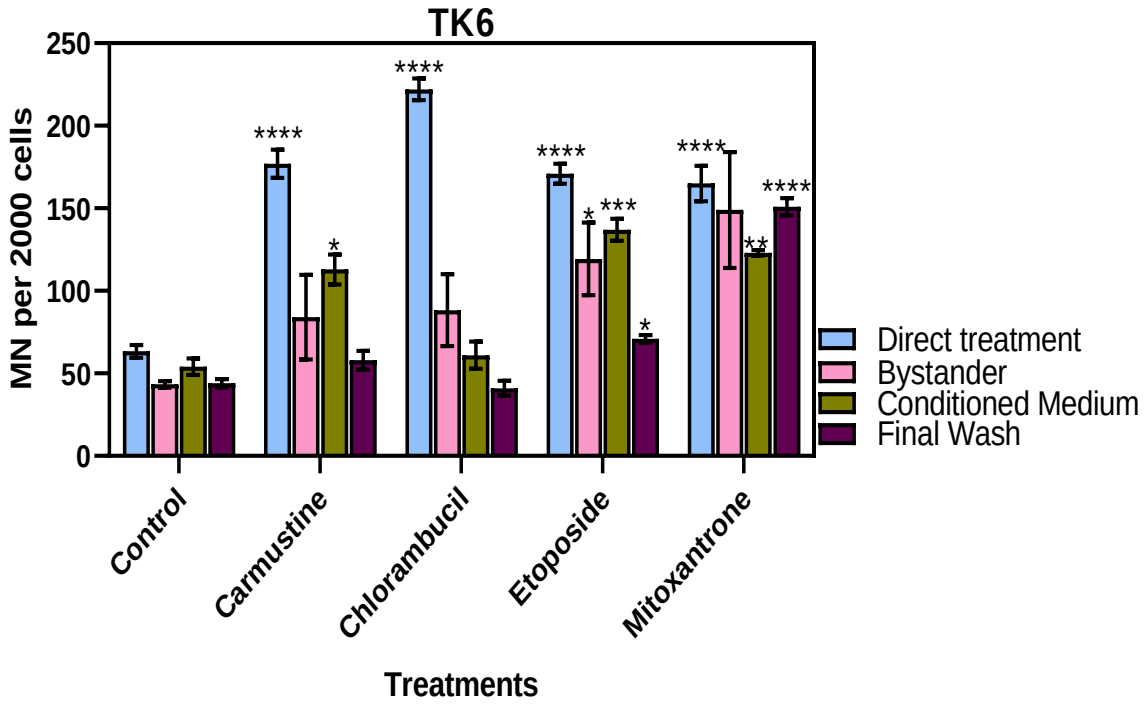

Figure 4.15: Effect of chemotherapy on induction of micronuclei in directly exposed and indirectly exposed TK6 cells. MN data of the indirectly (bystander) exposed cells of the co-culture model was compared to MN data acquired using the third (final) medium wash off of the HS-5 bone marrow cells after treatment, to incubate bystander TK6 cells for 24 hours. Direct comparison was prepared by treating the cells with the agents directly while the conditioned medium data was obtained from the harvested bystander TK6 cells co-cultured with the 24 hours incubated/conditioned fresh medium of HS-5 cells alone post treatment exposure. Mean ± SD of three independent experiments are represented and the asterisks depicts significance levels for $*p \leq 0.05$, $**p \leq 0.01$, $***p \leq 0.001$, $****p \leq 0.0001$ as analysed using the student T-test against their respective controls.

The cell viability data (Figure 4.16) of the medium transfer experiment and other conditions showed an overall good viability at about 60% and above, with the least viability evident in the direct treatment. The direct treatment showed reduction for all agents when compared with the untreated control. The reduction in all direct treatment was statistically significant ($**p \leq 0.01$) with etoposide at $*p \leq 0.05$. In the conditioned medium, while carmustine, chlorambucil and mitoxantrone showed viability at 80%, with mitoxantrone showing a statistical significance ($*p \leq 0.05$), etoposide cell viability was at 65% and was highly significant ($*p \leq 0.001$). The cell viabilities of the final wash was also very good, showing viabilities at about 70%; and while

they were less than the observed viabilities of the conditioned medium, they were however higher than the direct treatment.

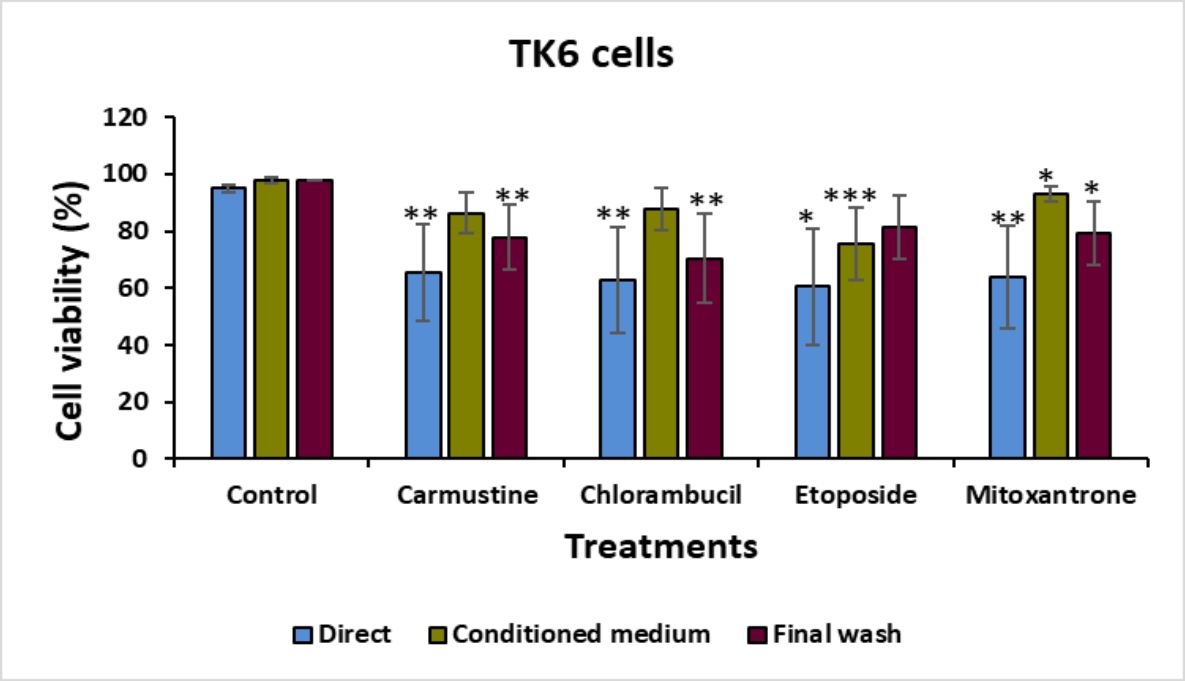

Figure 4.16: HPRT Cell viability assessment of TK6 cells in varying treatment conditions. TK6 cells directly exposed to clinically relevant doses of these four key chemotherapeutic agents was compared against the cell viabilities from HS-5 conditioned medium and final wash medium. Cell viabilities in all conditions were above the 50% threshold for all the agents relative to their separate controls. Data represents the mean ± SD of three separate experiments and the statistical significance shown as $*p \leq 0.05$, $**p \leq 0.01$, $***p \leq 0.001$, as extrapolated by student T-test.

4.4 Discussion

The use of chemotherapeutic agents for treatment cycles and conditioning regimen for haematological malignancies and solid tumours to include leukaemia, has been revolutionised in the past decade to reduce the common immediate side effects such as nausea, hair loss and vomiting. Chemotherapeutic agents exert their effects on both target DNA and non-targeted DNA. Although this effect is advantageous as it culminates in the induction-remission stages of most treatment, it is however not without complications (Partridge *et al.*, 2001). The different mechanism of actions of chemotherapeutic agents are discussed in section 1.4.

Whilst the functions of these agents are well described, there is however paucity of data about their genotoxicity in an *in vitro* bystander co-culture model. More so, the concept of CIBE, originated in the last 10 to 20 years, but has limited evidence of existing and has been demonstrated previously only in a few drugs and chemicals, e.g. cisplatin, bleomycin and some nitrosoureas (Chinnadurai *et al.*, 2011; Demidem *et al.*, 2006). The data presented in this thesis is the first time that CIBE has been demonstrated in such a wide (22) range of chemotherapeutics. Researchers utilise vital tools to discern the potential of these agents to cause genotoxicity, the result of which would aid biomonitoring and better efficacy with therapy. This chapter discussed the varied experiments performed in an attempt to unravel the likely indirect genotoxic potential of 22 different chemotherapeutic agents following exposure to HS-5 cell lines and co-culture with TK6, AHH-1 or Kasumi-1 cell lines. Elucidation of this indirectly induced DNA damage is important as it poses a detrimental effect on patients' health clinically, mainly in the concept of off-target effects and potential induction of mutagenic events in transplanted stem cells.

To study this effect, three known genotoxicity tests (comet, micronucleus and HPRT mutation assays) were utilised owing to their ability to measure varying endpoints that would facilitate proper conclusion of an agent's activity. Additionally, in order to specifically narrow down the type of damage detected by the micronucleus assay, the FISH technique was used by labelling the cells with a human pancentromeric probe. This latter technique focused on two cell lines (TK6 and Kasumi-1) based on their MN evidence of bystander effect (Figure 4.14) and as a representation of the lymphoid and myeloid bone marrow compartments. Only the four main drugs of this study was analysed.

4.4.1 Cytotoxicity assessment following co-culture of bystander cells

Assessing the viability of the exposed HS-5 cells is vital to the effective study of genotoxicity testing. Cytotoxic evaluation permits the determination of the lethal and tolerable dose of any chemotherapeutic agent; genotoxicity testing then allows the detection of that agent's capacity to cause DNA damage (Shi *et al*., 2010) providing toxicity is not excessive. In this study, the major method for determination of cell viability was the trypan blue exclusion assay whose principle relies on the capacity to exclude dead cells with stain uptake due to its compromised membrane integrity (Strober, 1997). Remarkably, the traditional trypan blue assay that is widely used in laboratories applies the laborious microscopic visual evaluation of cells. It is mostly limited to cell lines and well purified primary cell analysis (Chan *et al.*, 2012). However, this study utilised trypan blue both manually and an image based cytometry (LUNA counter) with capacity to visually mark-up live versus dead cells, by enabling the consistent use of a cell size specific protocol and an automated determination of total cells, live cells, dead cells and percentage viability of the cells. The speedy quantification of this method guarantees quick procedure and handling of the cells to avoid structural compromise and a precise detection of the genotoxic capacity of a chemotherapeutic agent, especially for comet assay with an increased tendency of possible repair capacity of the DNA damage. Additionally, a dual staining (acridine orange/propidium iodide) fluorescent technique was employed in the later part of this study after the initial 22 drug screening, following a recommendation for better and specific detection of cell viability by fluorescent dye. However, both methods generated comparable data. All approaches were used, depending on the stage of the research. Overall, the study subsequently relied on the cytotoxicity data generated by the LUNA cell counter image fluorescent technique, based on its earlier stated merits (section 2.2.7).

In this study, cell viability was key to every experiment that was performed. For all genotoxicity assessment, a determination of the cell viability was ascertained prior to using the adequate number of sample for each test. Except for where otherwise stated, samples were consistently above the 50% OECD guidelines prior to investigation. Cell viability was determined for all initial seeding density and post chemotherapeutic exposure for HS-5 as seen with its cytotoxicity data. Notably, the overall cell viability throughout the bystander cells was very good in all the experiments when compared with the viabilities of the direct measurements, relative to their respective controls. In a way, this is not surprising as the

chances are that viability can only be reduced if they were directly exposed to the agent or if the drug was eluting, then it would likely be at a lower dose than the directly exposed cells, thus probably reducing the overall toxicity. However, the data for genotox (to be discussed below), supports the idea that the drug is not eluting from the cells, as the genotox outcomes do not match what is expected for these drugs when directly exposed to the cells. For instance, one would expect an increased percentage DNA with the topoisomerase inhibitors or tail retardation with melphalan (alkylating agent), but this was not the case, although this study is however mindful that these outcomes were performed in a bystander model. Thus, the observed genotoxicity (section 4.4.2) relates to something else, which does not reduce viability as much. With the exception of Kasumi-1 cell line, all other cell lines that showed good viability are not leukaemic cell line and so their tolerability to these agents cannot be due a leukaemic origin. Given that genotoxicity can only manifest itself in a live cell, excellent viability here supports the idea that bystander could overall be more detrimental than direct exposure as the cells seem to survive the toxic insult.

4.4.2 Genotoxicity evaluation of bystander cells using the comet assay

The alkaline comet assay is a widely accepted tool for the assessment of DNA fragmentation and determination of DNA repair efficiency in eukaryotic cells (Collins, 2004 and Gunasekarana *et al.,* 2015). One advantage of DNA damage assessment methods is being rapid, simple, sensitive and the ability to detect damage to both proliferating and non-proliferating cells and this makes the technique of comet assay to stand out amongst other diagnostic methods (Liao *et al*., 2009). The versatility of this assay has been applied in numerous studies investigating DNA damage of genotoxic agents, biomonitoring of occupational exposures, DNA repair capacity (Azqueta *et al*., 2014), therapy monitoring for different diseases (Dusinska and Collins, 2008) and detection of sperm DNA damage in olizoospermic samples from infertile and cancer survivors (Flaherty *et al.,* 2008; Flarherty *et al.,* 2010).

Therefore, in this study comet assay was used to evaluate DNA strand breaks of all the bystander cell lines (TK6, AHH-1 and Kasumi-1) following co-culture with the treated bone marrow cell line, HS-5 (section 2.2.5). Overall, the DNA damaging capacity of 22 chemotherapeutic agents were investigated for TK6 and AHH-1, and with focus on four key agents (carmustine, chlorambucil, etoposide and mitoxantrone), the Kasumi-1 cell line was also studied. This assay was validated using H_2O_2 as a positive control and therefore certified

capable of detecting DNA damage. These data ranged between 30 to 40% and was the range accepted in-house for this agent at all times. The choice of H_2O_2 was due to its ability to induce strand breaks in cells (Driessens *et al.*, 2009). H_2O_2 is widely known for ability to induce strand breaks in human lymphocytes and as a potent DNA damaging agent (Andreoli *et al*., 1992; Raschke *et al.*, 2006). Although the extent of DNA damage was dependent on both exposure time and concentration of H_2O_2 (Benhusein *et al*., 2010), the assay was maintained for 5 minutes treatment at 50 µm and all images scored were typical comet with distinct head separated from elongated tail (section 2.5), and this was same for all the cell lines used.

There was no obvious evidence of substantial DNA damage for any particular agent in both the TK6 and AHH-1 cell lines. For TK6, some agents (5-FU and methotrexate) retarded the tail, which was intriguing as tail retardation is usually an effect of cross-linking agents. Neither 5-FU nor methotrexate are known to have the capability to cross-link the DNA, however this retardation was non-significant and a minimal reduction relative to the control. Most of the rest of the drugs were about the same level as the negative (untreated) control except for mechlorethamine and melphalan (both cross linkers), teniposide and mitoxantrone (both topoisomerase II inhibitors with ability to cause DNA strand breaks) and some DNA intercalators. Whilst it would not be surprising to see increases in percent DNA in the tail for the topoisomerase inhibitors (Salti *et al.*, 2000) and plant alkaloid (Branham *et al.*, 2000), this was not true for all the drugs tested. The current study for the two DNA intercalators (Ara-c and hydroxyurea) agrees with Guerci *et al.*, (2009) who demonstrated evidence for their ability to induce DNA fragmentation. Furthermore, mechlorethamine and melphalan would be expected to retard the tail as a cross-linker (Olive and Banath, 1997; Deans and West, 2011), as would the other alkylating agents tested. None of the alkylating agents retarded the tail rather carmustine and cisplatin data were same as basal level, and fragmentation due to mechlorethamine and melphalan, although statistically significant is in contrast to their known activity in directly exposed cells (Olive and Banath, 1995). The evidence of the initial screen for the four key agent (section 4.3.2.1) was comparable to the duration effect (section 4.3.4.2), showing percentage tail intensity for all agents <10% with exception of mitoxantrone which was originally at 17%. These slight discrepancy can be explained by the different times and use of different cell batches for these assays. However, they were all compared to their respective controls, thereby making the data valid. Collectively, these data strongly suggest

that bystander effect cannot be explained by simple elution/leakage of the native drug from the cells, as the DNA fragmentation observed is not in agreement with outcomes for direct exposure to this range of drugs. Whilst one could suggest that some drugs may be more competent in their ability to enter and leave the HS-5 cells, which might consequently alter the absolute concentration of drugs that the bystander cells could be suggested to be exposed to, it still does not explain the lack of crosslinking for alkylating agents, and elongation of the tail for mechlorethamine.

In AHH-1 cells, the DNA intercalators (daunorubicin and doxorubicin), bleomycin (induces DNA strand breaks), mitomycin C and melphalan (DNA crosslinkers) did show good significance. Understanding the mechanism of action of some of these agents (antibiotics), one could interpret these data as highly relevant and as a significant bystander effect, if the premise was that the drug enters the HS-5 cells, and some of it elutes out, directly affecting the AHH-1 bystander cells. However, DNA fragmentation by mitomycin C, cisplatin, mechlorethamine and melphalan contrary to the known tail retardation produced through direct exposure *in vitro*, thus not supporting this premise. Furthermore, comet induction is expected for topoisomerase inhibitors and has been evidenced for plant alkaloids, although the mode of action (as a microtubule inhibitor) is less obvious. While chlorambucil (alkylating agent) and mitoxantrone (topoisomerase inhibitor) evidenced same basal level as the untreated, carmustine showed some tail retardation but was not statistically significant. These varying outcomes for same class of agent within the same cell line suggests different drug activities in bystander effect.

Further to this, the assessed parameters of the comet assay can also influence the determined outcomes. Notably, tail moment appears to be the most popularly used parameter, however this parameter is a derived one with an absolute micrometre unit and some assay conditions (like electrophoresis time or the derived centre of gravity for the parameter) could affect relevant data. Hence, the recommendation for use of percentage DNA in the tail for use in regulatory purposes and utilisation in inter-laboratory data comparisons was used (Kumaravel *et al.*, 2009). Subsequently, the percentage tail intensity of the comets were used for the present study based on the report that it gave a better indication of what the comets looked like owing to its linear relationship to break frequency over a wide range (Collins, 2004).

Huang *et al.,* (2003) reported that the detection of DNA double strand breaks was based on drug concentration, where topotecan induced strong breaks but not mitoxantrone. The current

study utilised the clinically relevant doses as an initial screen, mainly to address the idea that chemotherapy could induce bystander effect following a clinically relevant dose and this is the first report for CIBE of this magnitude. Using the clinically relevant doses was vital to represent as much as possible the complications observed with these agents in various pathologies such as DCL (section 1.7). An acute dosing time of 1h was chosen for screening purposes. Based on the preliminary data from the screening, it was only proper to maintain this time for further assessments. Arguably, one could suggest that such time was not enough for full drug penetration, but because on the variabilities in the study outcome such as cell line variations, and due to the physical morphological disorientation (Figure 4.2a) observed each time following treatment, it does suggest good drug penetration. However, bearing in mind the varying cell line metabolism for different agents, more time points could be explored in future.

In particular, based on the earlier stated advantage of using tail intensity (Kumaravel *et al*., 2009) that rates DNA damage between 0 – 100%, implying that 'no damage' will score a zero and high damage a 100. This however is not practically obtainable as there are some basal levels of DNA fragmentation in cells. One such possibility could be during sampling and cell viability determination, where an aliquot was taken from a mixture of cell population that contained some fractions of early apoptotic and necrotic cells. These cells will introduce some measurement of 'DNA damage' into the assay and this would normally be queried in situations where high levels of 'damage' is obtained in the negative control sample. In addition, there is a general belief that apoptotic cells would normally appear as hedgehogs (atypical comets which appear with almost no head but large bright tail), but this is not a good assessment, as apoptotic cells are potentially lost during electrophoresis (Meinteres *et al*., 2003). Care was taken to exclude any visible form of hedgehogs through the exclusion of scores above 80% during image analysis. Additionally, care was taken to exclude other reported sources for variations such as the concentration of agarose, alkaline incubation time, electrophoresis duration, temperature and voltage gradient, staining and image analysis (Azqueta and Collins, 2013; Collins *et al*., 2014).

This study was planned for an acute dosing of 1h with these therapeutic agents, which also bears in mind the innate possibility of DNA repair for most single strand lesions (Cannan and Pederson, 2016). Consistent with previous studies (Bisnachi *et al*., 1995), the topoisomerase inhibitors of the AHH-1 cell line all evidenced a significant DNA fragmentation. However, in

contrast to the short time utilised in this study Jaxel *et al.,* (1988) in a direct study, reported a surprising ability of etoposide to induce DNA fragmentation and production of irreversible strand breaks following prolonged exposure (20 hours) in proliferating splenocytes. Godard *et al.,* (2002) reported the presence of DNA strand breaks with topoisomerase I & II inhibitors, such as etoposide and topotecan after 1h treatment but a disappearance of the breaks 24 hours post treatment. Within the current study, these agents also significantly induced DNA strand breaks in AHH-1 (but no strand breaks were induced in TK6), so it is reasonable to assume that DNA repair may be taking place in AHH-1. However, this assay was an indirect exposure, and the messages leaving the HS-5 and impinging on the AHH-1/TK6 cells could not be ascertained. As AHH-1 are metabolically competent (Crespi and Thilly, 1984), perhaps they are 'activating' the messenger to create breaks and then have the capacity to repair them, whereas TK6 may be unable to induce breaks at all or have other means of early detoxification. Clearly, the nature of the bystander cells plays a role in the outcome of viability and genotoxicity. Future studies on this may look into the possibility of a shortened co-culture period or sampling at different time points to ascertain the exact genotoxic capacity of these agents in a bystander model using comet assay. Such sampling will enable early detection of genotoxic insult and capacity to monitor the bystander cells ability to cope with such insult.

Notably, there was disparity between the two lymphoblastic cell lines and the differences in activities of different drugs, thereby poses a slight difficulty in interpretation of outcome. Whereas on the one hand, it may imply that the bystander effect is cell line specific, however it could also mean that there is more than one mechanism of action at play for a given drug, and different bystander cells may have differing capacity to respond to each mechanism. The inter-drug variation may be the influx or efflux rate of these agents within the HS-5 cell. If drugs are effluxed quickly, the determination of genotoxicity 24 hours later may rather be quite late. Overall, since the comet assay was employed for the measurement of DNA fragmentation in these bystander cells, these data suggest that genotoxicity via DNA fragmentation only exists for a few drugs. For these drugs, the percentage tail intensities were low and so to support the concept of genotoxicity through bystander effect, other assays and genetic endpoints need to be explored.

4.4.3 Genotoxicity evaluation of bystander cells using the micronucleus assay

The micronucleus assay was used in this study to further investigate the genotoxic potential of the 22 chemotherapeutic agents tested with the *in vitro* bystander model. Micronuclei (MN) are the result of numerical or structural chromosome aberrations generated in mammalian cells post exposure to toxic substances. MN are cytoplasmic nuclear bodies containing whole chromosome or fragments of chromosomes that were not incorporated at anaphase, and hence left outside the daughter nuclei at telophase, since lagging chromosomes cannot move through the spindle tubules to centrosome (Falck *et al.*, 2002 and Cimini *et al.*, 2002).

In this study, in order to investigate other modes of genotoxicity, the MN assay was utilised on all 22 chemotherapeutic agents using the TK6 and AHH-1 cell lines as bystander cells following HS-5 cells exposure to these agents. Considering the data accrued for both bystander cell lines, one can conclude that there was a high induction of micronuclei with all classes of drugs tested. With exception of 5-FU, chlorambucil and topotecan, all the agents in the AHH-1 cell line showed significant increases of micronuclei. All agents in TK6 were raised above the untreated control showing significant increase for carmustine, chlorambucil, cisplatin, melphalan, bleomycin, doxorubicin, topotecan, irinotecan and mitoxantrone.

Furthermore, there has been some report of increased MN frequency due to prolonged culture time (Falck *et al.*, 1997). MN formation is certainly a vital mechanism for chromosome loss and although it has been reported to be extruded from cells or accompany another daughter nucleus, its fate remains unclear (Norppa and Falck, 2003). The bystander *in vitro* co-culture model was designed to screen toxicity 24 hours post treatment. Since no cytochalasin B was used in this micronucleus assay (CBMN), the current study can be compared with other CBMN studies as the 24 hours sampling time post co-culture amounts to single cell division,

Some studies have reported the induction of bystander effect for chemotherapeutic agents such as mitomycin C, chloroethylnitrosourea, paclitaxel (Alexandre *et al*., 2007; Merle *et al*., 2008; Rugo *et al*., 2005). A lot of these studies were in murine models and some were in cell lines. While some have measured MN induction as an end point, others have concluded observation of bystander effect based on presence of soluble factors transferred to unexposed cells in conditioned medium experiments (Demidem *et al.*, 2006) or changes in gene expression such as the mitogen activated protein kinase (Asur *et al.*, 2010). Asur *et al.*, (2009) utilised MN as

an endpoint to identify mitomycin C and phleomycin's ability to cause bystander effect in normal human B lymphoblastoid cell lines in their conditioned medium experiment which showed 3 to 4 fold increase in MN, thus hypothesizing the release of soluble factors from the treated cells which cause bystander in untreated. In comparison to the 22 screened cells, MN induction of section 4.3.2.2 (MN ranging from 80 to 130) and 4.3.4.3 (MN ranges between 60 to 80) were relatively similar showing genotoxicity and evidence of bystander effect but differed in number of MN. This can be explained by the slight technical errors like the subjectivity with the MN scoring, assays performed at different cell passages, different season/time of the year and different cell batch. All of the above contribute to the varieties in the number of MN. The increased MN evidence in this study supports the phenomenon of CIBE for the 22 screened drugs and the good cell viabilities of the bystander cells at the time of assessment a true genotoxic outcome just as hypothesised for DCL.

Taken together, judging by the similarity of event outcomes in the two cell lines and having applied all reasonable precautions for this assay that is widely accepted for genotoxicity determination based on its ease and sensitivity, this study therefore suggests a possible role of CIBE. Comet assay suggests that DNA fragmentation may not play a role in CIBE while MN assay suggests that cytogenetic endpoints seem to be the outcome in CIBE. However, owing to the fact that the micronucleus assay determines both clastogenicity and aneugenicity, and since there was no correlation between the two endpoints (micronucleus and comet) thus far; this study warrants further investigation as to enable a differentiation of the increased MN as either chromosomal breaks or complete chromosome loss.

4.4.4 Genotoxicity evaluation of bystander cells by FISH

Use of the FISH technique with the MN assay is an advantage to genotoxicity testing (Shaposhnikov *et al.*, 2009). In this study, the initial screening of the 22 chemotherapeutic agents using the MN assay showed a very high MN induction for bystander cell lines following co-culture. However, since an exposure to a substance may induce MN either via chromosome loss or breakage, it therefore became essential to distinguish the phenomena of chromosomal fragments from whole lagging chromosomes. A detailed understanding of the MN origin in this study may improve the understanding of what mechanism(s) may cause a bystander effect through chemotherapeutics. An understanding about clastogenic and aneugenic carcinogens

are vital, as both structural and numerical aberrations can occur in various pathologies (Hovhannisyan, 2010), hence the justification for FISH assay in this study.

In order to study the bystander effect in more detail, four agents were chosen to be further investigated for the remainder of the research. These agents were two alkylating agents (carmustine and chlorambucil) and two topoisomerase II inhibitors (etoposide and mitoxantrone). In addition to the earlier reason stated (section 4.3.2) for these agents, the choice of this was to enable a more involved and focused study on few agents, with a view to discovering the mode of action of bystander effect for these compounds. To investigate the cytogenetics of MN formation, the usual bystander experiment was performed and micronucleus slides prepared for TK6 and Kasumi-1 co-cultures. Usually crosslinking agents are expected to be clastogenic, causing damage to chromosomes rather than DNA sequence (Nill *et al*., 2006). However, the two alkylating agents (carmustine and chlorambucil) evidenced slightly more aneugenicity than clastogenicity in both cell lines, however at approximately 60%:40% respectively would be considered of mixed mode of action within a bystander setting. Etoposide forms a ternary complex with DNA and the topoisomerase II enzyme, preventing the religation of DNA strands thereby causing strand breaks. Similarly, mitoxantrone acts by DNA intercalation and causes crosslinking and strand breaks (Woo *et al.*, 2008). Therefore, all the four agents would normally be expected to show clastogenicity rather than aneugenicity, but this was not the case. While none of the agents was strikingly aneugenic in TK6 cells, the proportion of the distribution tends to favour mixed events more with the exception of mitoxantrone which was clastogenic. Contrarily, the Kasumi-1 cell line depicts mainly mixed mode events for carmustine, chlorambucil and etoposide, while mitoxantrone was aneugenic. Norppa and Falck (2003) proposed the importance of specifically identifying the origin of MN since exposure to genotoxic substances induced only one MN type. Such identification could help explain the mode of action for the agent under study. However, the data accrued in this assay strictly does not show one major MN induction for any of these agents, but rather a mix of both. This outcome was supported by Schuler *et al*., (1995) who proposed that there are a few reported genotoxic agents, known to induce more than one MN type. Whilst this is the first report demonstrating mixed activity for these agents in a bystander study, there are few reports that support the induction of mixed events for some chemicals in direct treatments such as doxorubicin and fisetin (Olaharski *et al.*, 2005; Chondrou *et al.*, 2018).

Additionally, etoposide is mostly used in the treatment of leukaemia, lymphomas and other solid tumours. As a topoisomerase II inhibitor known to cause DNA strand breaks (Wang *et al*., 1990) it exerts clastogenicity. However, it has been reported with ability to induce both numerical and structural chromosome aberrations in somatic and germ cells (Baguley and Ferguson, 1998; Attia *et al.*, 2002; Attia *et al.*, 2003), which agrees with the findings of this research, although as a bystander model. This would infer a possible drug elution mechanism for the observed outcome, however the outcome for the comet measurement (section 4.3.2.1) does not support this, as the known clastogens were not able to induce DNA strand breaks. Similar to etoposide, cytochalasin B (a fungal metabolite) also has the capacity to the synthetic activities of the DNA and induce DNA fragmentation (Kolba *et al.*, 1990). Baseline MN frequency was reported to be increased in human lymphocytes treated with cytochalasin B but with increased culture time, to encourage the formation of more centromere positives than centromere negative MN (Falck *et al*., 1997). Such increase in culture time could be a possibility for the evidence of more aneugens than clastogens in this study. However, caution must be applied with the interpretation of this assay in comparison to a typical outcome of these agents with direct treatment, on the hypothesis that bystander mechanism differs with direct outcome. Currently it is unknown how the chemotherapeutic bystander effect occurs, and unless the drug directly elutes from the treated cell before impinging on the bystander cells then the outcomes of genotoxicity are not necessarily going to be the same. Where genotoxic outcomes are clearly very different, it supports the notion that other messengers are involved, however similar outcomes does not guarantee drug elution. Elhajouji *et al.*, (2011) and Hooyhannisyan (2010) both evidenced the clastogenic capacity of etoposide (topoisomerase inhibitor). However, in contrast to Elhajouji and Hoyhannisyan studies (Attia, 2003 and Attia, 2011), some studies have demonstrated using *in vivo* mouse models the clastogenic and aneugenic potential of two topoisomerase inhibitors (etoposide and teniposide), and thus support the mixed event observed for etoposide in this study. Whilst these studies were direct treatment outcomes, this is the first report to demonstrate the DNA distribution outcome for these agents in bystander co-culture model.

Use of pancentromeric probe was the choice in this study as centromere specific probe is more reliable and accurate in differentiating between the two MN types than anti-kinetochore antibody staining, since MN may show no kinetochore signal if formed from whole

chromosome with disrupted kinetochore (Schuler *et al.*, 1997). Overall, evidence from this FISH analysis reveal no specific type of MN induction with these agents, except mitoxantrone which showed aneugenic activity in Kasumi-1 but clastogenicity in TK6. All the other three agents tested presented a mixed mode of events.

4.4.5 Genotoxicity evaluation of bystander cells by the HPRT mutation assay

A mutagenic capacity of an agent depends on the efficiency of repair, formed adduct half-life and ability of miscoding during DNA replication (Jenkins *et al*., 2005). So far, the different genotoxicity testing assays used in this study have shown different outcomes. However, the exact messenger involved in bystander effect is not known and so there was a need to explore the 161 capacity of the released bystander factors to induce point mutation. The use of FISH with a pancentromeric probe, the comet and micronucleus earlier performed in this study, makes the genotoxicity study for these agents robust as it includes essential study endpoints, such as aneugenicity and clastogenicity. Therefore, with no knowledge of the mechanism involved in CIBE, inclusion of the HPRT adds mutagenicity endpoint to the study and these cumulative genotoxicity outcomes could help explain the possible mechanism of CIBE. In an attempt to investigate the possible implication of point mutation in CIBE, the alkylating agent MNU was used to validate the HPRT assay in the laboratory and upon determination of a working assay, this protocol was used to establish mutagenic potential of the bystander cells (AHH-1 and TK6). Normally cells were treated for the removal of any possible mutants prior to treatment using the HAT medium and upon recovery, cells were treated for 24 hours and four complementary plates set up for positive and negative selection of mutants (live colonies). Removal of mutants is vital to interpretation of the data outcome as it guarantees a true reflection of actual mutation. The choice of these cell lines was due to the already established research cell line protocols and due to the vast array of studies for which they had successfully been applied for this assay. It was also for the possibility of allowing a comparative thymidine kinase study alongside HPRT owing to their heterozygous possession of the TK locus (Morris *et al*., 1994; Doak *et al*., 2007 and Thomas *et al*., 2013). The HPRT loci is on the X chromosome and so use of male cell lines is vital to establishing mutagenicity (George, 2012). AHH-1 is a male cell line with heterozygous mutation of p53 gene but is metabolically competent; thus expressing high levels of native CYP1A1 that is necessary for drug metabolism and elimination (Morris *et al*., 1996). TK6 was constantly used in this study as an established

cell line for genotoxicity testing by most laboratory since it is a human derived cell line with functional p53, thus adding specificity to the HPRT forward mutation assay (Lorge *et al*., 2016 and Rees *et al*., 2017).

Evidence accrued from this study showed increased number of mutant frequencies for the bystander cells treated with carmustine, chlorambucil, etoposide and mitoxantrone in the order of lowest to highest in the AHH-1 cell line. Whilst the estimated bystander cell viabilities (section 4.17) of TK6 and AHH-1 prior plating the cells for colony formation were good, showing viability at 80%, they were still lower than the untreated control but with the exception of carmustine ($p \leq 0.01$), these increases were statistically insignificant. All the relative plating efficiencies were above the recommended 50% OECD guidelines and MNU outcome was comparable to the studies of Doak *et al.,* (2007) and Adams *et al.* (2013) with PE of highest doses at 100% and 60% respectively. The *HPRT* assay was validated with the use of MNU (positive control) and while there was no observed genotoxic effect level (NOGEL) with the doses tested for both cell lines, there was also no lowest observed genotoxic effect level (LOGEL) for the AHH-1, but arguably one can say LOGEL for TK6 in this study is at 0.01 µg/ml. This study however showed a non-linear dose response for both cell lines with increased MF. The observation of no NOGEL and LOGEL were consistent with the study of Doak *et al.* (2007), in which same significant dose of MF was observed. Contrary to this study, Thomas *et al*. (2013) reported NOGEL and LOGEL dose values as 0.0075 µg/ml (72.8nm) and 0.01 µg/ml (97nm) respectively, as estimated by the Dunnett post hoc analysis. The nonlinear dose response of this study for the MNU also agrees with other reports (Adams *et al.,* 2013; Bryce *et al.,* 2010 and Lynch *et al.,* 2011). Understanding the NOGEL and LOGEL doses of the positive control is vital to interpreting the increased MF observed in the bystander cells. One can suggest the presence of point mutation for the topoisomerase inhibitors (etoposide and mitoxantrone) in the bystander AHH-1 cell line and specifically for etoposide in TK6 bystander as its MF (5×10^{-5}) was higher than the MF (4×10^{-5}) at the LOGEL range of Thomas *et al.,* (2013). However, although the study utilised same cell number as reported for this assay, the number of plates for this forward mutation assay was considerably low compared to the reports of earlier studies (Adams *et al.*, 2013 and Doak *et al*., 2007).

Contrary to this study, chlorambucil has been reported with the capacity to cause mutation at the HPRT locus, however this was for direct exposure (Speit *et al*., 1992). Also, a direct

exposure of etoposide was not found to increase HPRT MF in a previous report (Dobrovolsky *et al.*, 2002), however, in the current study, etoposide was the only agent between the two cell lines that consistently showed clear evidence of increased HPRT MF. It should however be noted that in the previous studies, exposure to etoposide was direct, whereas here it is indirect, suggesting the messenger leaving the HS-5 cells is not etoposide itself. A search of the literature found evidence for HPRT induced mutation in RIBE (Zhou *et al.*, 2005 and Kinashi *et al.*, 2007), but no report was found for HPRT MF in CIBE or any other chemical, thus this is the first report to evidence this. With the lack of supporting evidence in the literature, together with the variations for the MF of both cell lines, which are very much similar with regards to the requirements for the HPRT assay, no conclusion can be made about any agent in particular. The data is suggestive that CIBE can cause HPRT mutation with some chemicals, but this is not necessarily 'group' specific, and again highlights the importance of the donor/bystander cell in the observed outcomes.

Furthermore, the sample size for this assay in this study may not have been adequate to draw a tangible conclusion. A total of four 96 well plates each were utilised per treatment or dose for the selective and non-selective MFs. More so, whilst AHH-1 represents data from three independent biological repeats, this study was limited to only two biological repeats of TK6. Future studies should take this into consideration and increase sample size to involve more plates, as well as perform the nucleotide sequence PCR for the HPRT gene to facilitate interpretation of outcome. On this note, this data is only indicative of a possible HPRT mutant for etoposide and/or mitoxantrone.

4.4.6 Evaluation of the duration of chemotherapy-induced bystander effect

Following the identification of high levels of micronuclei induced by all the agents tested and the possible dual genotoxicity type effect identified with the FISH, there became a further need for a deeper study into what bystander effect involved. Clinically, the treatment of most cancers initially relied on radiotherapy and surgery in the 1960s prior to the advent of combination chemotherapy (DeVita and Chu, 2008), which although improved survival outcome, it also posed a risk of relapse or secondary malignancies such as donor cell leukaemia, a phenomenon proposed to be a result of CIBE (Wiseman, 2011).

Despite the well described concept of RIBE, there are yet so many unanswered questions. This invariably imply that the field of CIBE will also have a plethora of unanswered questions, since CIBE involved multiple compounds with multiple activities, whereas RIBE largely refers to ionising radiation with some limited evidence of UV (Widel *et al.*, 2014 and Zhou *et al.*, 2005). One such question was to understand how long a bystander effect might last. In order to investigate this, this study designed an experiment that would last five days long. This duration was chosen because patients are normally allowed a two-day window for the effect of combined therapy or monotherapy to wear off, prior to stem cell transplant and a maximum time that patients could safely be left without a transplant was only about 5 days. Consequently, the established bystander model involved the modification of a daily replacement of new bystander cells, co-culturing with the same treated HS-5, followed by a cytotoxicity and genotoxicity assessment 24 hours later and for every 24 hours up to a total of 5 days. This assay was performed using the TK6 and Kasumi-1 cell lines, a choice that would closely mimic the bone marrow compartment with a pool of both lymphoid and myeloid cells of origin respectively. Kasumi-1 was also chosen here, as DCL largely manifests as AML, and it was of interest to explore if lymphoid and myeloid cells behaved differently in this experiment. All four key agents as mentioned earlier were tested. As seen with previous cytotoxicity data in this study, the cell viability in both cell lines for all five days when compared with their respective controls, were very good, thereby meeting the guidelines criteria for assessment of genotoxicity (OECD 1987; OECD, 2015). The comet assay in both TK6 and Kasumi-1 show a very good working positive control, showing almost a consistency at 40% for TK6 but varied in the Kasumi-1 cell line, with a slight decline at days 3 and 4.

The outcome of this study is suggestive of some active signal shared amongst the cells within the co-culture milieu. Since all the key four drugs in this longevity study have shown a capacity to cause DNA strand breaks after some days, there is possibility that there is either a trace drug or something that is eluting from the treated HS-5. Lehnert and Godwin (1997) reported a short-lived signal and a long-lived derived signal from their treated fibroblasts. In their study, they showed the induction of short-lived sister chromatid exchanges (SCEs) in conditioned medium with and without cells for few hours up to 24 hours post cell culture following low irradiation with α-particles. They also demonstrated a long survival of SCEs following 16 hours after freeze thawing of the conditioned medium and subsequent incubation of confluent unirradiated

cells with this medium. This would suggest that the treated compartment retains a longer effect that is continually released into the culture medium, hence the possibility for the increased MN on these days, however the effect of the current study was lost on day 5 and hence, does not support the long-lived signal transduction theory. Baskur (2010) in his *in vivo* studies demonstrated loss of DNA methylation in bystander spleen after acute radiation at 6 hours and 14 days, whereas fractionated irradiation led to hypomethylation in spleen bystander up to 14 days. Taking a different approach, Olobatuyi *et al.,* (2016) used a mathematical model to predict the lifespan of RIBE signals and concluded that both single and multiple irradiation resulted in signals that persisted temporarily or permanently. More so, the comet assay is widely known for its sensitivity, and should be capable to detect these signals, but this was not the case. This can either be explained by lack of DNA fragmentation (or fragmentation below the sensitivity of the assay), or effective and rapid repair capacity of the cells, therefore a method to assess this repair capacity is needed, in order to conclusively determine this effect.

Furthermore, RIBE was proposed to potentially be an induced genomic instability mechanism which persists for several generations (Seymour and Mothersill, 2000 and Lyng *et al.*, 2000). This would agree with the earlier findings of Pant and Kamada (1977), who reported a persistent bystander signal in atomic bomb victims after 31 years, although contrary to the lost MN induction on day 5. Arguably, it is possible that the bystander signals are short-lived hence the loss of MN induction in TK6 on day 5. It is also possible that the signals could cycle and reappear a few days later, however, only testing the cells for longer would confirm or deny this, but was a challenging experiment to do at this time due to limited use of the cell culture inserts.

More so, if this CIBE long lasting and short-lived effect was to hold true, it implies there is not really a safe window for transplant according to the clinician's suggestion of 5 days, however, further studies are needed by extending these days and studying its genotoxicity. In the interim, awareness of this possibility is vital to guide the clinical decision making when using these therapies and seek means to combat these traversal effects. Should a therapy or known chemotherapeutic be discovered to be safe, and /or produce minimal CIBE, then these may be used in preference for treatment. However, it is important to note that the bystander cell appeared influential in the outcome of genotoxicity and thus understanding the intrinsic risk factors (for example genetic polymorphism) of the bystander/donor cells, might implicate

which patients are, and are not at risk for DCL. This will enable the decision of who should then be treated with caution to some of the drugs shown to be more able to produce CIBE, but are known beneficial therapies.

In this study, the BM compartment and bystander cells were maintained at 1 x 10^5 cells/cm^2 and 5 x 10^5 cells/ml respectively. This HS-5 cell number was adequate to generate the signal transduction between cells in co-culture, whilst retaining enough space for cell growth. TK6 cell density was to allow for cell growth in the culture insert and cell death post co-culture. This TK6 starting seeding density also ensured the generation of the required cell numbers for testing post co-culture. Lyng *et al.*, (2000) suggest that the bystander effect is dependent on the number of cells present at the time of exposure. As this is the first investigation into CIBE longevity, it is suggested that the MN induction over a number of days is a clear indication of a signal transduction mechanism between the cells. Therefore, whilst caution is applied to the interpretation of CIBE relative to RIBE, as their mechanism would probably be entirely different (and possibly further influenced by the chemical used to induce CIBE), further investigation whereby cell numbers of the two compartments are varied would be necessary to partly help clarify the role of cell density involved in bystander effect.

4.4.7 Evidence of residual genotoxic chemical effect

To eliminate the possibility of drug elution for the increased MN observed in the bystander cells, an LCMS assay was to be optimised (chapter 3) but was not feasible as planned and so this assay was designed to assess the possible involvement of soluble factors or drug elution in bystander effect. To achieve this, directly exposed TK6 cells were compared with TK6 cells in co-culture and TK6 cells exposed to culture medium conditioned by treated HS-5 cells for 24 hours. Use of TK6 was thought appropriate for this investigation as this medium transfer experiment, as they were made a constant cell line factor in this study based on their robustness in genotoxicity assessment. Direct treatment was to prove a principle there was higher MN induction than bystander cells (indirect treatment), while conditioned medium was to evaluate soluble factors and the final wash to evaluate drug elution.

The direct treatment at these doses had a high MN induction in the TK6 cell line. There was an observation of different mechanisms such as the role of soluble factors and a possible drug elution occurring with these agents. One would expect (an assumption based on the few CIBE

experiments in the literature, but this is subject to future evaluation using the LCMS) that three washes was adequate to remove drugs from a treated cell culture and if so the MN induction of the final wash should be equivalent to control level. The outcome of carmustine, chlorambucil and etoposide final washes were not very different from the untreated control, whereas mitoxantrone witnessed a large rise in MN. Mitoxantrone's conditioned medium was similar to its bystander outcome, but carmustine and etoposide showed increased MN, while chlorambucil revealed a decline in MN induction, compared to bystander untreated control. The detection of MN with the transferred medium indicates the possibility of soluble factor influence within the culture medium compartment which contributes to the signals transferred onto the bystander cells. Data further reveal the provision of higher or relatively equal signal transduction in the bystander cells than conditioned medium.

The variations in the final wash could be explained by a possible difference in the influx and efflux rate of these agents in and out of HS-5 cells, since three washes appeared enough to wash the drugs off the cells in all but mitoxantrone. It could be that mitoxantrone is more stable than the other agent's, or is more likely to adhere to the exterior of the cell and requires more washes to be removed. Thus, whilst soluble factors appear evident for all agents, there is also a possibility of drug elution for mitoxantrone. With reference to RIBE mechanism, because it has been reported that not all cells have the capacity to generate or respond to bystander signals (Ryan, 2008), another study including more wash steps is required. For mitoxantrone, an assessment of drug elution is also required for all agents such as the LCMS (chapter 3); whilst also investigating influx and efflux rate of these agents may help provide clarity as to interpretation of the phenomenon for these outcomes.

A thorough literature search did not find any bystander conditioned medium experiments conducted for the chemotherapeutic agents, nor similar assays with these cell lines used in this study, therefore this would be the first demonstration for this. However, two DNA damaging agents bleomycin and mitomycin C according to Asur *et al*., (2009) show the occurrence of bystander effect devoid of residual chemical but due to soluble factors in the culture medium and possibly some stress indicators. Demidem *et al.,* (2006) demonstrated the induction of bystander effect in solid tumours following treatment with chloroethylnitrosourea (CENU). Other scholars like Soleymanifard *et al*., (2012) have argued a case of dose response relationship of bystander effect using conditioned medium as they observed a loss of effect

with low chemical doses but not with a high dose. The data presented by Asur *et al*., (2009), appeared to follow a linear dose increase in bystander and conditioned medium.

In summary, the weight of evidence clearly show higher cell death and genotoxicity with the direct exposure but less in the bystander, conditioned medium and washes. Thus, the exact factor playing a role in the co-culture that is not evident in the washes or even the conditioned medium remains a subject for further investigation (chapter 5).

4.5 Conclusion

The present study has been able to explore the genotoxic potential of 22 chemotherapeutic agents chosen from five major classes to include: alkylating agents, antimetabolites, antibiotics, topoisomerase inhibitors and the plant alkaloids. These agents were investigated using the bystander co-culture model and all agents evidenced the capacity to induce bystander effect using the micronucleus assay. The antibiotics, topoisomerase inhibitor and plant alkaloids but not alkylating agents and antimetabolites are indicative of a possible bystander effect in the comet assay.

The high induction of MN investigated for bystander effect by FISH technique for carmustine, chlorambucil, etoposide and mitoxantrone reveal both aneugenicity and clastogenicity potential for all except mitoxantrone, which shows an indication for aneugenic activity in the Kasumi-1 cell line, but mixed mode of action for TK6. Point mutation investigation in the HPRT assay reveals a clear mutant frequency for bystander cells exposed to etoposide and possibly mitoxantrone but not carmustine and chlorambucil.

An assessment of the possible duration for the observed bystander effect revealed a continual induction of micronuclei, which peaks off on day three for most agents, whereas the comet assay was not significant across all agents. This finding may imply that at least three to four days must elapse before it may be safe to allow for clearance of the chemotherapy and CIBE effect in a patient before actual stem cell transplant, which is likely impractical in a clinical scenario. Lastly, this study indicates that the CIBE is mediated by soluble factors in the medium, as evidenced from the absence of residual chemical for all agents except mitoxantrone, Hence, it is concluded that soluble factors certainly play a major role in CIBE within this study, but this is likely not the sole mechanism. Therefore, future studies could explore other mechanisms such as epigenetics, cytokine or microRNAs.

Chapter 5

Evaluating the Role of Reactive Oxygen Species in Chemotherapy-Induced Bystander Effect

5.1 Background

Reactive oxygen species (ROS) are partially reduced oxygen species derived from products of normal cell metabolism that are highly reactive and very unstable. ROS are generated through various processes which include: increased cell metabolism (Yang *et al*., 2018), oncogene activation (Vafa *et al*., 2002; Tanaka *et al.*, 2002), hypoxia induction in tumours (Azimi *et al.*, 2017), environmental toxins (Mouret *et al*., 2006) and alterations of signals associated with tumour transformation (Chiarugi *et al*., 2003). Thus, ROS can be generated both in pathological and non-pathological processes (Droge, 2002; Perl *et al*., 2004 and Valko *et al*., 2007).

Contrary to the traditional concept of ROS as just by-products of respiration interacting with cellular targets, current evidence indicates that ROS are necessary for cellular activities such as inhibition of pathogens, viruses and tumour proliferation (Conklin, 2004), cell signalling (Deem and Cook-Mills, 2004), detoxification (Wu and Yotunda, 2011) and regulation of blood flow (Griendling *et al*., 2000). Under normal physiologic state, a balance is maintained between production and internal cellular detoxification. However, when there is an imbalance between ROS production and the antioxidant control system, it results in oxidative stress that poses detrimental effects to cells (Pizzino *et al.*, 2017 and Tan *et al.*, 2018).

Some chemotherapeutic agents (doxorubicin, daunorubicin, bleomycin, cisplatin, etoposide, alkylating agents, taxanes and vinca alkaloids etc) are reported with the capacity to induce ROS (Alexandre *et al.*, 2007, Coklin, 2004 and Yang *et al.*, 2018). Also, there have been some studies on the role of oxidant and antioxidant systems in cancer development and most are indicative of a high contribution of oxidative stress in various pathologies (Patel *et al*., 2009, Bhagat *et al*., 2011). Also evidenced is the occurrence of increased genetic instability due to chemotherapy-induced ROS (Sallmyr *et al.*, 2008). However, the elevation of ROS during chemotherapy is attributed to increased mitochondrial ROS generation, lipid peroxidation and inhibition of antioxidant defence systems (Yang *et al.*, 2018). The exact role of ROS during

cancer chemotherapy remains unclarified, but a fact is that chemotherapy-induced cell death involves both ROS dependent and ROS independent pathways (Yang *et al.*, 2018).

Extended over activity of ROS causes a detrimental effect to cellular macromolecules such as proteins, DNA and lipids as well as possible further alteration in cell activity and function, potentially resulting in mutations and cancer. To combat these activities, there exist some internal control mechanisms in cells. Whilst most cells possess an efficient antioxidant mechanism, in a state of increased oxidative stress such systems become vulnerable, thus ROS have been implicated in the aetiology and progression of various diseases such as aging and other haematological malignancies like acute myeloid leukaemia (AML) and leukaemia relapse (Samimi *et al.*, 2018). Because most antineoplastic agents provoke oxidative stress, it is hypothesized that a promotion of the ROS repelling or control systems through a combination of antioxidants in chemotherapy may help alleviate side effects and improve treatment efficacy (Singh *et al.*, 2018).

Given that oxidative stress is in part responsible for some cell pathology including cancer, the regulation of the redox state is therefore imperative for the efficiency of cell function. Some effective antioxidants present in the blood plasma include SOD, GPx, CAT (Pouget *et al.*, 2018), glutathione (GSH/GSSG), cysteine/cysteine and TRX (He *et al.*, 2017) as well as vitamin E, vitamin C and beta-carotene (Conklin, 2004). The vast majority of studies have focused on the inhibitory effects of antioxidants in RIBE (Konopacka and Wolny, 2006 and Dahle *et al.*, 2005) but not CIBE.

Although cancer patients undergoing chemotherapy largely witness a better life quality, some were posed with cases of relapse, resistance to therapy and other therapy related complications such as donor cell leukaemia (DCL). While the literature tends to focus on cancer cells, and how to treat tumours successfully, few cases of research have focused on non-cancer (bystander) cells (Asur *et al.*, 2009; Chinnadurai *et al.*, 2012) unaffected by chemotherapy which may play a crucial role in relapse or secondary malignancies. However, the fact that the double-edged role of ROS in normal physiologic and pathological processes is not fully understood further complicates an understanding of the role ROS may play in inducing chemotherapy related complications, of particular relevance here is the relationship of ROS with the bystander cells - whether it is beneficial or harmful. On this note, this chapter attempts to understand the involvement of ROS and the likely evidence of oxidative stress in bystander

cells as a potential mechanism in CIBE. Such knowledge could help modulate therapeutic strategies, thereby creating a better efficacy of cancer treatment.

To investigate this ROS mechanism, this study utilised various techniques (enzyme modified comet assay, 2'7'-dichlorodihydrofluorescein diacetate (DCFDA) assay, western blotting, flow cytometry and the Agilent Seahorse XF mito stress test assay) to detect intracellular ROS, mitochondria functionality and some antioxidant expression levels. Briefly, the HS-5 bone marrow compartment was treated and evaluated directly with DCFDA, or using bystander cells following 24 hours co-culture. Bystander cells were investigated with all techniques with respect to the cellular effect of the four chemotherapeutic agents of interest (carmustine, chlorambucil, etoposide and mitoxantrone) with the addition of daunorubicin and doxorubicin in the mitochondrial stress test. Daunorubicin and doxorubicin are not the focus agents in this study, they were included in this assay because they exert their effect by generation of free radicals (Pourahmad *et al.*, 2016); thus served as a positive control.

5.2 Methods

5.2.1 DCFDA (2', 7'- dichlorofluorescein diacetate) assay

DCFDA assay is a sensitive technique that uses an intracellular probe for direct measurement of the redox state of a cell. Using the established method of Eruslanov and Kusmartsev (2010), this assay was utilised in this study to investigate the role of varying ROS as a potential mechanism of CIBE. TK6, AHH-1 and Kasumi-1 cell lines were investigated by flow cytometry, while the HS-5 assessment was performed with a fluorescent microplate reader. As HS-5 cells were directly exposed to the carmustine, chlorambucil, etoposide and mitoxantrone prior to assessment, the bystander cells were harvested as co-culture samples and then used for the assay (section 2.7).

5.2.2 Enzyme modified alkaline comet assay

The alkaline comet assay, when modified using the lesion specific endonucleases (Fpg and hOGG1), enables the detection of oxidative DNA damage in cells. This assay was used in this study to investigate the possible involvement of oxidative DNA damage in (CIBE) and was explored using the lymphoblast cell lines TK6 and AHH-1, and myeloid cell line Kasumi-1, following 24 hours co-culture with the previously treated bone marrow cell line (HS-5). This assay was performed according to the method of Smith *et al*., (2006) as detailed in section 2.4.3.

5.2.3 8-Hydroxy-2'-deoxyguanosine (8-OHdG) Assay

8-OHdG is the most frequent oxidative DNA damage product and serves as a biomarker for oxidative stress. This study used the anti DNA/RNA damage detection 8-OHdG antibody (ab1833933) purchased from Abcam (UK) to investigate the involvement of oxidative stress in the bystander cells. Following co-culture, the TK6, AHH-1 and Kasumi-1 cell lines were harvested, fixed, permeabilised and stained with the FITC conjugated antibody with high affinity and specificity to 8-OHdG (section 2.5) and quantified using flow cytometry alongside an isotype and an untreated negative control, with subsequent visualisation of localised cells on a confocal microscope.

5.2.4 Confocal microscopy

Following the antibody application with the 8-OHdG, while some samples were analysed by flow cytometry, some were aliquot and spun onto a slide for visualisation with the confocal microscope. This microscope was employed for its ability to resolve localisation of specific object details within a cell. This method was used to evaluate both treated and untreated samples using same parameters for inter and intra-day sample comparison.

5.2.5 Seahorse mitochondrial stress test

The endogenous sources of free radicals include the mitochondria, peroxisomes and endoplasmic reticulum; the cellular sites where oxygen consumption is very high. The mitochondria is the 'powerhouse' of cells and ROS are by-products of the mitochondrial electron transport chain and in response to environmental stress such as radiation and chemotherapy. The Agilent Seahorse XF mito stress test (section 2.8) is a gold standard extracellular flux assay for the assessment of the function of mitochondria through the measurement of oxygen consumption (OCR) and extracellular acidification rate (ECAR). Using the clinically relevant doses (Table 2.2) of carmustine, chlorambucil, etoposide, mitoxantrone, daunorubicin and doxorubicin, these chemotherapeutic agents were evaluated.

5.2.6 Western blot

The regulation of ROS within cells is vital for a balanced cell homeostasis. To investigate the defence of oxidative stress in the bystander cells, use of a western blot cocktail antibody (ab179843; Abcam, UK) enabled the determination of the expression levels of the three major antioxidants: superoxide dismutase (SOD1), catalase (CAT) and thioredoxin (TRX), through quantification of their abundance relative to a smooth muscle actin internal control. TK6, AHH-1 and Kasumi-1 cell lines following 24 hours co-culture, were harvested and lysed to quantify their protein levels for each chemotherapeutic agent and western blot analysis (section 2.9) was performed. Each protein resolved according to their expected molecular weights relative to a standard (14208S NEB, UK) by using a horseradish peroxidase linked anti-rabbit IgG secondary antibody (7074P2; NEB, UK).

5.2.7 Limitation of methods

DCFDA assay is known to have some limitations such as, it does not directly react with H_2O_2 and thus not a reliable measurement for H_2O_2. The formation of the intermediate compound DCF can rapidly react with oxygen to form superoxide whose dismutation further produces another H_2O_2, causing redox-cycling mechanisms that can lead to artefacts with potential disruption of fluorescent signal. Also, the cells possess cytochrome c (a mitochondria heme protein) which can oxidize DCFH into DCF thereby enhancing oxidant production (Kalyanaraman *et al.,* 2012). 8-OHdG assay had a disadvantage for cross reactivity of the detection antibodies with guanine and a possible overestimation of 8-OHdG background levels due to the oxidation of guanine to 8-OH-Gua during derivation step (Zhang *et al.,* 2013).

On the other hand, as well as its cost ineffectiveness, certain immortalized cell lines possess high glycolytic and reduced respiration and could be a limiting factor in the Seahorse assay (Horan *et al.,* 2012). Some cultured cells could impair measurement of some mitochondria functional parameters. Also, Seahorse assay was limited to use of only four substrates and OCR measurements in some cells does not always reflect mitochondria respiration as other oxygenase in cell could affect OCR (Koopman *et al.,* 2016). In western blot analysis, some antibodies can hit other cellular proteins exhibiting off target effects. Some commercial antibodies may detect the target protein and the technique is associated with many technical issues such as membrane transfer inefficiency, the quick decay of detection signal and lots of background detection (Gosh *et al.,* 2014).

Overall, despite the limitations of these assays they have been described as sensitive, simple and flexible enough to detect ROS. The methods used in this study utilised a combination of fluorescent probes, proteins and confocal methods, thus applying allow the detection of total ROS. Because of the low concentration and short lifetime, combining different methods ensured the full advantages of qualitative and quantitative methods thereby detecting a possible range of reactive species (Zhang *et al.,* 2018).

5.2.8 Statistical analysis

All experimental analysis are presented for three independent biological repeats. Results were analysed using the Graphpad Prism software by performing a two-way ANOVA and employing the Dunnett's multiple comparison post hoc test to determine statistical significance

between the treated cells and untreated control for all the relevant ROS assays. Statistical significance are considered when $p \leq 0.05$.

5.3 Results

5.3.1 Assessment of intracellular reactive oxygen species by DCFDA

In an attempt to elucidate the involvement of oxidative stress in this bystander study, it was necessary to evaluate all the involved compartments within the *in vitro* microenvironment. Therefore, to investigate ROS production from the HS-5 microenvironment intracellularly, the 2'-7'-dichlorodihydrofluorescein diacetate (DCFDA) assay was employed.

Following the optimisation of the DCFDA assay with H_2O_2 and $KBrO_3$ (chapter 3), the 'bone marrow'/HS-5 (treated) compartment upon exposure to the chemotherapeutic agents was evaluated for the presence of intracellular ROS. Results of this assessment (figure 5.1) showed no induction of ROS until one hour after exposure, although interestingly, only mitoxantrone had a fluorescent intensity lower than the untreated control. At three hours, there was a general increase in fluorescence intensity for all agents, including the untreated control, supporting basal cell activity and ROS accumulation, with similar differences between each drug and the control as for the data at one hour. However, it was not until 6 hours post exposure that the drug treated HS-5 began to demonstrate increased ROS activity over and above the control. At this point, mitoxantrone exceeded the control for fluorescent intensity and became similar to the other drugs. Intriguingly, despite being the drug that induced the most convincing evidence of oxidative DNA damage in the enzyme modified comet assay, mitoxantrone consistently produced the lowest ROS in HS-5 cells, of all four of the drugs. While chlorambucil and etoposide were statistically significant (****$p<0.0001$) from the untreated control at all time points, mitoxantrone was significantly different at baseline, non-significant for other time points until 18 (****$p<0.0001$) and 24 (****$p<0.0001$) hours, showing an accumulated oxidative ROS production over time.

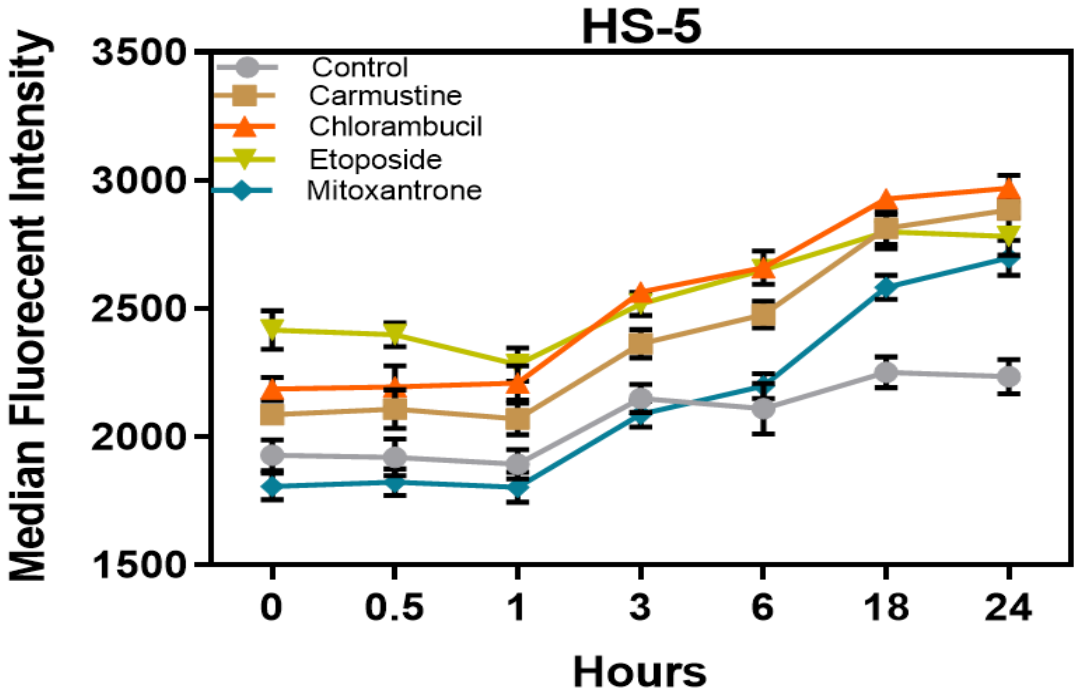

P-value	Time (hours)						
	0	0.5	1	3	6	18	24
Carmustine	0.0057	0.0007	0.0016	0.0001	<0.0001	<0.0001	<0.0001
	**	***	**	***	****	****	****
Chlorambucil	<0.0001	<0.0001	<0.0001	<0.0001	<0.0001	<0.0001	<0.0001
	****	****	****	****	****	****	****
Etoposide	<0.0001	<0.0001	<0.0001	<0.0001	<0.0001	<0.0001	<0.0001
	****	****	****	****	****	****	****
Mitoxantrone	0.0426	0.1506	0.1904	0.4956	0.2145	<0.0001	<0.0001
	*	ns	ns	ns	ns	****	****

Figure 5.1: Reactive oxygen species assessment by DCFDA in drug exposed HS-5 cells. HS-5 cells (1 x 10^4 cells/100µl) in a microplate were exposed to chemotherapeutic agents (carmustine, chlorambucil, etoposide and mitoxantrone) and incubated with DCFDA (1µM) in the dark for 45 minutes. The fluorescent intensities of these cells were measured for the presented time intervals up to 24 hours using a microplate reader. Mean ± SD is shown for three independent experiments, with statistical significance shown as *p<0.05, **p<0.01, ***p<0.001, ****p<0.0001; evaluated using two way ANOVA.

Further investigation of the impact of ROS in the bystander compartment was evidenced with the DCFDA assay using the bystander cell lines (TK6, AHH-1 and Kasumi-1 cell lines). These bystander cells were co-cultured for 24 hours with drug treated HS-5 cells, harvested and used to perform the DCFDA assay and analysed by flow cytometry.

Figure 5.2a shows the median fluorescent intensity (MFI) and percent positive cell response to the four chemotherapeutic agents in the TK6 cell line. All the agents (carmustine, chlorambucil, etoposide, mitoxantrone) in comparison to the untreated control revealed the same level (1.5 x 10^4) of fluorescence intensity. Percent positive cells were all very low (0% - indicative of no ROS signal production) except for mitoxantrone that showed positivity at 10%. The quantitative data was further supported with the graphical histogram overlay (Figure 5.2b) showing no obvious difference between the DCFDA treated control sample and all agents except mitoxantrone positive cells which was statistically significant (***$p \leq 0.001$).

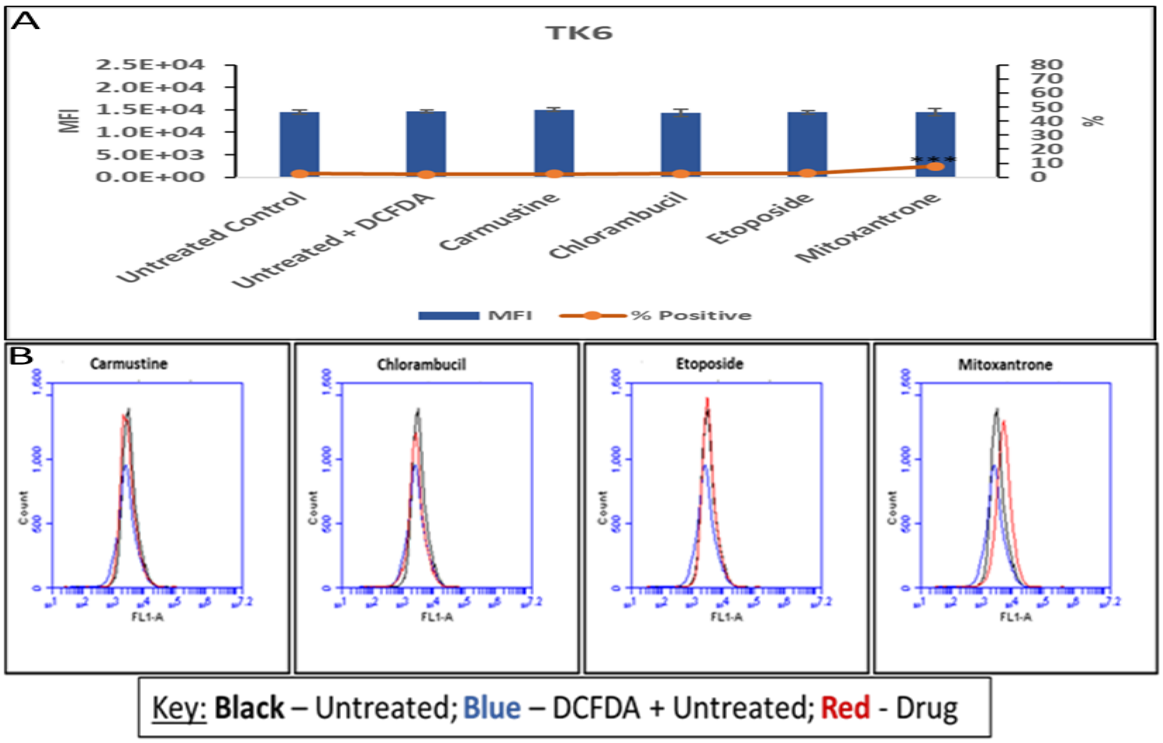

Figure 5.2: Median fluorescent intensity of TK6 bystander cells labelled with DCFDA. TK6 cells were harvested after 24 hours co-culture (pre-treated HS-5) and probed with DCFDA (1 µM) for 45 minutes in the dark at room temperature, then analysed with using the FL1 channel of flow cytometer. The data shows (a) mean values for the median fluorescent intensities and their corresponding percent positive cells; and (b) representative histogram overlay plots of the respective chemotherapeutic agents, (n=3). Statistical significance is shown for ***$p \leq 0.001$ for mitoxantrone positivity as estimated using two way ANOVA. Histogram indicates black=untreated control with no DCFDA, blue=untreated control with DCFDA, red=chemotherapeutic agent with DCFDA.

Contrary to the TK6, AHH-1 cells (Figure 5.3a) showed differing intensities between the control and the chemotherapeutic agents. The untreated control without DCFDA and untreated

control with DCFDA were similar showing MFI of 1 x 10^4 and no evidence of positive cells. All chemotherapeutic agents except chlorambucil and etoposide show significant increased MFI when compared to the untreated control plus DCFDA control. While carmustine was the highest with an MFI of 1.5 x 10^4 with over 60% significant (***$p \leq 0.001$) positive cells, chlorambucil had an MFI of 1 x 10^4 with 30% positive cells. Also, whilst the MFI of mitoxantrone was slightly raised (1.5 x 10^4), showing a significant (***$p \leq 0.001$) percent positive cells at 30%, etoposide showed the same level (1 x 10^4) of fluorescent intensity with the untreated plus DCFDA control and had only 10% of the cell population as positive.

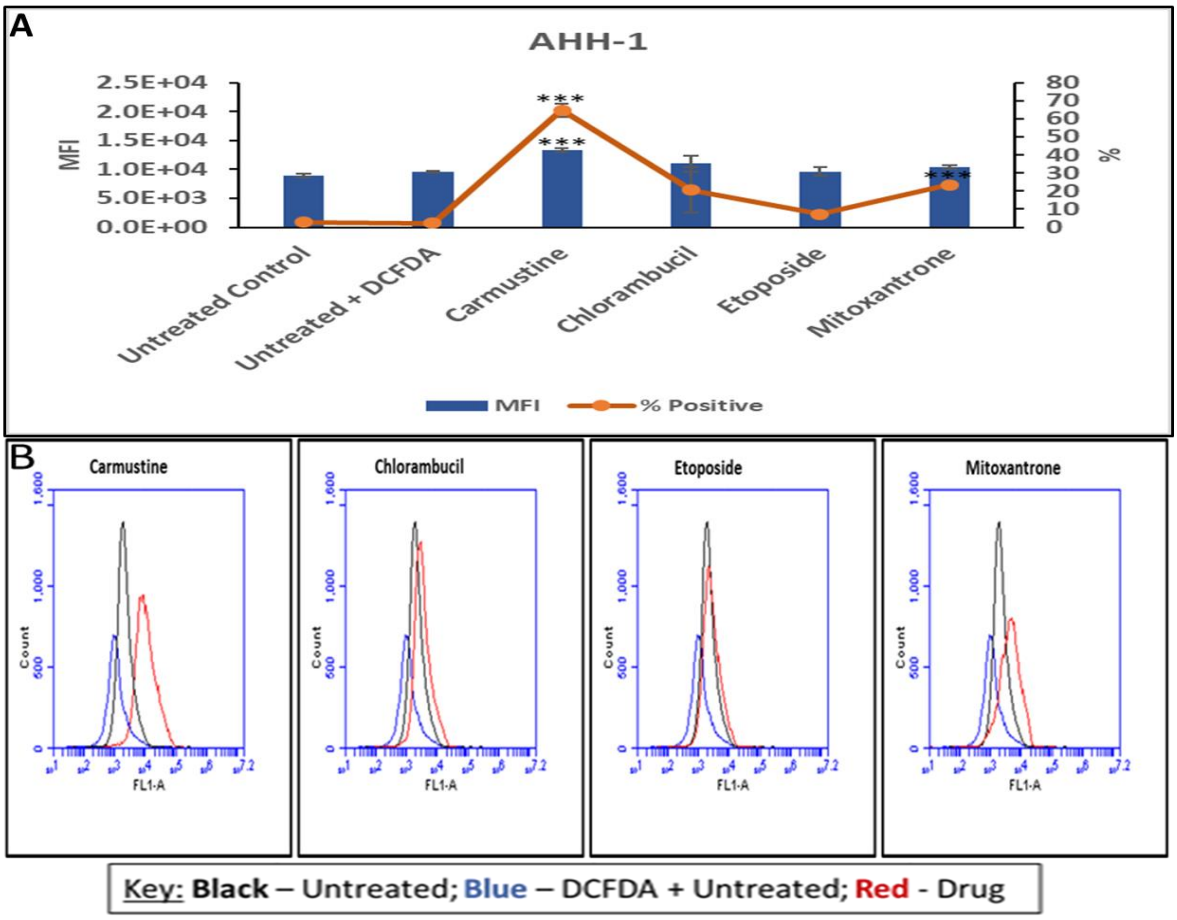

Figure 5.3 Determination of intracellular ROS in AHH-1 bystander cells. Bystander cells post co-culture were utilised in DCFDA assay and analysed by flow cytometry and show (a) fluorescent intensities of cells with and without DCFDA treatment and the relative cell positivity. (b) Representative flow cytometry histograms each comparing untreated control, DCFDA treated control and chemotherapeutic agents. Data depicts the mean ± SD of three separate biological repeats, with statistical relevance shown for ***$p \leq 0.001$.

Even though the MFI of carmustine, chlorambucil and mitoxantrone were raised above the controls, only carmustine was significantly increased (***$p \leq 0.001$). Also carmustine, etoposide and mitoxantrone all show statistical significance (***$p \leq 0.001$) for the number of positive cells. Qualitatively, as shown in the histogram (figure 5.3b) and in comparison to the untreated plus DCFDA control; carmustine and mitoxantrone were both seen with a clear shift to the right. Chlorambucil only had a slight shift and etoposide was almost unchanged; all these visual assessments of the agents correlate with the quantitative assessment.

Kasumi-1 (Figure 5.4a) bystander cells on the other hand, similar to TK6 was generally unaffected by the drugs, as evidenced by the DCFDA assay. For all the chemotherapeutic agents, the levels of fluorescent intensity were comparable to the untreated controls with and without DCFDA with MFI at 7×10^3, which notably is a lot less than the general MFI for TK6. However, mitoxantrone did show a slight increase of MFI (9×10^3) above the control, but these levels were not as high as for mitoxantrone with TK6 or AHH-1. The same observation was made with the percent positive cells which show 20% positivity for the untreated plus DCFDA control, chlorambucil and etoposide, whereas carmustine and mitoxantrone had a 10% positivity and the untreated control without DCFDA was 0%. The overlay histogram (Figure 5.4b) reflects this observation and shows almost a complete overlay for the untreated with and without DCFDA controls and the chemotherapeutic agents, as no visible shift to the right was observed.

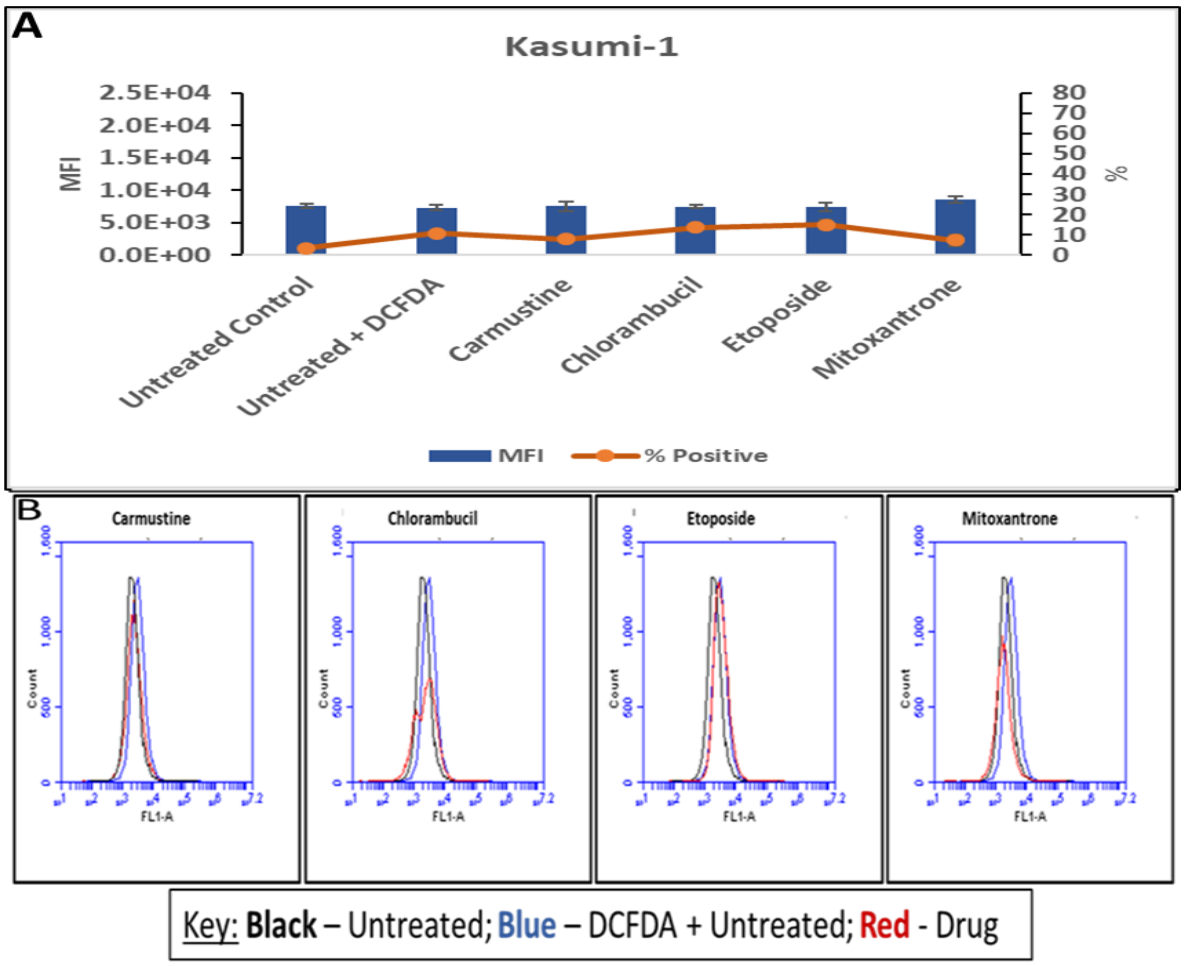

Figure 5.4: Evaluation of cellular reactive oxygen species in bystander Kasumi-1 cells. After co-culture with treated HS-5 cells, Kasumi-1 cells were harvested, treated with DCFDA (1 µM) in the dark for 45 minutes, and analysed using flow cytometry. The figures show (a) median fluorescent intensities and percent positive cells, and (b) representative overlay histograms of untreated cells and chemotherapeutic cells using the FL1 channel. The presented data are for three independent biological repeats, showing no statistical significance for any of the measured agents.

5.3.2 Oxidative damage detection using lesion specific endonucleases

Because one of the likely cause of mutations that may lead to cancer is the excessive endogenous or exogenous production of oxidative DNA damage by ROS (intracellular or extracellular insults). It follows that the accurate detection of the endpoint DNA lesions of these ROS types is paramount to achieving an efficient control mechanism to minimise damage. Given the disparity between the micronucleus and comet assay using the chosen chemotherapeutic agents for the investigation of CIBE and with the hypothesis of ROS as a likely CIBE mechanism, this research employed the use of lesion specific endonucleases

(hOGG1 and Fpg) to enable the specific detection of oxidative DNA damage. These enzymes in conjunction with the highly sensitive technique of alkaline comet assay potentiates a comparative assessment and distinction between DNA single strand and double strand breaks.

Representative images of the enzyme modified comet assay using the Kasumi-1 cell line are shown in figure 5.5. These images show the scored comets for each of the four agents, the hOGG1 and Fpg treated slides per treatment compared to the no enzyme treated slides. Visually, they describe the typical comet images with distinct head and tail.

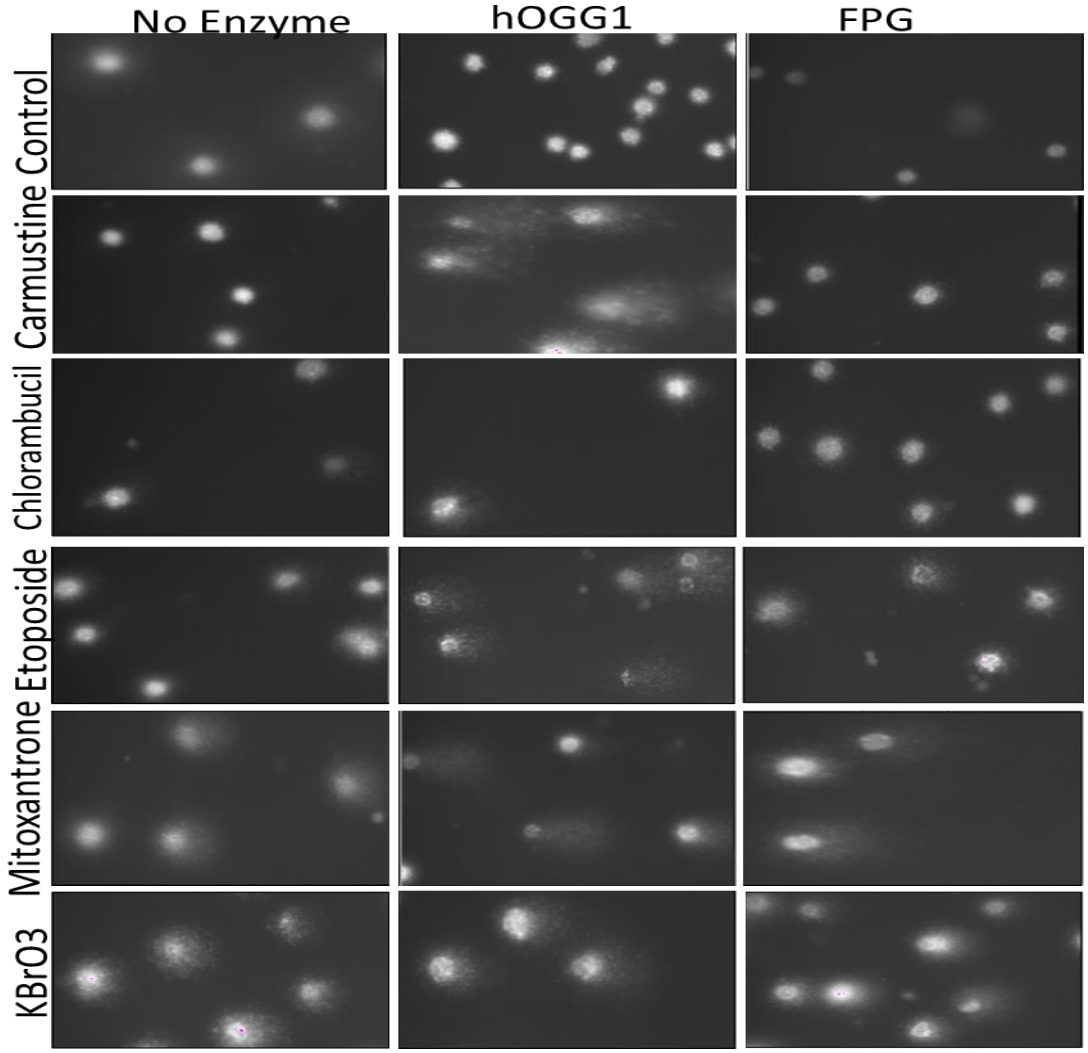

Figure 5.5: Representative comet images of the utilisation of lesion-specific endonucleases (hOGG1 and Fpg) and no-enzyme treated controls of the Kasumi-1 cell line. Comet tails were measured following co-culture of Kasumi-1 with the HS-5 cell line that was exposed to untreated control, carmustine, chlorambucil, etoposide, mitoxantrone, and potassium bromate ($KBrO_3$). Images are shown for the scored percentage DNA tail intensities. Fpg of mitoxantrone and $KBrO_3$ show tail elongation and so was carmustine in hOGG1; other agents does not show obvious difference from untreated control.

The results of the 24 hours post co-culture enzyme modified comet assay with TK6 (Figure 5.6) show no statistically significant increases in comet tail with or without the hOGG1 and Fpg, for all agents except mitoxantrone, all in comparison to their respective untreated control samples. For the hOGG1 treated cells, there was an observed increase over and above the treated control (10%) for carmustine (18%), chlorambucil (15%) and etoposide (19%) but these increase were not statistically significant; whereas mitoxantrone showed an increased statistically significant (*$p \leq 0.05$) oxidative lesion of 32%. Mitoxantrone was relatively comparable to the positive control $KBrO_3$ with a percent DNA tail intensity of 36%. For the Fpg treated cells, the all three agents (carmustine, chlorambucil and etoposide) showed similarity with % DNA tail intensity, to approximately 20%, which was all above the untreated control with 8%. Fpg treated mitoxantrone showed highest level of oxidative lesions with a value of 38% DNA tail intensity, to range higher than other agents, showing a statistical significance of **$p \leq 0.01$.

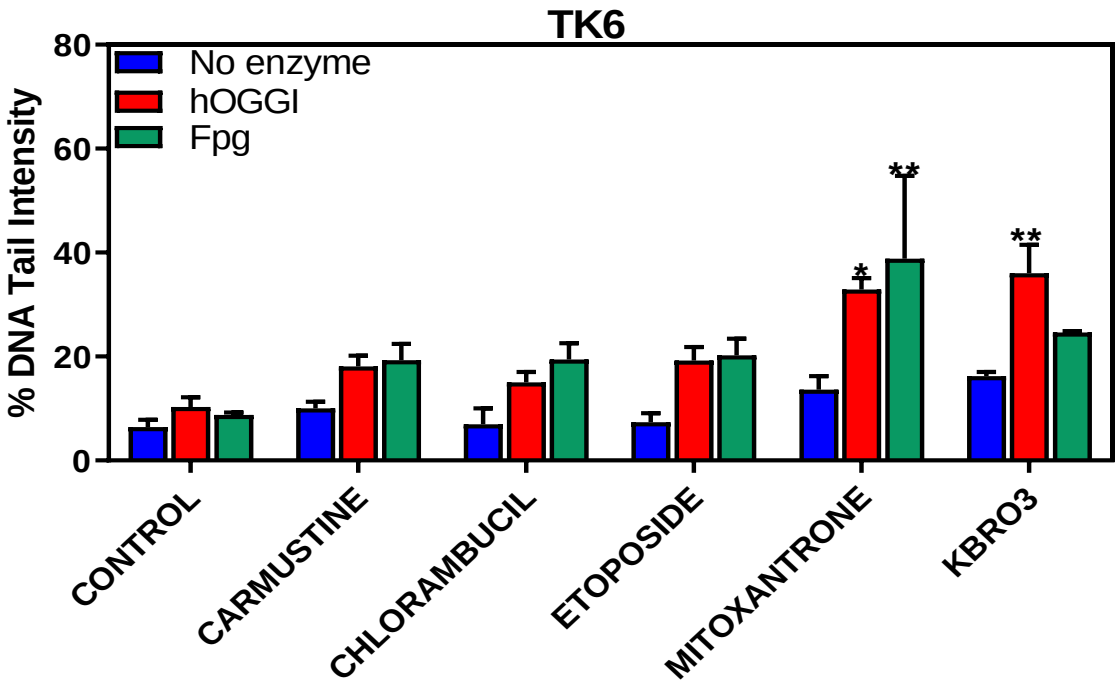

Figure 5.6: Percentage DNA in the tail of the TK6 bystander cell line with and without hOGG1 and Fpg. Following 24 hours co-culture of TK6 bystander cells and pre-treated HS-5, harvested cells were lysed, treated with hOGG1 and Fpg endonucleases prior to electrophoresis. Cells were compared against an untreated negative control and $KBrO_3$ positive control. Data is shown for three independent repeats as mean ± SD and its statistical significance represented as *$p \leq 0.05$ and **$p \leq 0.01$, as evaluated using the two way ANOVA.

Additionally, the untreated no enzyme treated control when compared to the enzyme treated, untreated controls were not statistically significant. All the no enzyme treated samples were reduced compared to the values of both enzyme treated samples, However, they all showed no statistical significance relative the no enzyme untreated control. The no enzyme treated KBrO3 positive control was relatively low and comparable to no enzyme treated mitoxantrone, showing %DNA tail intensity of about 15%. KBrO3 enzyme treated samples both showed increased %DNA tail intensity, but appeared more sensitive to hOGG1 enzyme with %DNA tail of 38%.

The data for the metabolically competent cell line AHH-1 (Figure 5.7) also shows an increase in comet tail for most agents tested when compared to their relative enzyme treated controls. Similar to the TK6, the percent DNA intensities for carmustine (19%; 15%), chlorambucil (25%; 19%) and etoposide (16%; 28%) for the respective enzymes (hOGG1; Fpg) were comparable and even though they were raised well above the controls (12%; 11%) they were not statistically relevant. However, similar to TK6, mitoxantrone (51%; 50%) and KBrO3 (55%, 43%) were both statistically significantly increased comet tails (***$p \leq 0.001$). Comparing AHH-1 samples which were not modified by either hOGG1 or Fpg, there is little difference between the bystander samples with the untreated control, although mitoxantrone is non-significantly raised. Only the positive control ($KBrO_3$) was significantly raised above the control without enzyme modification.

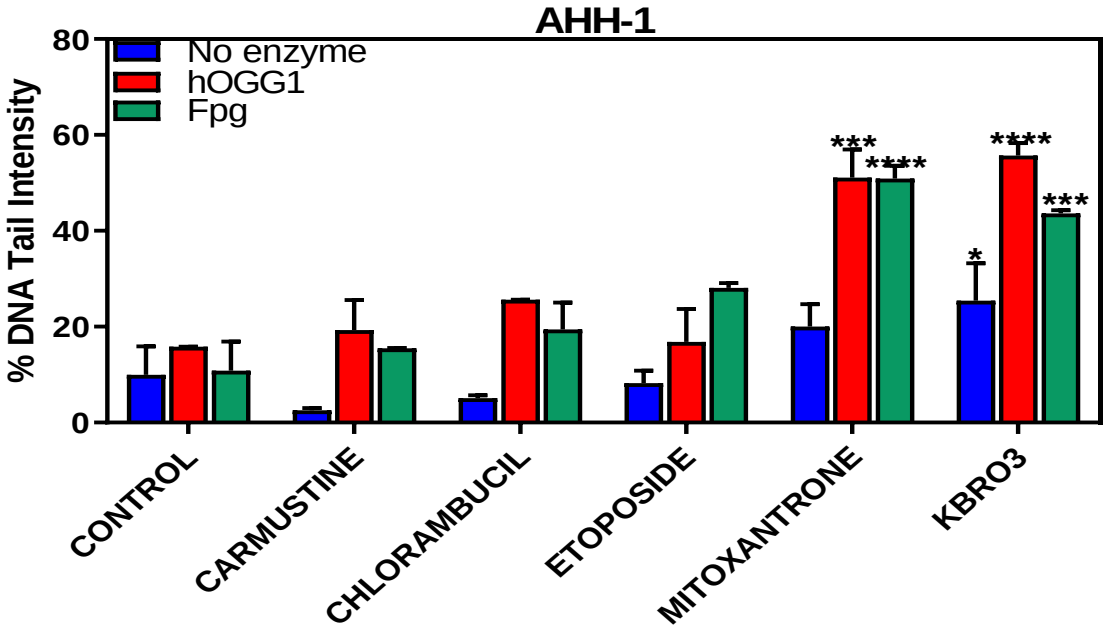

Figure 5.7: The effect of hOGG1 and Fpg on the AHH-1 cell line. Cells were harvested from the *in vitro* bystander co-culture model of this study. Post co-culture cells were harvested and utilised in the enzyme modified comet assay. Percent DNA in the tail was evaluated for the enzyme and non-enzyme treated cells. Comparisons of these were made for all chemotherapeutic agents against an untreated control. Data is represented as mean ± SD for three independent experiments, showing statistical significance as *$p \leq 0.05$ and ***$p \leq 0.001$; evaluated using two way ANOVA.

Additionally, in the Kasumi-1 cell line (Figure 5.8), the untreated controls showed no variation with DNA intensities of 10%, 12% and 11% for non-enzyme treated, hOGG1 and Fpg treated cells respectively. Similarly, all samples without enzyme modification show no statistical difference in comet tails, relative to the untreated controls, showing that enzyme modification is required to detect these lesions. Whilst carmustine showed increased DNA intensities of 28% and 20% for hOGG1 and Fpg respectively in comparison to the no-enzyme control, chlorambucil and etoposide presented similar values to each other, but were slightly higher for Fpg rather than for hOGG1 (24% and 28%). This suggests that different drugs might produce slightly different lesions during bystander effect, as recognised by the two different enzymes. Mitoxantrone intensities were the only comet tail increases that were statistically significantly different to the untreated control, at 42% for hOGG1 and 30% for Fpg. The positive control $KBrO_3$ showed similar DNA tail intensities to mitoxantrone with the respective enzymes,

suggesting that mitoxantrone has the capacity to induce similar DNA lesions at equivalent levels to the positive oxidative control.

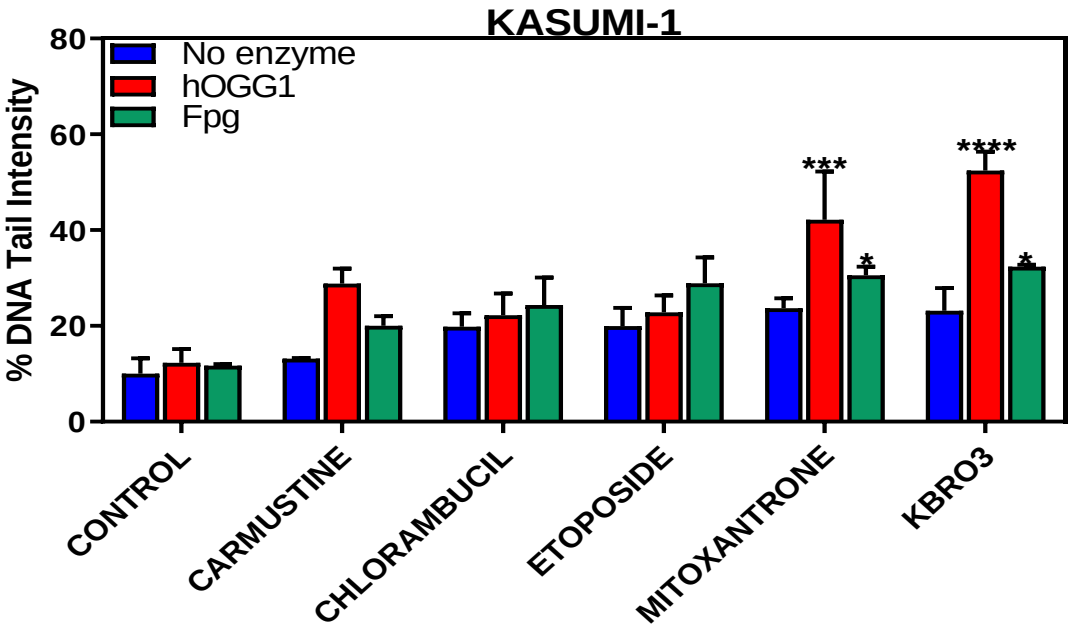

Figure 5.8: Assessment of oxidative DNA damage in Kasumi-1 bystander cells. After 24 hours co-culture of Kasumi-1 cells with HS-5 (pre-treated for 1h with clinically relevant doses of carmustine, chlorambucil, etoposide and mitoxantrone), two replicate slides for each enzyme per treatment was prepared for oxidative DNA damage assessment by the enzyme modified comet assay. Slides were scored, analysed and data represents three separate biological repeats with statistical significance presented as *$p \leq 0.05$ and ***$p \leq 0.001$; evaluated by two way ANOVA.

An overall comparative assessment of all the tested chemotherapeutic agents in the bystander assay shows that whilst all drugs have the capacity to induce lesions detected by Fpg and hOGG1, the only drug capable of statistically increasing the DNA intensity in the comet tail, and thus likely to induce bystander through ROS or other oxidative mechanisms is mitoxantrone. Mitoxantrone was comparable to the $KBrO_3$ positive control. Chlorambucil and etoposide were very similar with their intensities for both hOGG1 and Fpg treated. Carmustine, chlorambucil and etoposide however, were inconsistent in their comet tail intensities, dependent on which endonuclease was used and in which cell line tested; whereas chlorambucil and etoposide were more similar in Kasumi-1 and TK6, chlorambucil was more similar to carmustine for the AHH-1 cell line.

5.3.3 Assessment of oxidative DNA damage using 8-OHdG antibody

In this study a quantitative assessment of 8-OHdG using the bystander cells (TK6, AHH-1 and Kasumi-1) was evaluated following 24 hours co-culture with HS-5 cells previously exposed to carmustine, chlorambucil, etoposide and mitoxantrone. The confocal microscope was used to localise the antibody (Figure 5.9), while flow cytometry was used to quantitatively evaluate the amount of 8-OHdG present in the cells (Figure 5.10).

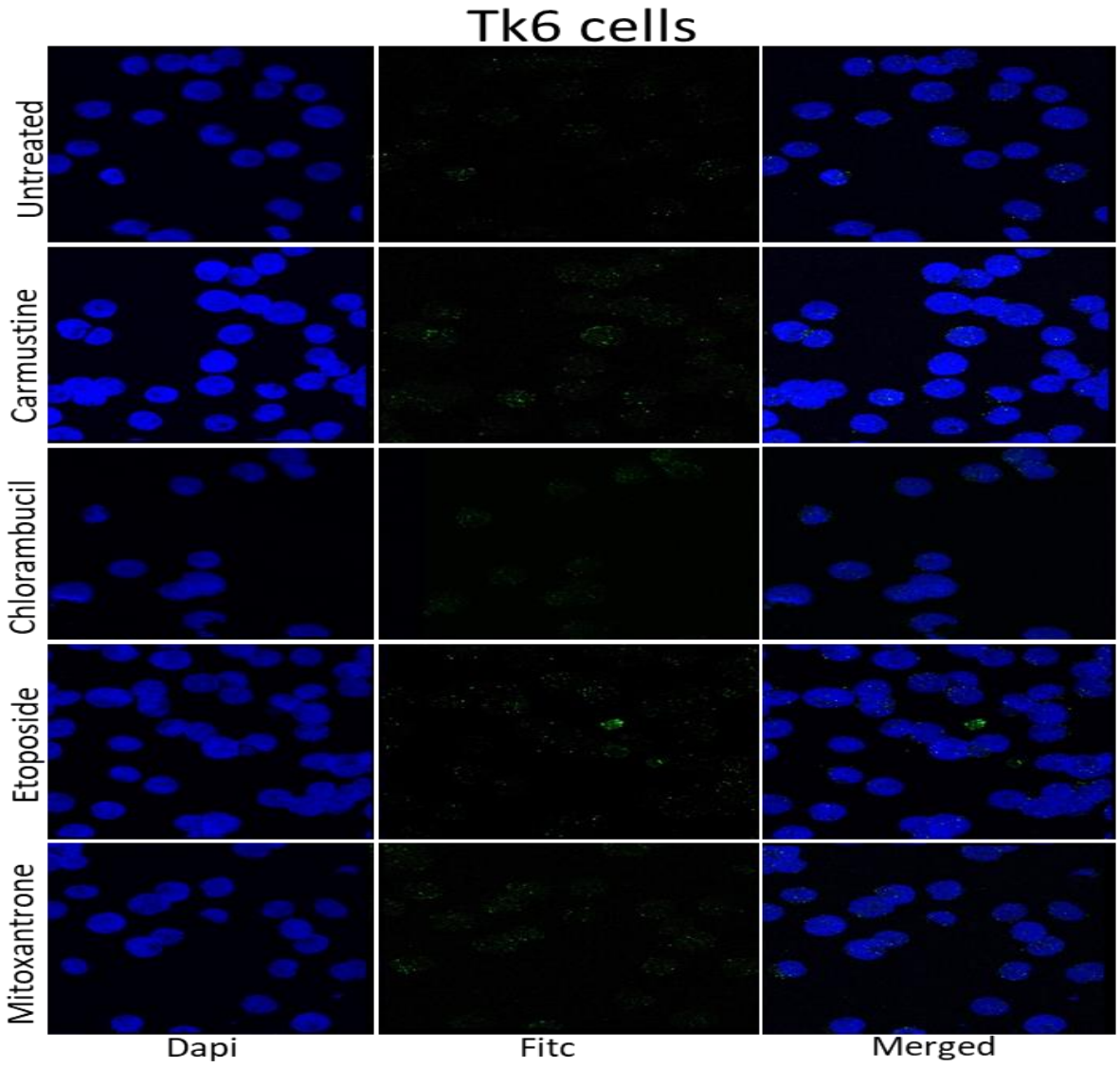

Figure 5.9: Confocal analysis for the bystander cells. Following 24 hours co-culture of bystander cells, cells were harvested, fixed and permeabilised. Using an anti-DNA/RNA antibody with specificity for detecting 8-OHdG damage, cells were stained overnight at 4^0C. Following washing of the unbound antibodies, slides were counter-stained with Dapi and visualised using the separate Dapi and Fitc microscope filters, then merged using ImageJ software. Data depicts representative images of three separate repeats.

There was little difference in MFI (Figure 5.10a) between the unlabelled untreated control and the isotype control, however, there was a slight increase of 8-OHdG labelled control sample, showing an MFI of 2 x 10^4 above the untreated control and this was used as baseline oxidative lesions in these bystander cells. Although all agents appear to be slightly raised above the untreated unlabelled control, they were relatively of similar MFI to the FITC (8-OHdG labelled control) treated except for carmustine which was significantly ($p<0.05$) increased with an MFI of 3.0 x 10^4. The unlabelled untreated control, 8-OHdG labelled untreated and isotype control showed no percent positive cells, whereas carmustine showed positivity of 5%, chlorambucil was 10%, etoposide was 15% and mitoxantrone was 20%, with only chlorambucil showing statistical significance ($p \leq 0.05$). These raised MFIs were however not statistically relevant and can be re-affirmed by the evidence of the histogram overlay (Figure 5.10b) for these agents. Data were all compared to the untreated control, labelled with the 8-OHdG antibody (called untreated +FITC throughout the assay).

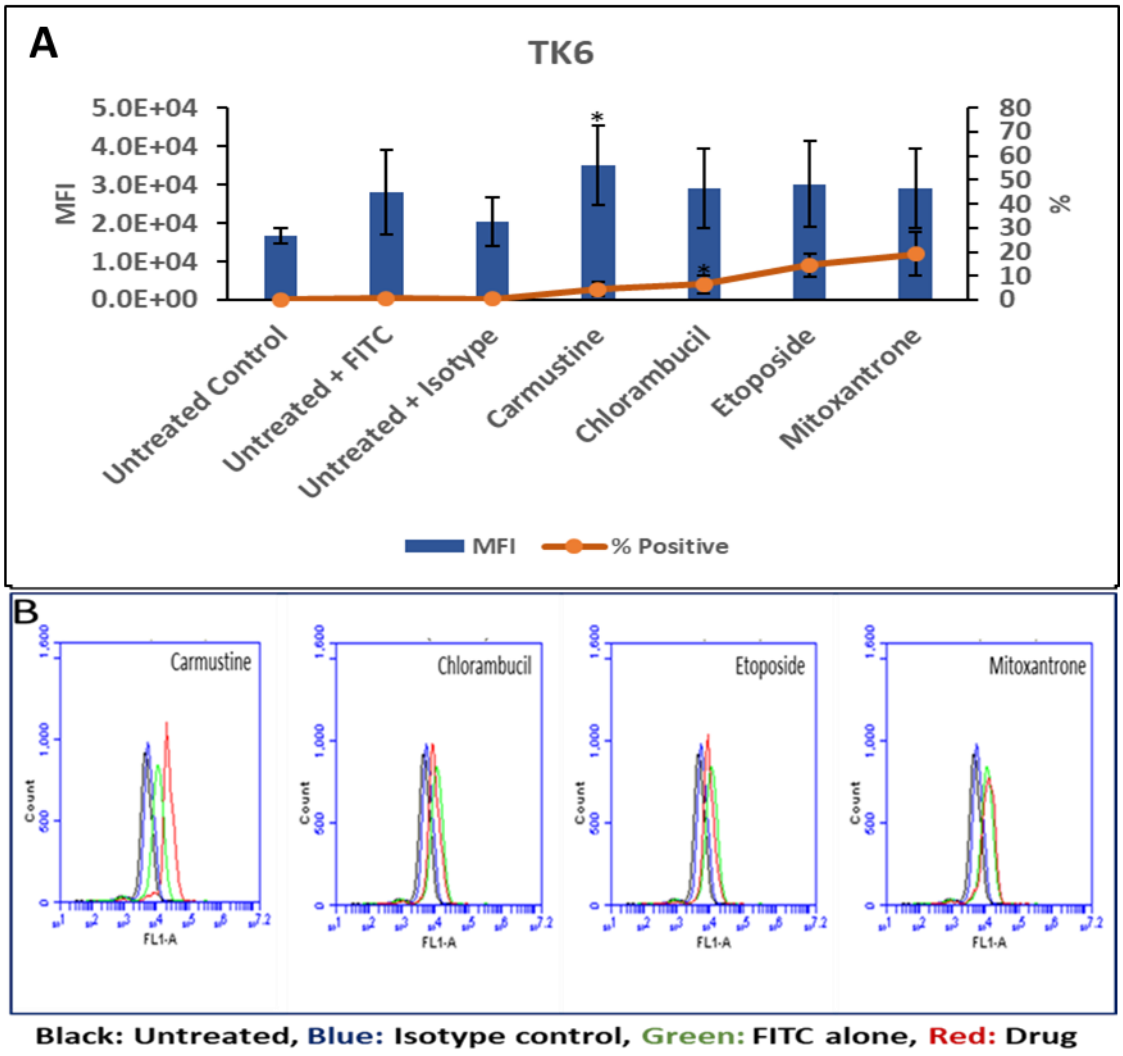

Figure 5.10: Evaluation of oxidative stress using 8-OHdG antibody. TK6 cells were harvested 24 hours post co-culture with HS-5 which had been pre-exposed to carmustine, chlorambucil, etoposide and mitoxantrone. The figures demonstrate (a) the median fluorescent intensity and percentage positivity of TK6 for the presence of 8-OHdG lesions and (b) representative histogram overlay plots evidencing the level of 8-OHdG lesions in the TK6 bystander cells. Except for carmustine's MFI, other agents were not statistically significant. Data is presented for three separate repeats and statistical significance is shown for *$p \leq 0.05$.

The MFI for the AHH-1 cell line (Figure 5.11a) was much lower for both treated and untreated cells in comparison to the TK6 bystander cells. While all the treated agents show an MFI of around 1 x 10^4, the isotype and unlabelled untreated control were similar showing an intensity of 8 x 10^3, but the FITC treated control had an MFI of 8 x 10^3, which was unexpected and suggest non-specificity for the AHH-1 cells. None of these chemotherapeutic agents showed a

significant MFI difference from the control. There were no positive cells for the unlabelled untreated control and the isotype control, whereas all the tested agents show same level of positivity at around 15% which was significantly raised ($p<0.01$) except carmustine, all in comparison to the 8-OHdG labelled untreated control (12% positive cells).

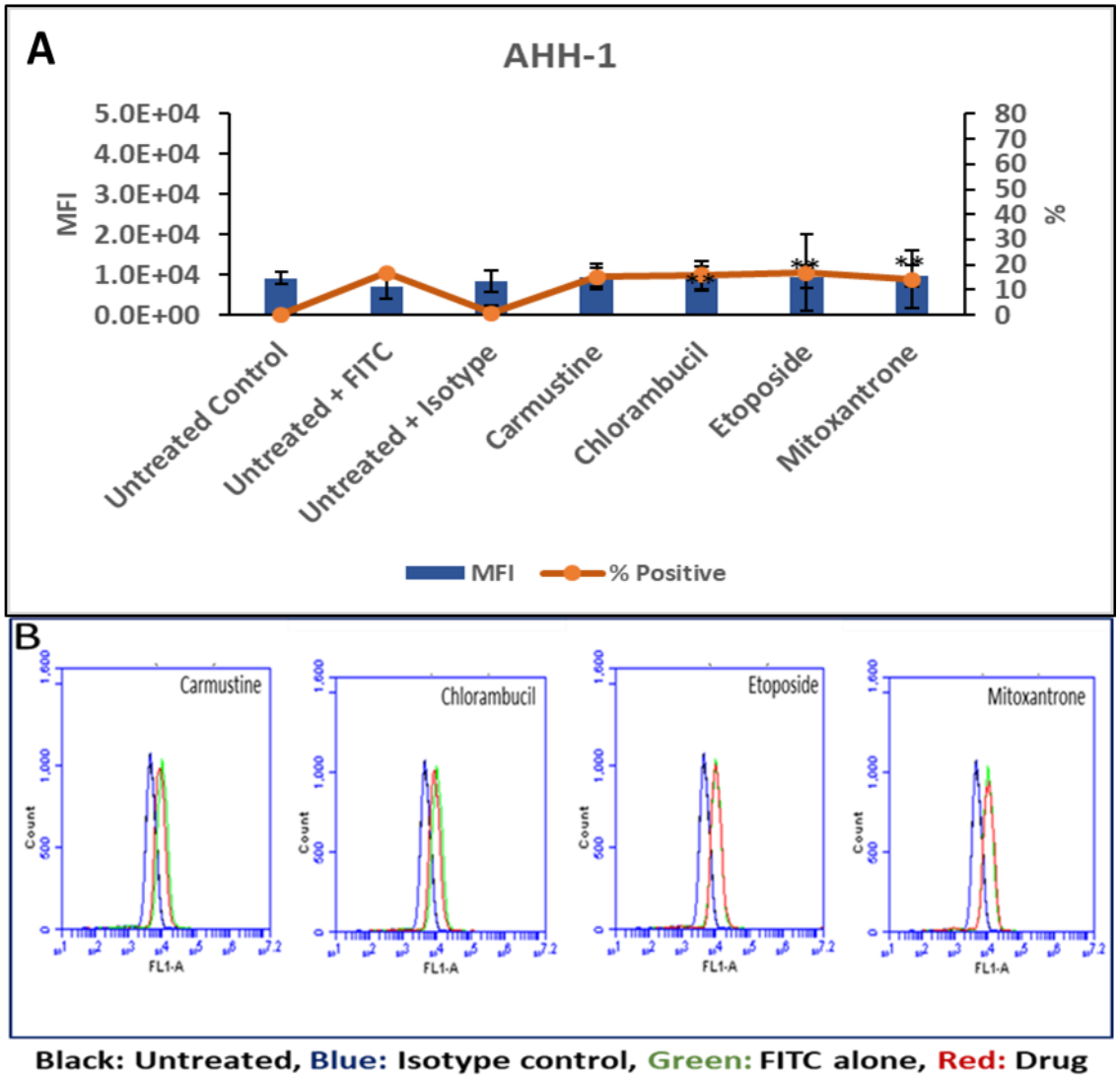

Figure 5.11: The levels of 8-OHdG in AHH-1 bystander cells assessed for some chemotherapeutic agents. The amount of 8-OHdG was measured using flow cytometry in AHH-1 cell line after 24 hours of co-culture with treated HS-5. Figure (a) show mean values of the median fluorescent intensities of carmustine, chlorambucil, etoposide and mitoxantrone; (b) shows representative histograms of AHH-1 cells showing comparison to the unlabelled untreated control, isotype control, 8-OHdG labelled untreated cells of the bystander cells from drug treatment. The data is representative of three separate repeats and although all MFI were non-significant, the percent positive cells statistical significance are shown as $**p \leq 0.01$.

Also in support of the accrued data for these agents, the qualitative evaluation of the histogram plots from flow cytometry for these agents, does reflect the untreated control for all agents to be very similar the isotype, whereas carmustine, chlorambucil, etoposide and mitoxantrone were relatively comparable to the treated FITC control cells. All of these show a slight shift to the right as a reflectively supported by the accrued significant positive data but with no major difference in MFI does not reflect oxidative ROS damage in AHHI-1 bystander cells for these agents.

Evidence from the myeloid cell line (Kasumi-1) for the expression of 8-OHdG levels (Figure 5.12a) in the treated and untreated samples reveal carmustine with a distinct and statistically significant ($p \leq 0.001$) MFI over and above the FITC untreated control (ie untreated control stained with the 8-OHdG antibody) and well raised above the other tested chemotherapeutic agents. The unlabelled untreated control, isotype control and untreated FITC stained control, all show the same MFI (8×10^3). While the MFI for etoposide and mitoxantrone ranges were 1×10^4 and 1.7×10^4, they were slightly increased when compared to the untreated FITC labelled control. Etoposide was however significant ($p \leq 0.05$) over the control although not as significant as carmustine ($p \leq 0.001$). With the increase in carmustine, this is likely suggestive of oxidative lesion in the bystander cells. Chlorambucil also had an increased MFI over the FITC labelled untreated control; but this was not statistically significant. For the other agents, chlorambucil and mitoxantrone show similar MFI and in comparison to the FITC labelled untreated control, they were not significant and appeared to have no change in the level of positive cells. The outcome of the percent positive cells were qualitatively reflected in the overlay histogram (Figure 5.11b) to show an unchanged or similar MFI for roughly all the agents when compared to against the untreated unlabelled sample, FITC treated and isotype control.

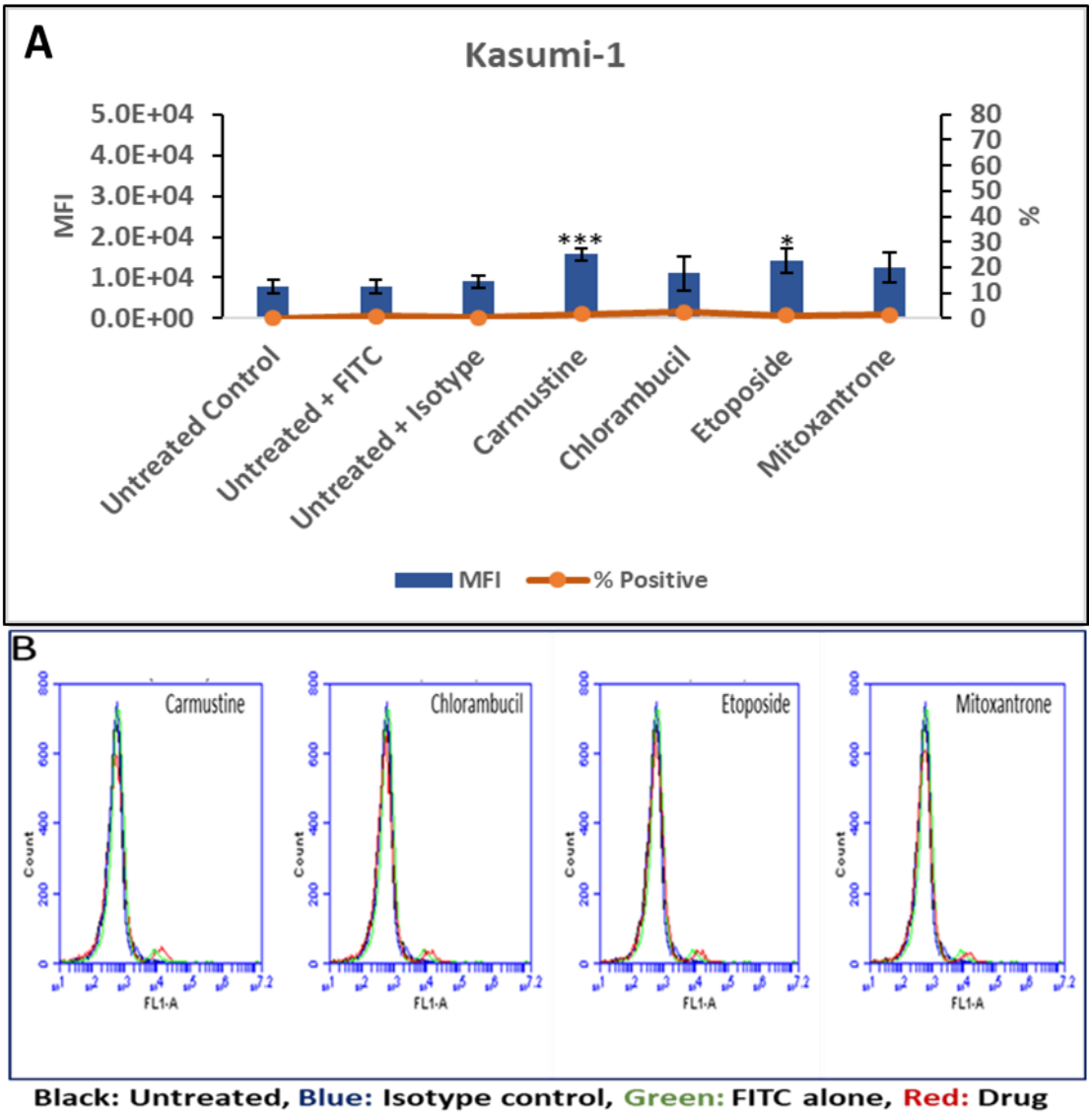

Figure 5.12: Determination of the amount of 8-OHdG in Kasumi-1 bystander cells after co-culture with drug treated HS-5 cells. Kasumi-1 cells were utilised in the 8-OHdG assay and analysed quantitatively by flow cytometry. Figure (a) shows the level of median fluorescence intensity which is indicative of the number of 8-OHdG lesions and (b) depicts a representative histogram plots from the flow cytometry for the tested agents in comparison with the untreated controls and isotype control. Data show possible ROS induced oxidative damage in the kasumi-1 cells. Data was repeated three different times and statistical relevance is shown as *$p \leq 0.05$ and ***$p \leq 0.001$; as evaluated using two way ANOVA.

5.3.4 Seahorse extracellular (XF) mito stress test

To assess the functionality of the mitochondria by the Agilent Seahorse analyser, different parameters (Figure 5.13) were measured upon addition of some reagents. Basal oxygen consumption rate (OCR) represents the rate of mitochondrial function for each cell type based on the conditions at which they are measured, and its measurement is dependent on oxygen, pyruvate, glucose and number of cells. Oligomycin inhibits the ATP synthase (complex V) and hence reflects the ATP producing capacity of the cells. Addition of carbonyl cyanide-4-(trifluoromethoxy) phenylhydrazone (FCCP) estimates the maximal respiratory capacity with any observed decline indicative of potential mitochondrial dysfunction. Addition of rotenone and antimycin A (a respiratory inhibitor) shuts down mitochondrial respiration allowing measurement of spare reserve capacity and non-mitochondria OCR (Tan *et al.*, 2015; Decleer *et al.*, 2018).

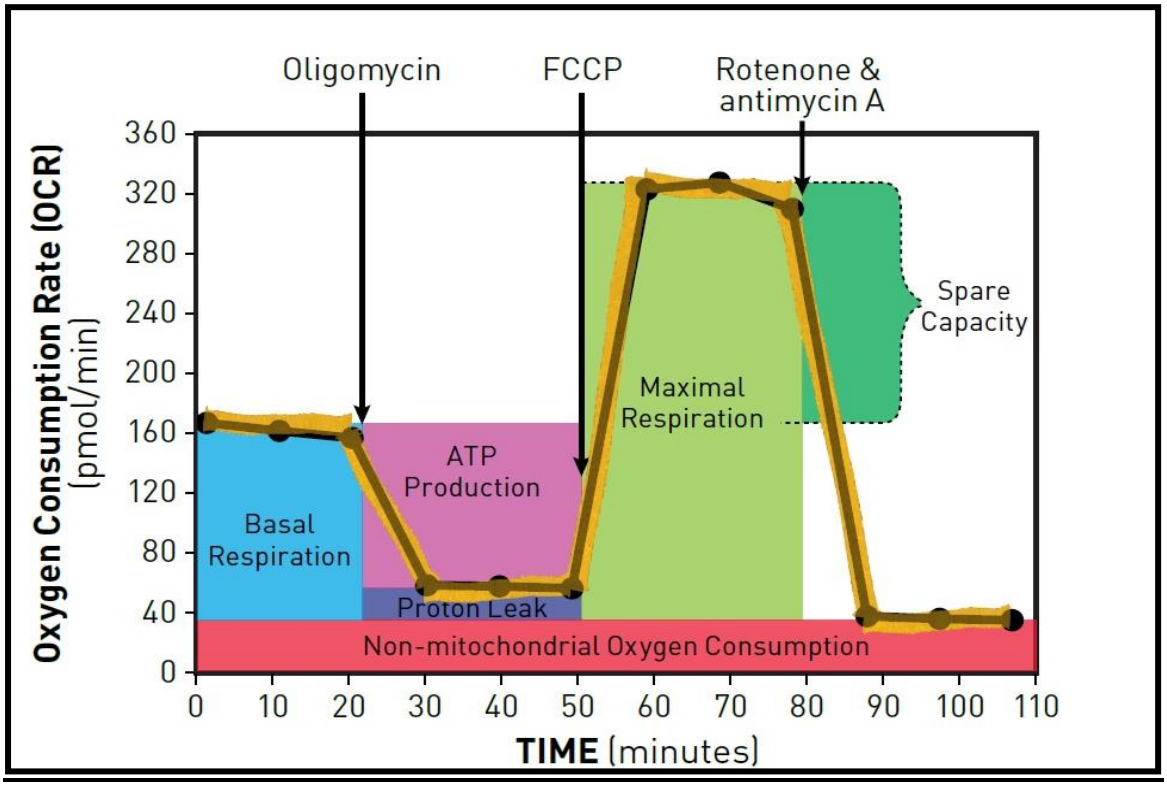

Figure 5.13: The bioenergetic scheme in theAgilent Seahorse XF mito stress test. Following the sequential delivery of oligomycin, FCCP, rotenone and antimycin A and depending on the programmed cycle times, basal respiration (blue), ATP dependent oxygen consumption (pink), proton leak (purple), maximal respiration (army green), non-mitochondria respiration (red) and spare reserve capacity (green) are measured and parameters corelated to their respective OCR. Image under with permission to use from seahore company.

The normal/standard seahorse XF mito stress test (normal implies when the cells are treated in the same way as the bystander cell culture model, by exposing the cells for 1h to chemotherapeutic agents prior to measurement) of HS-5 cells (Figure 5.14). All assessments were made in respect of the untreated control, and by the level of OCR of treated against untreated. Where there is an indication of reduction upon FCCP addition and with a decreased OCR, it is indicative of mitochondria disturbance. Figure 5.14a (OCR) shows the same OCR for untreated control and carmustine at 200 pmol/min. Whilst chlorambucil, mitoxantrone and doxorubicin showed a good basal respiration rate relative to the untreated control, etoposide was decreased and daunorubicin revealed a negative value. ECAR measurements (Figure 5.14b) show all agents as above 80mpH/min whereas etoposide and daunorubicin were between 60-80mpH/min. Both ECAR and OCR simultaneous measurements of glycolysis and mitochondria permits the detection of cellular response ETC and ATP demands, which are likely altered in the case of cancer and other pathologies.

The basal level measurement (Figure 5.14c) shows all the cells were almost actively functional (except for the decreased levels in etoposide and daunorubicin); an indication of good metabolism and possession of a good oxygen consumption activity within the cells. Also, the spare reserve (Figure 5.14c) capacity for carmustine, mitoxantrone and doxorubicin were relatively comparable to the untreated control with an OCR of 700 pmol/min. in comparison to the control, none of these agents showed a significant difference in either the basal respiration level or the spare reserve capacity. Chlorambucil and etoposide showed a very low reserve capacity and ATP production (Figure 5.14d), evidencing of good mitochondria activity. Daunorubicin's spare capacity was 400 pmol/min, with no evidence of ATP production at all, potentially a disturbance of mitochondria activity. This no ATP related OCR in daunorubicin showed a significant difference (***$p \leq 0.001$) and was the observed significant (*$p \leq 0.05$) decrease in etoposide ATP levels. Evidence of the proton leak was shown by chlorambucil, mitoxantrone and doxorubicin with values at 48 pmol/min, whilst the untreated control, carmustine and etoposide were 40 pmol/min, and a further decrease for daunorubicin at 30 pmol/min.

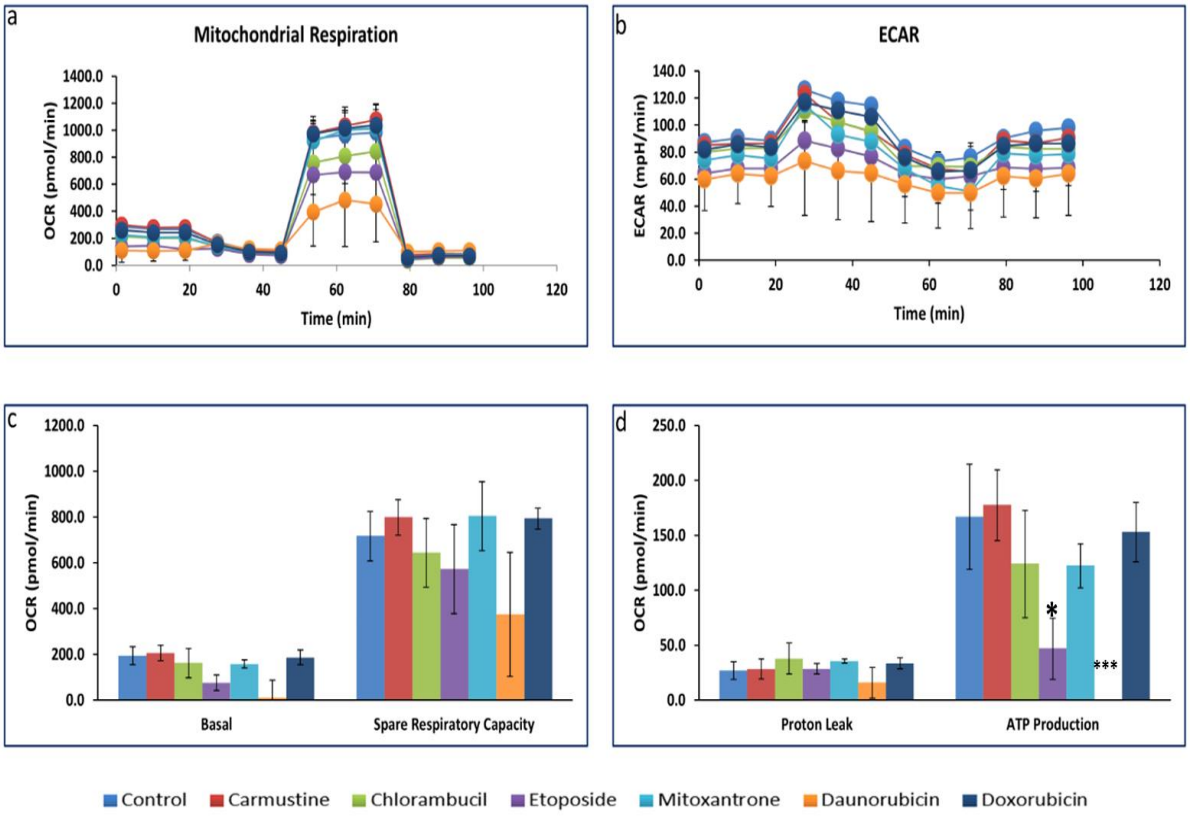

Figure 5.14: Assessment of mitochondrial respiration in HS-5 cells with and without drug treatment using normal seahorse assay. A mito stress test was performed using the XFe24 seahorse analyser by injecting oligomycin (1 µM), FCCP (1 µM), and rotenone (0.5 µM) with antimycin A (0.5 µM) in cells pre-treated for an hour with chemotherapeutic agents. Basal respiration was measured prior to injection of the reagents and post-exposure oxygen consumption rate, maximal respiration and spare reserve capacity was measured for these chemotherapeutic agents at their clinically relevant doses in real time. Data is representative of mean ± SD of three separate experiments and significant difference shown for *$p \leq 0.05$ and ***$p \leq 0.001$ as extrapolated against the untreated control by two way ANOVA.

In order to compare the individual chemotherapeutic agents in comparison to the untreated control as separate from the instrument generated data, the data is as shown in figure 5.15. Figures 5.15a and 5.15f respectively, reveal that both carmustine and doxorubicin are almost identical to the untreated control, with only small increases in each for maximal respiration at 1000 pmol/min while the untreated control OCR was 970 pmol/min. There was also no observed variation between mitoxantrone and the untreated control. However, there were marked differences between chlorambucil, etoposide and daunorubicin relative to the control.

They show OCR rates for the maximal respiration assessment of 800 pmol/min, 650 pmol/min and 400 pmol/min for chlorambucil, etoposide and daunorubicin respectively.

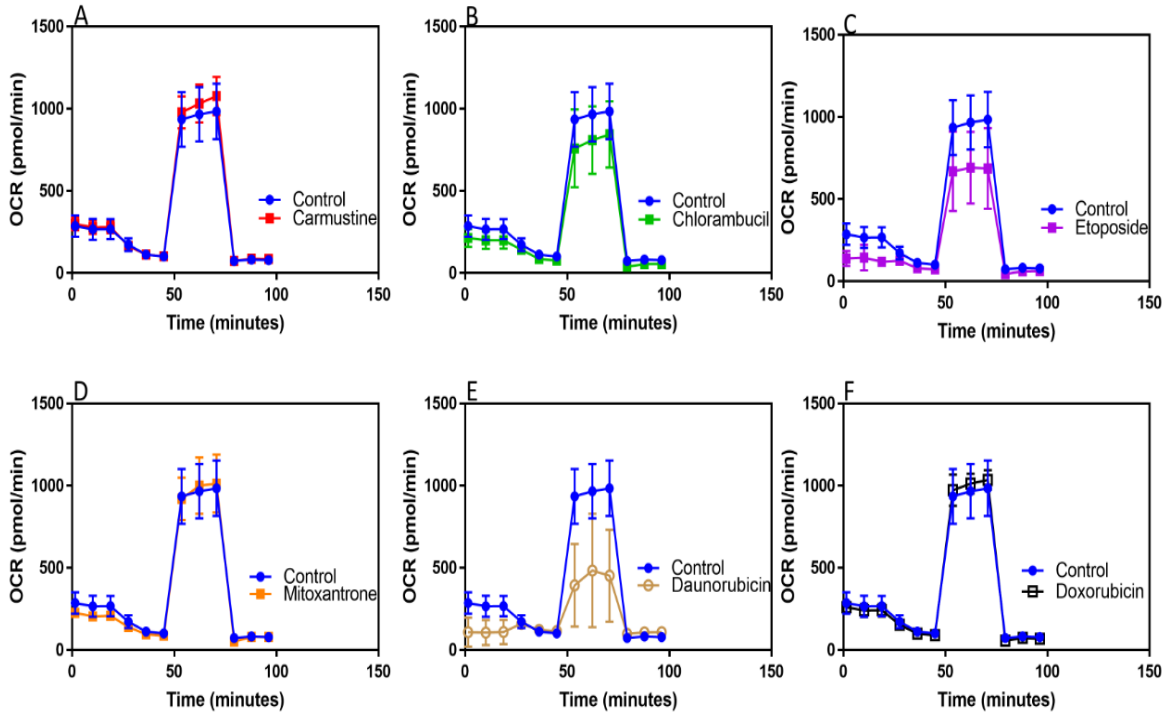

Figure 5.15: Qualitative comparison of the acute OCR of some chemotherapeutic agents relative to the untreated control in HS-5 cells. Carmustine (a), (b) chlorambucil, (c) etoposide, (d) mitoxantrone, (e) daunorubicin and (f) doxorubicin were compared to the untreated control. Following a 1h treatment of HS-5 cells with these agents, the Agilent Seahorse XF mito stress test template was used to measure the OCR in HS-5 cells in response to the various reagents (oligomycin, FCCP, rotenone and antimycin) delivered through the injection chamber. This experiment represents three individual repeats (n=3).

A close evaluation of the acute (implying no prior treatment and incubation of the cells with the chemotherapeutic agents for 1h before analysis. Rather once drugs were injected into the cells, they were put into the analyser for real time analysis) mitochondria stress test, show a good basal respiration (Figure 5.16c) for all agents except daunorubicin (with a negative OCR value) judging by OCR of at least 200pmol/min and relative to untreated control. All other agents were non-significant while daunorubicin had a significant (****$p \leq 0.0001$) decrease. With the exception of chlorambucil (180 pmol/min) and etoposide (185 pmol/min) which show a slight decrease in OCR, carmustine, mitoxantrone and doxorubicin were the same or above the OCR of the untreated control (200 pmol/min). The overall mitochondrial respiration (Figure 5.16c) and ECAR responses reveal a relatively stable mitochondrial activity and glycolysis

except for chlorambucil and daunorubicin which had decreased OCRs of 600 pmol/min and 400 pmol/min respectively. In comparison to the untreated control, this suggests a reduced mitochondria activity and showing a significant decrease of daunorubicin in basal and spare respiratory capacity respectively. Notably, in Figure 5.16d, there was no observed leakage of electrons during this real time assessment and only daunorubicin show a significant (***$p \leq 0.001$) decline in ATP production (40 pmol/min) compared to the untreated control (220 pmol/min). Daunorubicin is thus, suggested to have high ROS activity that potentially had led to inactivity of the mitochondria. This to be investigated further possibly trying different drug dosages. This is because there was an observed colour change upon addition of daunorubicin drug to the cells which may also account for a reduced pH in daunorubicin during the assay.

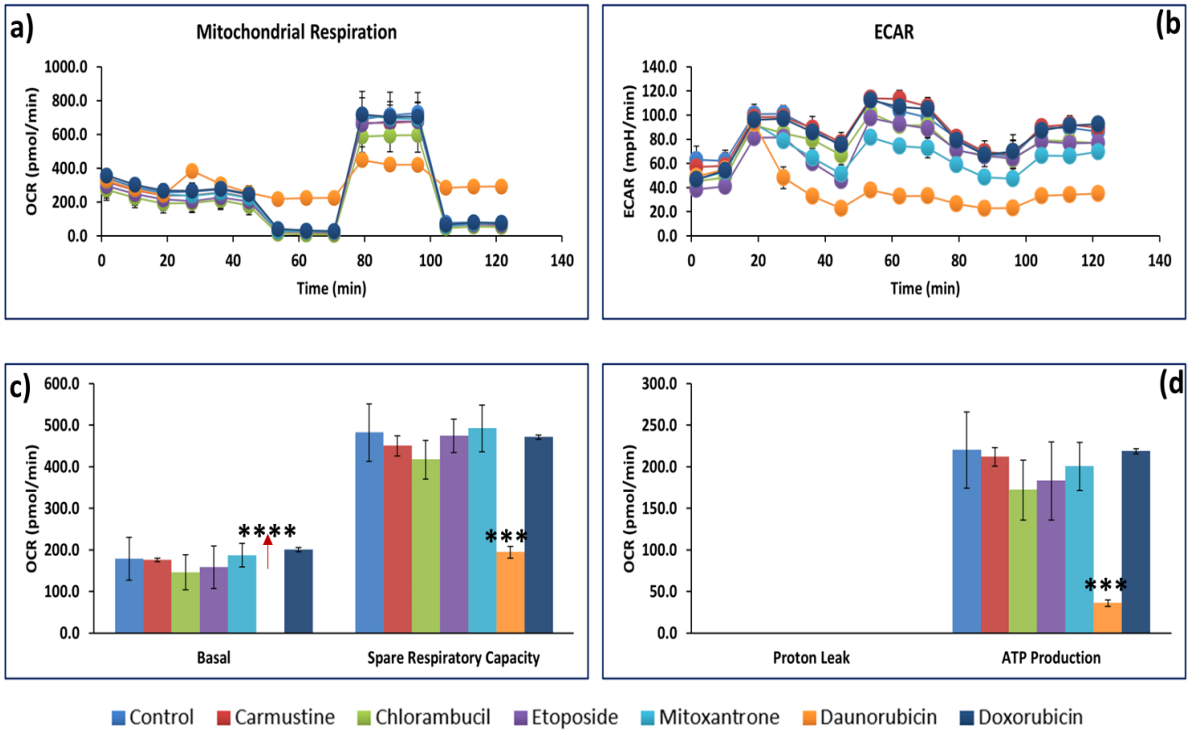

Figure 5.16: Quantitative assessment of some mitochondrial respiration parameters in the HS-5 cell line using the acute seahorse assay. HS-5 cells (25 x 10^4) were seeded in 500 µl of complete culture medium overnight, later replaced with freshly prepared seahorse complete medium and the cells exposed to carmustine, chlorambucil, etoposide, mitoxantrone, daunorubicin and doxorubicin. The evaluated OCR (a) and ECAR (b) were extrapolated following an acute injection of chemotherapeutic agents prior to addition of the three stressors oligomycin, Fccp and rotenone/actinomycin. Data is presented for (c) basal respiration and spare respiratory capacity; (d) proton leak and ATP production. The illustrated data is an average of three biological repeats and statistical significance shown as ***$p \leq 0.001$ and ****$p \leq 0.0001$; evaluated using two way ANOVA.

The individual graphic representation of the acute assay (Figure 5.17) more clearly reflects the differences between the OCRs of each of these agents and the untreated control. The data shows clear differences between the control and chlorambucil, and particularly in comparison with daunorubicin. With the untreated control OCR at approximately 800 pmol/min, chlorambucil and daunorubicin show OCR values of 600 and 420 pmol/min respectively. Mitoxantrone and doxorubicin were the same as the untreated control, similarly carmustine and etoposide show a negligible difference with the control. These agents with significant reductions from the untreated control are suggestive of mitochondrial disturbance.

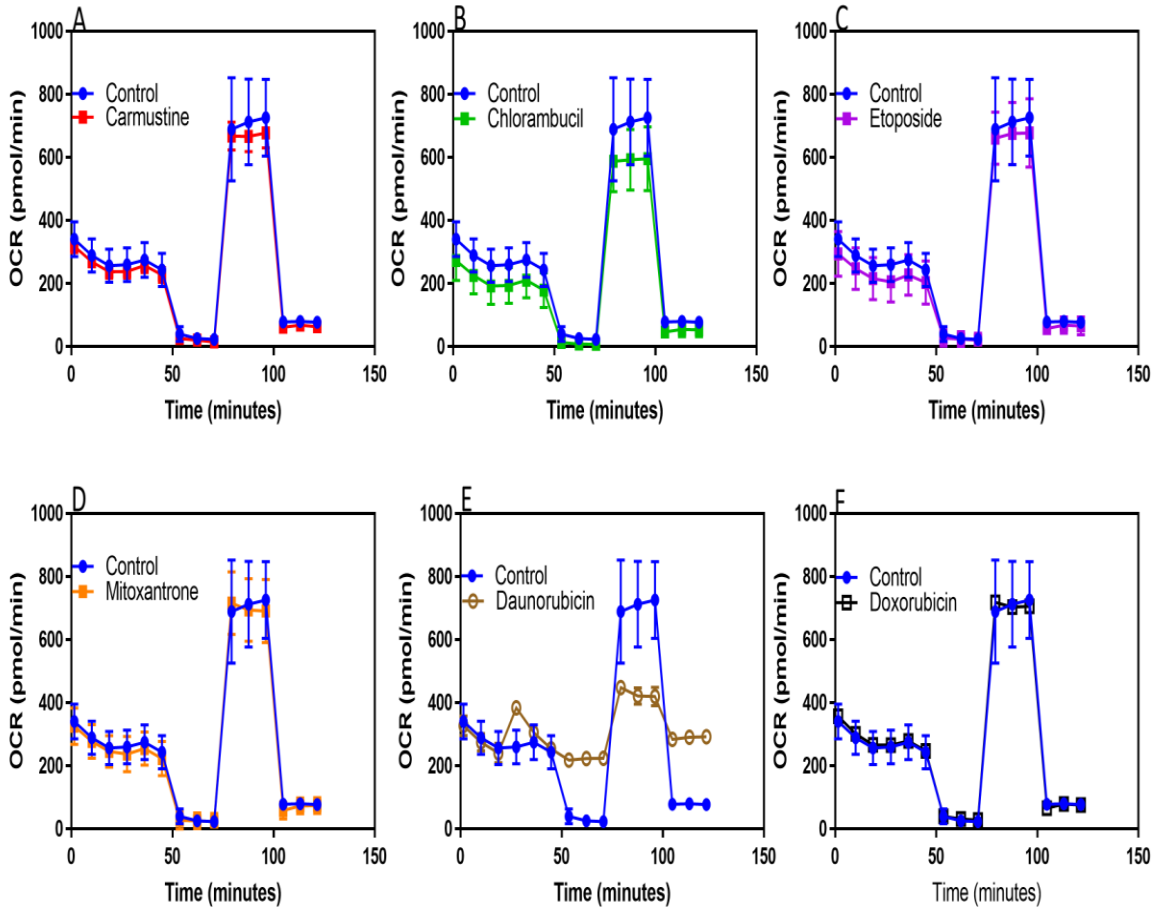

Figure 5.17: Qualitative representation of the effect of some chemotherapeutic agent on mitochondrial respiration. Using the mitochondria stress test, drugs were delivered after basal respiration was measured and before addition of oligomycin, FCCP and rotenone and antimycin A. This assay was performed using the seahorse acute mito mitochondria stress test and the presented data shows a comparative representation for mean ± SD of three independent repeats. A=carmustine, b=chlorambucil, c=etoposide, d=mitoxantrone e=daunorubicn, f=doxorubicin.

5.3.5 Evaluation of the expression of antioxidants by Western blotting

This study applied the western blot technique to investigate the expression levels of three key antioxidants (SOD1, CAT and TRX) within bystander cell lines (TK6, AHH-1 and Kasumi-1) co-cultured with chemotherapy treated HS-5 cells. Overall, the representative images (Figure 5.18) from the accrued repeats depicts low levels for CAT (except for the slight increase in Kasumi-1), moderate levels for SOD and high levels for TRX. This observation was supported by the quantitative evaluations of each enzyme with the corresponding internal control (β-actin) (Figure 5.19).

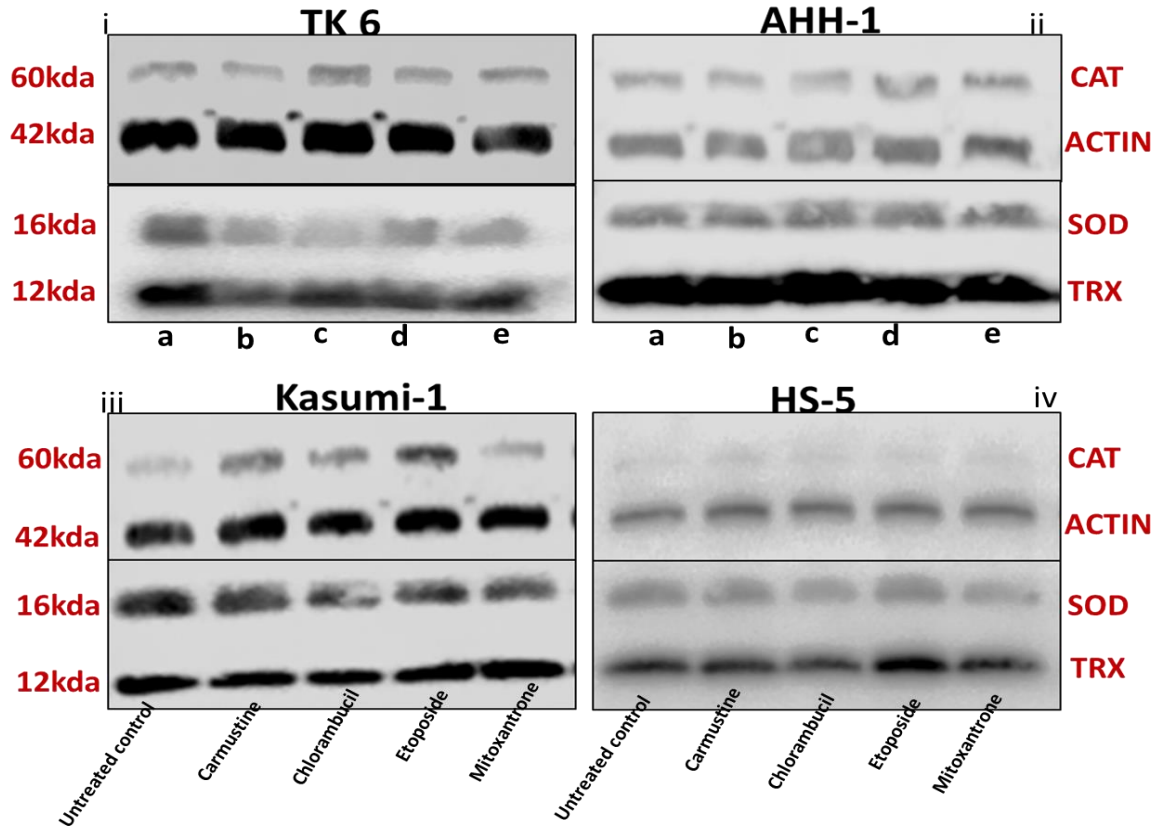

Figure 5.18: The protein levels of CAT, SOD and TRX in TK6, AHH-1, Kasumi-1 and HS-5 cell lines. The evaluation of protein expression was performed by the western blot assay using an antibody cocktail with β-actin as the internal loading control. Following 24 hours co-culture, cells were harvested and analysed for expression of these antioxidants and the densitometry quantified relative to their respective internal control. Presented herein is an immunoblot representative of an overall three biological repeats. a=untreated control, b=carmustine, c=chlorambucil, d=etoposide and e=mitoxantrone. i=TK6, ii=AHH-1, iii=Kasumi-1 and iv=HS-5.

In TK6 cells (Figure 5.19a), the results show an overall similarity between the untreated control and the indirect exposure to chemotherapeutic agents. In ascending order, CAT was least expressed, followed by SOD, with a further rise for the TRX. The untreated control, chlorambucil and mitoxantrone show similarity with the low levels of expression for CAT, whereas carmustine and etoposide show very little expression suggesting that CAT production is reduced relative to the control.

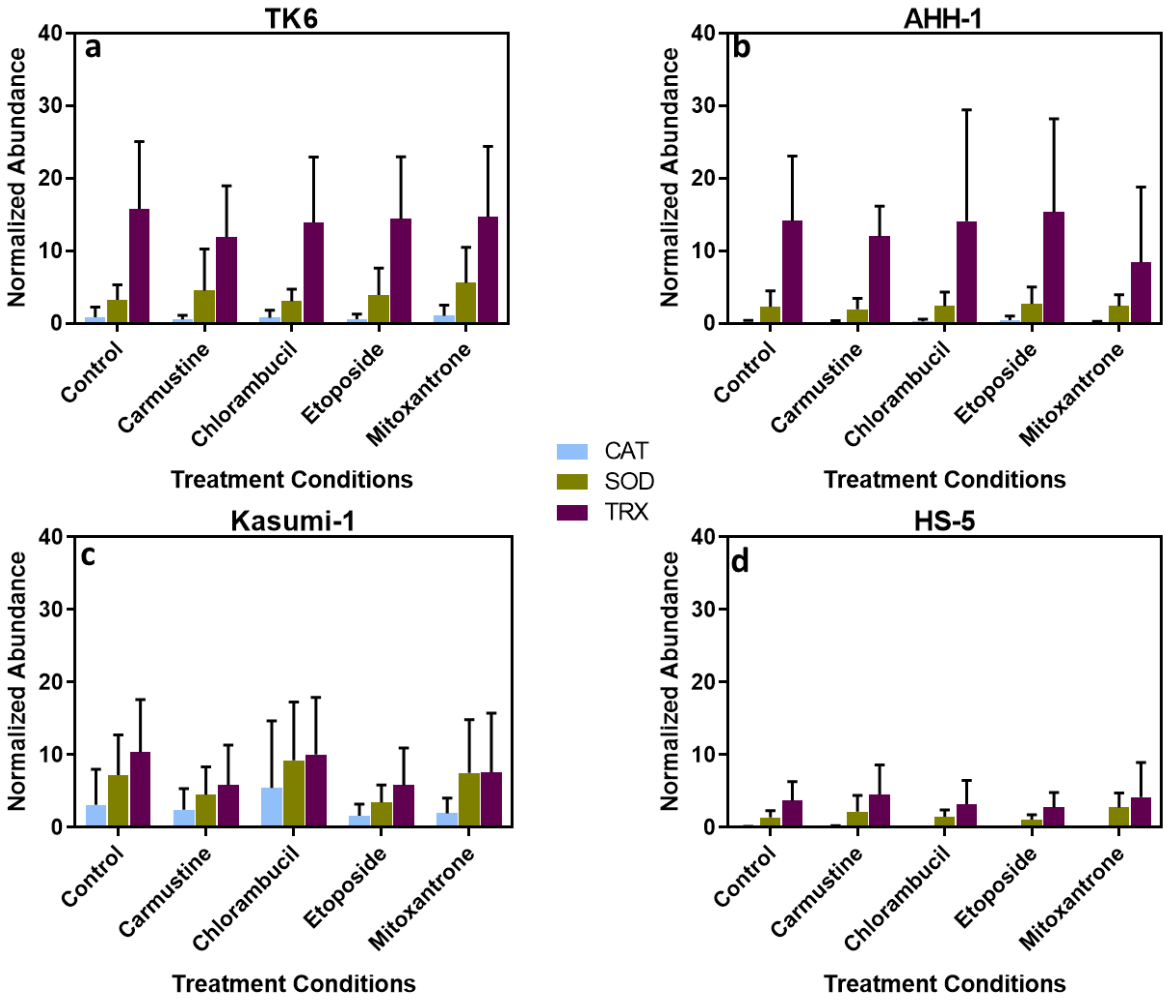

Figure 5.19: The relative abundance levels of CAT, SOD and TRX using western blot analysis. Bystander cells were harvested post co-culture with treated/untreated HS-5 cells, proteins quantified and immunoblotted against a cocktail antibody for three antioxidants. The data shows carmustine, chlorambucil, etoposide and mitoxantrone all compared to an untreated control for indirectly exposed TK6, AHH-1, Kasumi-1 cells, and directly exposed HS-5 cells. The data represents the mean ± SD of three independent experimental repeats and when chemotherapeutic agents were compared against untreated control, no agent showed statistical significance for the assessed antioxidants.

Carmustine and mitoxantrone did express higher levels of SOD in comparison to the untreated control, but etoposide showed the same levels of expression with the untreated control, while chlorambucil had a lower SOD expression when compared to the untreated control. Again when compared to the untreated control, all the tested chemotherapeutic agents had uniform expressions for TRX, with normalised abundance of carmustine slightly lower than that of the untreated control. None of the antioxidants were significantly expressed relative to the control, suggesting that either ROS were not highly expressed in TK6 cells, or that TK6 antioxidant capacity are very efficient to confer protective systems that are relatively unaffected by these treatment conditions.

The AHH-1 cells (Figure 5.19b) reveal almost a total absence of CAT for all agents except for etoposide (0.45), relative to the untreated control (0.2). SOD1 expression was also minimal, showing a deceased level for carmustine but an increased level for etoposide and mitoxantrone, all relative to the untreated control with a value of 2.3. TRX was the most highly expressed antioxidant in AHH-1, but there were no differences between any of the drug treatments either in comparison with each other, or with the untreated control.

Kasumi-1(Figure 5.19c) on the other hand, showed reasonable levels of expression for all three enzymes, with CAT and SOD generally more highly expressed than any of the other cell lines, but TRX generally below the expression for TK6 and AHH-1. However, despite overall higher levels of expression of these enzymes, none of the drug treatments induced a significant increase in expression relative to the untreated control. Compared to the control only chlorambucil showed an increase in relative expression of CAT, chlorambucil and mitoxantrone showed raised levels of SOD1, and TRX was the same for chlorambucil and untreated control, but lower for all three other drugs.

The HS-5 cell line, showed overall very low levels of expression of all three enzymes in comparison to the other three cell lines with almost a complete absence of CAT. SOD1 expression showed a non-significantly increase for all tested chemotherapeutic agents except etoposide, in comparison to the untreated control. TRX levels were only raised with carmustine and mitoxantrone relative to the untreated control but were not statistically significant.

5.4 Discussion

Free radicals generated during oxidative stress, exert their effects on different cellular targets including proteins, DNA and lipids. Lipid peroxidation for instance generates alkoxyl and peroxyl radicals, which are highly reactive but short-lived (Yang *et al.*, 2018). However, they also create secondary free radicals such as aldehydes that are more stable and can cross cell membranes to bind to nucleophilic amino acids such as cysteine, serine and tyrosine, to cause enzyme inhibition and alteration of cell structures (Conklin, 2004). When electrons leak out of electron transport chain, they react with oxygen to produce superoxide (O_2^-) which is converted to H_2O_2. Whilst O_2^- is highly reactive, H_2O_2 is slow reacting and can be produced from superoxide upon the dismutation activity of superoxide dismutase and can diffuse through the plasma membrane into the circulation, thus possess a long half- life. Such long-lived radicals could be a potential mechanism involved in CIBE. Therefore, following the establishment of genotoxic evidence for CIBE in this study and based on the awareness of some level of ROS generation by chemotherapeutic agents, this study sought to elucidate if the production of ROS could explain the observed bystander genotoxicity.

Because of the relatively short-lived radicals, measurement of ROS in general is a difficult task. Conventional ROS detection methods involve immunological and chemical approaches, but earlier versions relied upon fixed and static detection methods, and hence were limited in visualization and could be affected by cell viability and cell count (Eruslanov and Kusmartsev, 2010). On this note, this study utilised a range of varying assays (modified enzyme comet assay, 8-OHdG detection by antibody with flow cytometry, DCFDA, western blotting of antioxidant enzyme expression and Agilent seahorse XF mito stress test), harnessing their benefits to enable an adequate investigation of ROS.

5.4.1 Evaluation of intracellular ROS production by DCFDA

The use of DCFDA as a generalised assay for oxidative stress detection in some cases can also be used for detection of intracellular H_2O_2, although it is not a direct assay for H_2O_2 (Eruslanov and Kusmartsev, 2010). The DCFDA assay is a relatively easy to perform, highly sensitive technique and widely applied in the monitoring of redox changes in response to intra or extracellular oxidative production (Kalyanaraman *et al.*, 2012).

Based on the findings with the enzyme modified comet assay, this study decided to evaluate first the treated 'bone marrow compartment' using the HS-5 cells as a model. HS-5 cells post one hour treatment underwent the DCFDA assay while the bystander cells were used for same assessment 24 hours post co-culture.

HS-5 cells accrued data shows chlorambucil, etoposide and carmustine with ROS activity, but not mitoxantrone, which is unexpected given the higher levels of oxidative damage in the bystander cells from Mitoxantrone exposure. MFI of mitoxantrone in TK6 did not really shift despite the obvious shift in the histogram and the significant increase in percent positive cells. This may due the way the data was analysed by only considering the cells above the negative control peak. The events of other agents except mitoxantrone, although indicative of a possible ROS involvement cannot be distinguished as intra or extracellular. Mitoxantrone outcome is surprising as only mitoxatrone exhibited evidence of oxidative DNA damage. This may potentially be different types of ROS induced by these agents, and suggest varying mechanisms for all agents.

Examination of the outcome of this investigation shows no evidence of ROS involvement with the TK6, Kasumi-1 and AHH-1 cells, except for carmustine in AHH-1 which shows both increased MFI and a high number of fluorescently positive cells. Carmustine has shown possible ROS involvement in this study with the DCFDA assay and demonstrated some oxidative damage in the comet assay. Carmustine like most chemotherapeutic agents generates low levels amounts of ROS. This data is consistent with Ramesh *et al., (*2015*)* who reports carmustine's ability to induce oxidative cytotoxicity and its attenuation with an antioxidant transcription factor (nuclear factor erythroid-derived 2 like 2 - Nrf).

To conclude, this study investigated the possibility that the long-lived H_2O_2 or other ROS may be the cause of the observed DNA damage in the bystander cells. Data is inconclusive at the moment as some assays are supportive of ROS involvement but not consistent with any particular agent, while others are supportive of oxidative damage. However, due to limited supportive evidence for these agents on ROS production or involvement as a CIBE mode of action, both within the current study as well as in published literatures, further investigation is required such as the use of a more direct O_2^- or H_2O_2 assay. Also, whilst increases were apparent, much of these data were not statistically significant, and so ROS may play a role, but probably does not represent the whole story.

5.4.2 Oxidative DNA damage investigation by modified comet assay

The comet assay has been applied in different *in vitro* testing due to its sensitivity, specificity, rapid assessment and economic value. This further modification by incorporation of a DNA endonuclease enzyme such as hOGG1 and Fpg permits the measurement of oxidative damage through a quantitative evaluation of 8-oxoguanine levels (Azqueta and Collins, 2014). This evaluation measures increased strand breaks, data which is representative of the 8-OHdG lesions which the enzyme recognise. Investigation of oxidative damage in this study followed the low detection of DNA fragmentation for the earlier conventional alkaline comet screening (chapter 4) of twenty-two chemotherapeutic agents.

Four key drugs (carmustine, chlorambucil, etoposide and mitoxantrone) were utilised in this part of the study. Following 24 hours co-culture of TK6, AHH-1 and Kasumi-1, these cells were assessed using the modified comet assay. The data revealed all cell lines with a non-significant increased level of oxidative DNA damage than the non-enzyme treated. There were distinct outcomes for the different cell lines however. Most of the agents were more sensitive to Fpg, however increased sensitivity to hOGG1 was seen for carmustine in AHH-1 and Kasumi-1, chlorambucil in AHH-1 and mitoxantrone in AHH-1 and Kasumi-1. The outcome of this study with more sensitivity to Fpg may possibly be damage due to alkylated bases as suggested by Moller *et al.,* (2018). Smith *et al.,* (2006) suggested that both hOGG1 and Fpg recognizes oxidised purines, but hOGG1 specifically recognizes oxidative DNA damage, thus based on the data produced for the current study, it suggests that only mitoxantrone and carmustine show any likely evidence of oxidative damage. The observed cell line differences could suggest that some of these bystander cells may be good at neutralising ROS effect. Additionally, Tse *et al.,* (2017) reports evidence of oxidative DNA formation following fotemustine (carmustine analogue) exposure in melanoma cells and there is other evidence of some other chemotherapeutic agents to induce oxidative stress (Yokoyam *et al.,* 2017).

5.4.3 8-OHdG as an oxidative biomarker

There is increasing evidence of oxidative stress induced damage on cellular targets such as DNA, protein and lipids due to excess ROS (Kehrer, 1993; Valavanidis, Vlachogianni and Fiotakis, 2009). Several markers for oxidative stress such as 4-hydroxy-trans-hexenale (HHE),

aldehydes C_6-C_{12}, malondialdehyde (MDA), as well as nucleic acid oxidation markers (8-OHdG, 5-hydroxymethyl uracil (5-OHMeU), 8-oxo-7,8-dihydro-2-deoxyguanosine (8-oxodG)) and protein markers (o-tyrosine (o-Tyr), 3-nitrotyrosine (3-NOTyr)) have been evaluated widely in different research (Peclova *et al*., 2016). But for lack of automation and complexity of methods, a lot of these various parameters are not applicable for routine laboratory investigations.

ROS mostly interacts with cellular biomolecules producing peroxidised derivatives such as 8-OHdG, advanced oxidation protein products (AOPP) and advanced glycation end products (AGE), hence serum reactive oxygen metabolite by-products have been adopted as biomarkers for oxidative stress measurement (Pilger and Rudiger, 2006). However, 8-OHdG indicates endogenous oxidative DNA damage and its DNA base modification occurs following the attack of guanine by hydroxyl radicals and such modification can lead to mutagenicity and increased proliferation of cancer cells (Fenga *et al.*, 2017). More so, in nuclear and mitochondrial DNA, 8-OHdG is one of the major forms of oxidative damage induced base lesions and has been shown to be a good biomarker for estimating oxidative DNA damage following exposure to toxic chemicals as well as a risk factor indicator for other diseases including cancer (Valavanidis *et al*., 2009).

To evaluate the impact of oxidative stress in bystander cells, one of the predominant forms of nucleic acid oxidation products, 8-OHdG, was utilised as a biomarker in this study. 8-OHdG is considered an effective, versatile and widely used parameter for oxidative DNA damage measurement. As such, the biological significance for the alterations in 8-OHdG levels in cells is extensively explored in varying pathologies such as gastrointestinal disease (Ock *et al.*, 2012). The levels of oxidative stress biomarkers are usually low and therefore require a robust and sensitive method of detection for accuracy and reproducibility (Korkmaz *et al.*, 2018).

Methodologies for the detection of 8-OHdG include immunological methods such as enzyme linked immunosorbent assay (ELISA) and immunofluorescence (IF), and analytical assays e.g. high performance liquid chromatography (HPLC), tandem liquid chromatography mass spectrometry (LCMS/MS) and flow cytometry (Marrocco *et al.*, 2017 and Korkmaz *et al.*, 2018). In this study however, the 8-OHdG antibody was optimised for quantitative evaluation by flow cytometry and qualitative assessment using immunofluorescence. These methods are

reliable, fast and enabled an overall indication of the cell population as well as offering a single cell-based detection of oxidative damage.

In this study, use of the 8-OHdG antibody for the investigation of oxidative stress in the bystander cells reveal an increased MFI in TK6 and Kasumi-1 for both carmustine and etoposide. AHH-1 did not show a marked difference between control and bystander cells, but it had a statistically significant increase for all agents (carmustine, chlorambucil, etoposide and mitoxantrone) relative to the FITC stained untreated control. Only etoposide and mitoxantrone in TK6 show increased positivity when compared to the control. These findings suggest evidence of oxidative DNA damage for carmustine and etoposide potentially for TK6 and Kasumi-1. This study aligns with the low levels oxidative levels observed with etoposide in sperm cells, as well as when in combination with bleomycin and cisplatin (Baetas *et al.*, 2019), however, this was performed as a direct exposure not bystander.

Taken together, based on the high sensitive detection of flow cytometry, this quantitative assessment is highly reliable. Therefore, the altered MFI levels of 8-OHdG in TK6 and Kasumi-1, and the significant increase of AHH-1 cell line are indicative of oxidative stress in these bystander cells. Also the outcome of this assay was neither consistent between drugs nor cell line as evidenced (section 5.3.3).

5.4.4 Mitochondrial stress evaluation

Mitochondria are well established as the major intracellular source of ROS (especially complexes I and III) and as such are also the principal target of ROS; hence any mediated increase may lead to perturbations of the mitochondrial dynamics, various pathologies or mitochondrial dysfunction such as decreased respiration, reduced oxidative phosphorylation, and loss of mitochondrial membrane potential (Jezek *et al.*, 2018). Nemoto *et al.*, (2000) suggests that ROS production can lead to changes in mitochondria such as compromised electron transport chain with an associated increase in electron leakage that contemporaneously react with oxygen to produce superoxide.

To investigate the functionality of mitochondria in a ROS challenged environment potentially resulting from chemotherapy, we utilised the HS-5 cell and exposed it to different chemotherapeutic agents (carmustine, chlorambucil, etoposide, mitoxantrone, daunorubicin

and doxorubicin) at clinically relevant doses. The Agilent Seahorse extracellular flux (XF) mito stress test was has been reported as an efficient assay for measurement of mitochondria activity especially based on its assay detection cellular changes in real time (Nicholas *et al.*, 2017). XF analysis makes use of minimal cell seeding density to inform on a variety of mitochondrial parameters (basal respiration, proton leak, ATP production, spare respiratory capacity, non-mitochondrial respiration and maximal respiration). It also significantly excludes human or analytical software errors as it incorporates its own analytical software and background control wells, thereby allowing objective assessment and biological variability reduction.

To substantiate the hypothesis of this study, the accrued data reveal some level of disturbance within the mitochondria for some agents (daunorubicin, chlorambucil and etoposide) but not others (carmustine, doxorubicin and mitoxantrone). This disturbance is evident in the overall mitochondrial respiration (measured via OCR) as well as the glycolytic activity of the cell as measured via ECAR (Zhang and Zhang, 2019). A close look at the data shows that the basal respiration following exposure to all agents reduced except for carmustine and doxorubicin. There was a reduction in oxygen consumption of these same agents but unfortunately, this does not correlate completely with increased proton leak except for chlorambucil, doxorubicin and mitoxantrone. Also, there was a decline in ATP production for all agents except carmustine and doxorubicin as compared relative to the control. We observed another reduction in the capacity to cope with the stress condition as shown by the spare respiratory capacity for chlorambucil, etoposide, and daunorubicin.

Taken together, since proton leak depicts injury to the mitochondria and is responsible for the release of superoxide that reacts with oxygen, leading to formation of other radical or non-radicals, one can suggest a consistent relation of the activity of chlorambucil to increase ROS involvement as depicted by the assessed parameters. This is quite intriguing, chlorambucil showed an increase in oxidative damage in the comet assay, as well as in the 8OHdG assessment, although this was not generally statistically significant increases. One striking outcome of this study is that of daunorubicin and etoposide, which had a significant reduction in oxygen consumption but did not correlate with any electron leakage. Whilst their spare reserve capacity and ATP production were affected, these agents are potentially suggestive of creating a disruption with the mitochondrial respiration. For lack of any related study in this field, etoposide's outcome warrants further study. However, for a complete lack of the ATP

production in daunorubicin especially in the presence of its similar drug analogue doxorubicin which gave a positive production, together with evidence of only daunorubicin measurement without cells (data not shown) that showed a significant increase in OCR, whereas other agents were not metabolising for lack of cells. This effect may potentially be due to cell death, as the Seahorse assay measures live cells in real time (Figure 5.13), or that daunorubicin alters the measured parameters in Seahorse assay. This is probably due to a dosage effect and so demands further investigation for a fuller conclusion. Unfortunately, the capacity of this study could not accommodate this further investigation at this time.

Conversely, anthracyclines (such as doxorubicin and daunorubicin) are among the highest generators of ROS (Gammella *et al*, 2014) and so it is surprising that doxorubicin does not show increased ROS activity in this study. Doxorubicin disrupts ETC only upon reduction of quinone to semi-quinone, but this agent has been reported with inability to penetrate the inner membrane of mitochondria for certain cells (Conklin, 2004).

Furthermore, the outcome of these agents with mitochondrial dysfunction is an indicator to deciphering their induction of CIBE. This is because the mitochondrial DNA is very susceptible to ROS damage as they have a less efficient repair capacity (Pelicano *et al.*, 2009). Hence, if this damage, as seen with the OCR reduction, persists after the rapid activity of free radicals, it could translate to the bystander cells. To elucidate this further, it may be worth doing a mutation assessment of the mitochondria. This is because mutational events to the mitochondria would alter the functionality of the electron transport and thus oxidative phosphorylation. An alteration of this process would exacerbate ROS which would lead to further mutations and possibly end in a vicious cycle of mutation and ROS production.

Interestingly, there was no evidence of a proton leak from the acute measurement, indicating a non-likely involvement of ROS or that chemotherapeutic agents had not penetrated. With the exception of daunorubicin with a reduced basal respiration, ATP production and spare respiratory capacity, all other agents were relatively similar to the untreated control. The same observation was reflected with the OCR and ECAR measurements that show all agents excluding chlorambucil and daunorubicin as similar to the control, thereby indicating good mitochondrial function for most, but not all agents.

Overall, the standard Seahorse XF mito stress test suggests a role for mitochondrial dysfunction which may account for a bystander phenomenon induced by chemotherapy, as cells were exposed to chemotherapeutic agents for an hour prior to parameter measurement. However, the acute measurement injected these drugs after basal respiration measurement, and no changes in mitochondrial function suggests that more time is required between drug exposure and measurement of mitochondrial capacity. The variable outcome of acute measurement compared with the standard assay may partly be due to the inability of these agents to have penetrated sufficiently before the solvents addition, as thirty minutes elapsed between drug injection and first solvent (oligomycin) addition. This assertion is only made based on the fact that in the normal seahorse which show evidence of damage for some agents, drugs were on the cells for 1h and prior to oligomycin injection and other 30 minutes. However, this is a very interesting outcome of this study because the normal measurement reflects the activity occurring after drug exposure and therefore supports the possible ROS involvement for some of these agents and represents the scenario of treatment for bystander model. This is further supported by apparent maximal induction of MN 3 days after exposure (section 4.15). However, this would require evidence that ROS can be produced this long after drug exposure, or may result from more permanent dysfunction to mitochondrial activity. Alternatively, this outcome may be due to instability of these chemotherapeutic agents at 37^0C and therefore the imprecise activity of the agents. This is due to the discovery of drug instability at room temperature and since assay is performed at 37^0C, drug stability may likely have impact on the assay. The data presented here are the first attempts to use Seahorse analysis to explain CIBE and without supporting literature for this assay with these agents, this study raises interesting questions which require fuller evaluation.

5.4.5 Evaluation of the antioxidant defence system

As a way of coping with an elevated ROS production in biological systems, our bodies employ a complex antioxidant defence to scavenge any intra and extracellular formed ROS. Since different biological processes or pathogenic activities result in oxidative stress, cells deploy SOD, CAT and TRX and other enzymes to maintain cellular homeostasis (Balaban *et al.*, 2005). Oxidative stress induces the release of TRX, with reduced TRX scavenging H_2O_2, regulating different signal transduction pathways and acting as a good marker for oxidative

stress; SOD1 scavenges superoxides (O_2-) and catalase scavenges H_2O_2 (Ighodaro and Akinloy, 2018).

Western blot as a method of choice is generally a very sensitive technique detecting pictogram levels, and can produce a semi-quantitative assessment of the determined protein of interest (Ghosh, Gilda and Gomes, 2014). The western antibody cocktail of SOD1, CAT and TRX used in this study investigated the relative abundances in bystander cell lines (TK6, AHH-1 and Kasumi-1) indirectly exposed to chemotherapeutic agents at clinically relevant doses, and in the directly exposed HS-5 cell line.

CAT activity was the same or reduced relative to the control for TK6 and AHH-1, whereas Kasumi-1 showed decreased levels of CAT, with carmustine, etoposide and mitoxantrone in comparison to the control. Although there seems to be some cell specific disparity, this observation in Kasumi-1 potentially points towards a likely involvement of H_2O_2 and may partly be responsible for the observed damage in CIBE. Conversely, if the situation of low antioxidant levels does not imply exacerbation of ROS, then it goes to say that H_2O_2 is not the key player involved. This assertion will necessitate further assays specific for H_2O_2 to confirm it as true or false. SOD1 in Kasumi-1, on the other hand shows a slight increase for carmustine, etoposide and mitoxantrone but decreased levels with chlorambucil (section 5.3.5); it was unchanged in AHH-1 and revealed opposite events of TK6 in Kasumi-1. Based on this altered expression of SOD1 relative to the untreated control, one can suggest a clear O_2^- involvement with chlorambucil in Kasumi-1. TRX levels were generally was the same as for the control with all cell lines, except for the observed decrease for mitoxantrone in AHH-1, and decrease in carmustine, etoposide and mitoxantrone for Kasumi-1. HS-5 cells remained unchanged for all three antioxidants.

TRX, which exists in micromolar amounts in most cells (Chadwick and Goode, 2008), is surprisingly the most abundant of all tested antioxidants in both bystander cells and HS-5, followed by SOD and then CAT being the least highly expressed. During oxidative stress, it is expected that antioxidants would show increased levels in an attempt to combat the increased ROS activity. However, in extreme cases when ROS amounts overwhelms antioxidant defence, there exists decreased levels of these antioxidants (Tarlovsky, 2013). With the above data in mind, the observed low expressions of these enzymes typical in carmustine, etoposide and

mitoxantrone are either suggestive of no ROS involvement or an indication of a contained ROS effect; this is subject to further evaluations.

Whilst observations of antioxidant levels increasing or being overwhelmed are true for directly exposed cells, there is a lack of data for bystander cell responses. One might expect that if enough ROS were leaving the exposed HS-5, then bystander cells would similarly induce antioxidant expression in response. However as previously noted, ROS species likely to induce a bystander effect would need to be long-lasting and stable, able to leave the HS-5, travel through the medium and be taken up by the bystander cells. Thus, it is unlikely that ROS would be at concentrations high enough to overwhelm the cells and produce reductions in the antioxidants. Nevertheless, stable free radicals can produce high amounts of H_2O_2 and in the absence of contradictory evidence, it is possible that H_2O_2 levels might become high in bystander cells. The data from the increased presence of oxidative damage (comet) and 8OHdG (IF) would support this idea, however generally measurement of oxidative DNA damage was not significantly raised in bystander cells, nor did the DCFDA assay support large increases in ROS. Limitations in these assays, may not specifically measure the ROS of interest, and in the presence of changes in antioxidants, coupled with small increases in oxidative DNA damage, this study suggests that further research is warranted. Certainly, there is an obvious cell line disparity, which further supports a central role for the bystander cell itself.

The Kasumi-1 cell line evidenced measurable levels of all three proteins and expressed CAT at levels higher than the TK6, while CAT was virtually non-existent in the other two cell lines. TRX is highly expressed in TK6 and AHH-1 than the other two and SOD is generally highest in TK6 and Kasumi. This shows there is a lot of difference between the bystander cells. HS-5 cell line is very low for all three of these, and yet tends to be relatively 'resistant' to toxicity as observed in bystander experiment. This potentially suggests different mechanisms of detoxification and our research team believe that HS-5 expresses CYP450 owing to recent evidence (Alonso *et al*., 2015) that MSCs expresses CYP450, thus may help aid the way they metabolize or affected by these agents.

More so, the outcome of HS-5 was expected as this cell line has been reported with a significant level of GSH (the most abundant antioxidant in cells), and may therefore be responsible for the detoxification effect of these ROS. A question then posed, is that if HS-5 have the capacity to detoxify ROS through GSH, then why should the bystander cells show any increase in

oxidative DNA damage? It is possible that alternative active signalling molecules are released from the HS-5, which are unable to be detected using the techniques described here, but produce a unique oxidative stress response in the bystander cell itself, which might explain the disparity between each of the three bystander cell lines in the data presented here. Thus, the mechanism of action of CIBE might not specifically be ROS leaving HS-5 and travelling towards the bystander cells, but redox stress instead might be a 'side-effect' of another mechanism, which then has the capacity to induce oxidative DNA damage in the bystander cells, and possible mutagenic/leukaemogenic events, in the absence of significant cell death.

5.5 Conclusion

This study employed several methods of detection to evaluate a potential ROS involvement in bystander effect. The modified comet assay strongly suggested mitoxantrone as a ROS bystander enhancer. Carmustine was suggested by both the DCFDA and 8-OHdG assays as a major ROS inducer. The western blot antioxidant cocktail found no particular agent a high ROS generators in bystander cells. Whilst daunorubicin activity remains unexplained in the seahorse assay, chlorambucil was consistent in inducing ROS by both evaluation methods.

Summarily, evidence accrued from the use of various assay and techniques for all four main agents (carmustine, chlorambucil, etoposide and mitoxantrone), as well as the two antibiotics (daunorubicin and doxorubicin) included in the seahorse assay, point towards a potential ROS involvement in bystander effect. Although, no single chemotherapeutic agent was either consistent across all assays and/or showed cell line specificity, this data remains suggestive of oxidative stress in these cells, but is certainly not an absolute mechanism of CIBE. Oxidative/redox stress may instead be a side effect of a different more important signalling mechanism, but may contribute to the genotoxic outcome and/or signalling processes that promote survival of the bystander cells (Jang and Sharkis, 2007).

Chapter 6

Final discussion

6.1 Summary of findings

Chemotherapy is one of the treatment options for most cancer cases including leukaemia. While there has been many advances achieved through high quality randomized clinical trials, there remains adverse effects of chemotherapy to the treated patients such as therapy related leukaemia (Partridge, 2001). Another effect of chemotherapy is the possibility to remodel the tumour microenvironment (Liu *et al.*, 2017). Traditionally, the goal of cancer chemotherapy is the removal of tumour without damage to adjoining cells (Wang *et al.*, 2018), however, many first-line chemotherapeutic regimens have the capacity to affect both the cancer cells and the tumour microenvironment (Langley and Fidler, 2012). The tumour microenvironment represents the non-cancerous tissues surrounding the tumour such as the fibroblasts, cells of the blood vessels and proteins. Interactions of the cells within the tumour microenvironment can propagate the mutated clone and encourage development of the tumour.

The concept of tumour microenvironment's role in cancer initiation and progression was first demonstrated by Paget (1889). Within his study of post-mortem breast cancer tissues, he observed a non-random distribution of the metastasised cells and thus put forward the theory of 'seed and soil' hypothesis. This theory described the growth of tumour cells (seed) in a favourable microenvironment (soil). The above theory could potentially serve as a model to describe the bystander effect, whereby cells within the microenvironment can potentiate the development of cancer growth in neighbouring cells. This was hypothesised as a mechanism in donor cell leukaemia (DCL – Flynn and Kaufman, 2007); the pathological basis of this study which develops as a complication of stem cell transplant following chemotherapy.

This thesis aimed to develop a bystander model (chapter 3), that would be used to investigate the genotoxic capacity of 22 chemotherapeutic agents (chapter 4), with a focus to determine the impact of the redox microenvironment on a chemotherapy-induced bystander effect (chapter 5). Advances in the understanding of cellular responses and behaviour *in vivo* has been made possible through the advances in cell culture (Duval *et al.*, 2017). In an attempt to represent the BM microenvironment as closely as possible *in vitro,* different cell lines were utilised in this study. These cell lines were the human bone marrow mesenchymal stem cell line HS-5, the lymphoblast cell lines TK6 and AHH-1 and the myeloid cell line Kasumi-1;

choices that were an adequate representation of the interaction between the BM stroma and haematopoietic cells.

This study has demonstrated for the first time the capacity of all the tested chemotherapeutic agents to induce bystander effect. This discovery was made using clinically relevant doses of the chemotherapeutic agents, which were found to exhibit an overall maintenance of good cell viability for all the bystander cell lines. The idea of low bystander cell death coupled with genotoxicity might support the potential propagation of a mutagenic clone, potentially resulting in DCL. This assertion could be supported by the recent reports of an increase in the use of low intensity conditioning regimens coupled with increased reports (83% rise since 2000) of DCL (Suarez-Gonzalez *et al.,* 2018); here lower dosing might preserve the viability of the cells and allow proliferation of mutated clones (Atilla *et al.,* 2017). More so, evidence in the literature supports the ability to detect genotoxicity even at lower doses (Nohmi, 2018; Thomas *et al.,* 2015). It has also been reported that some tumours have the capacity to evade cell cycle and remain dormant in secondary organs (Barkan *et al.,* 2010), with no information about their further role with cells in the microenvironment. However, it has been proposed that the fate of a tumour cell is based on its interactions with cells in the microenvironment. Poo *et al.,* (2015) confirmed that cellular responses to DNA damage is through a series of communication signalling with the microenvironment to promote both cell survival and cell death. They further suggested that the decision between survival and death is linked to the pathways involved in cancer initiation and progression. This would infer that HS-5 cellular response to low toxicity and any chemotherapy damage may be a decision to repair rather than cell death and as such could propagate mutation in bystander cells in co-culture through transfer of bystander signals.

This study clearly demonstrated bystander cell line specificities with the various endpoints assessed. There was no consistent trend in genotoxicity identified for all three cell lines, as some agreed in one assay but varied in another. This outcome illustrates the importance of the transfused donor cells in any stem cell complication such a DCL, as this outcome infers a likely donor cell selectivity for bystander signals. In addition, this is supported by the observation that some cells have the capacity to receive bystander signals more than others, while some do not receive or generate bystander signals (Ryan, 2008). Further to this cell line variability was the observed differences with the chemotherapeutic agents. Again, no two drugs showed a consistent outcome either between the group of agents or within its chemotherapeutic class. The key agents chosen for this study were initially driven on the report (Cowell and Austin, 2012; Davies, 2001) that alkylating agents and topoisomerase inhibitors are highly implicated

in therapy related leukaemia (TRL). On the contrary, this research has demonstrated the tested agents potentiates bystander effect, irrespective of whether it is from either of these two groups. This clearly suggests that the mechanism of these agents in TRL is clearly different from DCL.

In line with the mechanism of DCL being different to TRL, this research evidenced a likely capacity of point mutation induction in some bystander cells by the HPRT mutation assay. It further demonstrated different mechanisms of chromosomal aberration with the four key agents tested, which in contrast to direct studies (Lynch, 2003; Elhajouji *et al.*, 2011) presented a mixed mode of activity for MN induction even in known clastogens. For instance, mitoxantrone would normally be clastogenic, but showed purely as aneugenic in Kasumi-1 bystander cells. It therefore supports the theory of multifactorial mechanisms in DCL. Also, TRL presents with point mutation and so does DCL, however, cytogenetics is considered as the primary outcome. TRL has been reported to present with deletions or loss of chromosomes 5 and 7 (Pedersen-Bjergaard *et al.*, 2000), while DCL reported cases has shown increased abnormality with chromosome 7 but an involvement of other complex karyotypes (Suarez-Gonzalez *et al.*, 2018). These findings does support this study whereby we observed more MN (anuegenicity) than point mutation.

Furthermore, DCL has been reported to occur as acute myeloid leukaemia, and appear to be exclusively AML in children, but can present as other leukaemia in adults, irrespective of the source or type of donor cells (Suarez-Gonzalez *et al*., 2018). This study showed a no drug, no cell line preference. In line with the knowledge that earlier reviewed DCL cases are majorly AML in nature but not every recipient stem cell transplant gets a DCL, it goes to say that at present every condition is unique regardless of donor origin, just as illustrated by the cell lines in this study. Currently, there is no evidence in the literature to support or refute alkylating agents or topoisomerase inhibitors as a major player, and since it wasn't evident in this study, this research area deserves further attention.

The outcome of this research has provided insight into stem cell transplantation, through the finding that the capacity to induce genotoxicity persists in bystander cells a few days after chemotherapy (section 4.3.4.3), thus warranting a discussion about a 'safe' period to transplant the donor cells after conditioning. This study observed that while the HS-5 remained viable and recovered completely by 3 days post-exposure, signals were still transferred to bystander cells to peak at around three days for carmustine, chlorambucil and etoposide but peak at day 4 for mitoxantrone, yet the inducing factor for such signal remains unknown. Although, these signals were not apparent in the comet assay (section 4.3.2.1); using the MN assay, this transfer

of soluble factors to bystander cells was however evident in the conditioned medium studies (section 4.3.4.4). Arguably, one can infer the no detection in comet as a possibility that DNA fragmentation occurred much earlier than the 24 hr time point measured and so much damage was repaired prior to sampling. However, this study evidenced an increased percent DNA tail intensity in the oxidative damage using enzyme modified comet assay (section 5.3), which clearly was not repaired within the 24hr time point, although this was only significant for mitoxantrone. Therefore, the outcome of high MN induction at day 3 infers a real signal from the microenvironment.

Clearly, using cells in co-culture in this study has demonstrated variable outcomes, with all the agents. However, standard genotoxicity testing currently involves measurements of the direct exposure of acute doses of these toxic agents *in vitro* (OECD, 2012). It therefore raises a question about the current approaches to genotoxicity testing. This is even more relevant in with the concept that intracellular communications plays a vital role to cancer initiation and outcome, is further complicated by the idea that genotoxicity may not only occur through direct exposure, but also through indirect signalling which may take several days to be detected. These ideas warrant a modification of the recommended monocultures utilised in genotoxicity testing; reconsidering the timeframes, dosing and multicellularity of the cultures to address these complications, such that a more relevant assessment of human risk can be determined. Such modification may involve the use of 3D multicellular models which better reflect *in vivo* studies than the current *in vitro* studies (Duvall *et al.,* 2017). Despite some evidence about misleading false positive data with genotoxicity assay (Kirkland *et al.,* 2007; Alder *et al.,* 2011), this study has been performed in line with current practice and as such the outcomes presented are relevant. Also, the current co-culture system utilises human cell lines, whereas *in vivo* pilot studies are performed in animals, and have been shown to produce different outcomes. Hayes *et al.,* (2013) demonstrated that glucocorticoids was negative in *in vitro* tests, but weakly positive *in vivo* in rodents. This shows that the *in vitro* testing is not always a good measure of what might happen *in vivo*. However, this interesting outcome of the study by Hayes *et al.,* demonstrates that a cause for concern with rodent assays; as glucocorticoids are widely used in humans and has not been known to create risk of genotoxicity in humans and therefore better development of a model more replicable of *in vivo* is paramount.

A major outcome of this study, evidenced through the LCMS study, was the observation that chemotherapeutic agents are unstable at room temperature and above, stable at 2-8 ^{0}C or less (chapter 3). This outcome does infer that if the drugs are unstable *in vitro,* then they may also

be unstable *in vivo* except if bound to a protein. This raises the question about the mechanisms involved in inducing bystander effect by these agents. Since different drugs induced an effect in at least one of the assays over and above the untreated control, it justifies the capacity of the HS-5 cells to uptake the drugs. However, judging by the very quick drug degradation during the LC-MS study (section 3.5.4) versus the timing of bystander signals, one can argue that simple elution of the drug and travel to the bystander cells, is unlikely to be the major mechanism of bystander. Indeed, human mesenchymal stem cells, from which HS-5 are derived, are not known to express the p-glycoprotein/multidrug resistance gene, which ordinarily might serve as a general mechanism to expel the majority of drugs from the cells (Bosco *et al.*, 2015), however currently it is not known if this is also true for HS-5, and can only be inferred.

Although some assays presented here support bystander induction (e.g. micronucleus assay) and others do not (e.g. the alkaline comet assay), one can also argue that the lack of detection of damage does not imply absence of damage. Indeed detection of damage can be governed by the sensitivity of the assay, whether the assay detects a lesion or a mutagenic event, and the concept of genotoxic thresholds, where there is a perception of balance between damage induction and DNA repair (Thomas *et al.*, 2015). Furthermore, the enzyme modified comet assay detected increases in DNA fragmentation over and above what was detected in the alkaline comet assay, demonstrating the presence of lesions that were not formerly detected. Whilst there was an increase of detected lesions in the presence of hOGG1 and Fpg, it was shown to be statistically significantly increased only for mitoxantrone; however, one must consider what is statistically relevant versus what is biologically relevant. What is clear from the data presented here is that the bystander cells were highly viable, and any mutagenic events could notionally be propagated through proliferation. Hence, what might not be statistically relevant at the time point measured, may become biologically relevant through clonal expansion, which aligns with the median time of incidence of DCL post-transplant. Additionally, the data here demonstrated for the first time that induction of bystander effect, even after just an hour's exposure to the drugs, peaks up to three days post exposure, and does not appear to cease until four or five days later, suggesting longer term mechanisms at play. Thus this research sought to investigate a likely mechanism for bystander effect.

While the mechanism of CIBE remains to be elucidated, RIBE has been well described and suggests amongst other things the influence of oxidative stress in bystander effect. Some of the evidenced RIBE endpoints include: increased chromosomal aberrations (Lorimore *et al.*, 1998), micronuclei (Azzam *et al.*, 2002), mutations (Zhou *et al.*, 2000), DNA double strand

breaks (Sedelnikova *et al.*, 2007) and sister chromatid exchanges (Nagasawa and Little, 1992). All these evidences led to two categorized mechanisms for RIBE: soluble factors induction and gap junction mediated cellular effects. Since stem cell transplant largely involves radiation and/or chemotherapy, this research investigated oxidative stress impact in CIBE.

This thesis sought to answer the question, 'does ROS play a role in bystander effect?' Various parameters were analysed such as the use of monoclonal antibodies to 8-OHdG to detect oxidative DNA damage. This outcome revealed the likely capacity of carmustine to induce oxidative stress in bystander which has been recognised elsewhere for carmustine (An *et al.*, 2011). This study optimised and developed a method using an antibody to 8-OHdG for detecting ROS induced DNA damage in the nucleus, but also revealed the presence of mitochondrial ROS induced DNA damage located within the cytoplasm. Contrary to the 8-OHdG visualisation, whilst the DCFDA assay generally showed an increase in ROS in HS-5 treated cells, the DCFDA assay did not evidence any ROS increases in bystander cells with the possible exception of carmustine in AHH-1 alone. The HS-5 cells were further explored for oxidative stress induction using a potent oxidative stress inducer diethylmaleate and the antioxidant N-acetylcysteine. However, no obvious increases or decreases in stress or damage was observed (section 3.3.1). This potentially argues other detoxification mechanisms or a chemo-resistance capacity of the HS-5 cell line, since it was observed that increased drug concentration did not affect the HS-5 cell viability. It is possible that HS-5 cells can metabolise these agents very quickly. At present, nothing is known about the metabolic capacity of the HS-5 cells aside from the recent evidence suggesting expression of CYP450 enzymes in human BM mesenchymal stem cells (Alonso *et al.*, 2015). It is also possible that the HS-5 cells possess an efficient intracellular antioxidant property and as such are resistant to oxidative influence, but may require stronger ROS inducers to exhibit a demonstrable effect.

The Agilent Seahorse XF mito stress test assessed the ability of mitochondrial disturbance via these agents. The mitochondria are well known for the ability to generate ROS. Additionally cytochrome C, an important protein in the mitochondria, responsible for signal generation, has been reported to mediate bystander effect (Yang *et al.*, 2009; He *et al.*, 2012). This study clearly showed a redox disturbance induced by all four agents, but because this outcome was not supported by the other assays (except for the mitoxantrone's oxidative DNA damage induction in the enzyme modified comet assay), none of these agents were considered to be a potent ROS inducer. Similarly, both the use of N-acetylcysteine as well as the western blot assessment of three key antioxidants (superoxide dismutase, catalase and thioredoxin), indicated that none of

them possessed the ability to change or reduce oxidative stress damage as detected by the assays. This does suggest that the ROS detected here do not play a major role in the generation of bystander effects. Arguably, these ROS are highly reactive and possess a very short half-life, however, H_2O_2 has been reported to exude the mitochondrial membrane upon production by superoxides to exert effects in the extracellular space (Lennicke *et al*., 2015). While there is no convincing evidence here that ROS plays a role in CIBE, ROS have been reported to be associated with chemotherapy treatment (Yan *et al.,* 2018; Conklin, 2004), but also to cause long term mutagenesis (Ahles and Saykin, 2007). ROS has also been linked to senescence, ageing and neurological disorders like Alzheimer's (An *et al.,* 2011; Tonnies and Trushina, 2017) and so remains an important concept to consider, especially for the mitoxantrone evidence demonstrated in this study.

In summary, the pathogenesis of DCL has previously been suggested to involve multifactorial processes, with different intrinsic and extrinsic influences (Flynn and Kaufman, 2006). The data presented within this thesis does support the idea that CIBE could be induced by any of the drugs investigated here, and any of these drugs could induce mutagenic events in the bystander cells which may align with the consequence for donated HSC within a DCL setting. Disruption to BM stromal functionality through chemotherapy as previously evidenced is long term (May *et al.,* 2018), and could alter the redox status, inferring that ROS potentially may play a role in CIBE, but is unlikely to be the sole mechanism involved. There are many soluble factors released from these cells as evidenced by other research within our group (data unpublished), all of which require further investigation. It is also possible that each drug may exhibit varying mechanisms relative to another and thus, there is much further work to be performed. The key to elucidating this mechanism is by understanding if either the recipient or the donor are more important in the generation of DCL/bystander, which may point towards parameters that promote risk. Further exploration of DCL cases may also inform on the concept of extended genotoxicity beyond direct exposure. This study has introduced new ideas about the scope of genotoxicity outcomes, and introduced new concepts regarding the influences of multicellularity in the test bed and the role of signalling pathways in both induction of damage and detoxification, which may prove to be highly complicated to investigate. The advent of more complex 3D models may help to address some of these outcomes.

6.2 Limitations of study

This study was limited to the use of only one bone marrow cell line as only HS-5 are available commercially, so further research requires the involvement of other cell lines or primary BM samples to make a comparative assessment of bystander effect. This would be a vital assessment to do because all three bystander cells showed differences, hence it will be interesting to determine any differences for the stromal BM compartment.

Overall, the genotoxicity assays used in this study are efficient and sensitive in detecting the observed damages. However, no technique is without a flaw, it will be highly relevant to utilise an automated or high throughput assay to replace the visual and manual counting of method of micronuclei used in this study and to reduce any subjectivity.

Furthermore, the exploration of ROS in the current study was largely limited to detection of the major DNA lesion 8-OHdG, which could be extended to other oxidative lesions, and specific ROS could also be measured (e.g. using electron parametric resonance).

However, as an initial determination of the scope of CIBE to exist, this study lays the foundation for significant future work and refinement.

6.3 Future considerations

The developed bystander model has served as a basis for the initial outcome of this study, but a better model to mimic the BM environment *in vitro* would be the use of three-dimensional (3D) cell culture. 3D cell culture has the advantage that cell morphology and polarity are maintained, and just like *in vivo* scenario, the cells in 3D cultures receives stimuli directly from the microenvironment. Another important consideration would be the use of primary cultures isolated directly from cancer patients, as these cells possess the correct genetic characteristic features of cancer cells *in vivo* and would represent the full scope of potential bystander signalling following combination chemotherapy protocols *in vivo*. Study of CIBE in patient samples would be highly beneficial in the perception of the risk and possible subsequent modulation of cancer chemotherapy.

This study involved acute dosing only (1hr) and there is a scope to investigate longer exposure and chronic dosing, which will ensure closer alignment to chemotherapy exposure and will be interesting to observe any further chemo-resistance or maintenance of cell viability over time. As mentioned in section 4.4.3, the duration assay can be performed in a different way to involve

varying both the cells of the BM compartment and the lymphoid or myeloid compartment for a comparative analysis that will help elucidate bystander mechanism. In the same vein, an exploration of the promptness of DNA repair in the bystander model could involve measurement of endpoints by sampling at various time points over a 24 hour period and beyond.

Also the study model has evaluated mostly soluble factors, and has only investigated MSC with bystander cells. Because of the need to replicate the BM microenvironment, it may be vital to develop a model that will accommodate in same culture other cells of the BM that may play a role (e.g. macrophages express significant ROS levels) without the use of culture inserts. In this setting, it would be beneficial to promote direct cellular contact, which may increase the detected bystander effect, but efficient methods to unequivocally distinguish exposed from bystander cells would need to be developed; such approaches are currently under development within our research group. This may complicate the *in vitro* model, but it is recommended as use of a cell lines in contact could inform other aspects of CIBE and show its relevance; for example, gap junctions. Other considerations include: an increased sample size to perform/confirm the HPRT assay (section 4.4.5); further exploring dosage effects to align with myeloablative versus non-myeloablative protocols; and possible integration of a mathematical model that may help calculate or predict duration effect as well as off-target genotoxic events.

6.3 Final conclusion

In this thesis, the research has addressed the phenomenon of chemotherapy-induce bystander effect using different genotoxic endpoints. Major impacts of this study are the potential clinical insights related to DCL, and the impact on human risk assessment related to genotoxicity it has provided through the various outcomes. This study has shown evidence in support of chemotherapy-induced bystander effect that is potentially long-lived and an important outcome to consider in stem cell transplant. This study posits that while mutagenicity is low with evidence of limited cytotoxicity following CIBE, any proliferation and clonal expansion of such mutated cells post stem cell transplant (and in the right microenvironment), could influence the presence and outcome of DCL in patients.

Nonetheless, DCL is relatively rare due to the infrequent combination of 'high risk' donor versus 'high risk' recipient cells. Although DCL has been previously reported with an incidence of 0.12 – 0.13%, following improvements in cytogenetic analysis to confirm donor origin of 'relapses', the number of cases that have been reported since the year 2000 accounts for over 80% of all reported cases. This suggests more awareness, better detection/diagnosis and a possible rise in stem cell transplant complications and so the implications of the current study could be highly important.

To summarise, this thesis has evidenced for the first time the phenomenon of chemotherapy-induced bystander effect of 22 chemotherapeutic agents. ROS as a mechanism of CIBE is probably not the clear mode of action but redox balance is definitely altered in CIBE; a factor dependent on the bystander cell and the chemotherapeutic agent. Ultimately, this redox disturbance is likely to cause varying complications based on its dual role in toxicity as well as normal cell signalling and as such a significant factor to be considered.

References

Abeloff, M., Armitage, J., Niederhuber, J., Kastan, M., McKenna, G.W. (2004) Clinical Oncology. 3rd ed. St. Louis, Mo.: Elsevier Churchill Livingstone. pp. 2834.

Aldini, G., Altomare, A., Baron, G., Vistoli, G., Carini, M., Borsani, L. and Sergio, F. (2018) N-Acetylcysteine as an antioxidant and disulphide breaking agent: the reasons why. *Free radical research*. *52* (7), pp.751-762.

Adler, S., Basketter, D., Creton, S., Pelkonen, O., Van Benthem, J., Zuang, V., Andersen, K.E., Angers-Loustau, A., Aptula, A., Bal-Price, A. and Benfenati, E. (2011). Alternative (non-animal) methods for cosmetics testing current status and prospects—2010. *Archives of toxicology*, *85*(5), pp.367-485.

Ahles, T.A. and Saykin, A.J. (2007). Candidate mechanisms for chemotherapy-induced cognitive changes. *Nature Reviews Cancer*, *7*(3), p.192.

Alexandre, J., Hu, Y., Lu, W., Pelicano, H. and Huang, P. (2007) Novel action of Paclitaxel against cancer cells: Bystander effect mediated by reactive oxygen species. *Cancer Research*. 67, pp. 3512-3517.

Alonso, S., Su, M., Jones, J.W., Ganguly, S., Kane, M.A., Jones, R.J. and Ghiaur, G. (2015). Human bone marrow niche chemoprotection mediated by cytochrome P450 enzymes. *Oncotarget*, 6 (17), p.14905

Ames, B. N., Shigenaga, M. K. and Hagen, T. M. (1993) Oxidants, antioxidants, and the degenerative diseases of aging (cancer/mutation/endogenous DNA adducts/oxygen radicals). *Proc. Natl. Acad. Sci. USA.* 90, pp. 7915-7922.

An, M.J., Sook Kim, S.S., Rhie, J.H., Shin, D.M., Seo, S.R., Seo, J.T. (2011) Carmustine induces ERK- and JNK-dependent cell death of neuronally-differentiated PC12 cells via generation of reactive oxygen species. *Toxicology in Vitro*. 25, pp. 1359–1365.

Ando, H., Kobayashi, M., Toda, S., Kikkawa, F., Masahashi, T. and Mizutani, S. (2000) Establishment of a ciliated epithelial cell line from human Fallopian tube. *Hum Reprod.* 15, pp. 1597-1603.

Andreoli, C., Leopardi, P., Rossi, S. and Crebelli, R. (1999) Processing of DNA damage induced by hydrogen peroxide and methyl methanesulfonate in human lymphocytes: analysis by alkaline single cell gel electrophoresis and cytogenetic methods. *Mutagenesis*. 14 (5), pp.497-504.

Anna, M., Yi, A., Lyu, L., Lin, C., Tsai, Y., Lau, J.Y., Wang, J.C. and Liu, F.L. (2007) Roles of DNA topoisomerase II isozymes in chemotherapy and secondary malignancies *Proc Natl Acad Sci U S A.* 104 (26): pp. 11014–11019.

Antin, J.H and Raley, D.Y (2009) Conditioning regimens. Manual of stem cell and bone marrow transplantation. Cambridge university press. pp. 23 – 33.

Antonio, M.D., McLuckie, K.I.E. and Balasubramanian, S. (2014) Reprogramming the Mechanism of Action of Chlorambucil by Coupling to a G-Quadruplex Ligand. *J Am Chem Soc.* 136 (16), pp. 5860–5863.

Apel, K. and Hirt, H. (2004) Reactive oxygen species: metabolism, oxidative stress, and signal transduction. *Annu Rev Plant Biol.* 55, pp. 373–399.

Apostolou, P., Toloudi, M., Kourtidou, E., Mimikakou, G., Vlachou, I., Chatziioannou, M. and Papasotiriou, I. (2014) Use of the comet assay technique for quick and reliable prediction of *in vitro* response to chemotherapeutics in breast and colon cancer. *J Biol Res.* 21 (1), pp. 14.

Araldi, R.P., Melo, T.C, Mendes, T.B., Luiz de Sa´ Ju´ nior, P., Nozima, B.H.N., Tiemi Ito, E., Franco de Carvalho, R., Barreiros de Souza, E. and de Cassia Stocco, R. (2015) Using the comet and micronucleus assays for genotoxicity studies: A review. *Biomedicine & Pharmacotherapy.* 72, pp. 74–82.

Arora, M. (2013) Cell culture media: a review. *Mater Methods.*3, pp. 175.

Asada, N. (2018) Regulation of malignant hematopoiesis by bone marrow microenvironment. *Front. Oncol.* 8, pp. 119.

Aslam M.S., Naveed, S., Ahmad, A., Abbas, Z., Gull, I. and Athar, M.A. (2014) Side effects of chemotherapy in cancer patients and evaluation of patinets opinion about starvation based differential chemotherapy. J*ournal of Cancer Therapy.* 5 (5), pp. 817 – 822.

Asur, R., Balasubramaniam, M., Marples, B., Thomas, R.A. and Tucker, J.D. (2010) Bystander effects induced by chemicals and ionizing radiation: evaluation of changes in gene expression of downstream MAPK targets. *Mutagenesis.* 25 (3), pp 271–279.

Asur, R.S., Thomas, R.A. and Tucker, J.D. (2009) Chemical induction of the bystander effect in normal human lymphoblastoid cells. *Mutat. Res.* 676, pp. 11–16.

Ataergin, S., Arpaci, F., Cetin, T., Guran, S., Yakicier, C., Beyzadeoglu, M. and Ozet, A. (2006) Donor Cell Leukemia in a Patient Developing 11 Months after an Allogeneic Bone Marrow Transplantation for Chronic Myeloid Leukemia. *American Journal of Hematology*. 81, pp. 370–373.

Attia, S. U., Schriever-Schwemmer, J. K., Badary, O. A. and Hamada, F. M. (2003) AdlerEtoposide and merbarone are clastogenic and aneugenic in the mouse bone marrow micronucleus test complemented by fluorescence in situ hybridization with the mouse minor satellite DNA probe. *Environmental and Molecular Mutagenesis*. 41 (2), pp. 99-103.

Atilla, E., Atilla, P.A. and Demirer, T. (2017). A review of myeloablative vs reduced intensity/non-myeloablative regimens in allogeneic hematopoietic stem cell transplantations. Balkan medical journal, 34 (1), pp.1-9.

Attia, S.M. (2011) Molecular cytogenetic evaluation of the aneugenic effects of teniposide in somatic and germinal cells of male mice. *Mutagenesis.* 27 (1), pp.31-39.

Attia, S.M., Kliesch, U., Schriever-Schwemmer, G., Badary, O.A., Hamada, F.M. and Adler, I.D. (2003) Etoposide and merbarone are clastogenic and aneugenic in the mouse bone marrow

micronucleus test complemented by fluorescence in situ hybridization with the mouse minor satellite DNA probe. *Environmental and Molecular Mutagenesis*. 41 (2), pp.99-103.

Attia, S.M., Schmid, T.E., Badary, O.A., Hamada, F.M. and Adler, I.D. (2002) Molecular cytogenetic analysis in mouse sperm of chemically induced aneuploidy: studies with topoisomerase II inhibitors. *Mutat Res.* 520, pp. 1–13.

Augustyniak, M., Gladysz, M. and Dziewiecka, M. (2016) The comet assay in insects – status, prospects and benefits for science. Mutation *Research/ reviews in Mutation Research*. 767, pp. 67-76

Austin, H., Delzell, E. and Cole, P. (1988) Benzene and leukemia. A review of the literature and a risk assessment. *Am J Epidemiol.* 127 (3), pp. 419–39.

Avendaño, C. and Menéndez, J.C (2015) DNA Alkylating Agents. *Medicinal Chemistry of Anticancer Drugs*. Second Edition, Elseveir Science print.

Azarova A.M., Lyu, Y.L., Lin, C.P., Tsai, Y.C., Lau, J.Y., Wang, J.C. and Liu, L.F. (2011) Roles of DNA topoisomerase II isozymes in chemotherapy and secondary malignancies. *Proc Natl Acad Sci.* 104 (26), pp. 11014-9.

Azimi, I., Petersen, R.M., Thompson, E.W., Roberts-Thomson, S.J. and Monteith, G.R. (2017) Hypoxia-induced reactive oxygen species mediate N-cadherin and SERPINE1 expression, EGFR signalling and motility in MDA-MB-468 breast cancer cells. *Sci Rep.* pp. 15474-15477.

Azqueta, A., Collins, A.R. (2013) The essential comet assay: a comprehensive guide to measuring DNA damage and repair Arch. *Toxicology.* 87 (6), pp. 949-968.

Azqueta, A., Slyskova, J., Langie, S.A.S., Gaivo, O. and Collins, A. (2014) Comet assay to measure DAN repair: approach and applications. *Front Genet.* 5, pp. 288.

Azzam, E.I. and Little, J.B. (2004) The radiation-induced bystander effect: evidence and significance. *Hum Exp Toxicol.* 23, pp. 61-65.

Azzam, E.I., de Toledo S.M. and Little, J.B. (2004) Stress Signaling from Irradiated to Non-Irradiated Cells. *Current Cancer Drug Targets.* 4, pp. 53-64.

Azzam, E.I., de Toledo, S.M. and Little, J.B. (2001) Direct evidence for the participation of gap junction-mediated intercellular communication in the transmission of damage Bystander effects AR Snyder 88 signals from alpha-particle irradiated to nonirradiated cells. *Proc Natl Acad Sci USA.* 98, pp. 473-478.

Azzam, E.I., De Toledo, S.M., Spitz, D.R. and Little, J.B. (2002) Oxidative metabolism modulates signal transduction and micronucleus formation in bystander cells from alpha-particle-irradiated normal human fibroblast cultures. *Cancer Res.* 62, pp. 5436–5442.

Bacigalupo, A., Ballen, K., Rizzo, D., Giralt, S., Lazarus, H., Ho, V., Apperley, J., Slavin, S., Pasquini, M., Sandmaier, B.M., Barrett, J., Blaise, D., Lowski, R. and Horowitz, M. (2009) Defining the Intensity of Conditioning Regimens: working definitions. *Biol Blood Marrow Transplant.* 15 (12), pp. 1628–1633.

Baguley, B.C. and Ferguson, L.R. (1998) Mutagenic properties of topoisomerase-targeted drugs. *Biochim Biophys Acta.* 1400, pp. 213–222.

Baker, M (2016) 1500 scientists lift the lid on reproducibility. *Nature.* 533, (7604), pp. 452 - 454.

Baldus, C.D., Mrózek, K., Marcucci, G. and Bloomfield, C.D. (2007) Clinical outcome of de novo acute myeloid leukaemia patients with normal cytogenetics is affected by molecular genetic alterations: a concise review. *Br. J. Haematol.* 137 (5), pp. 387–400.

Baron, F., Dresse, M.F. and Beguin, Y. (2003) Transmission of chronicmyeloid leukemia through peripheral-blood stem-cell trans-plantation. *Engl J Med.* 349, pp. 913-914.

Baskar, R. (2010) Emerging role of radiation induced bystander effects: Cell communications and carcinogenesis. *Genome Integrity.* 1, pp. 13.

Baskar, R., Balajee, A.S. and Geard, C.R. (2007) Effects of low and high LET radiations on bystander human lung fibroblast cell survival. *Int J Biochem and Cell Biol.* 83, pp 551-559.

Beerman, I., Luis, T. C., Singbrant, S., Celso, C. L. and Méndez-Ferrer, S. (2017) The Evolving View of the Hematopoietic Stem Cell Niche. *Exp Hematol.* 50, pp. 22–26.

Berg, K. D., Brinster, N. K. and Huhn K.M. (2001) Transmission of a T-cell lymphoma by allogeneic bone marrow transplantation. *Engl J Med.* 345, pp.1458-1463.

Berz, D., McCormack, E. M.,Winer, E. S., Colvin, G. A. and Quesenberry, P.J. (2007). Cryopreservation of Hematopoietic Stem Cells. *Hematol*. 82 (6): pp. 463–472.

Bhagat, S.S., Ghone, R.A., Suryakar, A.N. and Hundekar, P.S. (2011). Lipid peroxidation and antioxidant vitamin status in colorectal cancer patients. *Physiol Pharmacol.* 55, pp.72-6.

Bhattacharjee, M.K (2016) Antimetabolites: Antibiotics That Inhibit Nucleotide Synthesis.*Chemistry of Antibiotics and Related Drugs*. pp 95-108.

Bhattacharya, B. and Mukherjee, S. (2015) Cancer Therapy Using Antibiotics. *Journal of Cancer Therapy*. 6, 849-858.

Bhayat, F., Das-Gupta, D., Smith, C., McKeever, T. and Hubbard, R. (2009) The incidence of and mortality from leukaemias in the UK: a general population-based study. *BMC Cancer.* 9, pp. 252.

Binet, J.L., Auquier, A., Dighiero, G., Chastang, C., Piguet, H., Goasguen, J., Vaugier, G., Potron, G., Colona, P., Oberling, F., Thomas, M., Tchernia, G., Jacquillat, C., Boivin, P., Lesty, C., Duault, M.T., Monconduit, M., Belabbes, S. and Gremy, F. (1981) A new prognostic classification of chronic lymphocytic leukemia derived from a multivariate survival analysis. *Cancer*. 148 (1), pp. 198 - 206.

Bishop, R. (2010) Applications of fluorescence in situ hybridization (FISH) in detecting genetic aberrations of medical significance. *Bioscience Horizons.* 3 (1), pp. 85-95.

Bobadilla-Morales, L., Pimentel-Gutiérrez, H.J., Gallegos-Castorena, S., Paniagua-Padilla, J.A., Ortega-de-la-Torre, C., Sánchez-Zubieta, F., Silva-Cruz, R., Corona-Rivera, J.R., Zepeda-Moreno, A., González-Ramella, O. and Corona-Rivera, A. (2015) Pediatric donor cell leukemia after allogeneic hematopoietic stem cell transplantation in AML patient from related donor. *Molecular Cytogenetics.* 8, pp. 5.

Bolt, H. M., Foth, H., Hengstler, J. G. and Degen, G. H. (2004) Carcinogenicity categorization of chemicals-new aspects to be considered in a European perspective. *Toxicol Lett*. 151 (1), pp. 29-41.

Bolt, H.M., Stewart, J.D. and Hengstler, J.G. (2011) A comprehensive review about micronuclei: mechanisms of formation and practical aspects in genotoxicity testing. *Journal of Toxicology*. 85, pp. 861.

Bosco, D.B., Kenworthy R., Zorio, D.A., and Sang, Q.X. (2015) Human mesenchymal stem cells are resistant to Paclitaxel by adopting a non-proliferative fibroblastic state. *PLoS One.* 10 (6), e0128511.

Boulais, P. E. and Frenette, P. S. (2015). Making sense of hematopoietic stem cell niches. *Blood.* 126 (17), pp. 2621–2629.

Braña, M.F., Cacho, M., Gradillas, A., de Pascual-Teresa, B. and Ramos, A. (2001) Intercalators as anticancer drugs. *Curr Pharm Des.* 7 (17), pp. 1745-80.

Branham, M.T., Nadin, S.B., Vargas-Roig, L.M., Ciocca, D.R. (2004) DNA damage induced by paclitaxel and DNA repair capability of peripheral blood lymphocytes as evaluated by the alkaline comet assay. *Mutation Research,* 560 (1), pp. 11-7.

Brenner, D.J. and Hall, E.J. (2007) Computed tomography—an increasing source of radiation exposure. *N Engl J Med*. 357 (22), pp. 2277-2284.

Brüsehafer, K., Manshian, B.B., Doherty, A. T., Zaïr, Z. M., Johnson, G.E., Doak, S.H. and Jenkins, G.J.S. (2016) The clastogenicity of 4NQO is cell-type dependent and linked to cytotoxicity, length of exposure and p53 proficiency. *Mutagenesis*. 31, pp. 171–180.

Buffler, P.A, Kwan, M.L., Reynolds, P. and Urayama, K.Y. (2005) Environmental and genetic risk factors for childhood leukemia: appraising the evidence. *Cancer Invest.* 23 (1), pp. 60-75.

Burlinson, B., Tice, R.R., Speit, G., Agurell, E. and Brendler-Schwaab, S.Y. (2007) Fourth international workgroup on genotoxicity testing: Results of the *in vivo* comet assay workgroup. *Mutation Res./Genet. Toxicol. Environ. Mutagen*. 627, pp. 31-35.

Butler, J.M., Nolan, D.J., Vertes, E.L., Varnum-Finney, B., Kobayashi, H. and Hooper, A.T. (2010) Endothelial cells are essential for the self-renewal and repopulation of Notch-dependent hematopoietic stem cells. *Cell Stem Cell.* 6, pp. 251–64.

Bydlowski, S.P., Levy, D., Ruiz, J.M.L. and Pereira, J. (2013) Hematopoietic Stem Cell Niche: Role in Normal and Malignant Hematopoiesis. *Intech Open Science.* http://dx.doi.org/10.5772/55508.

Calini, V., Urani, C. and Camatini, M. (2002) Comet assay evaluation of DNA single- and double-strand breaks induction and repair in C3H10T1/2 cells. *Cell Biol Toxicol.* 18 (6), pp. 369-79.

Cannan, W. J. and Pederson, D. S. (2016) Mechanisms and Consequences of Double-strand DNA Break Formation in Chromatin. *J Cell Physiol*. 231 (1) pp. 3–14.

Cawkill, D. and Eaglestone, S.S. (2007) Evolution of cell-based reagent provision. *Drug Discov Today*. 12, pp. 820–5.

Chan, L. L., Wilkinson, A. R., Paradis, B. D. and Lai, N. (2012) Rapid Image-based Cytometry for Comparison of Fluorescent Viability Staining Methods. *Fluoresc.* 22 (5), pp. 1301-11.

Chandran, R., Hakki, M. and Spurgeon, S. (2012) *Infections in Leukemia*. In: Sepsis - An ongoing and significant challenge. *Intech.* pp 333-368.

Chang, X., Meyer, M.T., Liu, X., Zhao, Q., Chen, H., Chen, J., Qiu, Z., Yang, L., Cao J. and Shu, W. (2010) Determination of antibiotics in sewage from hospitals, nursery and slaughter

house, wastewater treatment plant and source water in Chongqing region of Three gorge reservoir in China. *Environmental pollution*. 158, pp. 1444-1450.

Chaudhry, M.A. (2006) Bystander effect: biological endpoints and microarray analysis. *Mutat Res.* 597, pp. 98–112.

Chauhan, P.S., Ihsan, R., Singh, L.C., Gupta, D.K., Mittal, V. and Kapur, S. (2013) Mutation of NPM1 and FLT3 Genes in Acute Myeloid Leukemia and Their Association with Clinical and Immunophenotypic Features. *Disease Markers.* 35 (5), pp. 581–588.

Cheung-Ong, K., Giaever, G. and Nislow, C. (2013). DNA-Damaging Agents in Cancer Chemotherapy: Serendipity and Chemical Biology. *Chemistry and Biology.* 20 (5), pp. 648 – 59.

Chiarugi, P., Pani, G., Giannoni, E., Taddei, L., Colavitti, R., Raugei, G., Symons, M., Borrello, S., Galeotti, T. and Ramponi, G. (2003) Reactive oxygen species as essential mediators of cell adhesion: the oxidative inhibition of a FAK tyrosine phosphatase is required for cell adhesion. *Cell Biol.* 161, pp. 933–944.

Chinnadurai, M., Chidambaram, S., Ganesan, V., Baraneedharan, I., Sundaram, L., Paul, S.F.D. and Venkatachalam, P. (2011) Bleomycin, neocarzinostatin and ionising radiation-induced bystander effects in normal diploid human lung fibroblasts, bone marrow mesenchymal stem cells, lung adenocarcinoma cells and peripheral blood lymphocytes. *Int. J. Radiat. Biol*. 87 (7), pp. 673–682.

Chinnadurai, M., Rao, B.S., Deepika R., Paul, S.F.D. and Venkatachalam, P. (2012) Role of Reactive Oxygen Species and Nitric Oxide in Mediating Chemotherapeutic Drug Induced Bystander Response in Human Cancer Cells Exposed In-Vitro. *World J Oncol*. 3 (2), pp 64-72.

Choi, S.W., Yeh, Y.C., Zhang, Y., Sung, H.W. and Xia, Y. (2010) Uniform beads with controllable pore sizes for biomedical applications. *Small.* 6 (14), pp. 1492-1498.

Chondrou, V., Trochoutsou, K., Panayides, A., Efthimiou, M., Stephanou, G. and Demopoulos, N.A., (2018). Combined study on clastogenic, aneugenic and apoptotic properties of doxorubicin in human cells in vitro. *Journal of Biological Research-Thessaloniki*, *25* (1), p. 17.

Cimini, D., Fioravanti,,D., Salmon,,E.D. and Degrassi,F. (2002) Merotelic kinetochore orientation versus chromosome mono-orientation in the origin of lagging chromosomes in human primary cells. *J. Cell Sci.* 115: pp. 507–515.

Clauson, C., Scharer, O.D. and Niedernhofer, L. (2013) Advances in Understanding the Complex Mechanisms of DNA Interstrand Cross-Link Repair. *Cold Spring Harb Perspect Biol*. 5.

Cole, R.J., Edwards, R.G. and Paul, J. (1965) Cytodifferentiation in cell colonies and cell strains derived from cleaving ova and blastocysts of the rabbit. *Exp Cell Res* 37, pp. 501-504.

Collins, A. R., Dobson, V. L., Du ̨sinská, M., Kennedy, G., and Štetina, R. (1997). The comet assay: what can it really tell us? *Mutat. Res.* 375, pp. 183–193.

Collins, A. R., Yamani, N. E. Lorenzo, Y., Shaposhnikov, S., Brunborg, G. and Azqueta, A., (2014) Controlling variation in the comet assay. *Front Genet.* 5, pp. 359.

Collins, A.R., Dusinska, M., Gedik, C.M. and Stetina, R. (1996) Oxidative Damage to DNA: Do We Have a Reliable Biomarker? *Environ Health Perspect*. 104 (3), pp. 465-469.

Collins, A.R., Oscoz, A.A., Brunborg, G., Gaiva˜o, I., Giovannelli, L., Kruszewski, M., Smith, C.C. and Rudolf S ˇ teˇtina (2008) The comet assay: topical issues. *Mutagenesis*. 23 (3), pp. 143–151.

Colmone, M., Amorim, L., Pontier, A., Wang, S., Jablonski, E. and Sipkins, D. A. (2008) Leukemic cells create bone marrow niches that disrupt the behavior of normal hematopoietic progenitor cells. *Science.* 322 (5909): pp. 1861–1865.

Conklin, K. A. (2004) Chemotherapy-associated oxidative stress: impact on chemotherapeutic effectiveness. *Integr Cancer Ther.* 3, pp. 294–300.

Conklin, K.A. (2004) Chemotherapy-Associated Oxidative Stress: Impact on Chemotherapeutic Effectiveness. *Integrative Cancer Therapies.* 3 (4), pp. 294-300.

Cook, G.J. and Pardee, T.S. (2013) Animal models of leukaemia: Any closer to real thing? *Cancer Metastasis rev.* 32 (0), pp. 63-76.

Cooley, L.D., Sears, D.A., Udden, M.M., Harrison, W.R. and Baker, K.R. (2000) Donor Cell Leukemia: Report of a Case Occurring 11 Years after Allogeneic Bone Marrow Transplantation and Review of the Literature. *American Journal of Hematology*. 63, pp. 46–53.

Cowell, I.G., Sondkaa, Z., Smith, K., Lee, K.C., Manvillea, C.M., Sidorczuk-Lesthuruge, M., Rancea, H.A., Padget, K., Jackson, G.H., Adachi, N. and Austin, C.A. (2012) Model for MLL translocations in therapy-related leukemia involving topoisomerase IIβ-mediated DNA strand breaks and gene proximity. *Cell Biology*. 109 (23), pp. 8989-94.

Craig, F.E. and Foon, K.A. (2008) Flow cytometric immunophenotyping for hematologic neoplasms. *Blood.* 111 (8), pp. 3941 – 67.

Crespi, C. L. Langenbachb, R. and Penmana, B.W. (1993) Human cell lines, derived from AHH-1 TK+/- human lymphoblasts, genetically engineered for expression of cytochromes P450. *Toxicology.* 82 (1-3), pp. 89-104.

Crespi, C.L. and Thilly, W.G. (1984) Assay for gene mutation in a human lymphoblast line, AHH-1, competent for xenobiotic metabolism. *Mutat Res.* 128 (2), pp. 221-30.

Crespi, C.L., Langenbach, R., Rudo, K., Chen, Y.T. and Davies, R.L. (1989) Transfection of a human cytochrome P-450 gene into the human lymphoblastoid cell line, AHH-1, and use of the recombinant cell line in gene mutation assays. *Carcinogenesis*, 10 (2), pp. 295–301.

Crespi, C.L., Liber, H.L., Behymer, T.D., Hites, R.A., and Thilly, W.G. (1985) A human cell line sensitive to mutation by particle-borne chemicals. *Mutat. Res.* 157, pp. 71-75.

Cutler, C. and Ballen, K. (2012). Improving outcomes in umblical cord blood transplantation: state of the art. *Blood Rev*. 26, pp. 241-246.

Davies, S.M. (2001). Therapy-Related Leukemia Associated With Alkylating Agents. *Medical and Pediatric Oncology.* 36, pp. 536-540.

Davis, A.S., Veira, A.J. and Mead, M.D. (2014) Leukaemia: an overview for primary care. *Am. Fam. Physician.* 89 (9), pp. 73 - 738.

Deans, A.J. and West, S.C. (2011). DNA interstrand crosslink repair and cancer. *Nature Reviews Cancer*. 11, pp. 467–480.

Decleer, M., Jovanovic, J., Vakula, A., Udovicki, B., Agoua, R. E. K., Madder, A., Saeger, S. and Rajkovic, A. (2018) Oxygen Consumption Rate Analysis of Mitochondrial Dysfunction Caused by *Bacillus cereus* Cereulide in Caco-2 and HepG2 Cells. *Toxins*. 10 (7), pp. 266.

Deem, T.L. and Cook-Mills, J. M. (2004) Vascular cell adhesion molecule 1 (VCAM-1) activation of endothelial cell matrix metalloproteinases: role of reactive oxygen species. *Blood.* 104, pp. 2385–2393.

Demidem, A., Morvan, D. and Madelmont, J. C. (2006) Bystander effects are induced by CENU treatment and associated with altered protein secretory activity of treated tumor cells: a relay for chemotherapy? *Int. J. Cancer*. 119, pp. 992–1004.

Dertinger, S.D., Phonethepswath, S., Weller, P., Nicolette, J., Murray, J., Sonders, P., Vohr, H.W., Shi, J., Krsmanovic, L., Gleason, C. and Custer, L., (2011) International Pig-a gene mutation assay trial: Evaluation of transferability across 14 laboratories. *Environmental and Molecular Mutagenesis*. 52 (9), pp. 690-698.

Desai, S., Kumar, A., Laskar, S. and Pandey, B.N., (2013) Cytokine profile of conditioned medium from human tumor cell lines after acute and fractionated doses of gamma radiation and its effect on survival of bystander tumor cells. *Cytokine*, 61 (1), pp.54-62.

DeVita,Jr. V.T. and Chu, E. (2008) A History of Cancer Chemotherapy. *Cancer Res.* 68 (21), pp. 8643–8653.

Dhakane, V.D. and Ubale, M.B. (2012), A Validated Stability-Indicating HPLC Related substances method for Carmustine in bulk drug. *Elixir Int. Journal.* 50, pp.10383-10386.

Di, X., Bright, A.T., Bellott, R., Gaskins, E., Robert, J., Holt, S., Gewirtz, D. and Elmore, L.W. (2008) A chemotherapy-associated senescence bystander effect in breast cancer cells. *Cancer Biology and Therapy*. 7 (6), pp. 864-872.

Ding, L. and Morrison, S.J. (2013) Haematopoietic stem cells and early lymphoid progenitors occupy distinct bone marrow niches. *Nature.* 495, pp. 231–235.

Doak, S. H., Jenkins, G. J., Johnson, G. E., Quick, E., Parry, E. M., and Parry, J.M. (2007) Mechanistic influences for mutation induction curves after exposure to DNA-reactive carcinogens. *Cancer Res.* 67 (8), pp. 3904–3911.

Dobo, K.L., Fiedler, R.D., Gunther, W.C., Thiffeault, C.J., Cammerer, Z., Coffing, S.L., Shutsky, T. and Schuler, M., (2011) Defining EMS and ENU dose–response relationships using the Pig-a mutation assay in rats. *Mutation Research/Genetic Toxicology and Environmental Mutagenesis*. 725 (1-2), pp.13-21.

Dobrovolsky, V.N., Shaddock, J.G. and Heflich, R.H. (2002) Mutagenicity of gamma-radiation, mitomycin C, and etoposide in the Hprt and Tk genes of Tk(+/-) mice. *Environ Mol Mutagen.* 39 (4), pp. 342-347.

Doherty, A.T. (2011) The In Vitro Micronucleus Assay. *Genetic Toxicology*. pp. 121–141.

Döhner, H., Estey, E.H., Amadori, S., Appelbaum, F.R., Büchner, T., Burnett, A.K., Dombret, H., Fenaux, P., Grimwade, D., Larson, R.A., Lo-Coco, F., Naoe, T., Niederwieser,

D., Ossenkoppele, G.J., Sanz, M.A., Sierra, J., Tallman, M.S., Löwenberg, B., Bloomfield, C.D. (2010) Diagnosis and management of acute myeloid leukemia in adults: recommendations from an international expert panel, on behalf of the European LeukemiaNet. *Blood.* 115, pp. 453–474.

Dolen, Y., Esendagli, G. and Eur. J. (2013) Myeloid leukemia cells with a B7-2+ subpopulation provoke Th-cell responses and become immunosuppressive through the modulation of B7 ligands. *Immunol*. 43 (3), pp. 747–757.

Domen, J., Wagers, A. and Weissman, I.L. (2006) Regenerative Medicine Bone marrow (Hematopoietic) stem cells. *National Institute of Health*. 2, pp. 14-28.

Drexler, H. G. (2011) Establishment and culture of leukemia-lymphoma cell lines. *Methods Mo.l Biol*. 731, pp. 181-200.

Donaldson, C. and Drexler, H.G. (2011) Establishment and culture of leukemia-lymphoma cell lines. *Methods Mol Biol*. 731, pp. 181-200.

Driessens, N., Versteyhe, S., Ghaddhab, C., Burniat, A., De Deken, X., Van Sande, J., Dumont, J.E., Miot, F. and Corvilain, B. (2009) Hydrogen peroxide induces DNA single-and double-strand breaks in thyroid cells and is therefore a potential mutagen for this organ. *Endocrine-related Cancer*. 16 (3), pp.845-856.

Droge, W. (2002) Free radicals in the physiological control of cell function. *Physiol.* 82, pp. 47–95.

Duval, K., Grover, H., Han, L., Mou, Y., Pegoraro, A.F., Fredberg, J. and Chen, Z. (2017) Modeling Physiological Events in 2D vs. 3D Cell Culture. *Physiology.* 32 (4), pp. 266–277.

Eden, T. (2010) Aetiology of childhood leukaemia. *Cancer Treatment Reviews*. 36 (4), pp. 286 – 297.

Ekwall, B., Silano, V., Paganuzzi-stammati, A. and Zucco, F. (1990) Toxicity Tests with Mammalian Cell Cultures. *Short-term Toxicity Tests for Non-genotoxic Effects.* John Wiley & Sons, Inc., New York, pp 75-97.

Elhajouji, A., Lukamowicz, M., Cammerer, Z. and Kirsch-Volders, M. (2011) Potential thresholds for genotoxic effects by micronucleus scoring. *Mutagenesis*. 26 (1), pp.199-204.

Eruslanov, E. and Kusmartsev, S. (2010) Identification of ROS using oxidized DCFDA and flow-cytometry. *Methods In Molecular Biology.* 594, pp. 57 -72.

Estaing, S. G., Lornage, J., Hadj, S., Boulieu, D., Salle, B. and Guerin, J.F. (2001) Comparison of two blastocyst culture systems: co-culture on Vero cells and sequential media. *Fertil Steril.* 76, pp. 1032-1035.

Esquivel-Velázquez, M., Ostoa-Saloma, P., Palacios-Arreola, M.I., Nava-Castro, K.E., Castro, J.I. and Morales-Montor, J. (2015) The role of cytokines in breast cancer development and progression. *Journal of Interferon & Cytokine Research*, *35*(1), pp.1-16.

Engvall, E. and Perlmann, P. (1972) Enzyme-linked immunosorbent assay, ELISA: III. Quantitation of specific antibodies by enzyme-labeled anti-immunoglobulin in antigen-coated tubes. *The Journal of Immunology.* 109 (1), pp.129-135.

Fairbairn, D.W., Olive, P.L. and O'Neill, K.L. (1995) The comet assay: a comprehensive review. *Mutation Research.* 339, pp. 37-59.

Falck, G., Catalan, J. and Norppa, H. (1997) Influence of culture time on the frequency and contents of human lymphocyte micronuclei with and without cytochalasin B. *Mutat. Res.* 392 (1-2) pp. 71-79.

Falck, G.C.M., Catalan, J. and Norppa, H. (2002) Nature of anaphase laggards and micronuclei in female cytokinesis-blocked lymphocytes. *Mutagenesis*. 17 (2), pp. 111–117.

Farhood, B., Goradel, N.H., Mortezaee, K., Khanlarkhani, N., Salehi, E., Nashtaei, M.S., Shabeeb, D., Musa, A.E., Fallah, H. and Najafi, M. (2019) Intercellular communications-redox

interactions in radiation toxicity; potential targets for radiation mitigation. *Journal of cell communication and signaling*. 13 (1), pp.3-16.

Fausel, C. (2007) Targeted chronic myeloid leukemia therapy: seeking a cure. *J Manag Care Pharm.* 13 *(8 Suppl A),* pp. 8–12.

Fellows, M. D. and O'Donovan, M. R. (2007) Cytotoxicity in cultured mammalian cells is a function of the method used to estimate it. *Mutagenesis*. 22, pp. 275–280.

Fellows, M.D., O'Donovan, M.R., Lorge, E. and Kirkland, D. (2008) Comparison of different methods for an accurate assessment of cytotoxicity in the *in vitro* micronucleus test II: Practical aspects with toxic agents. *Mutation Research*. 655 (1-2), pp. 4-21.

Fenech, M. (2000) The in vitro micronucleus technique. *Mutation Research/Fundamental and Molecular Mechanisms of Mutagenesis,* 455 (1-2): pp 81–95.

Fenech, M. (2008) The micronucleus assay determination of chromosomal level DNA damage. *Methods Mol Biol*. 410, pp.185-216.

Fenech, M., Kirsch-Volders, M., Natarajan, A. T., Surralles, J., Crott, J. W., Parry J. (2011) Molecular mechanisms of micronucleus, nucleoplasmic bridge and nuclear bud formation in mammalian and human cells. *Mutagenesis.* 26 (1), pp. 125–132.

Fialkow, P.J., Thomas, E.D., Bryant, J.L. and Neiman, P.E. (1971) Leukemic transformation of engrafted human marrow cells in vivo. *Lancet*. 1, pp. 251-255.

Flynn, C.M. and Kaufman, D.S. (2007). Donor cell leukemia: insight into cancer stem cells and the stem cell niche. *Blood.* 109, pp. 2688-2692.

Fox, E.J. (2004) Mechanism of mitoxantrone. *Neurology.* 63 (12 suppl 6), pp. S15 – 8.

François, M., Hochstenbac, K., Leifert, W. and Felix, M. (2014) Fenech1Automation of the cytokinesis-block micronucleus cytome assay by laser scanning cytometry and its potential application in radiation biodosimetry. *BioTechniques.* 57, pp. 309-312

Freedman, H. J., Parker, N. B., Marinello, A. J., Gurtoo, H. L., and Minowada, J. (1979) Induction, inhibition, and biological properties of aryl hydrocarbon hydroxylase in a stable human B-lymphocyte cell line, RPMI-1788. *Cancer Res.* 39, pp. 4612-4619.

Freedman, H.J., Gurtoo, H.L., Minowada, J., Paigen, B., and Vaught, J.B. (1979) Aryl hydrocarbon hydroxylase in a stable human B-lymphocyte cell line, RPMI-1788, cultured in the absence of mitogen. *Cancer Res.* 39, pp. 4605-4611.

Freshney, R.I. (2006) Basic principles of cell culture. Hoboken: John Wiley and Sons; Nutrional requirements for clonal growth of nontransformed cells. In: Katsuta H. (1978) editor. Nutritional requirements of cultured cells. Baltimore: University Park Press; pp. 423781 - 6803080.

Garrido, S.M., Appelbaum, F.R., Willman, C.L. and Banker, D.E. (2001) Acute myeloid leukemia cells are protected from spontaneous and drug-induced apoptosis by direct contact with a human bone marrow stromal cell line (HS-5). *Experimental hematology.* 29 (4), pp.448-457.

Ghazalla, M., Mutch, E . B., Aburawi, S. and Williams, F. M. (2010) Genotoxic effect induced by hydrogen peroxide in human hepatoma cells using comet assay. *Libyan J Med.* pp. 4637.

Ghosh, R., Gilda, J.E. and Gomes, A.V. (2014) The necessity of and strategies for improving confidence in the accuracy of western blots. *Expert Rev Proteomics.* 11 (5), pp. 549-560.

Giles, K. L. and Songstad, D. D. (1990) Plant Tissue Culture in the Twenty-First Century. *Developments in Crop Science*. 19, pp. 424-434.

Glasser, L., Meloni-Ehrig, A. and Greaves, W. (2009). Synchronous development of acute myeloid leukemia in recipient and donor after allogenic transplantation: report of a case with comments on donor evaluation. *Transfusion.* 49, pp. 555-562.

Gleitz, H., Kramann, R. and Schneider, R. K. (2018). Understanding deregulated cellular and molecular dynamics in the hematopoietic stem cell niche to develop novel therapeutics in bone marrow fibrosis: The hematopoietic stem cell niche in bone marrow fibrosis. *Pathology.* 245

Godard, T., Deslandes, E., Sichel, F., Poul, J.M. and Gauduchon, P. (2002) Detection of topoisomerase inhibitor-induced DNA strand breaks and apoptosis by the alkaline comet assay. *Mutat Res.* 520 (1-2): pp.47-56.

Goers, L., Freemont, P., Karen, M. and Polizzi, J. R. (2014). Co-culture systems and technologies: taking synthetic biology to the next level. *Soc. Interface.* 11, pp. 0065.

Graf, L., Iwata, M. and Torok-Storb, B. (2002) Gene expression profiling of the functionally distinct human bone marrow stromal cell lines HS-5 and HS-27a. *Blood.* 4 (100), pp. 1509-1511.

Greenbaum, A., Hsu, Y.M., Day, R.B., Schuettpelz, L.G., Christopher, M.J. and Borgerding, J.N. (2013) CXCL12 in early mesenchymal progenitors is required for haematopoietic stem-cell maintenance. *Nature.* 495, pp. 227–230.

Grem, J.L. and Keith, B. (2005) Mechanism of action of cancer chemotherapeutic agents: Antimetabolites John Wiley & Sons, Ltd.

Grifalconi, M., Celotti, L. and Mognato, M. (2007) Bystander response in human lymphoblastoid TK6 cells. *Mutat Res.* 625 (1-2), pp. 102-11.

Grigoropoulos, N.F., Petter, N., Van‘t Veer, M., Scott, M.A. and Follows, G.A. (2013) Leukaemia update. Part 1: diagnosis and management. *BMJ.* 346, pp.1660.

Groesser, T., Cooper, B. Rydberg B. (2008) Lack of bystander effects from high-LET radiation for early cytogenetic end points. *Radiat Res.* 170, pp. 794-802.

Guan, D., Qing, W., Ma, C., Zhang, Z., Wei, H. and Wu, G. (2018) Bone marrow stromal-cell line HS-5 affects apoptosis of acute myeloid leukemia cells HL-60 through GLI1 activation.

Güerci, A., Liviac, D., Marcos, R. (2009) Detection of excision repaired DNA damage in the comet assay by using Ara-C and hydroxyurea in three different cell types. *Cell Biol Toxicol,* 25 (1), pp. 73-80.

Guidance Document on Revisions to OECD Genetic Toxicology Test Guidelines (2015) http://www.oecd.org/env/testguidelines.

Guillermo Ruiz-Argüelles, J., Alejandro Ruiz-Argüelles and Javier Garcés-Eisele (2007) Donor cell leukemia: A critical review. *Leukemia & Lymphoma.* 48 (1), pp. 25-38.

Gunasekarana, V., Raj, G. V. and Chand, P. (2015) A comprehensive review on clinical applications of comet assay. *Journal of clinical and diagnostic research*. 9 (3), pp. GE01-GE05.

Gustafsson, B., Moell, J., LeBlanc, K., Barbany, G., So¨ derha¨ ll, S. and Winiarski, J. (2012) Donor cell-derived acute myeloid leukemia after second allogenic cord blood transplantation in a patient with Fanconi anemia. *Pediatr Transplantation*. 16, pp. E241–E245.

Gynn, L. and Gyurkocza, B. and Sandmaier, B.M. (2014) Conditioning regimens for hematopoietic cell transplantation: one size does not fit all. *Blood.* 124 (3), pp. 344-353.

Halliwell, B. (2006) Reactive Species and Antioxidants. Redox Biology Is a Fundamental Theme of Aerobic Life Plant. *Physiol*. 141 (2), pp. 312–322.

Halliwell, B. and Dizdaroglu, M. (1992) The measurement of oxidative damage to DNA by HPLC and GC/MS techniques. *Free Radic Res Commun*. 16, pp. 75-87.

Halliwell, B. and Whiteman, M. (2004) Measuring reactive species and oxidative damage in vivo and in cell culture: how should you do it and what do the results mean? *British Journal of Pharmacology*. 142, pp. 231–255.

Ham, R.G., MeKeehan, W.L., Freshney, R.I. (2005) Culture of animal cells: A manual of basic technique. 5th ed. New York: Wiley.

Hamerschlak, N. (2008) Leukemia: genetics and prognostic factors. *J Pediatr (Rio J).* 84 (4 Suppl), pp. S52-57.

Harada, T., Kashino, G., Suzuki, K., Matsuda, N., Kodama, S. and Watanabe M. (2008) Different involvement of radical species in irradiated and bystander cells. *Radiat Biol.* 84: pp. 809-814.

Hartmann, A. E., Agurell, C., Beevers, S., Brendler-Schwaab, B. and Burlinson P. (2003) Clay A. CollinsA. Smith G. Speit V. Thybaud, R.R. Tice.Recommendations for conducting the *in vivo*alkaline Comet assay. *Mutagenesis*. 18, pp. 45–51,

Hartung, T. Balls, M., Bardouille, C., Blanck, O., Coecke, S., Gstraunthaler, G. and LewisGood. D. (2002) Cell culture practice. ECVAM good cell culture practice task force report 1 *Altern. Lab. Anim*. 30, pp. 407-414

He, L., He, T., Farrar, S., Ji, L., Liu, T. and Ma, X. (2017) Antioxidants maintain cellular redox homeostasis by elimination of reactive oxygen species. *Cell Physiol Biochem*. 44, pp. 532–553.

He, M., Ye, S., Ren, R., Dong, C., Xie, Y., Yuan, D. and Shao, C. (2012) Cytochrome-*c* mediated a bystander response dependent on inducible nitric oxide synthase in irradiated hepatoma cells. *Br J Cancer*. 106 (5), pp. 889–895.

Hawkes, N., (2018) Childhood leukaemia: Novartis immunotherapy drug approved after deal with NHS.

Hayes, J.E., Doherty, A.T., Coulson, M., Foster, J.R., Cotton, P.T. and O'Donovan, M.R. (2013) Micronucleus induction in the bone marrow of rats by pharmacological mechanisms. I: glucocorticoid receptor agonism. *Mutagenesis.* 28 (2), pp. 227–232.

Hégarat, L.L., Huet, S. and Fessard, V. (2012) A co-culture system of human intestinal Caco-2 cells and lymphoblastoid TK6 cells for investigating the genotoxicity of oral compounds. *Mutagenesis*. 27 (6), pp. 631–636.

Hei, T.K. (2006) Cyclooxygenase-2 as a signalling molecule in radiation-induced bystander effect. *Mol Carcinogen*, 45, pp 455-460.

Helma, C. and Uhl, M. (2000) A public domain image-analysis program for the single-cell-gel-electrophoresis (comet) assay. *Mutat. Res.* 466, pp. 9–15.

Hempel, S.L., Buettner, G.R., O'malley, Y.Q., Wessels, D.A. and Flaherty, D.M. (1999) Dihydrofluorescein Diacetate Is Superior For Detecting Intracellular Oxidants: Comparison with 2',7'-Dichlorodihydrofluorescein Diacetate, 5 (and 6)-Carboxy-29, 79-Dichlorodihydrofluorescein Diacetate and Dihydrorhodamine 123. *Free Radical Biology & Medicine*. 27 (1/2), pp. 146–159.

Henzler, T. and Steudle, E. (2000) Transport and metabolic degradation of hydrogen peroxide in chara corallina: model calculations and measurements with the pressure probe suggest transport of H_2O_2 across water channels. *Exp Bot.* 51, pp. 2053–2066.

Hertenstein, B., Hambach, L., Bacigalupo, A., Schmitz, N., McCann, S., Slavin, S., Gratwohl, A., Ferrant, A., Elmaagacli, A., Schwertfeger, R., Locasciulli, A., Zander, A., Bornhäuser, M., Niederwieser, D. and Ruutu, T. (2005) Development Of Leukemia In Donor Cells After Allogeneic Stem Cell Transplantation--A Survey Of The European Group For Blood And Marrow Transplantation (EBMT). *The Hematology Journal*. 90 (7), pp. 969.

Herzog, D.P.A., Dohle, E., Bischoff, I. and Kirkpatrick, J. C. (2014) Cell communication in a Coculture System Consisting of Outgrowth Endothelial Cells and Primary Osteoblasts. *BioMed Research International.* 2014, 320123.

Hintzsche, H. (2017) Fate of micronuclei and micronucleated cells. *Mutat Res.* 771 pp. 85–98.

Hoffbrand, A.V., Moss, P.A.H. and Pettit, J.E. (2011) Essential Haematology. 7th ed. Oxford: Blackwell Publishing.

Hoffman, C.M. and Calvi L.M. (2014) Minireview: complexity of hematopoietic stem cell regulation in the bone marrow microenvironment. *Mol Endocrinol.* 28 (10), pp. 1592-601.

Hoffman, R. (2005) Hematology: Basic Principles and Practice. 4th. ed. St. Louis, Mo.: Elsevier Churchill Livingstone. pp. 1074–75.

Hoffman, R., Benz, E. J., Shattil, S. J., Furie, B., Cohen, H. J., Silberstein, L. E., and McGlave, P. editors. (2000) Hematology Basic Principals and Practice, 3rd ed. Churchill Livingstone, New York.

Hoffmann, S., Spitkovsky, D., Radicella, J.P., Epe, B. P and Wiesner, R. J. (2004) Reactive oxygen species derived from the mitochondrial respiratory chain are not responsible for the basal levels of oxidative base modifications observed in nuclear DNA of mammalian cells. *Free Radical Biology and Medicine.* 36, pp. 765–773.

Honma, M. (2011) Cytotoxicity measurement in in vitro chromosome aberration test and micronucleus test. *Mutation Research/Genetic Toxicology and Environmental Mutagenesis,* 724 (1-2) pp 86–87.

Horan, M.P., Pichaud, N. and Ballard, J.W.O. (2012) review: Quantifying mitochondrial dysfunction in complex diseases of aging. *Journal of Gerontol A Biol Sci Med Sci.* 67 (10), pp. 1022-1035.

Horwitz, M. (1997) The genetics of familial leukemia. *Leukemia*. 11 (8), pp. 1347–59.

Horwitz, M., Goode, E.L. and Jarvik, G.P. (1996) Anticipation in familial leukemia. *Am. J. Hum. Genet.* 59 (5), pp. 990–8.

Hovhannisyan, G.G. (2010) Fluorescence in situ hybridization in combination with the comet assay and micronucleus test in genetic toxicology. *Molecular Cytogenetics*, 3 (1), p.17.

https://www.hea,Mlth.harvard.edu/cancer/leukemia (2014). *Article of Leukaemia.*

Hua Wang, Li., Xiao Yang, Yi., Zhang, X., Huang, J., Hou, J., Jie Li., Xiong, H., Mihalic, K., Zhu, H., Xiao, W., Farrar, W.L. (2004) Transcriptional Inactivation of STAT3 by PPARγ Suppresses IL-6-Responsive Multiple Myeloma Cells. *Immunity*. 20 (2), pp. 205–218.

Huang, X., Traganos, F. and Darzynkiewicz, Z. (2003) DNA damage induced by DNA topoisomerase I- and topoisomerase II-inhibitors detected by histone H2AX phosphorylation in relation to the cell cycle phase and apoptosis. *Cell Cycle.* 2 (6), pp. 614-9.

Huang, Y. and Li, L. (2013) Transl DNA crosslinking damage and cancer - a tale of friend and foe. *Cancer Res.* 2 (3), pp. 144–154.

Ighodaro, O.M. and Akinloy, O.A. (2018) First line defence antioxidants-superoxide dismutase (SOD), catalase (CAT) and glutathione peroxidase (GPX): Their fundamental role in the entire antioxidant defence grid. *Alexandria Journal of Medicine.* 54, pp. 287-293.

In, I., Chio, C. and Tuveson. D. A. (2017) ROS in Cancer: the burning question. *Trends Mol Med*, 23 (5), pp. 411–29.

Ivanov, V.N., Hei, T.K., Zhou, H., Lien, Y.C. and Davidson, M.M., (2008) Mitochondrial Function and Nuclear Factor-KB–Mediated Signaling in Radiation-Induced Bystander Effects.

Iyer, R., Lehnert, B.E and Svensson, R. (2000) Factors underlying the cell growth-related bystander responses to alpha particles. *Cancer Res.* 60 (5), pp. 1290-1298.

Jabbour, E., O'Brien, S., Ravandi, F. and Kantarjian, H. (2015) Monoclonal antibodies in acute lymphoblastic leukemia. *Blood*. 125 (26), pp.4010-4016.

Jairam, V., Park, H.S.M. and Yu, J.B. (2018) Treatment-related complications of chemotherapy and radiation therapy: an analysis of the nationwide emergency department sample. *Radiation Oncology*. 102 (3), pp. e416 – e417.

Jang, Y.Y and Sharkis, S.J. (2007) A low level of reactive oxygen species selects for primitive hematopoietic stem cells that may reside in the low-oxygenic niche. *Blood.* 110, pp. 3056-3063.

Jaruga, P. and Dizdaroglu, M. (1996) Repair of products of oxidative DNA base damage in human cells. *Nucleic Acids Res.* 24, pp. 1389–94.

Jaxel, C., Taudou, G., Portemer, C., Mirambeau, G., Panijel, J. and Duguet, M. (1988) Topoisomerase inhibitors induce irreversible fragmentation of replicated DNA in concanavalin A stimulated splenocytes. *Biochemistry*. 27 (1), pp. 95-99.

Jedrzejczak-Silicka, M. (2017) History of cell culture. *Intech*. 10 pp. 5772-66905.

Jenkins, G. J., Doak, S. H., Johnson, G. E., Quick, E., Waters, E. M., and Parry, J. M. (2005) Do dose response thresholds exist for genotoxic alkylating agents? *Mutagenesis* 20: pp. 389–398.

Jenkins, G. J., Zaïr, Z., Johnson, G. E. and Doak, S. H. (2010) Genotoxic thresholds, DNA repair, and susceptibility in human populations. *Toxicology*. 278, pp. 305–310.

Jenkins-Baker, P. G., Bigelow, A., Marino, S. and Charles R. (2004) Detection of chromosomal instability in -irradiated and bystander human fibroblasts Brian. *Geard Mutation Research.* 568, pp. 41–48.

Jha, A.N. (2008) Ecotoxicological applications and significance of comet assay. *Mutagenesis.* 23 (3), pp. 207-221.

Jiménez, P., Alvarez, C.J., Garrido, P., Lorente, A.J., Palacios, J. and Ruiz-Cabello, F. (2012) Acute Myeloid Leukaemia of Donor Cell Origin Developing 17 Years after Allogenic Hematopoietic Cell Transplantation for Acute Promyelocytic Leukaemia. *Int J Biomed Sci.* 8 (4), pp. 244-248.

Johnson, G.E. (2012). Mammalian cell HPRT gene mutation assay: Test methods. In: Genetic Toxicology: Principles and method. (Parry J. M., Parry E. M., editors), *Springer*. pp. 55–67.

Joseph, B., Paul, C.A., Navneet, M., Miguel-Angel, P., David, M.I., Paul, S., Joseph, P., Helen, L.L., John, W. and Bipin, S.N. (2014) Conditioning Chemotherapy Dose Adjustment in Obese Patients: A Review and Position Statement by the American Society for Blood and Marrow Transplantation Practice Guideline Committee Biology. *Blood and Marrow Transplantation*. 20 (5), pp. 600-616.

Joseph, J.S., malindisa, S.T. and Ntwasa, M. (2018) Two-dimensional (2D) and three-dimensional (3D) cell culturing in drug discovery. *Intec open access Journal.* pp.81552.

Karaszkiewicz, J.W. (2005) Critical factors in immunoassay optimization. *Gaithersburg, MD.*

Karl, K.K., Vincent, E.C. and Gibson, J. N. (2017) Antineoplastic Drugs. *Pharmacology and Therapeutics for Dentistry.* pp. 530-562

Katrina, J., Cooper, F. and Strich, R. (2000) Reactive Oxygen Species and Mitochondrial Dynamics: The Yin and Yang of Mitochondrial Dysfunction and Cancer Progression. *Antioxidants.* 7 (1), pp. 13.

Kattal, N., Cohen, J. and Barmat, L.I. (2008) Role of co-culture in human in vitro fertilization: a meta-analysis. *Fertil Steril*. 90 (4), pp. 1069-1076.

Kaufmann, S. H. and Earnshaw, W.C. (2000) Induction of apoptosis by cancer chemotherapy. *Exp Cell Res.* 256, pp. 42-49.

Kaur, P., Kalia, S. and Bansal, M.P. (2006) Effect of diethyl maleate induced oxidative stress on male reproductive activity in mice: Redox active enzymes and transcription factors expression. *Molecular and Cellular Biochemistry.* 291 (1-2), pp.55-61.

Kayser, S., Dohner, K., Krauter, J., Kohne, C.H., Horst, H.A., Held, G., Lilienfeld-Toal, M.V., Wilhelm, S., Kundgen, A., Gotze, K., Rummel, M., Nachbaur, D., Schlegelberger, B., Gohring, G., Spath, D., Morlok, C., Zucknick, M., Ganser, A., Dohner, H. and Schlenk, R.F. (2011) The impact of therapy-related acute myeloid leukemia (AML) on outcome in 2853 adult patients with newly diagnosed AML. *Blood.* 117 (7), pp 2137-2145.

Kehrer, J.P. (1993) Free radicals as mediators of tissue injury and disease. *Critical Reviews in Toxicology.* 23, pp. 21–48.

Khalade, A., Jaakkola, M.S., Pukkala, E. and Jaakkola, J.J. (2010) Exposure to benzene at work and the risk of leukemia: a systematic review and meta-analysis. *Environ Health*. 9, pp. 31.

Kimura, A., Miyata, A. and Honma, M. (2013) A combination of in vitro comet assay and micronucleus test using human lymphoblastoid TK6 cells. *Mutagenesis. 23,* pp. 583-590.

Kinashi, Y., Masunaga, S., Nagata, K., Suzuki, M., Takahashi, S. and Ono, K. (2007) A Bystander Effect Observed in Boron Neutron Capture Therapy: A Study of the Induction of Mutations in the HPRT Locus. *Int J Radiat Oncol Biol Phys.* 68 (2), pp. 508–514.

Kirkland, D., Reeve, L., Gatehouse, D. and Vanparys, P. (2011) .A core in vitro genotoxicity battery comprising the Ames test plus the in vitro micronucleus test is sufficient to detect rodent carcinogens and in vivo genotoxins. *Mutat Res.* 721 (1), pp. 27-73.

Kirsch-Volders, M. (2011) Origin and fate, biological significance, protocols, high throughput methodologies and toxicological relevance. *Arch Toxicol* 85, pp. 873–899.

Kirsch-Volders, M., Sofuni, T., Aardemac, M., Albertini, S., Eastmond, D., Fenech, M., Ishidate, M., Kirchner, S., Lorge, E., Morita, T., Norppa, H., Surrallés, J., Vanhauwaert, A. and Wakata, A.M. (2003) Report from the *in vitro* micronucleus assay working group. *Mutat. Res.* 540, pp. 153–163.

Kolber, M.A., Broschat, K.O. and Landa-Gonzalez, B. (1990) Cytochalasin B induces cellular DNA fragmentation. *The FASEB journal.* 4 (12), pp.3021-3027.

Koopman, M., Michels, H., Dancy, B.M., Kamble, R., Mouchiroud, L., Auwerx, J., Nollen, E.A.A. and Houtkooper, R.H. (2016) A screening-based platform for the assessment of cellular respiration in Caenorhabditis elegans. *Nat Protoc.* 11 (10), pp. 1798-1816.

Korbling, M. and Freireich, J. (2011) Twenty-five years of peripheral blood stem cell transplantation. *Blood.* 117 (24), pp. 6411-6416.

Krishna, G. and Hayashi, M. (2000) In vivo rodent micronucleus assay: protocol, conduct and data interpretation. *Mutation Research*. 455, pp. 155–166.

Kumaravel, T. S., Vilhar, B., Faux, S. P., Jha, A.N. (2009) Comet Assay measurements: a perspective. *Cell Biol Toxicol.* 25, pp. 53–64.

Kumaravel, T.S. and Jha, A.N. (2006) Reliable Comet Assay measurements for detecting DNA damage induced by ionising radiation and chemicals. *Mutation Research.* 605, pp. 7–16.

Kuznetsova, I.S., Labutina, E.V. and Hunter, N. (2016) radiations risks of leukaemia, lymphoma and multiple myeloma incidence in the mayak cohort: 1948-2004. *PLoS One.* 11 (9), pp. e0162710.

Kwok, K.K., Vincent, E.C. and Gibson, J.N. (2017) Antineoplastic drugs. Pharmacology and Therapeutics for dentistry (7th Edition). pp. 530-562.

Landsberger, M. and Brinkmeier, H. (2018) Immunoblot Analysis of DIGE-Based Proteomics. *Methods Molecular Biology*. 1664, pp. 287-299.

Larizza, L., Magnani, I. and Beghini, A. (2005) The Kasumi-1 cell line: at (8; 21)-kit mutant model for acute myeloid leukemia. *Leukemia & lymphoma.* 46 (2), pp.247-255.

Lazennec, G., Bresson, D., Lucas, A., Chauveau, C. and Vignon, F. (2001) ER beta inhibits proliferation and invasion of breast cancer cells. *Endocrinology.* 142, pp. 4120–4130.

Le Hégarat, L., Huet, S. and Fessard, V. (2012) A co-culture system of human intestinal Caco-2 cells and lymphoblastoid TK6 cells for investigating the genotoxicity of oral compounds. *Mutagenesis*. 27 (6), pp.631-636.

Lehnert B.E. and Goodwin, E.H. (1997). A new mechanism for DNA alterations induced by alpha particles such as those emitted by radon and radon progeny. *Environ Health Perspect.* 105 (5), pp 1095-101.

Lennicke, C., Jette Rahn, J., Lichtenfels, R., Wessjohann, L.A. and Seliger, B. (2015) Hydrogen peroxide – production, fate and role in redox signaling of tumor cells. *Cell Communication and Signaling*. 13, p. 39

Lester, M.A. (2005) Bacterial Topoisomerase Inhibitors: Quinolone and Pyridone Antibacterial Agents. *Chemical Reviews.* 105 (2), pp. 559–92.

Levy, J.A., Buell, D.N., Creech, C., Hirshaut, Y. and Silverberg, H. (1971). Further characterization of the WI-L1 and WI-L2 lymphoblastoid lines. *J. Natl. Cancer Inst.* 46, pp. 647-654.

Levy, J.A., Virolainen, M. and Defendi, V. (1968) Human lymphoblastoid lines from lymph node and spleen. *Cancer.* 22, pp. 517-524.

Liao, W., McNutt, M. and Zhu, W. (2009) The comet assay: A sensitive method for detecting DNA damage in individual cells. *Methods.* 48 (1), pp. 46-53.

Lichtman, M.A. (2010) Obesity and the risk for a hematological malignancy: leukemia, lymphoma, or myeloma. *Oncologist*. 15 (10), pp. 1083-1101.

Liviac, D., Creus, A. and Marcos, R. (2010) Genotoxicity testing of three monohaloacetic acids in TK6 cells using the cytokinesis-block micronucleus assay *Mutagenesis*. pp. 1–5.

Lobo, N.A., Shimono, Y., Qian, D. and Clarke, M.F. (2007) The biology of cancer stem cells. *Annual Review of Cell Developmental Biology.* 23, pp. 675 – 99.

Long, X., Perlaky, L., Man, C. T. and Redell, M. S. (2014) Stromal CYR61 Confers Resistance to Mitoxantrone Via Spleen Tyrosine Kinase Activation in Human Acute Myeloid Leukemia. *Blood.* 124, pp. 2228.

Lorge, E., Hayashi, M., Albertini, S. and Kirkland, D. (2008) Comparison of different methods for an accurate assessment of cytotoxicity in the *in vitro* micronucleus test. Theoretical Aspects. *Mutation Research.* 655, pp. 1-3.

Lorge, E., Moore, M.M., Clements, J., O'Donovan, M., Fellows, M.D., Honma, M., Kohara, A., Galloway, S., Armstrong, M.J., Thybaud, V. and Gollapudi, B. (2016) Standardized cell sources and recommendations for good cell culture practices in genotoxicity testing. *Mutation Research/Genetic Toxicology and Environmental Mutagenesis.* 809, pp.1-15.

Lorimore, S.A., Coats, P.J., Scobie, G.E., Milne, G. and Wright, E.G. (2001) Inflammatory-type responses after exposure to ionizing radiation in vivo: a mechanism for radiationinduced bystander effects? *Oncogene.* 20, pp. 7085-7095.

Lorimore, S.A., Kadhim, M.A., Pocock, D.A., Papworth, D., Stevens, D.L., Goodhead, D.T. and Wright, G. (1998) Chromosomal instability in the descendants of unirradiated surviving cells after alpha-particle irradiation. *Proc. Natl. Acad. Sci.* 95, pp. 5730–5733.

Lund, J. E. (2000) Toxicologic effects on blood and bone marrow, in Schalm's Veterinary Hematology, 5th ed. (B. F. Feldman, J. G. Zinkl, and N. C. Jain, eds.). Lippincott, Williams and Wilkins, Philadelphia, PA. pp. 44—50.

Luo, W., Gurjuar, R., Ozbal, C., Taghizadeh, K., Lafleur, A., Dasari, R., Zarbl, H. and Thilly, W.G. (2003) Quantitative Detection of Benzo[a]pyrene Diolepoxide-DNA Adducts by Cryogenic Laser Induced Fluorescence *Chem. Res. Toxicol.* 16, pp. 74-80.

Lynch, A., Harvey, J., Aylott, M., Nicholas, E., Burman, M., Siddiqui, A., Walker, S. and Rees, R. (2003) Investigations into the concept of a threshold for topoisomerase inhibitor-induced clastogenicity. *Mutagenesis.* 18 (4), pp. 345 – 353.

Lyng, E M., Seymour, C. B. and Mothersill, C. (2002) Early events in the apoptotic cascade initiated in cells treated with medium from the progeny. *Radiation Protection Dosimetry.* 99 (1-4), pp.169-72

MacKenzie, A., Wilson, H.L., Kiss-Toth, E., Dower, S.K., North, R.A. and Surprenant, A., (2001) Rapid secretion of interleukin-1β by microvesicle shedding. *Immunity.* 15 (5), pp. 825-835.

Maele-Fabry, V.G, Gamet-Payrastre, L., Lison, D. (2019) Household exposure to pesticides and risk of leukemia in children and adolescents: Updated systematic review and meta-analysis. *Int J Hyg Environ Health.* 222 (1), pp. 49-67.

Maloney, D.G., Sandmaier, B.M., Mackinnon, S. and Shizuru, J.A. (2002) Non-Myeloablative Transplantation. *American Society of Haematology.* 2002, pp. 392-421.

Maria, D. and Collins A.R. (2008) The comet assay in human biomonitoring: gene-environment interactions. *Mutagenesis.* 23 (3), pp. 191-205.

Marin, A., Margarita, M., Liñán, O., Alvarenga, F., López, M., Fernández, L., Büchser, D. and Cerezo, L. (2015). Bystander effects and radiotherapy. *Rep Pract Oncol Radiother.* 20 (1), pp. 12–21.

Mangerich, A., Debiak, M., Birtel, M., Ponath, V., Balszuweit, F., Lex, K., Martello, R., Burckhardt-Boer, W., Strobelt, R., Siegert, M. and Thiermann, H. (2016) Sulfur and nitrogen mustards induce characteristic poly (ADP-ribosyl) ation responses in HaCaT keratinocytes with distinctive cellular consequences. *Toxicology letters. 244*, pp.56-71.

Marmont, A.M., Horrowitz, M.M., Gale, R.P., Sobocinski, K., Ash, R.C., van Bekkum, V.M., Champlin, R.E., Dicke, K.A., Goldman, J.M. and Good, R.A. (1991) T-cell depletion of HLa-identical transplants in leukaemia. *Blood.* 78 (8), pp. 2120-2130.

Matsumoto, H., Hayashi, S., Hatashita, M., Ohnishi, K., Shioura, H., Ohtsubo, T., Kitai, R., Ohnishi, T. and Kano, E. (2001) Induction of Radio-resistance by a Nitric Oxide-Mediated Bystander Effect. *Radiation Research.* 155 (3), pp. 387-396.

McCann, S. and Wright, E. (2003) Donor leukaemia: perphaps a more common occurrence than we thought. *Bone Marrow Transplant.* 32, pp. 455-457.

May, J.E., McCann, S. and Wright, E. (2003) Donor leukaemia: perphaps a more common occurrence than we thought. *Bone Marrow Transplant.* 32, pp. 455-457.

McEvoy, G.K. (2006) Drug Information. Bethesda, Maryland: American Society of Health-System Pharmacists, *Inc. AHFS Drug Information.* pp. 975-978.

McNamee, J.P., McLean, J.R.N., Ferrarotto, C.L. and Bellier, P.V. (2000) Comet assay: rapid processing of multiple samples. *Mutation Research/Genetic Toxicology and Environmental Mutagenesis*. 466 (1), pp. 63-69.

Meintières, S., Nesslany, F., Pallardy, M. and Marzin, D. (2003) Detection of ghost cells in the standard alkaline comet assay is not a good measure of apoptosis. *Environ Mol Mutagen.* 41 (4), pp. 260-9.

Merle, P., Morvan, D., Caillaud, D. and Demidem, A. (2008) Chemotherapy-induced Bystander Effect in response to Several Chloroethylnitrosoureas: An Origin Independent of DNA Damage? *Anticancer Research.* 28, pp. 21-28.

Miki, Y., Ono, K., Hata, S., Suzuki, T., Kumamoto, H. and Sasano, H. (2012) The advantages of co-culture over mono cell culture in simulating in vivo environment. *J Steroid Biochem Mol Biol.* 131 (3-5), pp. 68-75.

Mikkola, H.K.A. and Orkin, S.H. (2006) The journey of developing hematopoietic stem cells. *Development.* 133, pp. 3733 – 3744.

Metafuni, E., Chiusolo, P., Laurenti, L., Sorà, F., Giammarco, S., Bacigalupo, A., Leone, G. and Sica, S. (2018) Allogeneic hematopoietic stem cell transplantation in therapy-related myeloid neoplasms (t-MN) of the adult: monocentric observational study and review of the literature. *Mediterranean journal of hematology and infectious diseases*. 10 (1).

Metayer, C., Colt, J.S, Buffler, P.A, Reed, H.D, Selvin, S., Crouse, V. and Ward, M.H (2013) Exposure to herbicides in house dust and risk of childhood acute lymphoblastic leukaemia. *Journal of Exposure Science and Environmental Epidemiology.* 23, pp. 363-370.

Miller, B. and Potter-locher, F. (1998) Evaluation of the in vitro micronucleus test as an alternative to the in vitro chromosomal aberration assay: position of the GUM working group on the in vitro micronucleus test. *Mutation Research*. 410, pp. 81–116.

Mitchell, S.A, Randers-Pehrson, G. Brenner, D.J. and Hall, E. J. (2004) The bystander response in C3H 10T1/2 cells: the influence of cell-to-cell contact. *Radiat Res.* 161 (4), pp. 397-401.

Mitchelmore, C.L. and Chipman, J.K. (1998) Detection of DNA strand breaks in brown trout (*Salmo trutta*) hepatocytes and blood cells using the single cell gel electrophoresis (comet) assay. *Aquat. Toxicol.* 41, pp. 161–182.

Mitkevich, V.A., Petrushanko, I.Y., Spirin, P.V., Fedorova, T.V., Kretova, O.V., Tchurikov, N.A., Prassolov, V.S., Ilinskaya, O.N. and Makarov, A.A. (2011) Sensitivity of acute myeloid

leukemia Kasumi-1 cells to binase toxic action depends on the expression of KIT and AML1-ETO oncogenes. *Cell Cycle.* 10 (23), pp. 4090-4097.

Moore, G.E., Gerner, R.E. and Franklin, H.A. (1967) Culture of Normal Human Leukocytes. *JAMA*. 199, pp. 519-524.

Mondal, B.C., Majumdar, S., Dasgupta, U.B., Chaudhuri, U., Chakrabarti, P. and Bhattacharyya, S. (2006) BCR–ABL fusion transcript in typical chronic myeloid leukaemia: a report of two cases. *Journal of clinical pathology*. 59 (10), pp.1102-1103.

Moore, G.E., Gerner, R.E. and Franklin, H.A. (1967) Culture of Normal Human Leukocytes. *JAMA*. 199, pp. 519-524.

Morris, S.M., Manjanatha, M.G., Shelton, S.D., Domon, O.E., McGarrity, L.J. and Casciano, D.A., (1996). A mutation in the p53 tumor suppressor gene of AHH-1 tk+− human lymphoblastoid cells. *Mutation Research/Fundamental and Molecular Mechanisms of Mutagenesis*. 356 (2), pp.129-134.

Morris, S.M., Domon, O.E., Delclos, K.B., Chen, J.J. and Casciano, D.A. (1994). Induction of mutations at the hypoxanthine phosphoribosyl transferase (HPRT) locus in AHH-1 human lymphoblastoid cells. *Mutation Research/Fundamental and Molecular Mechanisms of Mutagenesis.* 310 (1), pp 45-54.

Morrison, V.A., Rai, K.R., Peterson, B.L., Kolitz, J.E., Elias, L., Appelbaum, F.R., Hines, J.D., Shepherd, L., Larson, R.A.and Schiffer, C.A. (2002) Therapy-related myeloid leukemias are observed in patients with chronic lymphocytic leukemia after treatment with fludarabine and chlorambucil: results of an intergroup study, cancer and leukemia. *J Clin Oncol.* 20 (18) pp 3878-84.

Morse, H.R. (2018) Chemotherapy-induced genotoxic damage to bone marrow cells: long-term implications. *Mutagenesis*. 33 (3), pp.241–251,

Mothersill, C. and Seymour C. (2001) Radiation-induced bystander effects: past history and future directions. *Radiat Res.* 155, pp. 759-767.

Mothersill, C. and Seymour, C. (2005) Radiation-induced bystander effects: are they good or bad or both. *Med Confl Surviv.* 21, pp. 101-110.

Mothersill, C. and Seymour, C. (2006) Radiation-induced bystander and other non-targeted effects: novel intervention points in cancer therapy? *Curr Cancer Drug Targets*. 6, pp. 447-454.

Mothersill, C. and Seymour, C.B. (2006) Radiation-induced bystander effects and the DNA paradigm: an "out of field" perspective. *Mutat Res.* 597, pp. 5–10.

Mothersill, C. and Seymour, C. (1997) Medium from irradiated human epithelial cells but not human fibroblasts reduces the clonogenic survival of unirradiated cells. *Int J Radiat Biol.* 71 (4), pp. 421-427.

Mothersill, C.E., Moriarty, M.J. and Seymour, C.B. (2004) Radiotherapy and the potential exploitation of bystander effects. *Radiat Oncol Biol Phys.* 58, pp. 575-579.

Mothersill. C. and Seymour, C.B. (1998) Mechanisms and implications of genomic instability and other delayed effects of ionizing radiation exposure. *Mutagenesis.* 13 (5), pp. 421-26.

Mouret, S., Baudouin, C., Charveron, M., Favier, A., Cadet J. and Douki T. (2006) Cyclobutane pyrimidine dimers are predominant DNA lesions in whole human skin exposed to UVA radiation. *Proc Natl Acad Sci*. 103, pp. 13765–13770.

Muelas, M.W., Ortega, F., Breitling, R., Bendtsen, C. and Westerhoff, H.V. (2018) Rational cell culture optimization enhances experimental reproducibility in cancer cells. *Scientific Reports.* 8, p. 3029.

Murphy, J.E., Nugent, S., Seymour, C. and Mothersill, C. (2005) Mitochondrial DNA point mutations and a novel deletion induced by direct low-LET radiation and by medium from irradiated cells. *Mutation Research/Genetic Toxicology and Environmental Mutagenesis.* 585 (1-2), pp.127-136.

Nagamura-Inoue, T., Kodo, H. and Takahashi, Mugishima, H., Tojo, A. and Asano, S. (2007) Four cases of donor cell-derived AML following unrelated cord blood transplantation for adult patients: Experiences of the Tokyo Cord Blood Bank. *Cytotherapy.* 9, pp. 7.

Nagarathna, P.K.M., Wesley, M. J., Reddy, P. S. and Reena. K. (2013) Review on Genotoxicity, its Molecular Mechanisms and Prevention. *Int. J. Pharm. Sci. Rev. Res.* 22 (1), pp. 236-243.

Nagasawa, H. and Little, J.B. (1999) Unexpected sensitivity to the induction of mutations by very low doses of alphaparticle radiation: evidence for a bystander effect. *Radiat Res.* 152, pp. 552-557.

Nagasawa, H. and Little, J.B. (1992) Induction of sister chromatid exchanges by extremely low doses of alpha-particles. *Cancer Res.* 52 (22), pp. 6394–6396.

Najafi, M., Fardid, R., Hadadi, G.H. and Fardid, M. (2014). The Mechanisms of Radiation-Induced Bystander Effect. *Biomed Phys Eng.* 4 (4), pp. 163–172.

Negreira, N., Lopez de Alda, M. and Barcelo, D. (2014) Cytostastic drugs and metabolites in municipal and hospital wastewaters in Spain: Filtration, occurrence, and environmental risk. *Science of the Total Environment.* 497-498, pp. 68-77.

Nemoto, S., Takeda, K., Yu, Z.X., Ferrans, V.J. and Finkel, T. (2000) Role for mitochondrial oxidants as regulators of cellular metabolism. *Mol. Cell. Biol.* 20, pp. 7311-8.

Neumann, H. G. (2009) Risk assessment of chemical carcinogens and thresholds. *Crit Rev Toxicol*. 39 (6), pp. 449-461.

Ng, A.P. and Alexander, W.S. (2017) Haematopoietic stem cells: past, present and future. *Cell death discovery*. *3*, pp.17002.

Newton, H. B. (2006) Clinical Pharmacology of Brain Tumor Chemotherapy. *Handbook of Brain Tumor Chemotherapy.* pp. 21-43

Nitiss, J. L. (2009) Targeting DNA topoisomerase II in cancer chemotherapy. *Nat Rev Cancer.* 9 (5), pp. 338–350.

Nobili, S., Lippi, D., Witort, E., Donnini, M., Bausi, L., Mini, E. and Capaccioli, S. (2009). Natural compounds for cancer treatment and prevention. *Pharmacological Research.* 59, pp. 365–378.

Nohmi, T., (2018) Thresholds of genotoxic and non-genotoxic carcinogens. *Toxicological research*, *34*(4), p.281.

Noll, D. M., Mason, T, M. and Miller, P. S. (2006) Formation and Repair of Interstrand Cross-Links in DNA. *Chem Rev*. 106 (2), pp. 277–301.

Nombela-Arrieta, C., Ritz, J. and Silberstein, L.E. (2011) The elusive nature and function of mesenchymal stem cells. *Nature reviews Molecular cell biology.* 12 (2), p.126.

Norppa, H. and.Falck, G.C.M. (2003) What do human micronuclei contain? *Mutagenesis*. 18 (3), pp. 221–233.

Nussenzweig, A. (2017) Endogenous DNA Damage as a Source of Genomic Instability in Cancer.

Nwajei, F. and Konopleva, M. (2013) The Bone Marrow Microenvironment as Niche Retreats for Hematopoietic and Leukemic Stem Cells. *Advances in Hematology.* (13), 953982.

Ock, C., Kim, E., Choi, D.J., Lee, H.J., Hahm, K., Chung, M.H (2012) 8-Hydroxydeoxyguanosine: Not mere biomarker for oxidative stress, but remedy for oxidative stress-implicated gastrointestinal diseases. *World J Gastroenterol.* 18 (4), pp. 302-308.

OECD (1998) Introduction to the OECD Guidelines on Genetic Toxicology Testing and 1664 leGuidance on the Selection and Application of Assays." In the Third Addendum to the OECD 1665 Guidelines for Testing of Chemicals. OECD Publications.

OECD (2012) Guidelines For The Testing Of Chemicals, Proposal For Updating Test Guideline 487, *In Vitro* Mammalian Cell Micronucleus Test.

O'Flaherty, C., Hales, B.F., Chan, P., Robaire, B. and Steril, F. (2010) Impact of chemotherapeutics and advanced testicular cancer or Hodgkin lymphoma on sperm deoxyribonucleic acid integrity. *Fertility and Sterility.* 94 (4), pp. 1374-9.

O'Flaherty, C., Vaisheva, F., Hales, B.F., Chan, P. and Hum, R. B. (2008) Characterization of sperm chromatin quality in testicular cancer and Hodgkin's lymphoma patients prior to chemotherapy. *Reprod.* 3 (5), pp. 1044-1052.

Olaharski, A.J., Mondrala, S.T. and Eastmond, D.A. (2005) Chromosomal malsegregation and micronucleus induction in vitro by the DNA topoisomerase II inhibitor fisetin. *Mutation Research/Genetic Toxicology and Environmental Mutagenesis*. 582 (1-2), pp.79-86.

Olive, P.L. and Banath, J.P. (1995) Sizing Highly Fragmented DNA in Individual Apoptotic Cells Using the Comet Assay and a DNA Crosslinking Agent. *Experimental Cell Research,* 221 (1), pp. 19-26.

Olive, P.L. and Banath, J.P. (1997) Multiceli Spheroid Response to Drugs Predicted with the Comet Assay *Cancer Research,* 57, pp. 5528-5533.

Olive, P.L., Durand, R.E., Banfith, J.P. and Evans, H.H. (199la) Etoposide sensitivity and topoisomerase I1 activity in Chinese hamster V79 monolayers and small spheroids. *Int. J Radiat. Biol*. 60, pp. 453-466.

Olobatuyi, O., de Vries, G. and Hillen, T. (2017) A Reaction-diffusion model for radiation-induced bystander effects. *Journal of Mathematical Biology*. 75 (2), pp 341-372.

Olson, B.J.S.C. (2016) Assays for Determination of Protein Concentration. *Current Protocols in Pharmacology,* 73, A.3A.1–A.3A.32.doi:10.1002/cpph.3.

Ostling, O. and Johanson, K.J. (1984) Microelectrophoretic study of radiationinduced DNA damages in individual mammalian cells. *Biochem. Biophys. Res. Commun*. 123, pp. 291-298.

Otero, L., Daiane Correa de Souza, Rita de Cássia Tavares, Bernadete Evangelho Gomes, Padilha, T.F., Bouzas, L.F., Teresa de Souza Fernandez and Abdelhay, E. (2012) Monosomy 7 in donor cell-derived leukemia after bone marrow transplantation for severe aplastic anemia: Report of a new case and review of the literature. *Genetics and Molecular Biology*. 35 (4), pp. 734-736.

Pal, D., Blair, H. J., Elder, A., Dormon, K., Rennie, K. J., Coleman, D.J.L., Weiland, J., Rankin, K. S., Filby, A., Heidenreich, O. and Vormoor, J. (2016) Long-term *in vitro* maintenance of clonal abundance and leukaemia-initiating potential in acute lymphoblastic leukaemia. *Leukemia.* 30, pp. 1691–1700.

Palanca-Wessels, M.C. and Oliver, W. (2014) Press Advances in the treatment of hematologic malignancies using immunoconjugates. *Blood*, 123, pp 2293-2301.

Panousis, C., Kettle, A.J. and Phillips, D.R. (1995) Myeloperoxidase oxidizes mitoxantrone to metabolites which bind covalently to DNA and RNA. *Anticancer Drug Des.* 10 (8), pp. 593 – 605.

Pant, G.S., Kamada, N. (1977) Chromosome aberrations in normal leukocytes induced by the plasma of exposed individuals. *Hiroshima Journal of Medical Sciences.* 26 (2–3), pp 149–154.

Paris, France. (1998) Introduction to the OECD Guidelines on Genetic Toxicology Testing and 1664 leGuidance on the Selection and Application of Assays." In the Third Addendum to the OECD 1665 Guidelines for Testing of Chemicals. OECD Publications.

Park, D., Sykes, B. D. and Scadden, D. T. (2012) The hematopoietic stem cell niche. *Frontiers in Bioscience*. 17, pp. 30-39.

Parry, E. M., Parry, J.M., Corso, C., Doherty, A., Haddad, F., Hermine, T.F., Johnson, G., Kayani, M., Quick, E. and Warr, T. (2002) Detection and characterization of mechanisms of action of aneugenic chemicals. *Williamson J Mutagenesis.* 17 (6) pp. 509-521.

Patel, J.B., Shah, F.D., Shukla, S.N., Shah, P.M. and Patel, P.S. (2009) Role of nitric oxide and antioxidant enzymes in the pathogenesis of oral cancer. *Cancer Res Ther.* 5, pp. 247-253.

Payne, S. and Miles, D. (2008) Mechanisms of Anticancer Drugs. *http://cw.tandf.co.uk/scottbrownent/sample-material/Chapter-4-Mechanisms-of-anticancer-drugs*. CRC Press, pp. 34-46.

Parker, B.S., Buley, T., Evison, B.J., Cutts, S.M., Neumann, G.M., Iskander, M.N. and Phillips, D.R. (2004) A molecular understanding of mitoxantrone-DNA adduct formation: effect of cytosine methylation and flanking sequences. *J Biol Chem.* 279 (18), pp. 18814-23.

Partridge, A.H., Burstein, H.J. and Winer, E.P. (2001) Side effects of chemotherapy and combined chemo hormonal therapy in women with early-stage breast cancer. *JNCI Monographs*. (30), pp.135-142.

Pedersen-Bjergaard, J., Andersen, M.K. and Christiansen, D.H. (2000) Therapy-related acute myeloid leukemia and myelodysplasia after high-dose chemotherapy and autologous stem cell transplantation. *Blood*. 95, pp. 3273-3279.

Pedersen-Bjergaard, J., Andersen, M.K., Christiansen, D.H. and Nerlov, C. (2002) Genetic pathways in therapy-related myelodysplasia and acute myeloid leukemia. *Blood*. 99 (6), pp. 909-1912.

Pelclova, D., Zdimal, V., Kacer, P., Fenclova, Z., Vlckova, S., Syslova, K., Navratil T., Schwarz, J., Zikova, N., Barosova, H., Turci, F., Komarc, M., Pelcl, T., Belacek, J., Kukutschova, J. and Zakharov, S. (2016) Oxidative stress markers are elevated in exhaled breath condensate of workers exposed to nanoparticles during iron oxide pigment production. *Journal of Breath Research.* 10 (1) pp. 016004.

Percival, M.E., Lai, C., Estey, E. and Hourigan, C.S. (2017) Bone marrow evaluation for diagnosis and monitoring of acute myeloid leukemia. *Blood Rev*. 31 (4), pp. 185–192.

Perl, A., Gergely, P. and Banki K. (2004). Mitochondrial dysfunction in T cells of patients with systemic lupus erythematosus. *Int Rev Immunol*. 23 pp. 293–313.

Pesce, A.J., Mendoza, N., Boreisha, I., Gaizutis, M.A. and Pollak, V.E., (1974) Use of enzyme-linked antibodies to measure serum anti-DNA antibody in systemic lupus erythematosus. *Clinical chemistry*. 20 (3), pp.353-359.

Peter, M. (2011) Apoptosis Meets Necrosis. *Nature.* 471, pp. 310-311.

Phillips, H. J. (1973) Dye Exclusion Tests for Cell Viability. *Tissue Culture,* pp. 406–408.

Philomena, G. (2011) Concerns regarding the safety and toxicity of medicinal plants -An overview. *Journal of Applied Pharmaceutical Science.* 1 (6), pp. 40-44.

Pilger, A. and Rüdiger, H.W. (2006) 8-Hydroxy-2′-deoxyguanosine as a marker of oxidative DNA damage related to occupational and environmental exposures. *Int. Arch. Occup. Environ. Health.* 80 (1), pp. 1–15.

Plessis, S.S., Agarwal, A., Mohanty, G. and Van der Linde, M. (2015) Oxidative phosphorylation versus glycolysis: what fuel do spermatozoa use? *Asian J Androl.* 17 (2) pp. 230–235.

Podszywalow-Bartnicka, P., Kominek, A., Wolczyk, M., Kolba, M.D., Swatler, J. and Piwocka, K., (2018) Characteristics of live parameters of the HS-5 human bone marrow stromal cell line cocultured with the leukemia cells in hypoxia, for the studies of leukemia–stroma crosstalk. *Cytometry Part A.* 93 (9), pp.929-940.

Pokharel, M. (2012) Leukemia: A review article. *International Journal of Advanced Research in Pharmaceutical Bio Sciences*. 2 (3), pp. 397-407.

Poliquin, C.M. (1990) Post-Bone Marrow Transplant Patient Management. *The Yale Journal of Biology and Medicine.* 63, pp. 495-502.

Prise, K. M., Folkard, M. and Michael, B. D. (2003) A review of the bystand-er effect and its implications for low-dose exposure. *Radiat. Prot. Dosimetry*. 104, pp. 347-355.

Prise, K.M. and O'Sullivan, J.M. (2009) Radiation-induced Bystander Signaling in Cancer Therapy. *Nat Rev Cancer*. 9 pp. 351-360.

Purdie, J. (2017). https://www.healthline.com/health/leukemia-hereditary genetic-vs-hereditary.

Qu, Y., Franchi, L., Nunez, G. and Dubyak, G.R. (2007) Nonclassical IL-1β secretion stimulated by P2X7 receptors is dependent on inflammasome activation and correlated with exosome release in murine macrophages. *The Journal of Immunology*. 179 (3), pp.1913-1925.

Radivoyevitch, T., Sachs, R.K., Gale, R.P., Molenaar, R.J., Brenner, D.J., Hill, B.T., Kalaycio, M.E., Carraway, H.E. and Mukherjee, S. (2015) Defining AML and MDS second cancer risk dynamics after diagnoses of first cancers treated or not with radiation. *Leukemia*. 258.

Rajkovic, A. (2018) Oxygen Consumption Rate Analysis of Mitochondrial Dysfunction Caused by *Bacillus cereus* Cereulide in Caco-2 and HepG2 Cells. *Toxins*. 10 (7), pp. 266.

Rai, K.R., Sawitsky, A., Cronkite, E.P., Chanana, A.D., Levy, R.N. and Pasternack, B.S., (1975). Clinical staging of chronic lymphocytic leukemia. *Blood*, *46* (2), pp.219-234.

Raisuddin, S. and Jha, A.N. (2004) Relative sensitivity of fish and mammalian cells to sodium arsenate and arsenite as determined by alkaline single cell gel electrophoresis and cytokinesis block micronucleus assay. *Environ Mol Mutagen*. 44, pp. 83–9.

Ralhan, R. and Kaur, J. (2007) Alkylating agents and cancer therapy *Expert Opin. Ther*. 17 (9), pp. 1061-1075

Raschke, M., Rowland, I.R., Magee, P.J. and Pool-Zobel, B.L. (2006) Genistein protects prostate cells against hydrogen peroxide-induced DNA damage and induces expression of genes involved in the defence against oxidative stress. *Carcinogenesis.* 27 (11), pp.2322-2330.

Redza-Dutordoir, M. and Averill-Bates, D.A. (2016). Activation of apoptosis signalling pathways by reactive oxygen species. *Biochim Biophys Acta.* 1863 (12), pp. 2977-2992.

Rees, B.J., Tate, M., Lynch, A.M., Thornton, C.A., Jenkins, G.J., Walmsley, R.M. and Johnson, G.E., (2017). Development of an in vitro PIG-A gene mutation assay in human cells. *Mutagenesis*. 32 (2), pp. 283-297.

Renew, J.E. and Huang, C. (2004) Simultaneous determination of fluoroquinolone, sulphonamide, and trimethoprim antibiotics in waste water using tandem solid phase extraction and liquid chromatography-electrospray mass spectrometry. *Journal of Chromatography A.* 1042, pp. 113-121.

Robert, W.P., Schubach, W., Neiman, P., Martin, P. and Thomas, D.E. (1985) Donor cell leukemia developing six years after marrow grafting for acute leukemia. *Blood.* 65 (5), pp. 1172-1174.

Roecklein, B.A, Torok-Storb, B. (1995) Functionally distinct human marrow stromal cell lines immortalized by transduction with the human papilloma virus E6/E7 genes. *Blood.* 85 (4), pp. 997-1005.

Rojas, E., Lopea, M.C. and Valverde, M. (1999) Single cell gel electrophoresis assay: methodology and applications. *J. Chromatogr. B.* 722, pp. 225–254.

Rollie, S. and Sundmacher, K. (2012) Designing biological systems: systems engineering meets synthetic biology. *Chem. Eng. Sci.* 69, pp. 1 – 29.

Rosefort, C., Fauth, E. and Zankl, H. (2004) Micronuclei induced by aneugens and clastogens in mononucleate and binucleate cells using the cytokinesis block assay.1 *Mutagenesis*. 19 (4), pp. 277-284.

Roness, H., Kalich-Philosoph, L. and Meirow, D., (2014) Prevention of chemotherapy-induced ovarian damage: possible roles for hormonal and non-hormonal attenuating agents. *Human reproduction update*, 20 (5), pp.759-774.

Rugo, R.E., Almeida, K.H., Hendricks, C.A., Jonnalagadda, V.S. and Engelward, B.P. (2005) A single acute exposure to a chemotherapeutic agent induces hyper-recombination in distantly descendant cells and in their neighbors. *Oncogene.* 24, pp. 5016–5025.

Ruiz-Arguelles, G.J., Ruiz-Arguelles, A. Garces-Eisele, J. (2007) Donor cell leukaemia: a critical review. *Leuk Lymphoma.* 48 (1), pp. 25 – 38.

Rzeszowska-Wolny, J, Przybyszewski, W.M., Widel, M. (2009) Ionizing radiation-induced bystander effects, potential targets for modulation of radiotherapy. *European Journal of Pharmacology*. 625, pp. 156–164.

Sabine, A., Langie, S., Koppen, G., Desaulniers, D., Al-Mulla, F., Al-Temaimi, R., Amedei , A., Azqueta, A., Bisson, W.H., Brown, D., Brunborg, G., Charles, A.K., Tao Chen , Annamaria Colacci, Firouz Darroudi, Stefano Forte, Laetitia Gonzalez, Hamid, R.A., Knudsen, L. E., Leyns, L., Salsamendi, A. L., Memeo, L., Mondello, C., Mothersill, C., Olsen, A., Pavanello1, S., Raju, J., Rojas, E., Roy, R., Ryan, E., Ostrosky-Wegman, P., .Salem, H. K., Scovassi, I., Singh, N., Vaccari, M., Schooten, F. J.V., Valverde, M., Woodrick, J., Zhang, L., Larebeke, N., Kirsch-Volders, M. and Collins, A. R. (2015) Causes of genome instability: the effect of low dose chemical exposures in modern society. *Carcinogenesis*. *Supplement*, 36: pp. S61–S88.

Salceda, J., Ferna´ndez, X. and Roca, J. (2006) Topoisomerase II, not topoisomerase I, is the proficient relaxase of nucleosomal DNA. *The EMBO Journal*. 25, pp. 2575–2583.

Sallmyr, A., Fan, J., Datta, K., Kim, K.T., Grosu, D., Shapiro, P., Small, D. and Rassool, F. (2008) Internal tandem duplication of FLT3 (FLT3/ITD) induces increased ROS production, DNA damage, and misrepair: *implications for poor prognosis in AML*. 111 (6), pp. 3173-3182.

Salman, Z., Balandrán-Juárez, J. C., Pelayo, R., Monica, L. and Guzman, A. (2015) Novel Three-Dimensional Co-Culture System to Study Leukemia in the Bone Marrow Microenvironment. *Blood.* 126, pp. 1864.

Sakamoto, S., Putalun, W., Vimolmangkang, S., Phoolcharoen, W., Shoyama, Y., Tanaka, H. and Morimoto, S. (2018) Enzyme-linked immunosorbent assay for the quantitative/qualitative analysis of plant secondary metabolites. *Journal of natural medicines*. 72 (1), pp.32-42.

Salti, G.I., DasGupta, T.K. and Constantinou, A.I. (2000) A novel use for the comet assay: detection of topoisomerase II inhibitors. *Anticancer Res.* 20 (5A), pp. 3189-93.

Sanz, G.F., Sanz, M.A., Vallespí, T., Cañizo, M.C., Torrabadella, M., García, S., Irriguible, D. and San Miguel, J.F. (1989) Two regression models and a scoring system for predicting survival and planning treatment in myelodysplastic syndromes: a multivariate analysis of prognostic factors in 370 patients. *Blood.* 74 (1), pp. 395–408.

Sawal, H.A., Asghar, K., Bureik, M. and Jala, N. (2017) Bystander signalling via oxidative metabolism. *Onco Targets Ther.* 10, pp. 3925-3940.

Schmid, W. (1975). The micronucleus test. *Mutation. Research.* 31, pp. 9–15.

Schmidmaier, R., Baumann, P. and Meinhardt, G. (2006) Cell-cell contact mediated signalling — no fear of contact. *Exp Oncol.* 28 (1), pp. 12–15.

Schmidt, T., Masouleh, B. K. and Loges, S. (2011) Loss or inhibition of stromal-derived PlGF prolongs survival of mice with imatinib resistant Bcr-Abl1+ leukemia. *Cancer Cell.* 19 (6): pp. 740–753.

Schuler, M., Rupa, D.S. and Eastmond, D.A. (1997) A critical evaluation of centromeric labeling to distinguish micronuclei induced by chromosomal loss and breakage in vitro. *Mutat Res.* 392 (1-2), pp. 81-95.

Schuz, J. and Erdmann, F. (2016) Environmental exposure and risk of childhood leukaemia: An overview. *Arch Med, Res.* 47 (8), pp. 607-614.

Scuto, A., Krejci, P., Popplewell, L., Wu, J., Wang, Y., Kujawski, M., Kowolik, C., Xin, H., Chen, L., Wang, Y., Kretzner, L., Yu, H., Wilcox, W.R., Yen, Y., Forman, S. and Jove, R. (2011) The novel JAK inhibitor AZD1480 blocks STAT3 and FGFR3 signaling, resulting in suppression of human myeloma cell growth and survival. *Leukemia.* 25 (3), pp. 538–550.

Sedelnikova, O.A., Nakamura, A., Kovalchuk, O., Koturbash, I., Mitchell, S.A., Marino, S.A., Brenner, D.J. and Bonner, W.M. (2007) DNA double-strand breaks formin bystander cells after

microbeam irradiation of three-dimensional human tissue models. *Cancer Res.* 67: pp. 4295–4302.

Seymour, C. B. and Mothersill, C. (2004) Radiation-induced bystander effects — implications for cancer. *Nature Reviews Cancer*. 4 (2), pp. 158–164.

Shafat, M. S., Gnaneswaran, B., Bowles, K. M. and Rushworth, S.A. (2017) The bone marrow microenvironment–Home of the leukemic blasts. *Blood Reviews*. 31, pp. 277–286.

Shaker, G.H. and Melake, N.A. (2012) Use of the single cell gel electrophoresis (comet assay) for comparing apoptotic effect of conventional antibodies versus nanobodies. *Saudi Pharmaceutical Journal*. 20, pp. 221–227.

Shao, C., Aoki, M. and Furusawa, Y. (2001) Medium-mediatedb ystander effects on HSG cells co-cultivatedw ith cells irradiatedb y X-rayso r a 290 MeV/u carbon beam. *Radiat. Res.* 42, pp. 305-316.

Shao, C., Folkard M., Michael, B.D. and Prise, K.M. (2005) Bystander signalling between glioma cells and fibroblasts targeted with counted particles. *International Journal of Cancer.* 116, pp. 45-51.

Shao, C., Prise, K. M. and Folkard, M. (2008) Signaling factors for irradiated glioma cells induced bystander responses in fibroblasts. *Mutat. Res.* 638, pp. 139–145.

Shigenaga, M.K., Aboujaoude, E.N., Chen, Q. and Ames, B.N. (1994). Assays of oxidative DNA damage biomarkers 8-oxo-2'-deoxyguanosine and 8-oxoguanine in nuclear DNA and biological fluids by high-performance liquid chromatography with electrochemical detection. *Methods Enzymol*. 234, pp. 16-33.

Shiozaki, H., Yoshinaga, K., Kondo, T., Imai, Y., Shiseki, M., Mori, N., Teramura, M. and Motoji, T. (2014) Donor cell-derived leukemia after cord blood transplantation and a review of the literature: Differences between cord blood and BM as the transplant source. *Bone Marrow Transplantation*. 49 (1), pp. 102 – 109.

Shugart, L.R. (2000) DNA damage as a biomarker of exposure. *Ecotoxicology*. 9, pp. 329–340.

Siddik, Z.H. (2002) Mechanisms of Action of Cancer Chemotherapeutic Agents: DNA-Interactive Alkylating Agents and Antitumour Platinum-Based Drugs. The Cancer Handbook 1st Edition. Edited by Malcolm R. Alison 2002 John Wiley & Sons, Ltd.

Singh, N.P., McCoy, M.T., Tice, R.R. and Schneider, E.L. (1988) A simple technique for quantitation of low levels of DNA damage in individual cells. *Exp. Cell Res*. 175, pp. 184-191.

Singh, N.P., McCoy, M.T., Tice, R.R. and Schneider, E.L. (1988) A simple technique for quantitation of low levels of DNA damage in individual cells. *Exp. Cell Res*. 175, pp. 184-191.

Siu, W.H.L., Cao, J., Jack, R.W., Wu, R.S.S., Richardson, B.J., Xu, L. and Lam, P.K.S. (2004) Application of the comet and micronucleus assays to the detection of B[*a*]P genotoxicity in haemocytes of the green-lipped mussel (*Perna viridis*). *Aquatic Toxicology*. 66 (4), pp. 381–392.

Skladanowski, A. and Konopa, J. (2000) Mitoxantrone and ametantrone induce interstrand cross-links in DNA of tumour cells. *British journal of Cancer.* 82, pp. 1300-1304.

Skopek, T.R., Liber, H.L., Penman, B.W. and Thilly, W.G. (1978) Isolation of a human lymphoblastoid line heterozygous at the thymidine kinase locus: possibility for a rapid human cell mutation assay. *Biochem. Biophys. Res. Commun.* 84, pp. 411-416.

Smith, C. C., O'Donovan, M. R. and Martin, E. A. (2006) hOGG1 recognizes oxidative damage using the comet assay with greater specificity than FPG or ENDOIII. *Mutagenesis.* 21 (3), pp. 185–190.

Snyder, A.R. (2004) Review of radiation-induced bystander effects. *Human and Experimental Toxicology*. 23, pp. 87-89.

Sosaa, V., Molinéa, T., Somozaa, R., Paciucci R., Kondohc, H., Matilde, E.and Leonart, L. (2013) Oxidative stress and cancer. *Ageing Research Reviews.* 12, pp. 376–390.

Speit, G., Menz, W., Röscheisen, C. and Köberle, B. (1992) Cytogenetic and molecular characterization of the mutagenicity of chlorambucil in V79 cells. *Mutat Res.* 283 (1), pp. 75-81.

Spinelli, O., Giussani, U., Borleri, G., lazzari, M., Michelato, A., Dotti, G., Barbui, T. and Rambaldi, A. (2000) Need for an accurate molecular diagnosis to assess the donor origin of leukemia relapse after allogeneic stem cell transplantation. *Haematologica*. 85 (2000), pp. 1153-1157.

Stamell, E.F., Wolchok, J.D., Gnjatic, S., Lee, N.Y. and Brownell, I. (2013) The abscopal effect associated with a systemic anti-melanoma immune response. *Radiat Oncol Biol Phys.*, 85, pp. 293–295.

Stieglitz, E. and Loh, M.L. (2013) Therapeutic Advances in Hematology Review Genetic predispositions to childhood leukemia. *Ther Adv Hematol*. 4 (4), pp. 270 –290.

Strober, W. (1997) Trypan Blue Exclusion Test of Cell Viability. *Current Protocols in Immunology.* A3B.1-A3B.2.

Suarez-Gonzalez, J., Martinez-Laperche, C., Kwon, M., Balsalobre, P., Carbonell, D., Chicano, M., Rodriguez-Macias, G., Serrano, D., Gayoso, J., Diez-Martin, J.L. and Buno, I. (2018) Donor cell-derived haematological neoplasms after hematopoietic stem cell transplantation. A systematic review. *Biology of Blood and Marrow Transplantation.* 24 (7), pp. 1505 – 1513.

Syslová, K., Böhmová, A., Mikoška, M., Kuzma, M., Pelclová, D. and Kačer, P. (2014) Oxidative Medicine and Cellular Longevity. Multimarker Screening of Oxidative Stress in Aging. 14.

Tanaka, H., Matsumura, I., Ezoe, S., Satoh, Y., Sakamaki, T., Albanese, C., Machii, T., Pestell, R.G. and Kanakura, Y. (2002) E2F1 and c-Myc potentiate apoptosis through inhibition of NF-kappaB activity that facilitates MnSOD-mediated ROS elimination. *Mol Cell.* 9, pp. 1017–1029.

Taylor, G.M. and Birch, J.M. (1996) The hereditary basis of human leukemia. In Henderson, E.S., Lister, T.A. and Greaves, M.F. *Leukemia.* 6th ed. Philadelphia: WB Saunders. pp. 210.

Tavor, S., Petit, I., Porozov, S., Avigdor, A., Dar, A., Leider-Trejo, L., Shemtov, N., Deutsch, V., Naparstek, E., Nagler, A. and Lapidot, T. (2004) CXCR4 regulates migration and development of human acute myelogenous leukemia stem cells in transplanted NOD/SCID mice. *Cancer research.* 64 (8), pp.2817-2824.

Wang, H., Shi, T., Qian, W., Liu, T., Kagan, J., Srivastava, S., Smith, R.D., Rodland, K.D. and Camp, D.G. (2016) The clinical impact of recent advances in LC-MS for cancer biomarker discovery and verification. *Expert Rev Proteomics*. 13 (1), pp. 99–114.

Taylor, G.M. and Birch, J.M. (1996) The hereditary basis of human leukemia. In Henderson, E.S., Lister, T.A. and Greaves, M.F. *Leukemia.* 6th ed. Philadelphia: WB Saunders. pp. 210.

Thiede C. (2004) Diagnostic chimerism analysis after allogeneic stem cell transplantation: new methods and markers. *Am J Pharmacogenomics*. 4 (3), pp. 177-87.

Thirumaran, R., Prendergast, G.C and Gilman, P.B. (2007) Cytotoxic chemotherapy in clinical treatment of cancer. Cancer immunotherapy: immune suppression and tumor growth. *Elsevier.* pp. 101 -116.

Thomas, A. D., Jenkins, G. J. S., Kaina, B., Bodger, O. G., Tomaszowski, K., Lewis, P.D., Doak, S.H. and Johnson, G.E. (2013) Influence of DNA Repair on Nonlinear Dose-Responses for Mutation. *Toxicological Sciences*. 132 (1), pp. 87–95.

Thomas, A.D., Fahrer, J., Johnson, G.E. and Kaina, B. (2015) Theoretical considerations for thresholds in chemical carcinogenesis. Mutat Res Rev Mutat Res. 765, pp. 56-67.

Tice, R. R., Agurell, E., Anderson, D., Burlinson, B., Hartmann, A., Kobayashi, H., Miyamae, Y., Rojas, E., Ryu, J.C. and Sasaki. Y. F. (2000) Single Cell Gel/Comet Assay: Guidelines for *in vitro* and *in vivo* Genetic Toxicology Testing. *Environmental and Molecular Mutagenesis.* 35, pp. 206-221.

Tome, W.A., Fenwick, J.D. Bentzen, S.M. (2006) Dose a local bystander effect necessitate a revision of TCP models that are based on observed clinical data? *Acta Oncol.* 45, pp. 406-411.

Tönnies, E. and Trushina, E. (2017) Oxidative Stress, Synaptic Dysfunction, and Alzheimer's Disease. *J Alzheimers Dis.* 57 (4), pp.1105-1121.

Torane, V.P. and Shastri, J.S. (2008) Comparison of ELISA and rapid screening tests for the diagnosis of HIV, hepatitis B and hepatitis C among healthy blood donors in a tertiary care hospital in Mumbai. *Indian journal of medical microbiology*. *26* (3), pp.284-285.

Torok-Storb, B., Iwata, M., Graf, L., Gianotti, J., Horton, H., Byrne, M.C. (1999) Dissecting the marrow microenvironment. *Ann. N.Y. Acad. Sci*. 872, pp. 164–170.

Torra, O.S. and Loeb, K.R. (2011) Donor Cell–Derived Leukemia and myelodysplastic Neoplasm: Unique Forms of Leukemia. *Am J Clin Pathol*. 135, pp. 501-504.

Trott, K. R. (2001) Non-targeted radiation effects in radiotherapy. *Acta Oncol.* 40, 976-980.

Usuludin, S.B.M., Cao, X., Lim, M. (2012) Co-Culture of Stromal and Erythroleukemia Cells in a Perfused Hollow Fiber Bioreactor System as an In Vitro Bone Marrow Model for Myeloid Leukemia. *Biotechnology and Bioengineering*. 109 (5), pp. 148 – 58.

Vafa, O., Wade, M., Kern, S., Beeche, M., Pandita, T.K., Hampton, G.M. and Wahl, G.M. (2002) C-Myc can induce DNA damage, increase reactive oxygen species, and mitigate p53 function: a mechanism for oncogene-induced genetic instability. *Mol Cell*. 9 pp. 1031–1044.

Valko, M., Leibfritz, D., Moncol, J., Cronin, M.T., Mazur, M. and Telser, J. (2007) Free radicals and antioxidants in normal physiological functions and human disease. *Biochem Cell Biol*. 39, pp. 44–84.

Vanderstichel, R., Dohoo, I. and Markham, F. (2015) Applying a kinetic method to an indirect ELISA measuring Ostertagia ostertagi antibodies in milk. *Canadian Journal of Veterinary Research*. 79 (3), pp.180-183.

Veskoukis, A.S., Tsatsakis, A.M. and Kouretas, D. (2012) Dietary oxidative stress and antioxidant defense with an emphasis on plant extract administration. *Cell Stress and Chaperones.* 17, pp. 11–21.

Vlachogianni, T. and Fiotakis, C. (2009) A Critical Biomarker of Oxidative Stress and Carcinogenesis Athanasios Valavanidis. *Environmental Science and Health.* 27, pp. 120–139.

Vollmer, T., Stewart, T. and Baxter, N. (2010) Mitoxantrone and cytotoxic drugs mechanism of action. *Neurology.* 74 (1), pp. S41- S46.

Walshauser, M.A., Go, A., Sojitra, P., Venkataraman, G. and Stiff, P. (2014) Donor Cell Myeloid Sarcoma. *Case Reports in Hematology*. 2014, 153989.

Wang, E., Hutchinson, C.B., Huang, Q., Mark Lu, C., Crow, J., Wang, F., Sebastian, S., Rehder, C., Lagoo, A., Horwitz, M., Rizzieri, D., Jingwei Yu, Goodman, B., Datto, M. and Buckley, P. (2011) Donor Cell–Derived Leukemias/Myelodysplastic Neoplasms in Allogeneic Hematopoietic Stem Cell Transplant Recipients. A Clinicopathologic Study of 10 Cases and a Comprehensive Review of the Literature. *Am J Clin Pathol*. 135, pp. 525-540.

Wang, Q., He, Y., Shen, Y., Zhang, Q., Chen, D., Zuo, C., Qin, J., Wang, H., Wang, J. and Yu, Y., (2014) Vitamin D inhibits COX-2 expression and inflammatory response by targeting thioesterase superfamily member 4. *Journal of Biological Chemistry*. 289 (17), pp.11681-11694.

Wasnik, S., Kantipudi, S., Kirkland, M.A. and Pande, G. (2016) Enhanced *Ex Vivo* Expansion of Human Hematopoietic Progenitors on Native and Spin Coated Acellular Matrices Prepared from Bone Marrow Stromal Cells. *Stem Cells Int.* 7231567.

Watson, G.E., Lorimore, S.A., Macdonald, D.A. and Wright, E.G. (2000) Chromosomal instability in unirradiated cells induced in vivo by a bystander effect of ionizing radiation. *Cancer Res.* 60, pp. 5608-5611.

Weinberg, F., Hamanaka, R., Wheaton, W.W., Weinberg, S., Joseph, J., Lopez, M., Kalyanaraman, B., Mutlu, G.M., Budinger, G.R. and Chandel, N.S. (2010) Mitochondrial metabolism and ROS generation are essential for Kras-mediated tumorigenicity. *Proc Natl Acad Sci.* 107, pp. 8788–8793.

Whitesides, G.M. (2006) The origins and the future of microfluidics. *Nature.* 442 (7101), pp. 368-73.

Widel, M. (2012) Bystander effect induced by UV radiation; why should we be interested? *Postepy Hig Med.* 66, pp. 828-837.

Widel, M., Przybyszewski, W.M., Cieslar-Pobuda, A., Saenko, Y.V. and Rzeszowska-Wolny, J. (2012) Bystander normal human fibroblasts reduce damage response in radiation targeted cancer cells through intercellular ROS level modulation. *Mutat Res.* 731, pp. 117-124.

Widel, M., Krzywon, A., Gajda, K., Skonieczna, M. and Rzeszowska-Wolny, J. (2014) Induction of bystander effects by UVA, UVB, and UVC radiation in human fibroblasts and the implication of reactive oxygen species. *Free Radic Biol Med.*, 68, pp 278-87.

Wider, N., Beguin, A., Rochat, B., Buclin, T., Kovacsovics, T., Duchosal, M.A., Leyvraz, S., Rosselet, J., Biollaz, J. and Decosterd, L.A. (2004) Determination of imatinib (Gleevec) in human plasma by solid-phase extraction-liquid chromatography-ultraviolet absorbance detection. *Journal of Chromatography B.* 803, pp. 285-292.

Witherspoon, R.P., Schubach, W., Neiman, P., Martin, P. and Thomas, E.D. (1985) Donor cell leukemia developing six years after marrow grafting for acute leukemia. *Blood*. 65, pp. 1172-1174.

Wiseman, D.H. (2011) Donor Cell Leukemia: A Review. *Biol Blood Marrow Transplant*. 17, pp. 771-789.

Woo, D.A., Collins, R.H., Rossman, H.S., Stüve, O. and Frohman, E.M. (2008) Mitoxantrone-Associated Leukemia in Multiple Sclerosis: Case Studies. *Int J MS Care.* 10, pp. 41–46.

Woods, D. and Turchi, J. J. (2013) Chemotherapy induced DNA damage response, *Cancer Biology & Therapy*. 14 (5), pp. 379-389.

World Health Organisation. (2002) Non-Ionizing Radiation, Part 1: Static and Extremely Low-Frequency (ELF) Electric and Magnetic Fields (IARC Monographs on the Evaluation of the Carcinogenic Risks) *Geneva*. pp. 332–333.

Wright, E.G. (2010) Manifestations and mechanisms of non-targeted effects of ionizing radiation. *Mutat Res.* 687: pp. 28–33.

Wu, J.H. and Jones, N.J. (2012) Assessment of DNA interstrand crosslinks using the modified alkaline comet assay. Genetic Toxicology: Principles and Methods. *Methods in Molecular Biology.* 817, pp. 165-181.

Yang, G., Wu, L., Chen, S., Zhu L., Huang, P., Tong, L., Zhao, Y., Zhao, G., Wang, J., Mei, T., Xu, A. and Wang, Y. (2009) Mitochondrial dysfunction resulting from loss of cytochrome c impairs radiation-induced bystander effect. *Br J Cancer.* 100 (12), pp. 912-6.

Yang, L., tan, Y., Shi, J., Zhao, Y., Zhu Y., Hu, Y., Pan, W., Ye, Y., He, J., Zheng, W., Sun, J., Cai,Z., Huang, H., Luo, Y. (2018) Allogeneic hematopoietic stem cell transplantation should be in preference to conventional chemotherapy as post-remission treatment for adults with lymphoblastic lymphoma. *Bone Marrow Transplant.* 53 (10), pp. 1340-1344.

Yang, H., Villani, R. M., Wang, H., Simpson, M. J., Roberts, M. S., Tang, M. and Liang, X. (2018) The role of cellular reactive oxygen species in cancer chemotherapy. *Journal of Experimental and Clinical Cancer Research.* 37, pp. 266

Yang, J., Bai, W.L., Chen, Y.J. and Gao, A. (2015) 1, 4-benzoquinone-induced STAT-3 hypomethylation in AHH-1 cells: Role of oxidative stress. *Toxicology reports.* 2, pp. 864-869.

Yao, T. and Asayama Y. (2017) Animal cell culture media: History, characteristics, and current issues. *Reprod Med Biol.* 16 (2), pp. 99–117.

Yee, K.W. and O'Brien S.M. (2006) Chronic lymphocytic leukemia: diagnosis and treatment. *Mayo Clin Proc*. 81 (8), pp. 1105-1129.

Yong, A.S.M. and Goldman, J.M. (1999) Relapse of chronic myeloid leukaemia 14 years after allogenic bone marrow transplantation. *Bone Marrow Transplant.* 23, pp. 827-828.

Yoshinaga, S., Mabuchi, K., Sigurdson, A.J., Doody, M.M. and Ron, E. (2004) Cancer risks among radiologists and radiologic technologists: review of epidemiologic studies. *Radiology*. 233 (2), pp. 313–21.

Yves, P., Elisabetta, L., HongLiang, Z. and Christophe, M. (2010) DNA Topoisomerases and Their Poisoning by Anticancer and Antibacterial Drugs. *Chem.Biol.* 17 (5), pp. 421-433.

Zanetta, F., Montecucco, A. and Biamonti, G. (2015) Molecular mechanisms of etoposide. *Excli.* 14, pp. 95–108.

Zeeb, H. and Blettner, M. (1998) Adult leukaemia: what is the role of currently known risk factors? *Radiat Environ biophys.* 36 (4), pp. 217 – 28.

Zeyneloğlu, H., Kahraman, S. and Pirkevi, C. (2011) J Reprod Co-culture techniques in assisted reproduction: history, advances and the future. *Stem Cell Biotechnol*. 2 (1), pp. 29-40.

Zhang, C., Nestorova, G., Rissman, R.A. and Feng, J. (2013) Detection and quantification of 8-Hydroxy-2-Deoxyguanosine in Alzheimers transgenic mouse urine using capillary electrophoresis. *Electrophoresis.* 34 (15), pp. 2268-2274.

Zhang, J. and Zhang, Q. (2019) Using Seahorse machine to measure OCR and ECAR in cancer cells. *Methods Mol. Biol.* 1928, pp. 353-363.

Zhang, Y., Dai, M. and Yuan, Z. (2018) Methods for the detection of reactive oxygen species. *Anal. Methods.* 10, pp. 4625.

Zhao, F., Mancuso, A., Bui, T.V., Tong, X., Gruber, J.J., Swider, C.R., Sanchez, P.V., Lum, J.J., Sayed, N., Melo, J.V., Perl, A.E., Carroll, M., Tuttle, S.W. and Thompson, C.B. (2010) Imatinib resistance associated with BCR-ABL upregulation is dependent on HIF-1 alpha-induced metabolic reprograming. *Oncogene.* 29 (20), pp. 2962-72.

Zhao, M., Li, H., Li, L. and Zhang, Y. (2014) Effects of a gemcitabine plus platinum regimen combined with a dendritic cell-cytokine induced killer immunotherapy on recurrence and survival rate of non-small cell lung cancer patients. *Exp Ther Med.* 7 (5), pp. 1403–1407.

Zhao, H., Wang, Y., Jin, Y., Liu, S., Xu, H. and Lu, X. (2016) Rapid and sensitive analysis of melatonin by LC-MS/MS and its application to pharmacokinetic study in dogs. *Asian Journal of Pharmaceutical Sciences.* 11 (2), pp. 273 – 280.

Zhou, H., Ivanov, V. N., Gillespie, J., Geard, C. R., Amundson, S. A., Brenner, D.J., Yu, Z., Lieberman, H.B. and Hei, T. K. (2005) Mechanism of radiation-induced bystander effect: role of the cyclooxygenase-2 signalling pathway. *Proc natl Acad Sci.* 102 (41), pp. 14641 – 6.

Zhou, H., Randers-Pehrson, G., Waldren, C.A., Vannais, D., Hall, E.J and Hei, T.K. (2000) Induction of a bystander mutagenic effect of alpha particles in mammalian cells. *Proc. Natl. Acad. Sci.* 97, pp. 2099–2104.

Zhou, Z., Zwelling, L.A., Ganapathi, R. and Kleinerman, E.S. (2001) Enhanced etoposide sensitivity following adenovirus-mediated human topoisomerase II alpha gene transfer is independent of topoisomerase. *Cancer*. 85 (5), pp. 747-51.

Ziraldo, R., Andreas Hanke, S. and Levene. S.D. (2019) Kinetic pathways of topology simplification by Type-II topoisomerases in knotted supercoiled DNA. *Nucleic Acids Research*. 47 (1) pp. 69–84.